Nalcor Energy – Lower Churchill Project

Iceberg Risk to Subsea Cables in Strait of Belle Isle

ILK-CC-CD-8110-EN-RP-0001-01

Comments:	Total # of Pages (Including Cover): 206

V1	**Jan. 2011**	**Initial Draft**					
V2	**June, 2011**	**Additional Routes**					
Status/ Revision	Date	Reason For Issue	Prepared By	Checked By	IMS Lead	Dept. Manager Approval	Project Manager Approval
CONFIDENTIALITY NOTE:	This document contains intellectual property of the Nalcor Energy – Lower Churchill Project and shall not be copied, used or distributed in whole or in part without the prior written consent from the Nalcor Energy – Lower Churchill Project.						

Additional Signatures (where required)

Status/ Revision	Date	Reason For Issue	Prepared By	Checked By	IMS Lead	Dept. Manager Approval	Project Manager Approval

Professional Engineers Stamp:
(where required)

Iceberg Risk to Subsea Cables in Strait of Belle Isle

C-CORE Report
R-10-039-781 V2

Prepared for:
Nalcor Energy

June 2011

Captain Robert A. Bartlett Building
Morrissey Road
St. John's, NL
Canada A1B 3X5

T: (709) 864-8354
F: (709) 864-4706

Info@c-core.ca
www.c-core.ca

This page is intentionally left blank

Iceberg Risk to Subsea Cables in Strait of Belle Isle

Prepared for:
Nalcor Energy

Prepared by:
C-CORE
Fugro GeoSurveys Inc.

C-CORE Report:
R-10-039-781 V2

June 2011

Innovative Engineering Solutions
Captain Robert A. Bartlett Building
Morrissey Road
St. John's, NL
Canada A1B 3X5

T: (709) 864-8354
F: (709) 864-4706

Info@c-core.ca
www.c-core.ca

The correct citation for this report is:

C-CORE (2011). Iceberg Risk to Subsea Cables in Strait of Belle Isle. Report prepared by C-CORE and Fugro GeoSurveys Inc. for Nalcor Energy, C-CORE Report R-10-039-781 V2, June 1, 2011.

Project Team:
Tony King (C-CORE, Project Manager)
Laurie Davis (Fugro GeoSurveys Inc., Interpretation and Reporting Manager)
Andrea Caines (Fugro GeoSurveys Inc., Geomatics Specialist)
Robyn Clements (Fugro GeoSurveys Inc., Geomatics Specialist)
Todd Ralph (Fugro GeoSurveys Inc., Hydrographic Support Manager)
Chris Woodworth-Lynas (Geologist)

REVISION HISTORY

VERSION	NAME	COMPANY	DATE OF CHANGES	COMMENTS
V1 (Draft)	Tony King	C-CORE	January 5, 2011	Draft for Nalcor Review
V1	Tony King	C-CORE	January 17, 2011	C-CORE Review Completed
V2	Tony King	C-CORE	June 1, 2011	Routes Added, Text Modified

DISTRIBUTION LIST

COMPANY	NAME	NUMBER OF COPIES
Nalcor Energy	Bernard Madden	1 (digital)

EXECUTIVE SUMMARY

Nalcor Energy is in the process of conducting a feasibility study on the subsea installation of cables across the Strait of Belle Isle, which will comprise part of the Lower Churchill Transmission Project linking Gull Island, Labrador, and Soldier's Pond, Newfoundland. The Strait of Belle Isle is frequented by icebergs which pose a hazard to any cables either placed on, or trenched into, the seabed. This report describes the application of a model to assess iceberg risk to cables laid on the seabed in the Strait of Belle Isle. Model output was compared with iceberg scour data derived from multibeam surveys.

The iceberg scour dataset described in this report is the first systematic assessment of the scour regime in the Strait of Belle Isle. The scour data was derived from ~ 706 km^2 of multibeam data acquired in 2007 and 2009, covering a water depth range of 1 to 128 m. The data population consists of 1,910 measured scours with 36,093 cross-sectional profiles. Table 1 gives a summary of the scour parameters. The scour orientation is highly directional, with a dominant southwest-northeast orientation. The observed spatial distribution of iceberg scours was unexpected, with the majority of scours occurring in deeper water in areas thought to be sheltered by bathymetric highs (banks) immediately to the northeast of the cable-crossing site (see Figure 1). These features are thought to be predominantly relict features associated with previous glacial events and not indicative of the modern iceberg scour regime. An analysis of the scour data indicated a change, generally in the 70 - 75 m water depth range, characterized by deeper, wider, and longer scours with higher berms, steeper sidewall slopes and increased rise-ups. However, it should be noted that criteria have never been established for characterizing relict scours on the basis of geometry, and there is no basis for definitively stating that all scours in deeper water depths in the area of interest are relict features.

Table 1 Scour parameter summary

Parameter	Mean	Std. Dev.	Maximum
Density (#/km^2, using 2 × 2 km grid)	2.70	3.64	18.5
Scour Depth (m)	0.81	0.50	4.73
Incision Width (m)	39.1	16.8	132.1
Berm-to-Berm Width (m)	52.8	20.3	155.0
Berm Height (m, excluding 9.2% zeros)	0.42	0.32	3.90
Depth of Disturbance – Max. (m)	1.35	0.75	7.77
Sidewall Slope – Max (º)	4.81	2.89	34.9
Length (m)	365.7	439.4	5,505.8
Rise-Up (m)	2.40	2.49	20.8

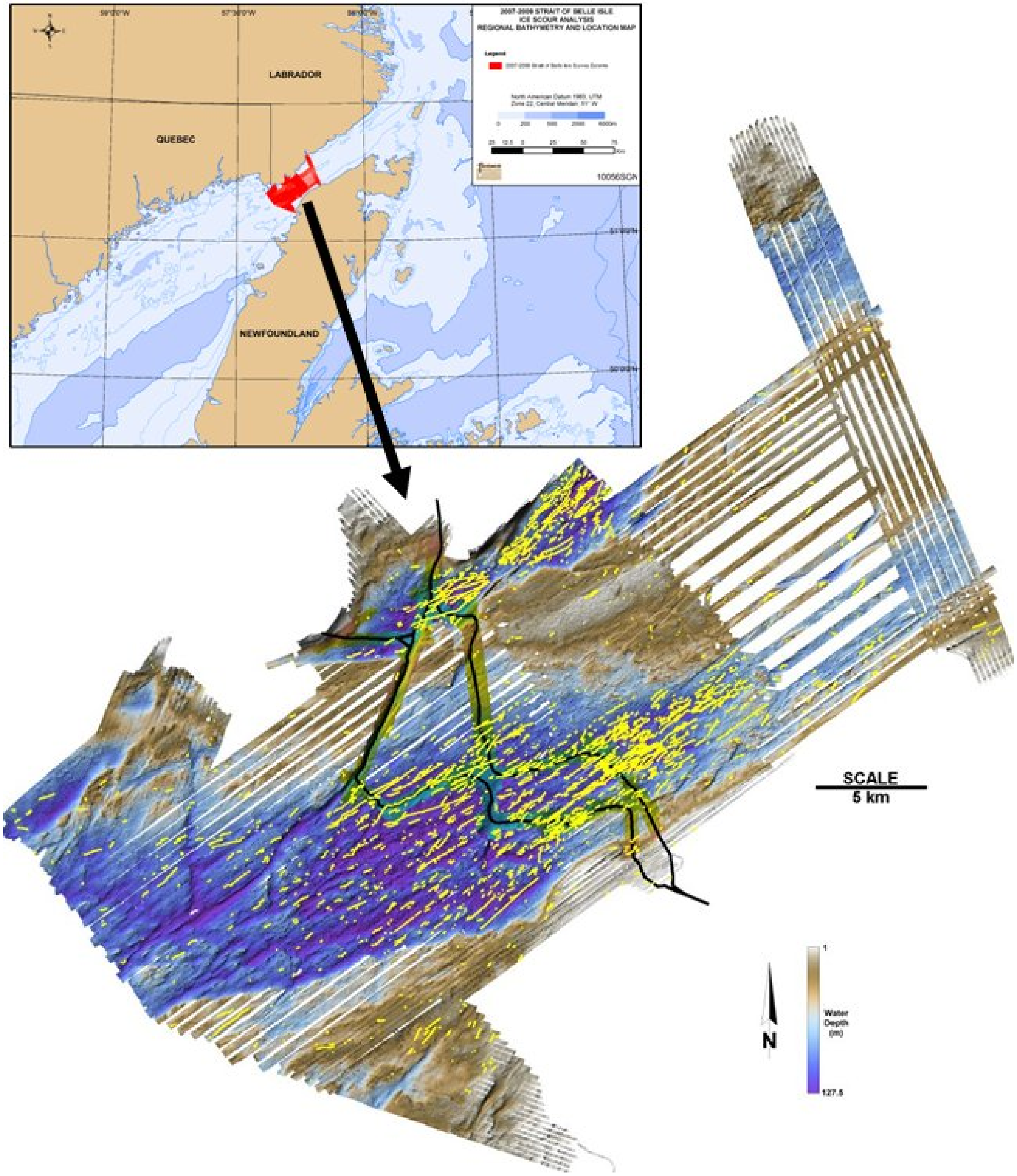

Figure 1 Multibeam survey coverage with proposed cable routes (black) and mapped scours (yellow)

The iceberg risk analysis uses output from a Monte Carlo iceberg contact simulation that models the distribution of iceberg groundings and incidences where iceberg keels are close enough to contact a cable on the seabed (nominally 100 – 120 mm diameter). Simulated icebergs are introduced at a location northeast of the cable crossing site, assigned initial waterline lengths, masses and drafts and then moved into the Strait of

Bell Isle in 1-hour time steps using a simple autoregressive drift model. As the simulation progresses, the mass of the iceberg is reduced to simulate the deterioration (i.e. melting) process and the draft is reduced accordingly. Since icebergs are observed to roll and change drafts, the iceberg draft is occasionally adjusted within the constraints of the mass/draft relationship. During each time increment, the water depth at the iceberg location is checked against the iceberg draft. If the iceberg draft exceeds the water depth, the iceberg is considered grounded and is immobile until its draft decreases sufficiently through melting to refloat. Locations where the draft exceeds the water depth, or the keel is within 1 m of the seabed, are saved. Once the iceberg mass decreases to a defined minimum value (roughly equivalent to a bergy bit) the simulation is terminated. Figure 2 shows the distribution of modeled iceberg rates, which overall agrees with the distribution of iceberg groundings inferred from trajectory data, but shows a trend opposite that suggested by the scour data (which supports the hypothesis that these are primarily relict features).

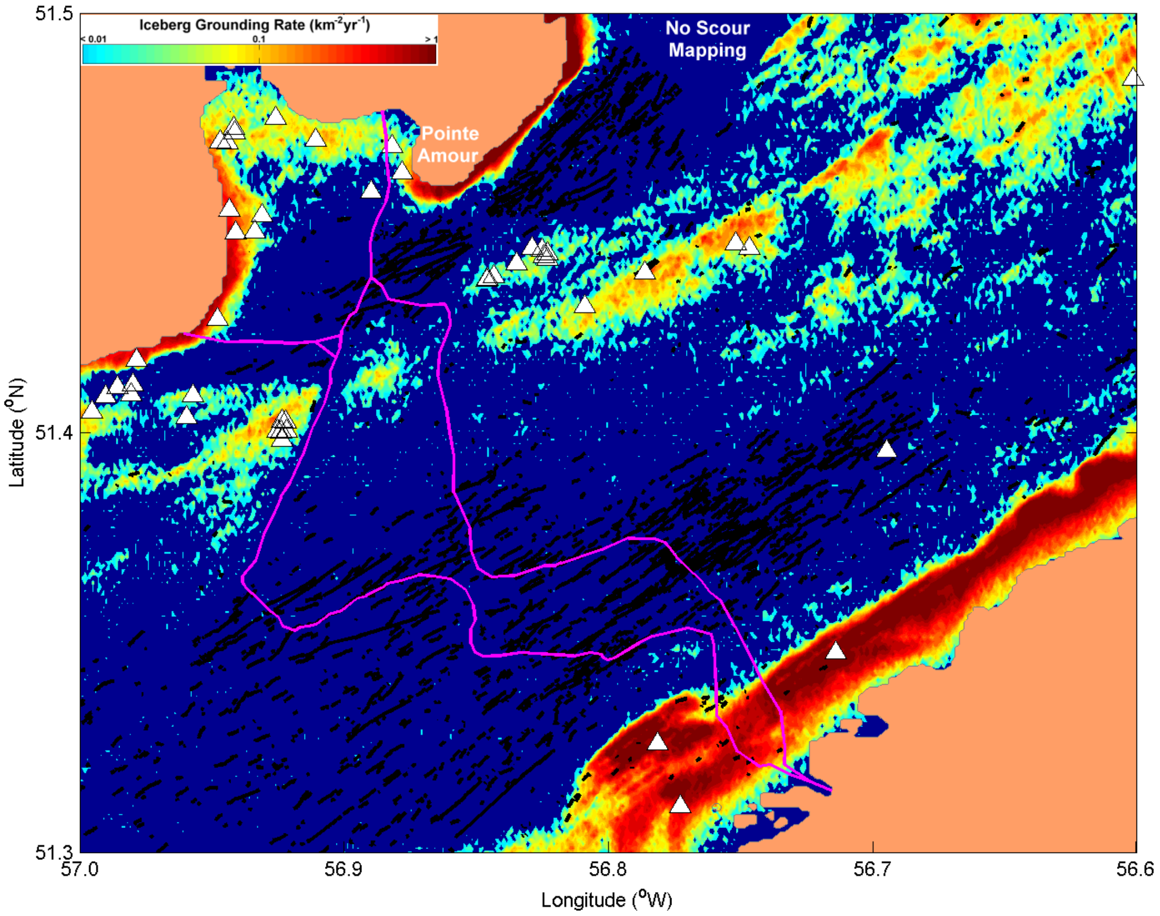

Figure 2 Modeled iceberg grounding rates, cable routes (magenta), mapped scours (black) and iceberg grounding events (Δ) inferred from iceberg trajectory data

The Monte Carlo model used to simulate iceberg movement and grounding at the site indicated that iceberg rolling and associated draft adjustments provide a mechanism for icebergs to drift over bathymetric highs and ground on the seabed in areas otherwise considered sheltered from iceberg keels. Further data, in particular iceberg rolling frequencies and magnitudes of the associated changes in draft, is vital in order to properly characterize this phenomenon. The Monte Carlo model itself is computationally intensive, slow and exhibits significant scatter in the results. These types of problems are not unusual with Monte Carlo models; however, further refinement of the model or the application of additional computing resources may be required in the future.

Multiple subsea cables will be required at the Strait of Belle Isle, and additional analysis was performed to address the issue of "simultaneous" contact with more than one cable. The separation distance between cables was compared to the observed scour length distributions and it was noted that the probability of contacting multiple cables is reduced with increased separation distance.

As an addendum to the analysis described above, a risk analysis was performed for the revised cable routes shown in Figure 3. These cables have a different Newfoundland landfall (near Shoal Cove) and are spaced at 150 m, reduced to 50 m in the narrow channel between the banks on the Labrador side of the Strait of Belle Isle (to avoid high modeled iceberg grounding rates on the bank tops). The iceberg contact rate was calculated for the various scenarios (iceberg rolling frequencies) using the assumption that directional drilling is used to avoid iceberg contact in shallow water. Table 2 gives iceberg contact rates for transition between directional drilling to installation on the seabed at 50 m, 60 m and 70 m water depths.

Table 2 Iceberg contact frequency as a function of directional drilling seabed piercing water depth for various scenarios (mean return period in brackets)

Mean Iceberg Rolling Frequency	Seabed Piercing Water Depth (m)		
	50 m	60 m	70 m
3 days (Base Case)	0.015 yr^{-1} (67 years)	0.007 yr^{-1} (140 years)	0.005 yr^{-1} (200 years)
1 Day	0.016 yr^{-1} (63 years)	0.008 yr^{-1} (125 years)	0.005 yr^{-1} (200 years)
10 Days	0.009 yr^{-1} (110 years)	0.002 yr^{-1} (500 years)	0.001 yr^{-1} (1,000 years)
No rolling	0.006 yr^{-1} (160 years)	0.0001 yr^{-1} (10,000 years)	N.A.

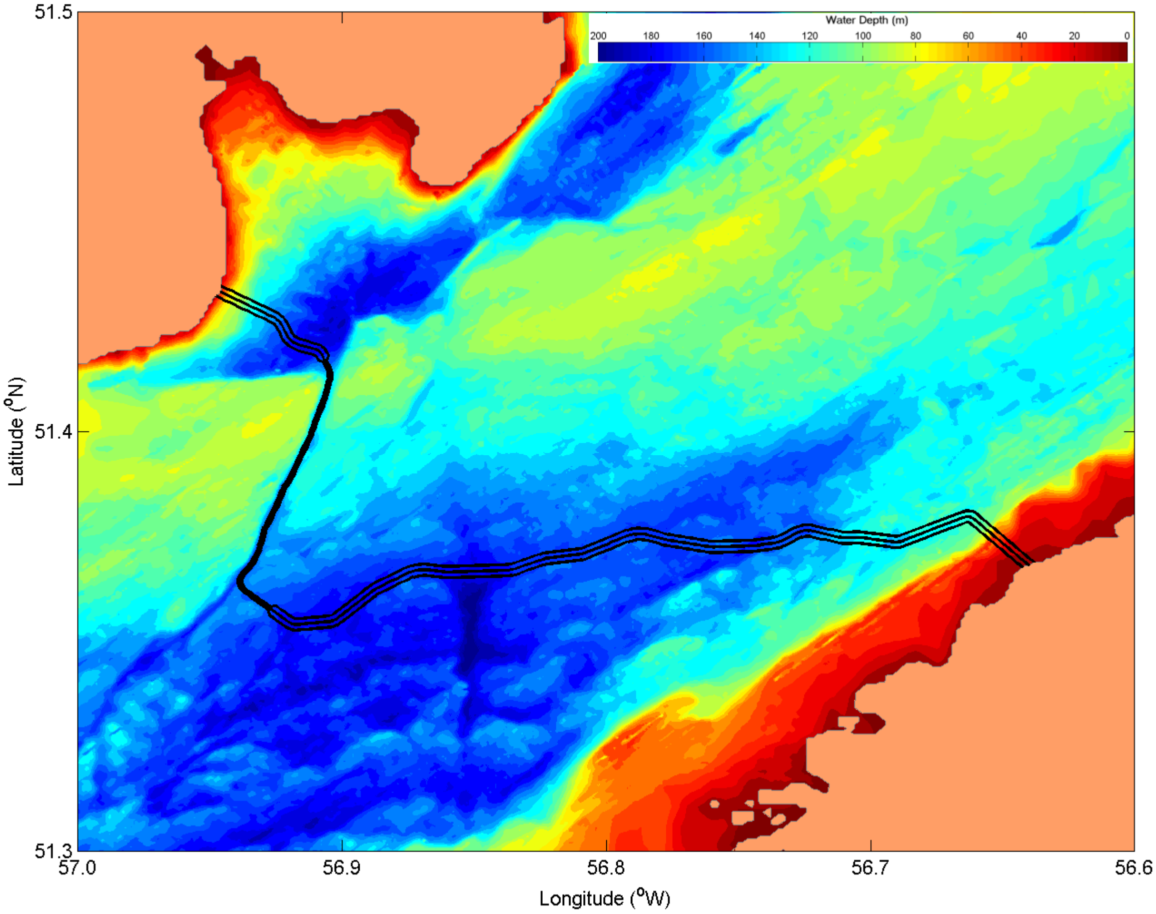

Figure 3 Revised cable routes, with Newfoundland landfall near Shoal Cove

It should be noted that the risk model and analyses described in this report have a number of conservative elements, which is typical when there is some degree of uncertainty in the relevant parameters. These conservative elements include the following:

- an estimation of iceberg frequency based on the entire degree square containing the cable crossing site (whereas iceberg frequency at the cable crossing site is likely lower);
- mean scour lengths in deeper water that are likely based on relict scours, and thus are longer than would be the case for modern scours at this site (and thus overestimate the scouring iceberg encounter rate with the cables);
- the assumption that all iceberg grounding events result in scour formation (when it is considered likely that only a fraction of icebergs have sufficient driving forces to initiate scour formation);
- the relatively high rolling rate (3 days) used in the base case;

- the assumption that iceberg rolling is equally likely to result in a deeper iceberg draft or a shallower draft (when, logically, rolling will tend to be biased towards producing shallower, more stable drafts);
- the rock berm planned for the cables laid on the seabed would likely deflect some free-floating iceberg keels that would otherwise contact the cables; and
- all iceberg contacts result in damage to the cables, whereas in some case the cables may simply be displaced.

Further data collection and analysis are recommended to better characterize conditions at the Strait of Belle Isle and refine the iceberg risk assessment for the cable crossing. These primarily fall into two categories: characterization of icebergs and related parameters, and improved understanding of the iceberg scour record on the seabed. Iceberg data required are:

- iceberg frequency (i.e. satellite imagery analysis) ;
- iceberg drift data (from radar or beacons) for drift statistics/grounding locations;
- site specific iceberg size (length, mass) and deterioration rates; and
- iceberg rolling rates and associated draft changes.

The collection of current data and the development of a current model for the site would provide a basis for understanding and modeling iceberg drift patterns at the site.

Various avenues for improved understanding of the iceberg scour process are as follows:

- differentiation of recent and relict ice scour populations;
- characterization of recent ice scour distributions and metrics;
- improved understanding of bathymetric controls on ice grounding potential;
- improved understanding of ice keel-soil interaction and substrate limitations on keel penetration (relative to cable protection requirements); and
- estimation of recent ice grounding frequency.

TABLE OF CONTENTS

LIST OF TABLES

LIST OF FIGURES

1 INTRODUCTION

1.1 Background

Nalcor Energy is in the process of conducting a feasibility study on the subsea installation of cables across the Strait of Belle Isle which will comprise part of the Lower Churchill Transmission Project linking Gull Island, Labrador, and Soldier's Pond, Newfoundland (see Figure 1-1). Potential landing sites and routes for the Strait of Bell Isle cable crossing are shown in Figure 1-2.

The Strait of Belle Isle, which has a width of approximately 18 km at its narrowest point, is frequented by icebergs which pose a hazard to any cables either placed on, or trenched into, the seabed. This report considers iceberg risk to cables laid on the seabed. A cable laid on the seabed is at risk from scouring and free-floating icebergs. A scouring iceberg contacts the seabed and is pushed along by environmental forces (i.e. currents, wind, waves and pack ice) while a free-floating iceberg does not contact the seabed (but may be in very close proximity). The dominant factors influencing risk from scouring icebergs are the iceberg scour formation rate and the mean scour length, while for free-floating icebergs the dominant factors are the iceberg frequency, draft distribution and mean drift speed. This report describes the application of a Monte Carlo iceberg contact model (C-CORE, 2004a; C-CORE, 2010) to assess iceberg risk to subsea cables laid on the seabed in the Strait of Belle Isle. Output from the model was compared with iceberg scour data derived from multibeam surveys of the Strait of Belle Isle cable crossing site.

1.2 Objectives

The objectives of this project were to:

- develop an iceberg contact simulation for the Strait of Belle Isle to model iceberg scour rates on the seabed and free-floating contact frequencies with cables and structures extending above the seabed;
- analyze multibeam data from the Strait of Belle Isle to extract iceberg scour metrics for model evaluation and risk analysis; and
- assess iceberg risk to cables laid on the seabed for routes and configurations specified by the client.

Figure 1-1 Transmission link between Gull Island, Labrador and Soldier's Pond, Newfoundland (from Nalcor, 2009)

Figure 1-2 Potential landing sites and corridors for Strait of Belle Isle cable crossings (from Nalcor, 2009)

2 ICEBERG SCOUR SURVEY

2.1 Introduction

2.1.1 Background

This section presents the results of an iceberg scour mapping and measurement study conducted by Fugro GeoSurveys Inc. in the Strait of Belle Isle, between Labrador and insular Newfoundland (Figure 2-1). Fugro Jacques GeoSurveys Inc. (FJGI) became Fugro GeoSurveys Inc. (FGI) in 2010, thus references change accordingly. Ice scour mapping was based on extensive multibeam bathymetry data coverage that was acquired by FGI on behalf of Nalcor in 2007 and 2009, for the purpose of subsea HvDC cable installation planning (FJGI, 2007, 2008, 2010a,b; Enclosure 1). The material presented in Sections 2.1 and 2.2 were extracted from the report "Strait of Belle Isle Ice Scour Analysis, 2007 & 2009 Survey Data" (FGI, 2010). Section 2.3 presents an analysis of ice scour data. Ice scour databases are included on the accompanying DVD, as well as geo-referenced seabed imagery (.tif) and visualization files (IVS Fledermaus® format). The required software (iView4D) is available at http://www.ivs3d.com/products/iview4d.

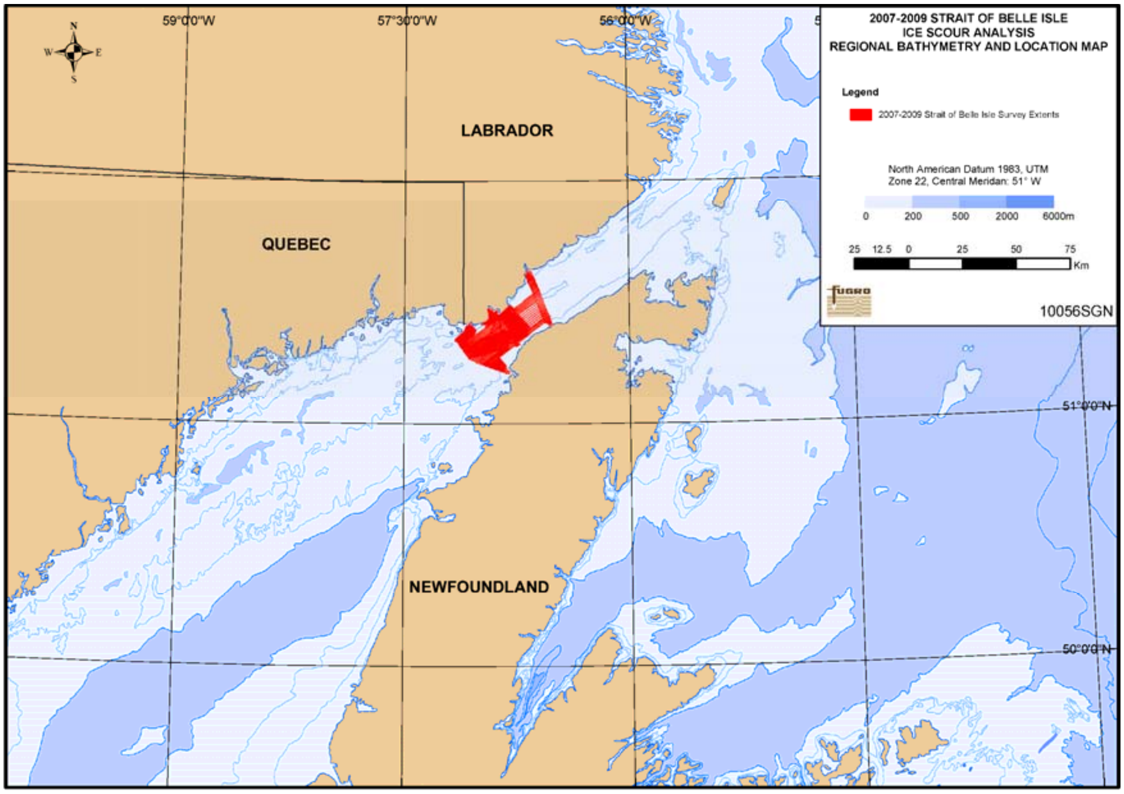

Figure 2-1 Regional bathymetry and location map, 2007-2009 Strait of Belle Surveys (FGI, 2010)

2.1.2 Datasets

The present Strait of Belle Isle ice scour mapping study was based on multibeam bathymetry datasets acquired by FGI on behalf of Nalcor in 2007 and 2009, as part of geophysical survey programs designed to assist with HvDC cable installation planning. The surveys are summarized below, with emphasis on acquisition and processing of multibeam echosounder bathymetry data.

In 2007, a geophysical survey program was conducted on behalf of Nalcor Energy (then Newfoundland and Labrador Hydro) by FJGI in the Strait of Belle Isle from August-October (FJGI, 2008). The survey plans were guided by a preceding desk study compilation of existing data on the area's natural and socioeconomic environments, as well as a reconnaissance multibeam bathymetry survey that provided regional seafloor topographic information (FJGI, 2008). The original, regional study area was approximately 40 km by 50 km in size (Figure 2-2), and extended from approximately L'Anse au Clair to the Pinware River on the Labrador coast, and from St. Barbe Bay (between Anchor Point and Black Duck Cove) to Green Island Brook on the Newfoundland side of the Strait. A reconnaissance multibeam echosounder survey was carried out in this region to assess seafloor topography and assist in the identification of potential submarine cable corridors for the later dedicated geophysical corridor survey. The regional multibeam survey data were acquired by the MV Marine Eagle using a Reson SeaBat 8101 system operating at a frequency of 240 kHz. The analysis of the 2007 reconnaissance survey identified two potential submarine cable corridors across the Strait, each approximately 500 m in width.

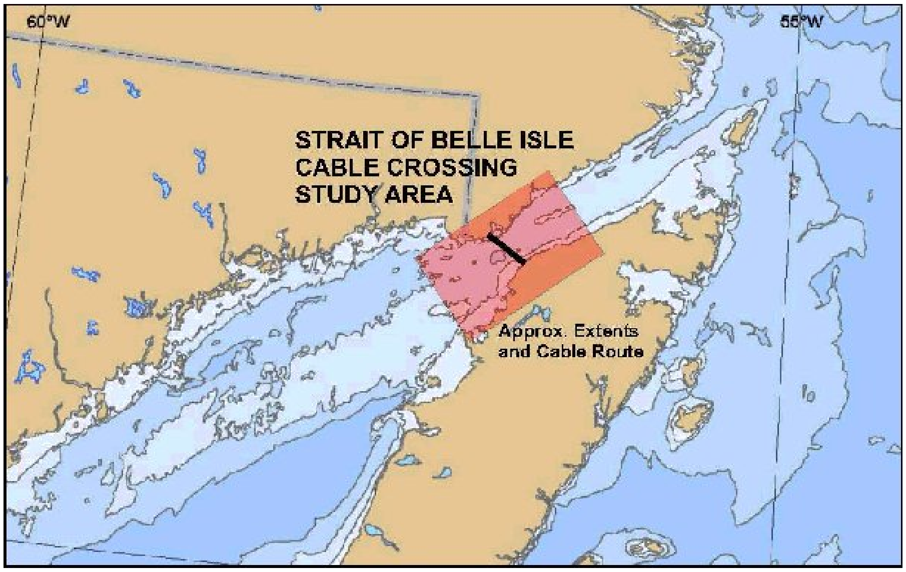

Figure 2-2 Approximate study area of the 2007 geophysical survey program (FGI, 2010)

The subsequent 2007 geophysical route survey program involved the collection of detailed sidescan sonar imagery, high resolution multibeam echosounder data and sub-bottom profile data within the two submarine cable corridors, with a total surveyed area of approximately 28 km^2. The purpose of this survey was to characterize the bathymetric and seafloor conditions along the two potential corridors. A total of 890 km of geophysical survey lines were shot, comprising:

- 772 km of deep water offshore survey (including near Forteau Point);
- 92 km of nearshore survey at Mistaken Cove / Yankee Point; and
- 26 km of nearshore survey at L'Anse Amour.

The deep water geophysical data collected as part of the corridor surveys included:

- side scan data, acquired by an Edgetech DF-1000 digital side scan sonar operating at both 100 kHz and 380 kHz at 150 m slant range on both channels;
- multibeam bathymetry, acquired by a Reson SeaBat 8111 system operating at a frequency of 100 kHz; and
- sub-bottom profiler data acquired by a Huntec boomer Deep Tow System (DTS) operating at 240/135 Joules with a frequency range between 0.5 – 6 kHz (centre frequency 2.5 kHz) and 0.5 second firing rate.

The nearshore geophysical data collected included the following:

- side scan data, acquired by a Klein 3000 digital side scan sonar operating at both 100 kHz and 500 kHz at 150 m slant range on both channels;
- multibeam bathymetry, acquired by a Reson SeaBat 8125 system operating at a frequency of 455 kHz; and
- sub-bottom profiler data acquired by a surface-towed IKB Seistec system operating at 200 Joules with a frequency range between 0.5 – 6 kHz and 0.5 second firing rate.

Subsequent to the geophysical route survey, additional seabed groundtruth data (sediment samples and video) were collected and used to refine seabed interpretations for substrate habitat assessment (FJGI, 2010a; Amec, 2009).

In July of 2009, geophysical surveys were conducted in the Strait of Belle Isle on behalf of Nalcor to assist with engineering planning and feasibility assessment of a sub-surface tunnel option for HvDC cable installation (FJGI, 2010b). Three types of geophysical information were acquired during the 2009 marine surveys, including: multibeam echosounder bathymetry data, used for creating high resolution seafloor bathymetry maps; sub-bottom profiler data, used to interpret the thickness of unconsolidated seafloor sediments above bedrock, and; 2-Dimensional High Resolution (2DHR) data, used to interpret bedrock depth and structure. Surveying was divided into nearshore and offshore components. A nearshore survey conducted from a small, shallow-drafted vessel, the MV 'Cansea' was necessary in order to collect data in the nearshore regions of Point Amour / Fox Cove and Forteau Point where the water was too shallow and navigation too hazardous for a larger vessel. Offshore survey data were collected from a larger, ocean-going survey vessel, the M/V 'Anticosti'.

Multibeam echosounder data were collected during the offshore and nearshore surveys, using different systems best suited to the surveying conditions in deep and shallow water, respectively. 2DHR seismic data were acquired during the offshore survey only. Nearshore and offshore surveys were designed with appropriate overlap so that multibeam and sub-bottom data could be linked and interpreted as a single dataset. The 2009 survey data used for the present ice scour study was limited to multibeam bathymetry, and are detailed below.

Nearshore Survey

Multibeam data were collected with a Reson 8125 system deployed from a pivot arm on the port side of the nearshore survey vessel, M/V 'Cansea'. The 8125 system operates at a frequency of 455 KHz, receiving 240 depth soundings per cycle. The update rate of the multibeam system varied with water depth but ranged from 4 Hz in water depths of 50 m to 2 Hz in water depths of 110 m. The Reson 8125 is rated to measure water depths up to 120 m with a range resolution of 6 mm, and to obtain a swath width of 3.5 times the water depth. Experience with the system shows that acceptable swath coverage is typically three to four times the water depth. Update rate is a function of water depth and speed of sound in water, peaking at a rate of 40 times per second. Beam aperture is 1° in the along ship direction and 0.5° in the athwart ship direction, and spaced at equiangular intervals of 0.5°, yielding total sector coverage of 120°. Sound velocity profiles were obtained using an AML SVplus velocimeter. Soundings were obtained while the vessel was stationary.

Offshore Survey

Multibeam data were collected with a Reson 8101 system deployed through a dedicated moonpool onboard the M/V 'Anticosti'. The Reson 8101 system operates at a frequency of 240 KHz, receiving 101 soundings per cycle. It measures depths up to approximately 300 m with a range resolution of up to 1.25 cm (depending on water depth and system settings), and obtains a maximum swath width of 7.4 times the water depth. Update rate is a function of water depth and speed of sound in water, peaking at a rate of 40 times per second. Beam aperture is 1.5° in both alongship and athwartship directions and spaced at equiangular intervals of 1.5°, yielding a total sector coverage of 150°. Regular Sound Velocity profiles were obtained every six to eight hours during data collection to calibrate the multibeam data using a combination of a Seabird SBE19plus CTD instrument and Sippican XBT T6 probes.

Data Processing

Nearshore and offshore multibeam bathymetry data were processed with the CARIS/HIPS software suite. This software allows for interactive QC of all associated sensors. Bathymetric data were reduced to local chart datum (LLWLT) by use of predicted tides obtained from the Canadian Hydrographic Service. Predicted tides are accurate to between 20 cm and 30 cm, largely dependent on existing atmospheric conditions.

As a method to substantiate the absolute accuracy and repeatability achieved by the multibeam survey, random spot checks were conducted against the data collected in the Strait of Belle Isle for Nalcor in 2007 and also against the nearshore data collected onboard the Cansea in 2009; it was found that on average the datasets agreed to within 0.4% of the measured water depth. A total of 1190 line km of multibeam data were collected.

2.1.3 Regional Setting

The Strait of Belle Isle is an open marine passage between Labrador and insular Newfoundland, with water depths exceeding 100 m in places (Enclosure 1). The seabed topography is strongly influenced by sedimentary bedrock structure, sculpted by Quaternary glaciations. Seabed sediments, where present, consist mainly of coarse granular glacial deposits, reworked by marine processes. The region has experienced relative sea level changes related to glaciation, eustatic variations and isotatic rebound, with over 150 m of coastal emergence occurring since the last ice glacial retreat (Grant, 1992). The setting and physiography of the Strait are summarized below, as context for the present study of ice scour features and distributions.

Bedrock in the region consists predominantly of the Lower Paleozoic Labrador and Port au Port Group sedimentary rocks. These rocks dip gently to the east and southeast at < 3°, and the erosion of these well layered rocks has resulted in numerous, curved scarp and dip slopes that are best expressed on the top of Bank B and in the deep waters of the Central Trough (Figure 2-3). The hummocky seafloor of parts of nearshore Forteau Bay and the region between 6 km and 9 km offshore from Pinware River may reflect the presence of basement rocks of Precambrian gneisses covered by a thin mantle of glacial and post-glacial sediments.

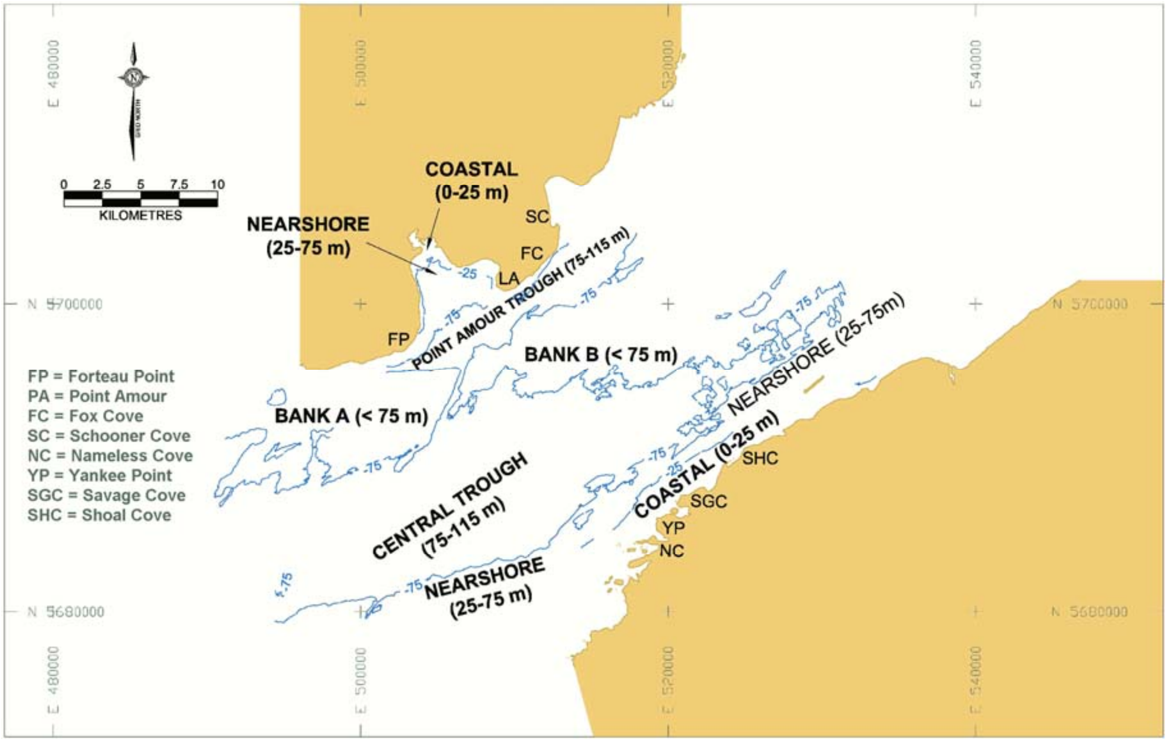

Figure 2-3 Regional seafloor physiography of the Strait of Belle Isle (FGI, 2010)

On the Labrador side of the Strait, the seafloor deepens rapidly from the coastline across a narrow Coastal zone (0 - 25 m water depth) that is mostly less than 500 m wide. Depths increase in a Nearshore zone that extends from the 25 m to the 75 m isobath. This zone is less than 500 m wide offshore from Point Amour and Fox Cove, the 75 m isobath being no more than 900 m from the shoreline. The Nearshore zone widens in Forteau Bay to 4.5 km, and to 7 km on the shallow Bank A.

Beyond the Labrador Nearshore zone the seafloor deepens into a broad hour glass-shaped depression, informally referred to as the Point Amour Trough. The Trough is oriented northeast-southwest and reaches maximum water depths of 115 m. The Trough reaches a maximum width of between 2 km and 3 km, narrowing to a saddle 1 km wide and shoaling to 80 m water depth off Point Amour, the shallowest region in the Trough.

Seaward of Point Amour Trough, the seabed shoals onto a broad plateau, referred to as Bank B, where water depths decrease to less than 75 m. Bank B is separated from Bank A by a distinct north-northeast – south-southwest oriented channel that is 250 – 300 m wide (Figure 2-4). The channel floor has a minimum water depth of 84 m at its junction with the Point Amour Trough at the north end, deepening to a maximum of 106 m where it enters the Central Trough. This channel forms part of the proposed route for seafloor HvDC cables and is described in detail in FJGI (2008). Local relief on both Banks is between 5 and 10 m.

Beyond the two Banks, the seafloor deepens to between 75 and 115 m in the Central Trough, a wide, east-northeast to west-southwest - trending depression. The Trough trends obliquely across the centre of the Strait towards the coast on the Island of Newfoundland. The Trough narrows progressively towards the northeast from a maximum width of 9 km, between L'Anse au Clair and Winter Cove, to 5 km offshore Yankee Point and disappears as a recognizable feature north of Green Island Cove. Channels B and C converge in the central part of the trough in a water depth of 115 m. The northern margin of the Central Trough slopes gradually upwards towards Bank A and Bank B. The southern margin of the Trough is marked by a pronounced, regional, steep north-northwest – facing slope. The base of the slope shallows progressively from 100 m in the southwest to 65 m in the northeast. Similarly, the slope crest shallows from 70 m in the southwest to 20 m in the northeast. Three kilometres seaward of Yankee Point, the slope arcs 1 km towards the shore, and is marked by a small north-facing gully. Local relief in the Central Trough varies from as much as 25 m in the southwest and deepest region to less than 5 m in the northeast.

The Nearshore zone on the Newfoundland side is 10 km wide offshore from St. Barbe, narrowing to between 1 km and 2 km in the region offshore between Yankee Point and Shoal Cove, and widening again to 5 km offshore of Green Island Cove. Local relief in the Nearshore zone is generally less than 5 m but increases to 25 m at a prominent southwest-trending ridge 6 km offshore from St. Barbe. In places, this discontinuous ridge shoals to between 15 and 30 m.

In marked contrast to the Labrador side of the Strait, the extensive, relatively flat-floored, Newfoundland Coastal zone extends from between 1 and 5 km from shore. On a regional scale, the seabed deepens gradually out to the 25 m isobath and, with the exception of minor bedrock scarps, generally less than 2 m high, is relatively flat and featureless.

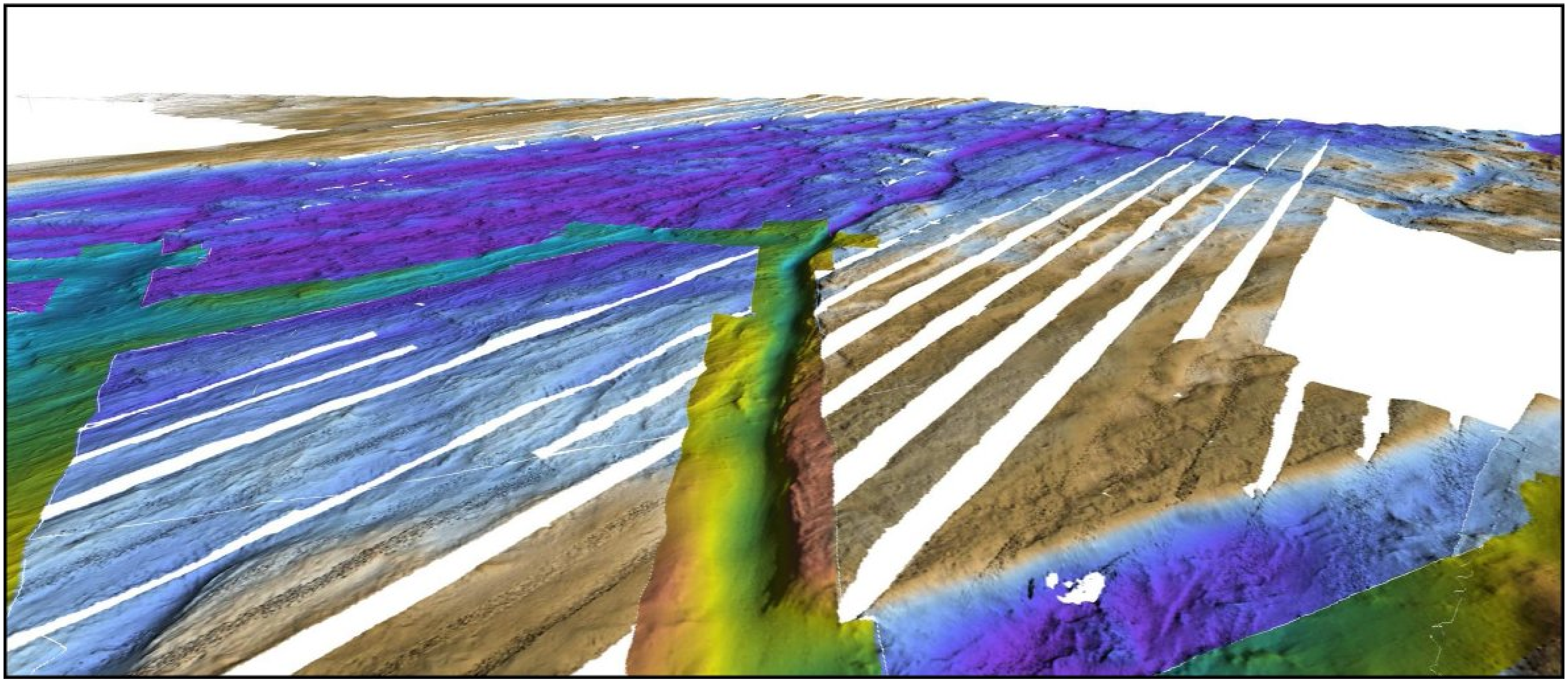

Figure 2-4 3D Perspective View (S) of Seabed Topography, Strait of Belle Isle - note: bedrock channel extending southward through the centre of the image forms part of the potential western HvDC cable route (FGI, 2010)

2.2 Methodology

2.2.1 Ice Scour Analysis Tools

This project utilized proprietary ice scour analysis software tools developed by FGI. The software uses Visual Basic and AutoCAD applications to extract scour measurements from digital seabed terrain data acquired with multibeam sonar (Davis et al., 2005).

The method involves scour mapping (digitization) by the interpreter, followed by automated cross-sectional and planimetric data extraction, and editorial review. A key feature of the software tools is the ability to define a pre-scour 'undisturbed' seabed surface, which is used as a reference datum for measurement of cross-sectional scour dimensions (Section 2.2.4).

2.2.2 Ice Scour Mapping

Ice scour mapping was performed in an AutoCAD workstation environment, using the bathymetry datasets summarized in Section 2.1.2. The data were rendered as a number of georeferenced color coded, shaded relief images, and combined as a bathymetry mosaic (Enclosure 1). Artificial illumination and shading of the seabed surface accentuates scours for improved detection and mapping. Transparencies were applied to areas with data gaps, to allow underlying images to show through. The color palette shows shallow water regions as white to brown and deeper water areas as blue to purple. The 2007 route survey bathymetry data are distinguished by a "rainbow" color palette with shallow water regions shown as red to yellow and deep as green to blue. As noted in Section 2.1.2, the total area of (partially overlapping) seabed coverage from the 2007 and 2009 surveys is 706 km^2, with a water depth range of 1 m to 128 m, Lower Low Water Large Tide (LLWLT).

The bathymetry mosaic was used as a backdrop for iceberg scour mapping (Enclosure 1). Centre-line vectors were digitized by an interpreter as 2D polylines along the axis of each scour. Mapping was limited to features with visible relief in the shaded relief imagery that could be interpreted with confidence as being formed by ice contact events. Scour detection and interpretation was complicated in places by seabed and nearsurface bedrock lineations with similar alignment, and by other seabed features of glacial origin. In some instances, nearsurface bedrock structure appeared to influence the path of ice movement during grounding and scouring, making it difficult to differentiate scours from the underlying seabed texture. Visual cues for scour interpretation included (but were not limited to) the presence of well-defined incisions, constructional berms, apparent cross-cutting and erosion of older scours and glacial moraines, and morphologic indicators of ice keel-seabed interaction (e.g. chatter marks).

Where possible, scours were traced along their full visible length, including through cross-cut areas and across small data gaps. This was done in an effort to capture unique ice grounding events with a single scour vector and ID, rather than as a series of segmented polylines; however, it was not always possible to trace scours across broad data gaps. Differences in bathymetry, data density and continuity across the study area (Section 2.1.2) meant that the scour detection and mapping was more confident and continuous in some places than others, introducing some spatial bias (e.g. scour length).

2.2.3 *Cross-Sectional Profile Generation*

The scour vectors were un-named when digitized. Once digitizing was completed across the study area, the scours were ordered numerically according to x-y position (west to east) and assigned unique identification numbers (e.g. SOBI_0001). Cross-sectional profile lines were created perpendicular to each mapped scour vector (e.g. Figure 2-5) and assigned a separate, sequential ID (e.g. SOBI_0001_0001, SOBI_0001_0002, etc.).

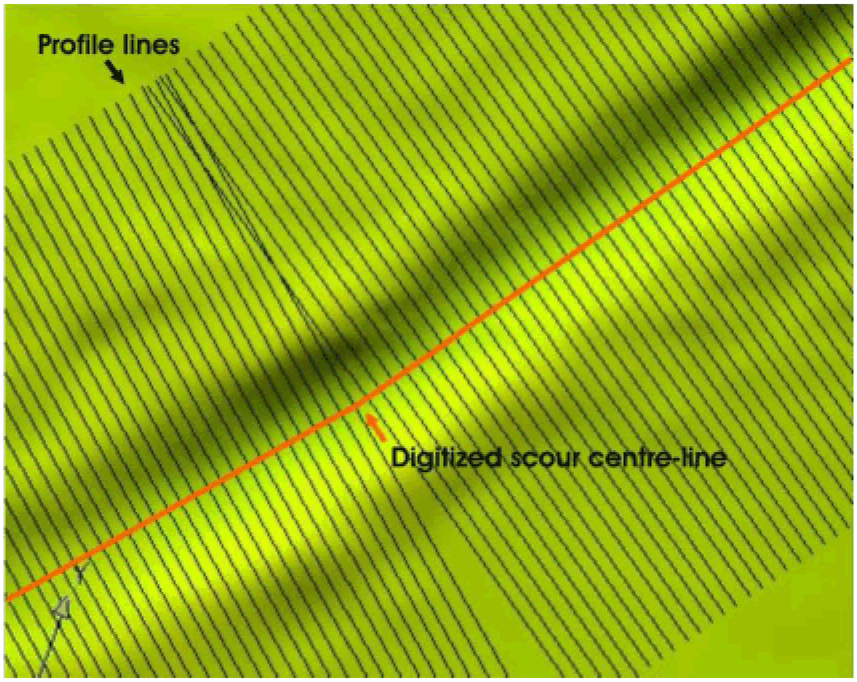

Figure 2-5 Shaded relief image of an ice scour with digitized center-line and cross-sectional profile line overlays (FGI, 2010)

The profile lines were spaced 10 m apart (along each scour axis) and were 250 m in length; sufficient to span the largest scour features. Profiles were generated by sampling the underlying DTM surfaces at 1 m spacing along each 250 m profile line. When sampling the DTMs, the software scanned for the highest resolution bathymetry data at each location, using the best of the available, overlapping datasets. Spatial resolution of the DTM grids ranged from 2 m in the nearshore zones, to 3 m along the high data density route corridors, to 5 m across the regional 2007 survey and 2009 Strait crossing corridor. Scour metrics were derived at each cross-sectional profile location, using the methods described below.

2.2.4 *Seabed Reference Datum*

In order to measure the cross-sectional dimensions of an ice scour, such as depth, width or berm height, a datum representing the pre-scour, undisturbed seabed must be defined. Depths and heights are measured as elevation differences relative to the seabed reference datum, as illustrated in Figure 2-6 (Scour Profile Viewer). The upper panel illustrates a seabed ice scour profile and auto-picked reference datum, using the Derivative Method. The lower panel shows the difference in elevation between the seabed profile and datum (Δz). The shaded relief image in the upper right provides a plan-view of the profile location. The intersections between the bathymetry profile and datum define the zero-crossing points, used to measured incision width.

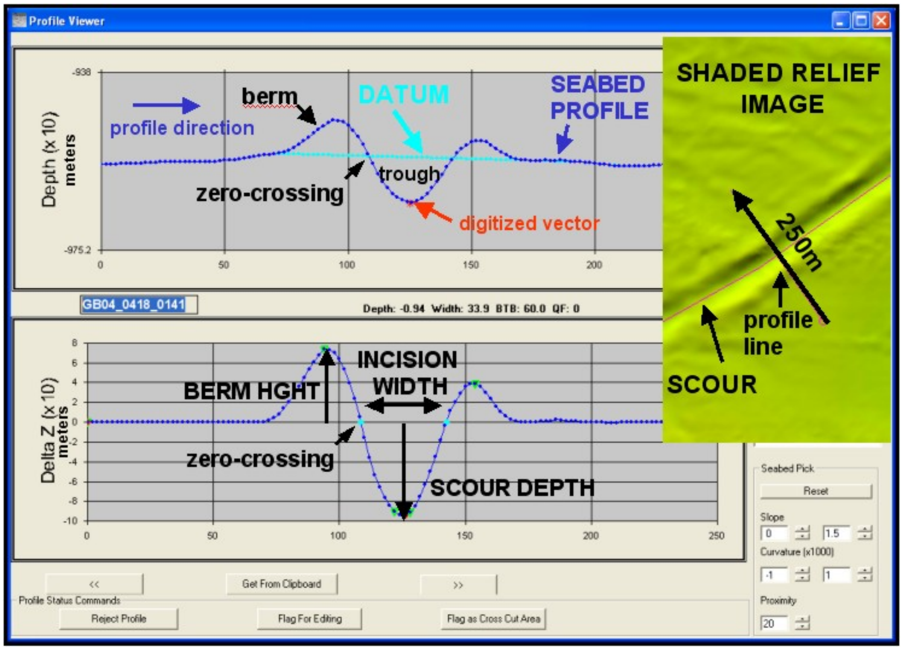

GB04_0418_0141

Depth: -0.94 Width: 33.9 BTB: 60.0 QF: 0

Slope: 0 1.5
Curvature (x1000): -1 1
Proximity: 20

Figure 2-6 Scour profile viewer (FGI, 2010)

The FGI scour analysis tools offer two methods for deriving a reference datum from seabed digital terrain data. The first is based on seabed surface derivatives, and involves filtering out areas of 'disturbed' seabed based on slope and curvature threshold criteria. Seabed DTM points with high slope and curvature (scour berms and incisions) are removed from the surface, and the datum is interpolated between areas of relatively undisturbed, native seabed. The second method uses least-squares polynomial regression to derive a reference datum from seabed DTM data. The polynomial method of datum selection is designed for use in regions of irregular terrain and intensively scoured seabed, where remnants of undisturbed seabed are isolated and limited. It is less sensitive to seabed roughness than the derivative datum-picking method, and therefore returns a higher percentage of profile measurements that pass the Quality Flag filter criteria (as compared to the Derivative Method). Both of the seabed datum selection methods are automated, objective and reproducible.

2.2.5 Seabed Datum Polynomial Method

The polynomial method of datum selection was used for the present study, due to the compexity of seabed topography. The method uses least-squares polynomial regression to derive a 2D cross-sectional datum line fitted to each bathymetry data profile. The polynomial exponent is selected to provide the best approximation of the cross-sectional bathymetry profile trend, with the datum line passing about mid-way between berm tops and base of scouring (see Figure 2-7). A 5th order polynomial function was mainly used for the present analysis. A small subset (22) of large scour was processed with a 3rd order polynomial, which better captured the form of the seabed profile across these features.

It is noted that the mathematically derived polynomial curve sometimes passes either above or below small scours that are superimposed on an irregular or sloping seabed, as the curve conforms to the general bathymetric profile shape. In these cases, the datum line fails to capture the target scour, and does not yield a valid scour profile measurement. However, these occurrences are auto-detected by the Profile Viewer tool, and the polynomial exponent is increased through a series of iterations until the small target scour is intersected by the tightly constrained datum line.

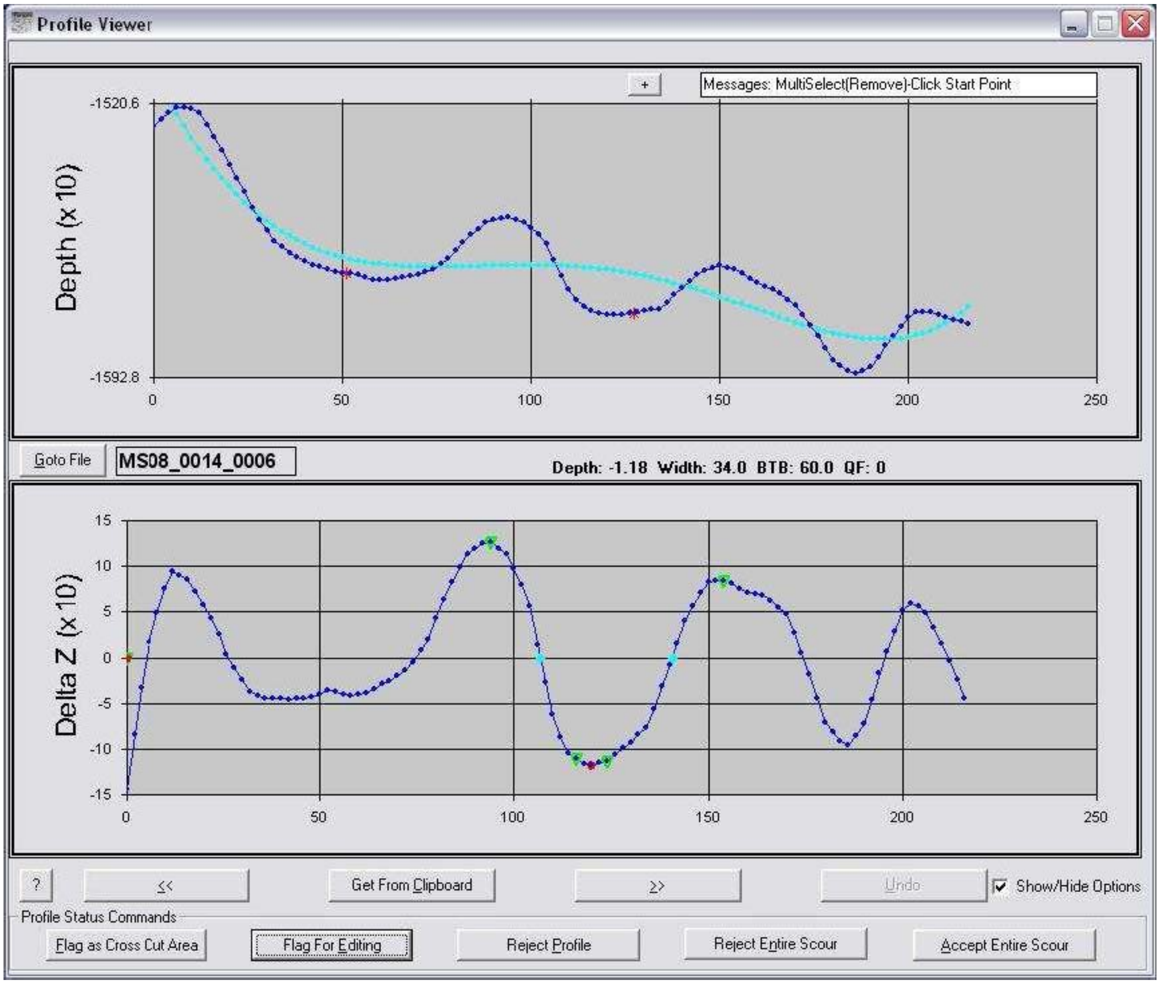

Messages: MultiSelect(Remove)-Click Start Point

MS08_0014_0006

Depth: -1.18 Width: 34.0 BTB: 60.0 QF: 0

Figure 2-7 Profile Viewer showing 5th-order polynomial curve fitted to bathymetry profile data - first step of Polynomial Datum Method (FGI, 2010)

Once the polynomial curve is derived, a vertical shift is applied to raise it to a level approximating the pre-scour, undisturbed seabed surface (Figure 2-8). The appropriate vertical shift is gauged by empirical testing. For the SOBI study area, the datum was scaled to ~68% of the mean vertical distance between berm top(s) and scour base. This vertical scale factor was applied to all polynomial datum lines to better approximate the pre-scour seabed surface elevation. Once the polynomial curve is raised, a straight line is fitted between the resultant profile zero-crossing points, to remove the effect of upward or downward polynomial curvature across the scour incision. The scour depth measurement is then made from the straight datum reference line (Figure 2-9).

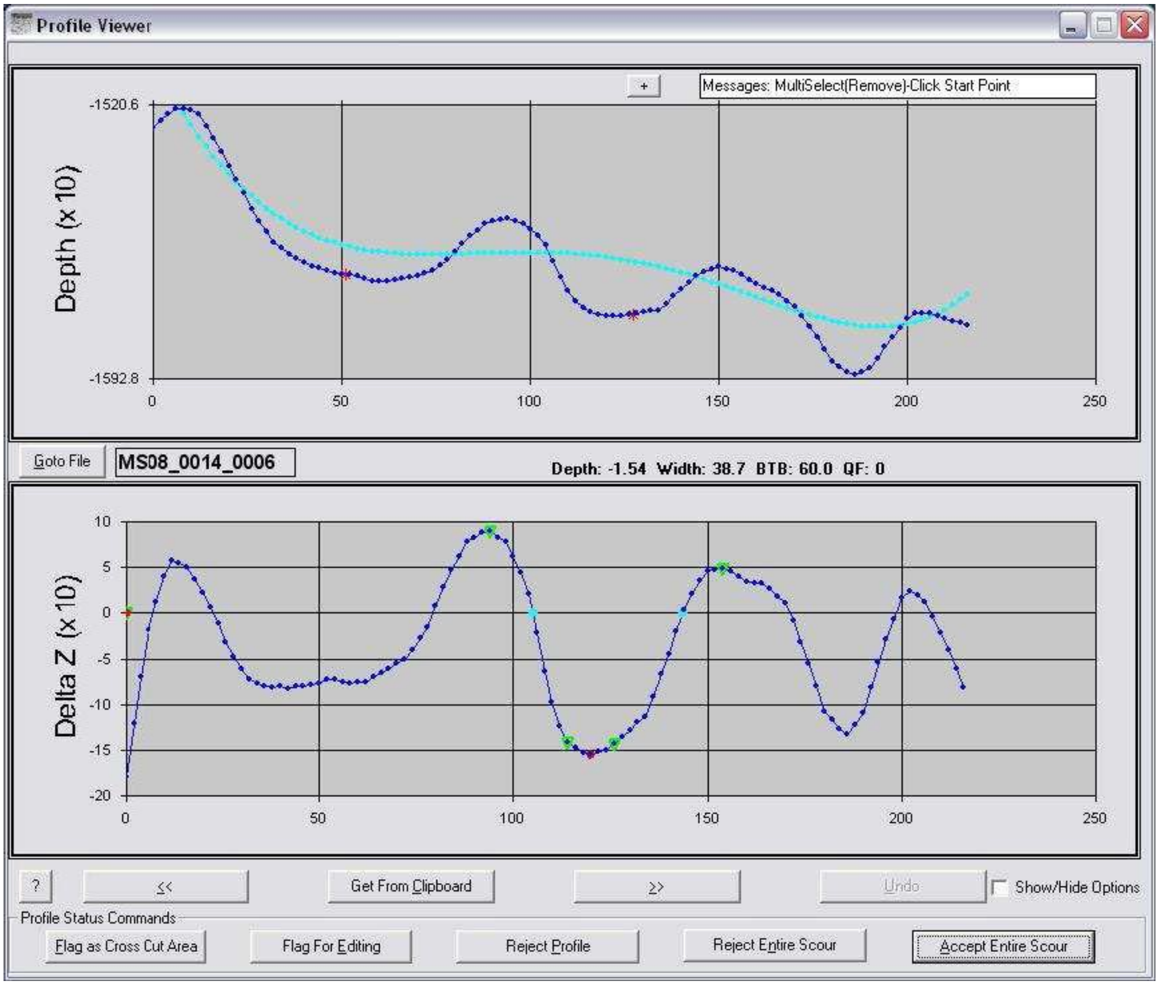

Messages: MultiSelect(Remove)-Click Start Point

MS08_0014_0006

Depth: -1.54 Width: 38.7 BTB: 60.0 QF: 0

Figure 2-8 Profile Viewer showing 5th order polynomial curve fitted to bathymetry profile data, and shifted vertically to 68% of elevation range between berm tops and base of scour - second step of Polynomial Datum Method (FGI, 2010)

While the datum scaling was appropriate to the scour population overall, it was sometimes higher than the surrounding ‘native’ seabed in cases where scours are flat-based with pronounced berms, since the vertical datum shift is a statistical ratio that assumes average berm development. This results in an occasional deep bias in scour depth measurements, of up to 20%.

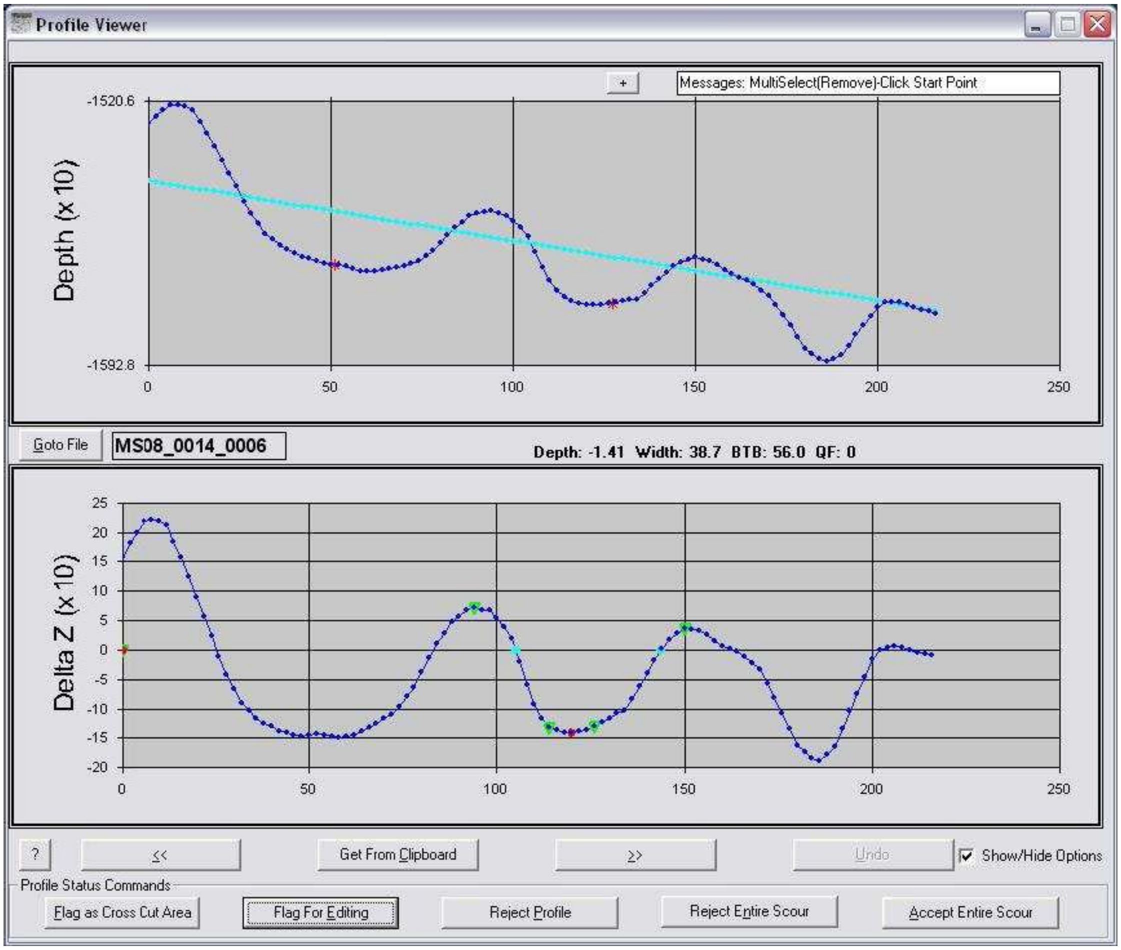

Messages: MultiSelect(Remove)-Click Start Point

MS08_0014_0006

Depth: -1.41 Width: 38.7 BTB: 56.0 QF: 0

☑ Show/Hide Options

Figure 2-9 Profile Viewer showing straight line datum interpolation between zero-crossing points defined by scaled polynomial function - third step of Polynomial Datum Method (FGI, 2010)

2.2.6 Quality Flags

A number of filters are used to ensure that the auto-picked seabed datum used for scour profile measurements is valid, and also to identify any datum picks that may require screening by the interpreter. The filters are used to screen the profile data for a number of conditions, and then set various Quality Flags (QF) depending on the particular conditions identified (Appendix A).

The user can either automatically reject data based on Quality Flags, or manually edit the seabed datum and accept the profiles back into the dataset. Quality Flags were used to screen and target datum picks that required screening, and for final filtering of the scour profile dataset during export (Section 2.2.7).

2.2.7 Cross-Sectional Scour Metrics

Once the seabed reference datum is defined, the Profile Viewer calculates the difference in elevation (Δz) between the datum profile and the actual seabed profile (refer to Figure 2-6). The profile elevation differences (Δz) are used to determine the gouge depth and berm heights; but first the program defines the actual limits of the incision based on the position of the datum zero-crossing (z-c) points. To do this, the program flags the position of the digitized centerline on the cross-sectional profile, and then scans left and right of the centre line to identify the points at which the seabed profile rises up to meet or cross the datum line (i.e. the zero-crossings). The position and spacing of the zero-crossing points determines the incision width, and the maximum depth (Δz) between the zero-crossings is logged as the local gouge depth (Figure 2-6). The maximum gouge depth point on the profile is typically near the mapped centre line but does not always coincide with it; depending on the interpreter's visual perception of the position of the gouge axis and the level of detail used in digitizing.

The presence or absence of berms is indicated by whether or not the Δz values become positive beyond the z-c points. In order to determine the position and height of the berm tops (where present), the program continues to track the Δz value outward from the z-c points until the Δz+ values peak, and then decline. The detected Δz+ peaks are marked as berm tops, and are used as reference points for measuring berm heights and the berm-to-berm width of the gouge. A related metric is the "depth of disturbance", which is effectively the elevation range from berm top to base of scour, measured on both sides of the feature. This metric gives an indication of the maximum seabed relief associated with a scour feature. It is noted that the apparent maximum relief from berm top to scour base may increase as a scour runs along a sloping seabed (see Figure 2-10).

Gouge sidewall slopes are recorded at the zero-crossing points and between the z-c and maximum depth point (see schematic cross-section below; Figure 2-11). Slopes are measured on both sidewalls (left and right of the gouge axes) between the datum zero-crossing points and base of gouge, and reported as minimum, maximum and average values. The sidewall slope is also measured locally at each datum zero-crossing.

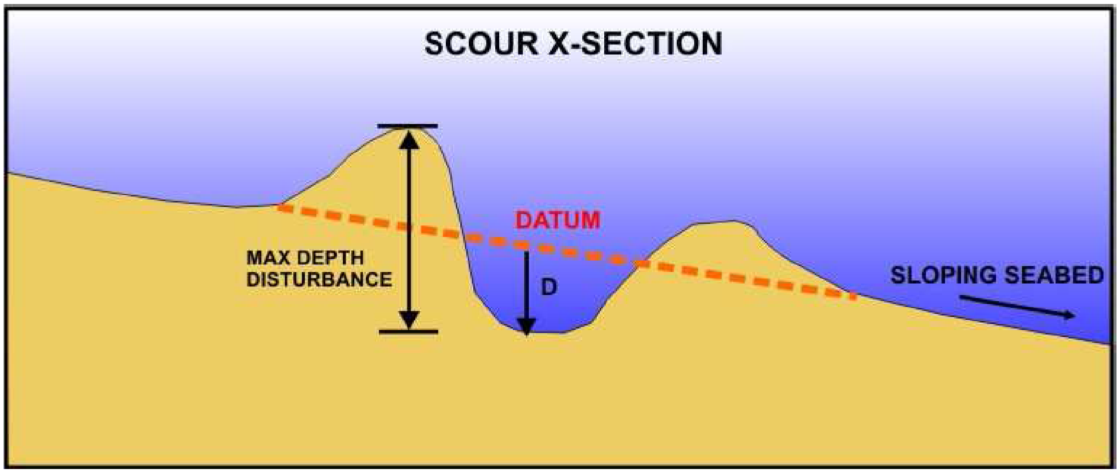

Figure 2-10 Schematic cross-section of ice scour showing depth of disturbance measurement (FGI, 2010)

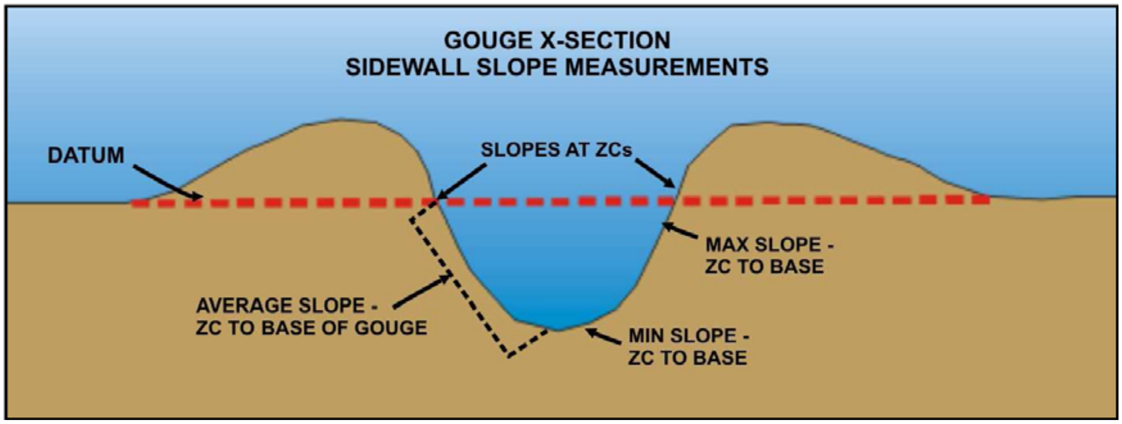

Figure 2-11 Schematic cross-section of ice scour showing sidewall slope measurements (FGI, 2010)

The slope calculator occasionally returns null values (999) in cases where gouges are very narrow and are defined by a limited number of profile data points. These typically represent a small proportion of the total slope dataset. The cross-sectional gouge symmetry can be assessed by comparing the relative slopes of opposing sidewalls, and the relative heights of berms on each side of the gouge profile. For a symmetrical gouge, the sidewall slopes are similar, while asymmetrical gouges show significantly different slopes on opposite sides of the axis.

A cross-sectional shape parameter termed the base-to-incision width ratio is calculated to differentiate gouges that are U-shaped versus more V-shaped in profile. The base width of the gouge is the cross-sectional width measured at an elevation above the base of the gouge that equals 10% of the total incision depth. The shape parameter is then calculated as the ratio between the base width and the incision width. A deep and narrow V-shaped gouge has a low width ratio, while a broad, U-shaped gouge typically has a higher ratio.

2.2.8 Data Review and Export

The scour profile data were reviewed using the Profile Viewer before final export. Quality Flags were used to screen the data for possible datum mis-picks related to complex seabed topography. The accuracy of datum picks was also screened in plan view, by overlaying zero-crossing points on the bathymetry mosaic. The data review was assisted by an AutoCAD interface that auto-zooms to selected profile locations on the seabed imagery, in order to visualize the plan-view morphology of the scours.

In some instances, profile datum selection was not viable where the imaged scours became too shallow, or were affected by data artifacts such as residual motion and/or gaps and seams between overlapping datasets. These mis-picks were apparent in profiles and in the distribution of zero-crossing points on the bathymetry mosaic. Profiles with invalid datum picks were rejected from the dataset, with some smaller, more subtle scours being rejected entirely in terms of metrics output (Enclosure 1).

Once the data were fully screened and edited, a data export module was used to output the scour parameter data generated by the Profile Viewer. Quality Flags were set to reject any residual noise from the final data output. The output filters include rejection of scour with apparent depth less than 5 cm, which is below the effective resolution of the bathymetry data. Output data included the individual profile metrics (Appendix B) as well as scour summary data (Appendix C). The summary data include normal statistics such as the minimum, maximum and mean of the cross-sectional dimensions, as well as scour lengths and orientations. The exported digital data on the enclosed DVD are described in Appendix D.

2.3 Results

2.3.1 *Introduction*

A total of 2,186 interpreted iceberg scour features were mapped within the area of SOBI multibeam data coverage (Enclosure 1, Figure 2-12). The estimated density of scours within the study area is approximately 3 per km^2. Scour density is locally much higher, but the overall average is reduced by the limited number of scours occurring in areas of exposed bedrock on the central plateau and in some nearshore regions (Figure 2-13).

Scour metrics were sampled at a 10 m interval along the axis of each feature. This density of profile sampling was considered appropriate to the volume and complexity of seabed bathymetry data. As discussed in Section 2.2, profile editing was restricted to automated Quality Flag filtering and manual rejection of profiles with apparent datum mis-picks. The final SOBI profile metrics dataset consists of 36,093 observations from 1,910 measured scours. An additional 276 mapped features were rejected from the metrics database due to scour depth and data limitations.

The planform shape of the observed iceberg scours varies from straight, to arcuate to sinuous. Scours occasionally show changes in trajectory that appear to be due to ice keel interaction with complex seabed topography. Cross-sectional shape ranges from singular steep-walled, V shaped incisions, to broad U shaped incisions; and in rare cases display multiple ridges and grooves formed by irregular ice keels. Some scours are flat-based with prominent marginal berms. It is inferred that the shape and depth of these features is at least partly substrate controlled, with shallow bedrock inhibiting ice keel penetration. Seabed soils were displaced laterally to form distinct berm accumulations with limited erosion of the bedrock-floored substrate.

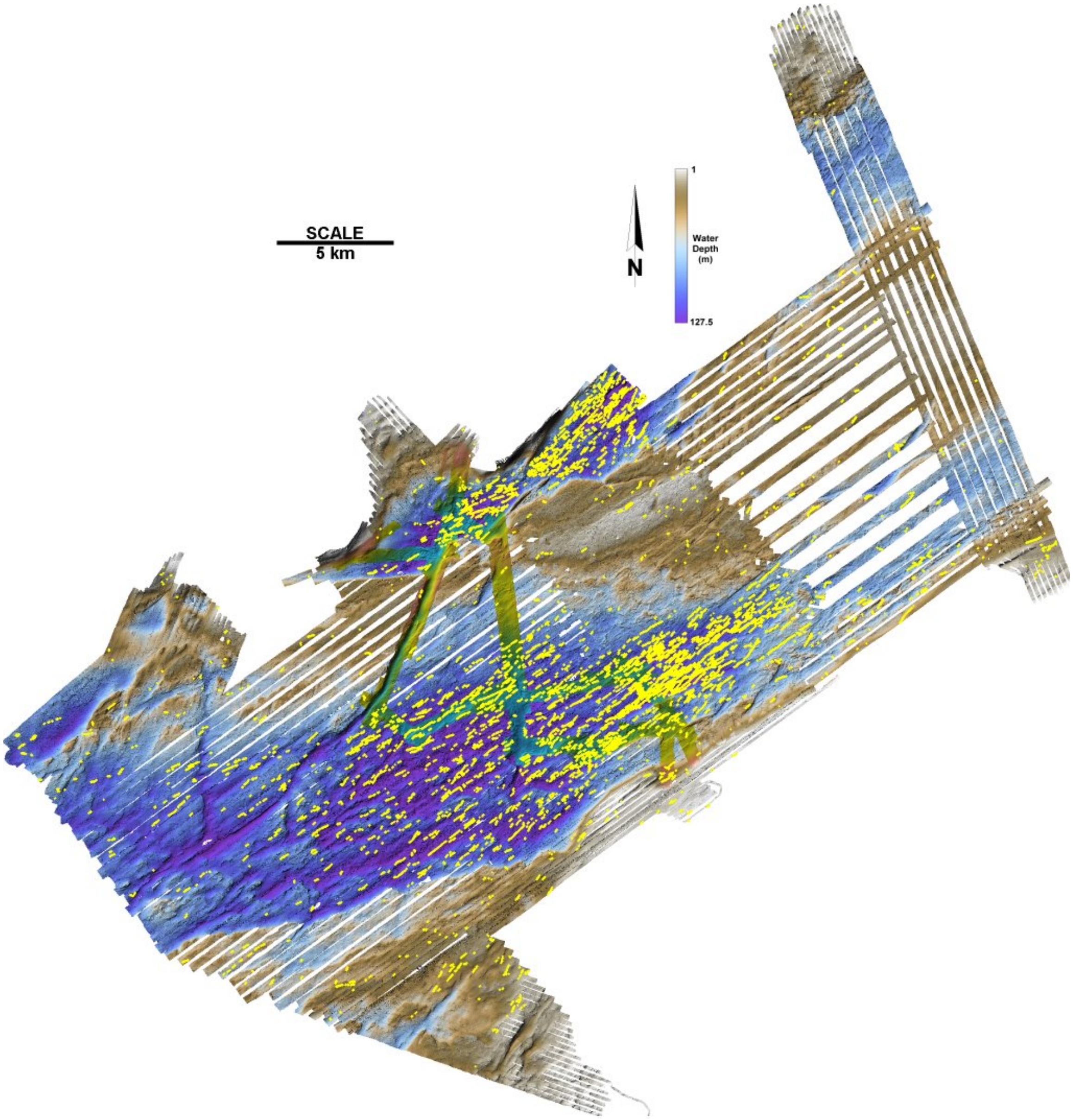

Figure 2-12 Scour profile locations (yellow)

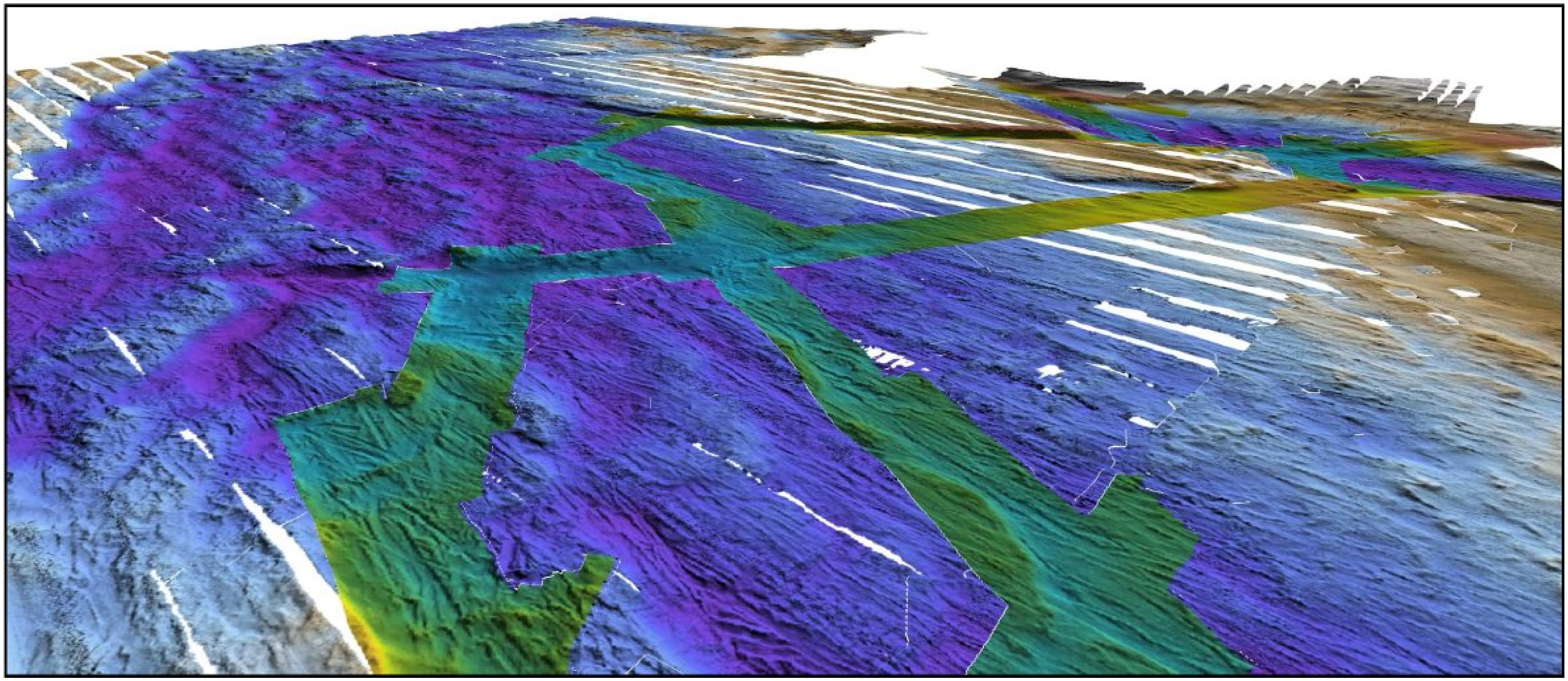

Figure 2-13 Perspective view of Strait of Belle Isle bathymetry, looking to the west - note iceberg scours concentrated in low-lying areas in the image foreground (FGI, 2010)

2.3.2 Scour Density

One of the motivations for extracting iceberg scour data from the multibeam data was to compare observed iceberg scour densities and modeled iceberg grounding locations. Scour densities were calculated by counting the number of iceberg scours located within, or passing through, each 2 km × 2 km cell. Cells with less than 50% multibeam coverage were excluded from the analysis, and scour densities in cells with less than 100% multibeam coverage were adjusted accordingly. The mean water depth was also calculated for each cell. Figure 2-14 shows a scatter plot of scour density and water depth, along with mean values per 10 m water depth bin. The mean overall scour density calculated using this grid size is 2.70 km^{-2}, with a standard deviation of 3.64 km^{-2} and a maximum of 18.50 km^{-2}. The peak average density is 7 km^{-2} in the 105 to 115 m water depth range. The spatial distribution of scour density is shown in Figure 2-15.

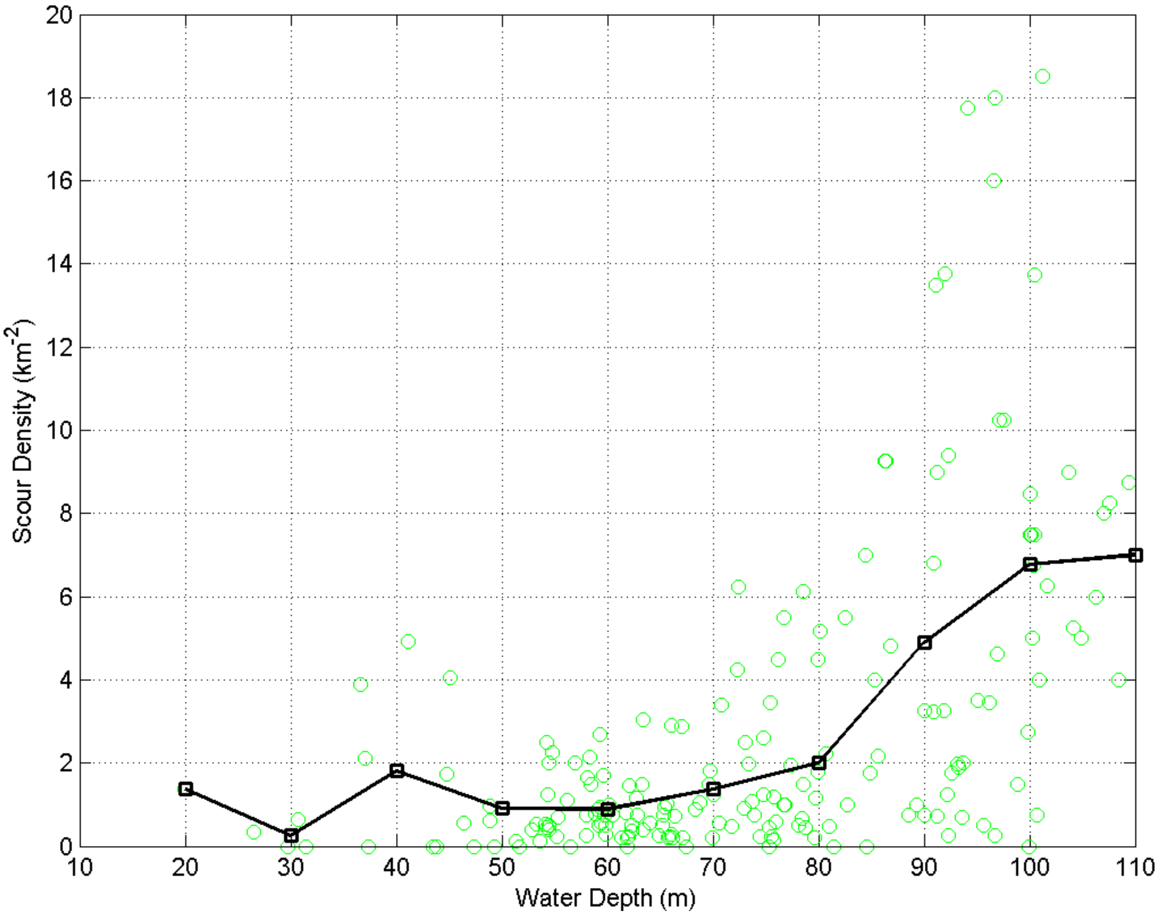

Figure 2-14 Scour density and water depth, and mean density per 10 m water depth bin

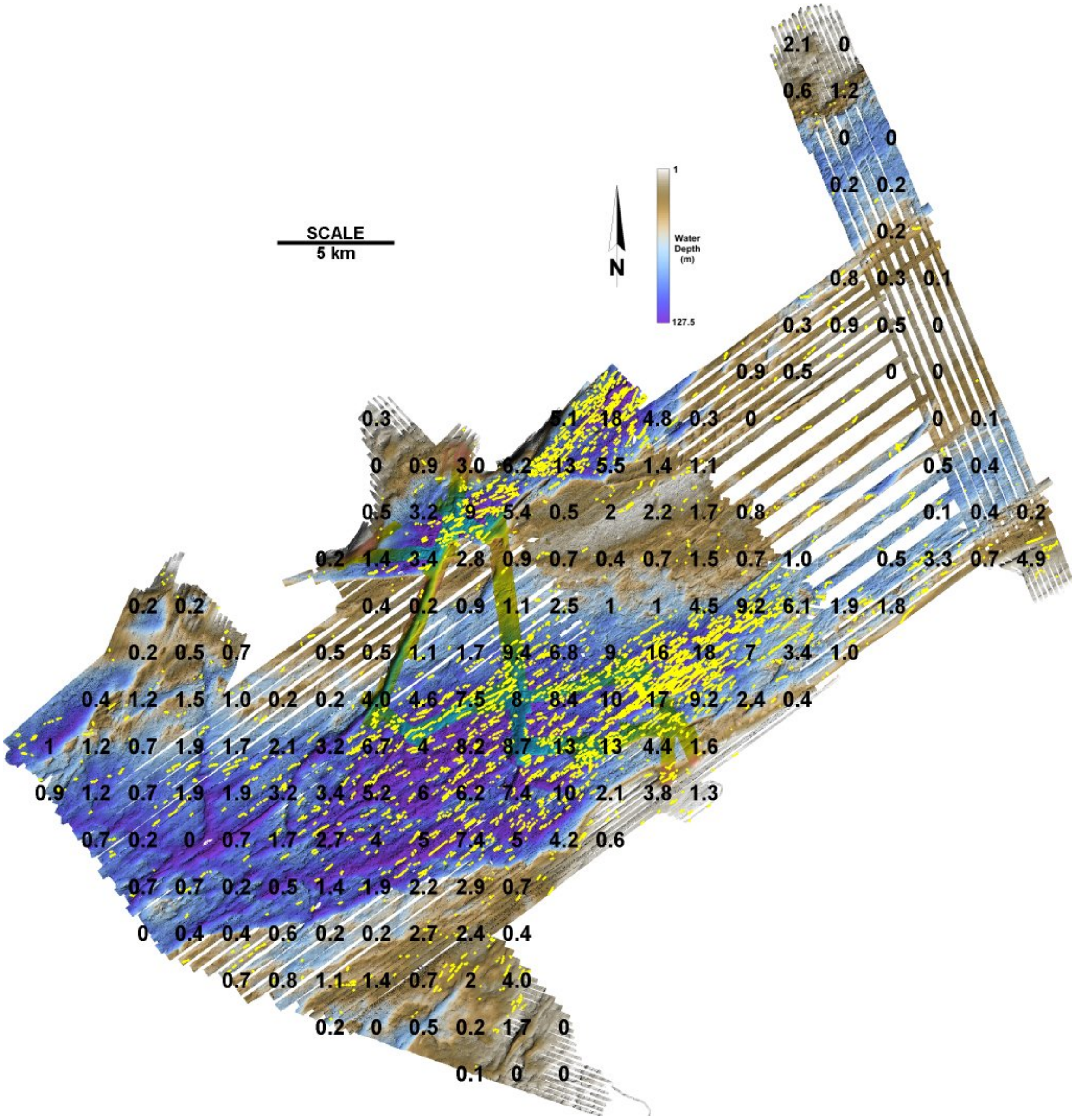

Figure 2-15 Spatial distribution of scour density

2.3.3 Scour Depth

Scour depth is measured with reference to the undisturbed seabed (seabed datum) and is a measure of the depth of the iceberg keel penetration into the seabed during the scouring process. Two phenomena which influence the observed distribution of furrow depths are:

- the presence of relict iceberg scour features; and
- sediment infill.

Relict scour (furrow and pit) features, which are thousands of years old and remnants of previous climate regimes, tend to be deeper and are observed in deeper water depths than modern scour features. Including these features into statistical models of furrow size (depth) tends to lead to an overestimation of risk, as relict scours are generally deeper than modern scours. Conversely, sediment infill makes the depth distribution appear shallower than the actual case, and can lead to an underestimation of the associated risk. Both of these effects are likely to be significant in the Strait of Belle Isle. Most, if not all, of the scours observed in the deeper water portions of the cable routes are thought to be relict, and high current speeds common in the Strait of Belle Isle would likely cause scour infill in shallower water where mobile sediments are present. There is currently no basis for assessing the influence of these effects on the scour depth distribution. Ideally, scour depth parameters should be based on new scours identified through repetitive mapping. Table 2-1 gives scour depth statistics as a function of water depth. Figure 2-16 shows a scatter plot of scour depth and water depth, as well as the mean and standard deviation of scour depth in 10 m water depth bins. A significant increase can be seen in both the mean and standard deviation of scour depth at 70 m water depth.

Iceberg scour depths on the Grand Banks and Labrador Shelf typically follow a lognormal distribution (King et al., 2009; King and Sonnichsen, 2010). The scour depth distribution for the Strait of Belle Isle was best characterized by a lognormal distribution in water depths less than 85 m (Figure 2-17), but in water depths greater than 85 follows a gamma distribution (Figure 2-18). This difference may be due to seabed conditions (i.e. sediment type of thickness), or may be indicative of the transition depth between the modern and relict scour populations. The spatial distribution of scour depth is shown in Figure 2-19.

Table 2-1 Scour depth as a function of water depth

Water Depth (m)	No. Profiles	Mean (m)	St. Dev. (m)	Max. (m)
> 5 & ≤ 15	19	0.18	0.08	0.36
> 15 & ≤ 25	59	0.26	0.18	0.92
> 25 & ≤ 35	114	0.22	0.11	0.67
> 35 & ≤ 45	226	0.33	0.16	0.91
> 45 & ≤ 55	1,104	0.39	0.27	1.69
> 55 & ≤ 65	1,346	0.41	0.33	2.79
> 65 & ≤ 75	1,361	0.67	0.60	4.73
> 75 & ≤ 85	3,056	0.76	0.49	4.20
> 85 & ≤ 95	8,409	0.79	0.47	3.46
> 95 & ≤ 105	16,013	0.88	0.48	4.47
> 105 & ≤ 115	4,362	0.94	0.54	4.08
> 115 & ≤ 125	24	0.90	0.53	2.38
All	36,093	0.81	0.50	4.73

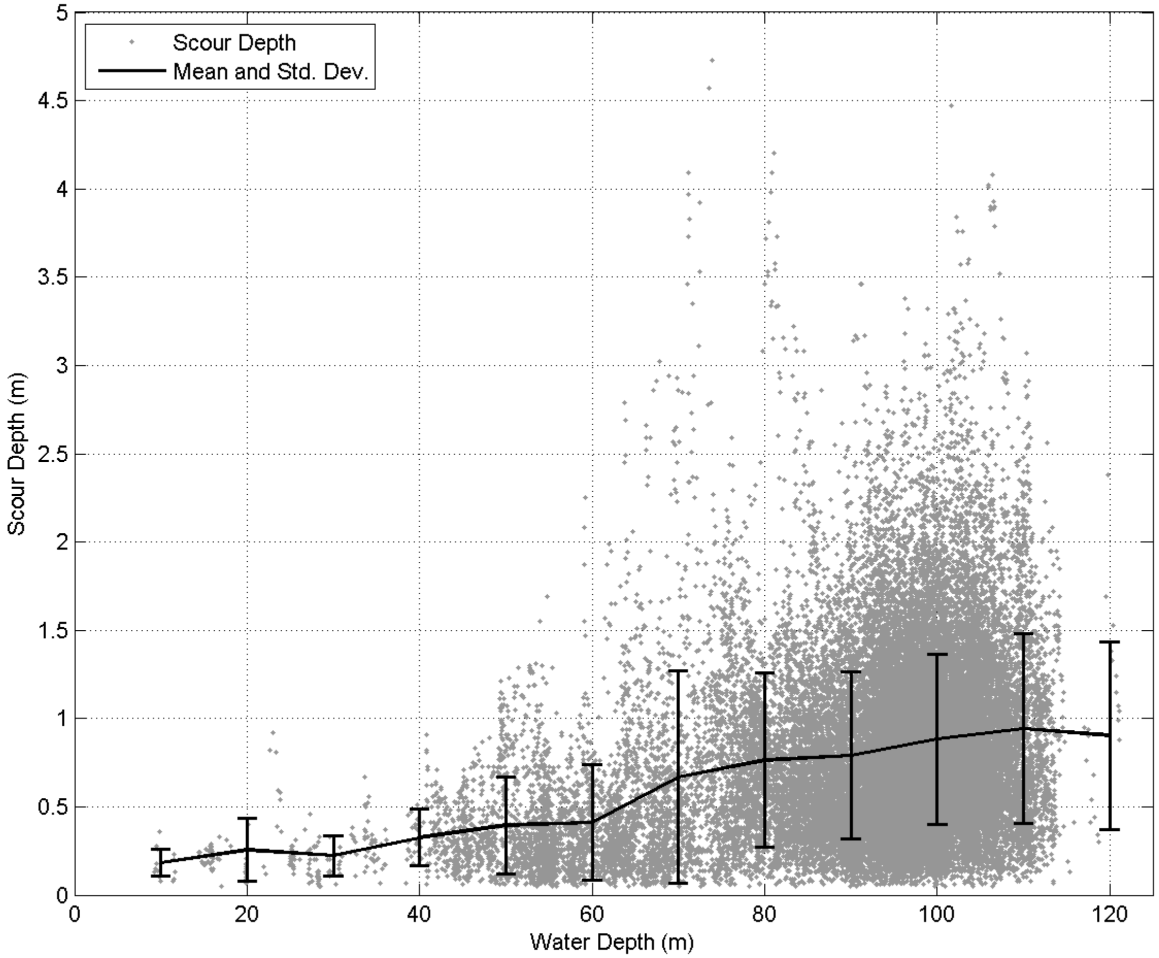

Figure 2-16 Scour depth as a function of water depth

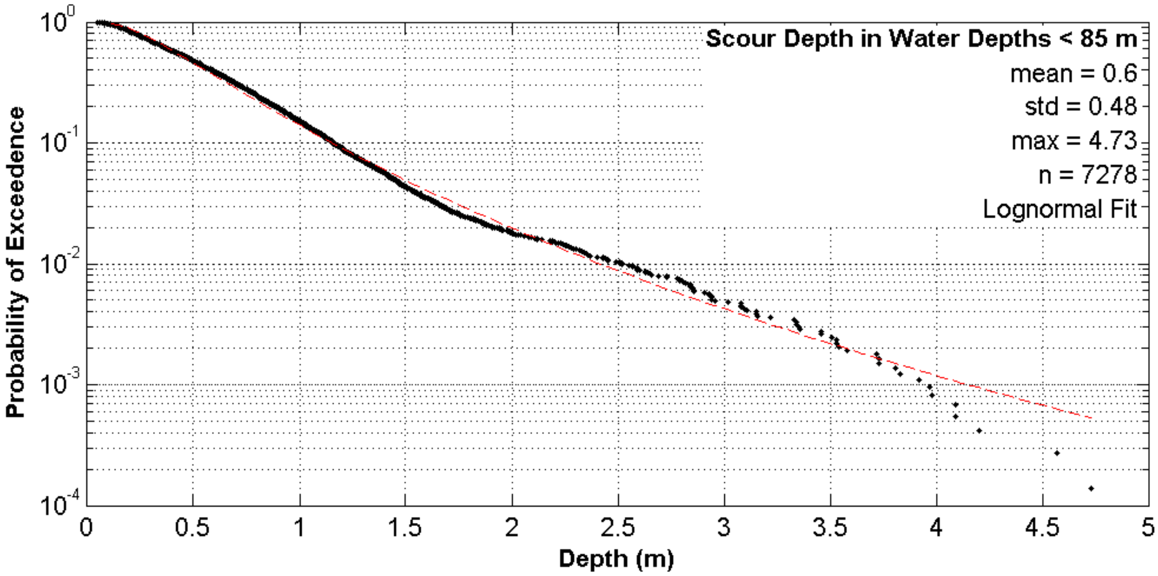

Figure 2-17 Scour depth distribution in water depths less than 85 m

Figure 2-18 Scour depth distribution in water depths greater than 85 m

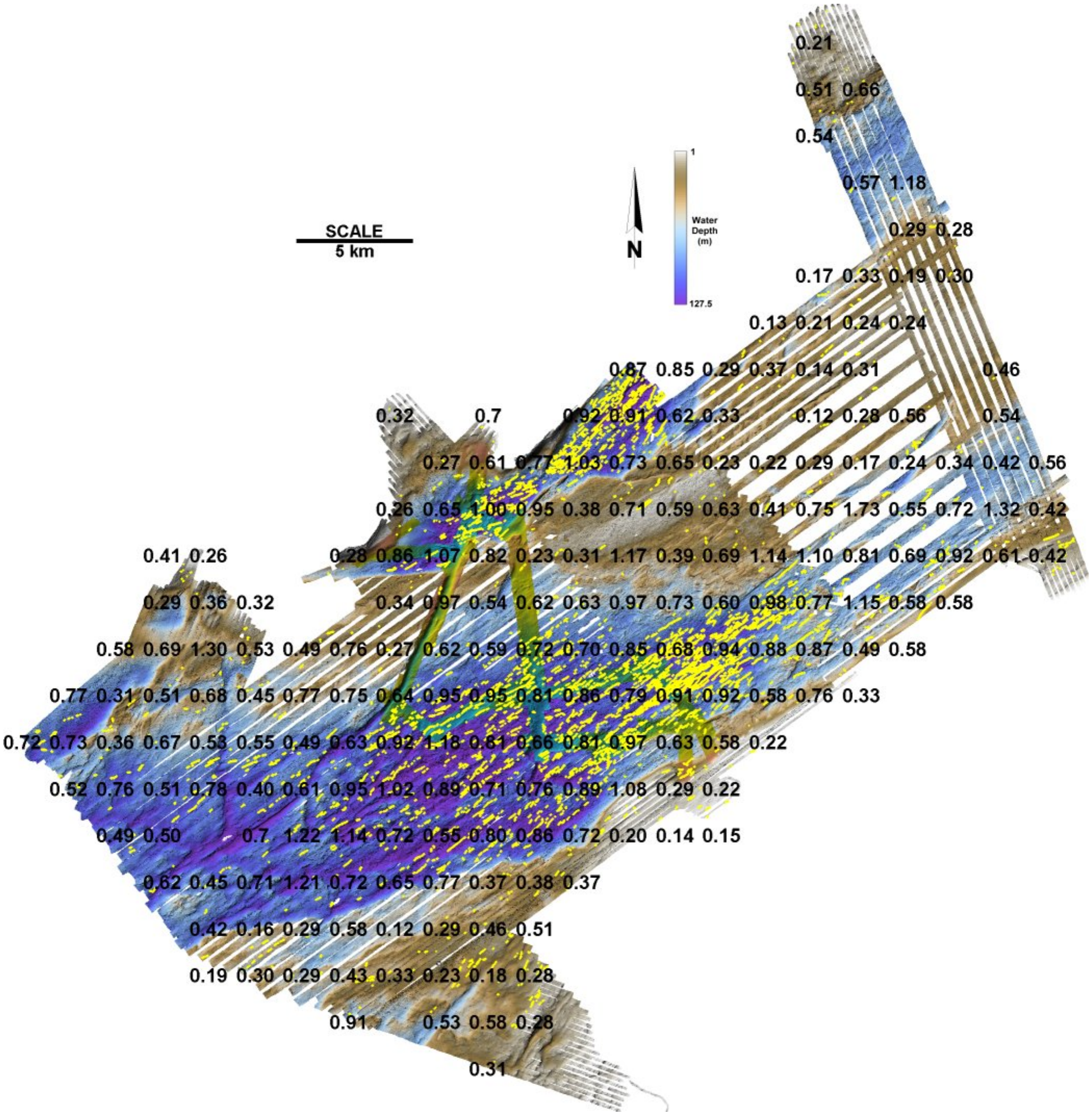

Figure 2-19 Spatial distribution of mean scour depth

2.3.4 Scour Incision Width

The scour incision width is the width of the depression the iceberg keel creates in the seabed, measured relative to an undisturbed seabed datum, and does not include the berms of displaced material on either side. Table 2-2 gives a breakdown of furrow incision width in the Strait of Belle Isle survey area. A noticeable increase in mean incision width is observed above 70 m water depth. Scour incision width is usually (but not always) best characterized using a lognormal distribution (e.g. King et al., 2009). It was found that the Strait of Belle Isle scour incision widths were equally well characterized by either the lognormal or gamma distributions in all water depth ranges. Figure 2-20 shows a scatter plot of scour incision width and water depth, as well as the mean and standard deviation of incision width in 10 m water depth bins. Figure 2-21 shows the distribution of incision widths for the full dataset with a gamma distribution. Figure 2-22 shows a scatter plot of furrow incision width and depth, along mean and standard deviations of scour depth in 10 m incision width bins. This shows the positive correlation between scour width and depth. Figure 2-23 shows the ratio of scour depth and incision width as a function of water depth, which indicates a changing scour cross-sectional shape with water depth. Figure 2-24 shows the spatial distribution of mean scour width over the multibeam survey area.

Table 2-2 Scour incision width as a function of water depth

Water Depth (m)	No. Profiles	Mean (m)	St. Dev. (m)	Max. (m)
> 5 & ≤ 15	19	10.8	3.5	17.2
> 15 & ≤ 25	59	20.2	6.8	40.9
> 25 & ≤ 35	114	21.6	7.7	44.8
> 35 & ≤ 45	226	24.9	9.8	55.1
> 45 & ≤ 55	1,104	27.9	12.9	79.4
> 55 & ≤ 65	1,346	27.9	13.1	88.7
> 65 & ≤ 75	1,361	36.4	15.5	93.0
> 75 & ≤ 85	3,056	42.4	17.7	117.8
> 85 & ≤ 95	8,409	39.4	17.0	115.5
> 95 & ≤ 105	16,013	39.0	14.8	125.4
> 105 & ≤ 115	4,362	45.2	20.7	132.1
> 115 & ≤ 125	24	38.5	18.5	61.6
All	36,093	39.1	16.8	132.1

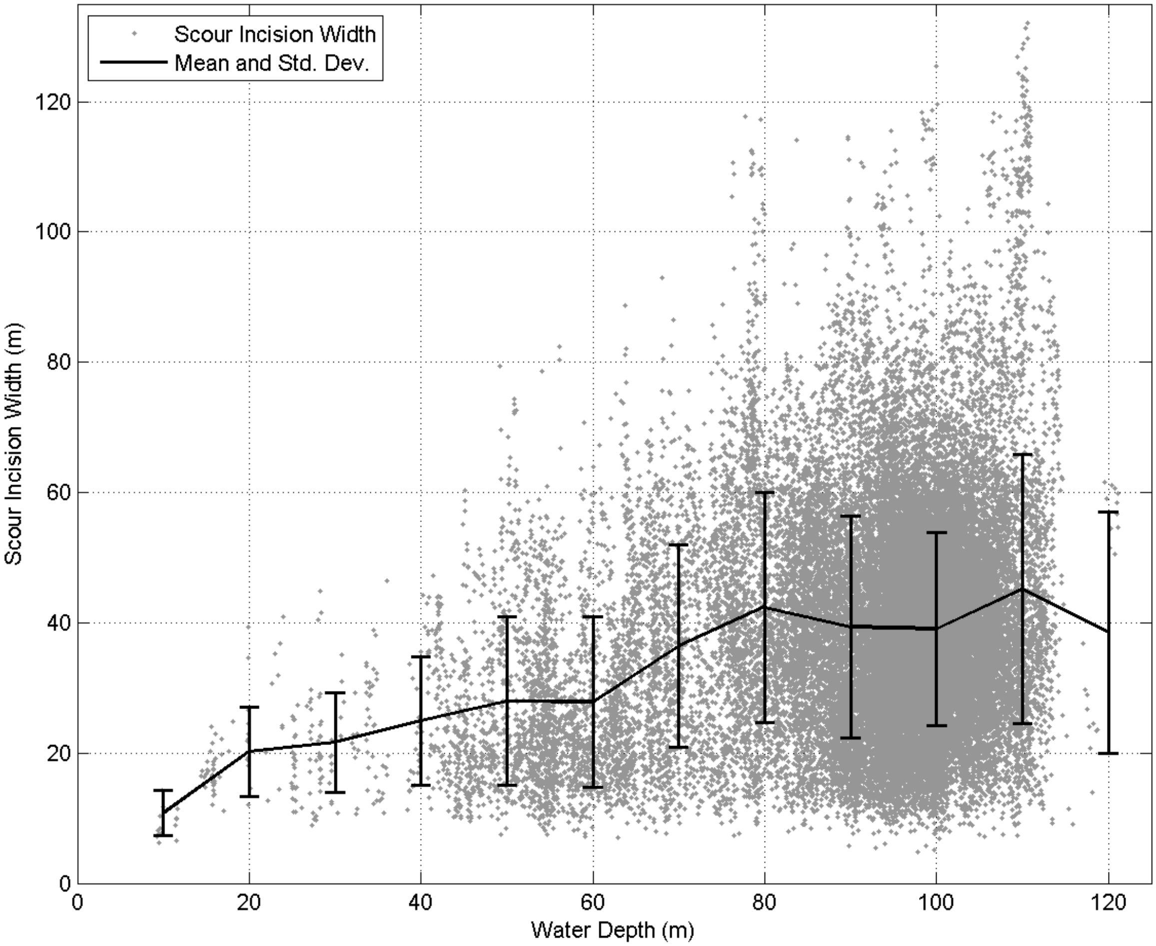

Figure 2-20 Scour incision width as a function of water depth

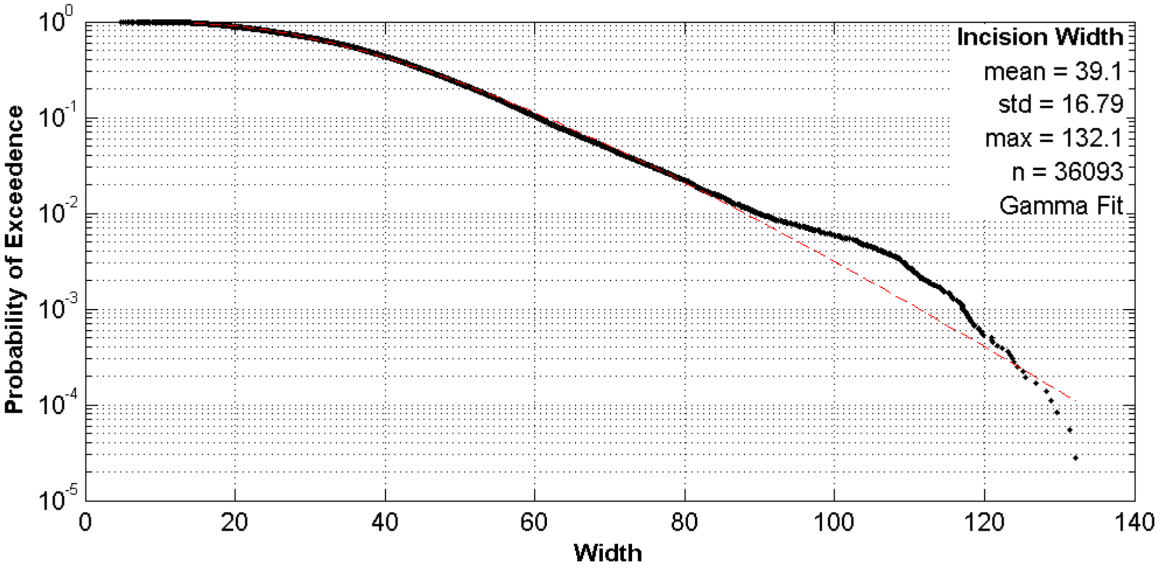

Figure 2-21 Distribution of scour incision width

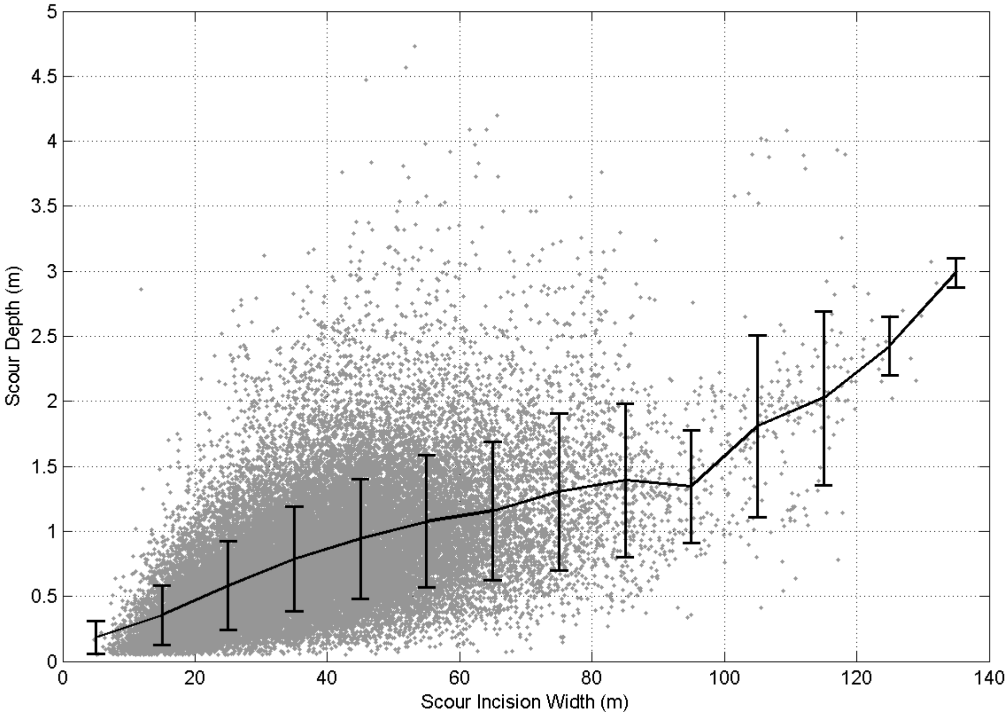

Figure 2-22 Scatter plot showing scour depths and incision widths

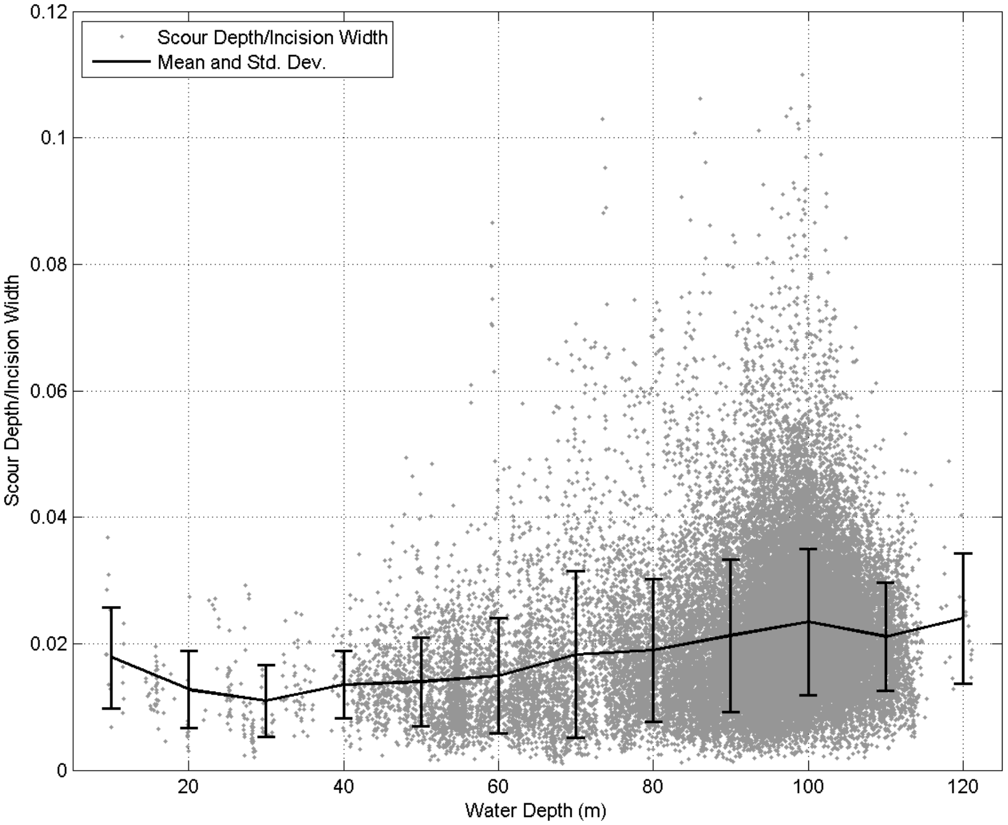

Figure 2-23 Scour depth/width ratio as a function of water depth

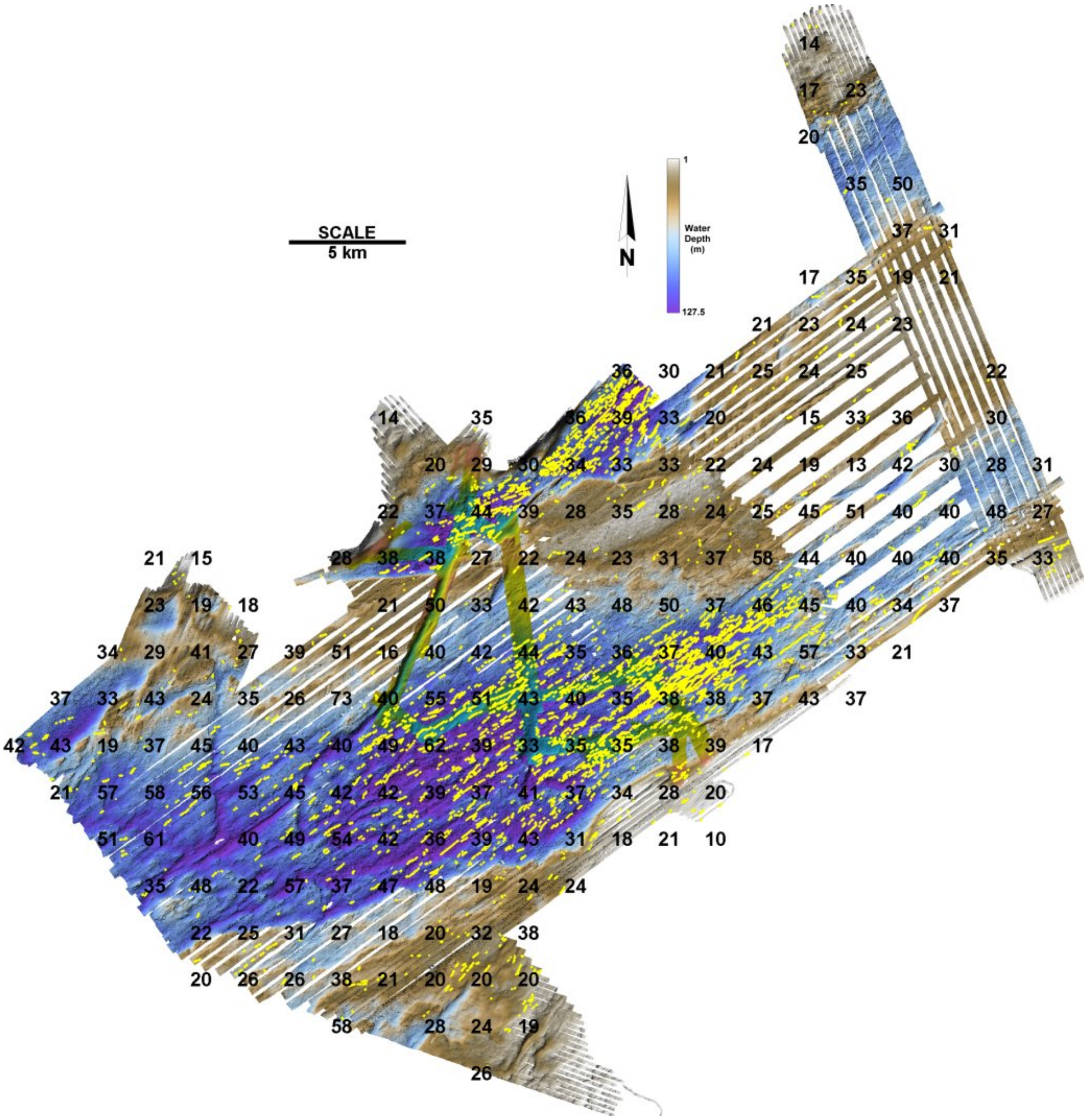

Figure 2-24 Spatial distribution of mean scour incision width

2.3.5 Scour Berm-to-Berm Width

The scour berm-to-berm width is the distance between the tops of the berms (sediment displaced during the scour formation process) on either side of the scour. The minimum possible berm-to-berm width is the incision width. The mean berm-to-berm width is 52.8 m, with a standard deviation of 20.3 m and a maximum of 155.0 m. Figure 2-25 shows a scatter plot of scour incision and berm-to-berm widths. The mean ratio of berm-to-berm to incision width is 1.4 (Figure 2-26), with a standard deviation of 0.2 and a maximum of 3.5 (incision width of 5.4 m and a berm-to-berm width of 19 m). Figure 2-27 shows a scatter plot of the berm-to-berm to incision width ratio and water depth. The mean of the ratio consistently decreases with water depth, although there are no transitions that would suggest a relationship with scour age.

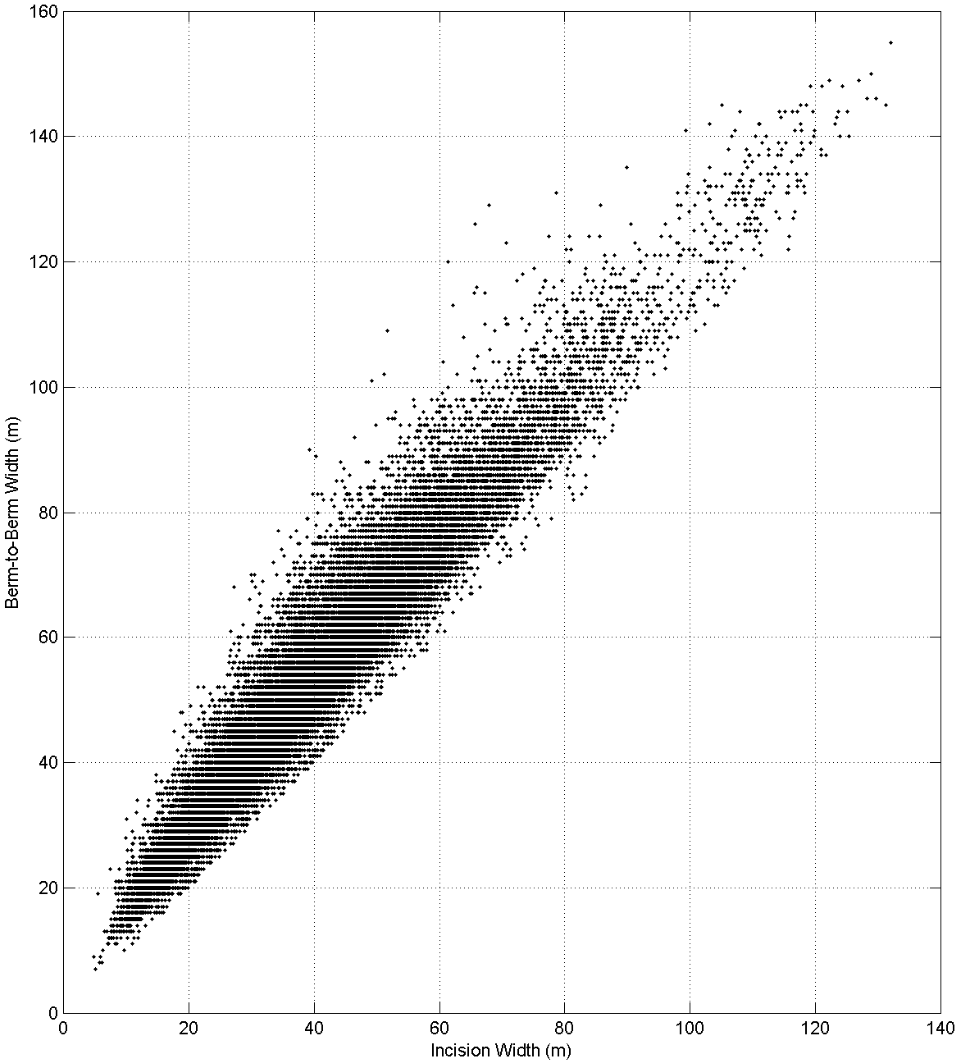

Figure 2-25 Scour incision and berm-to-berm width

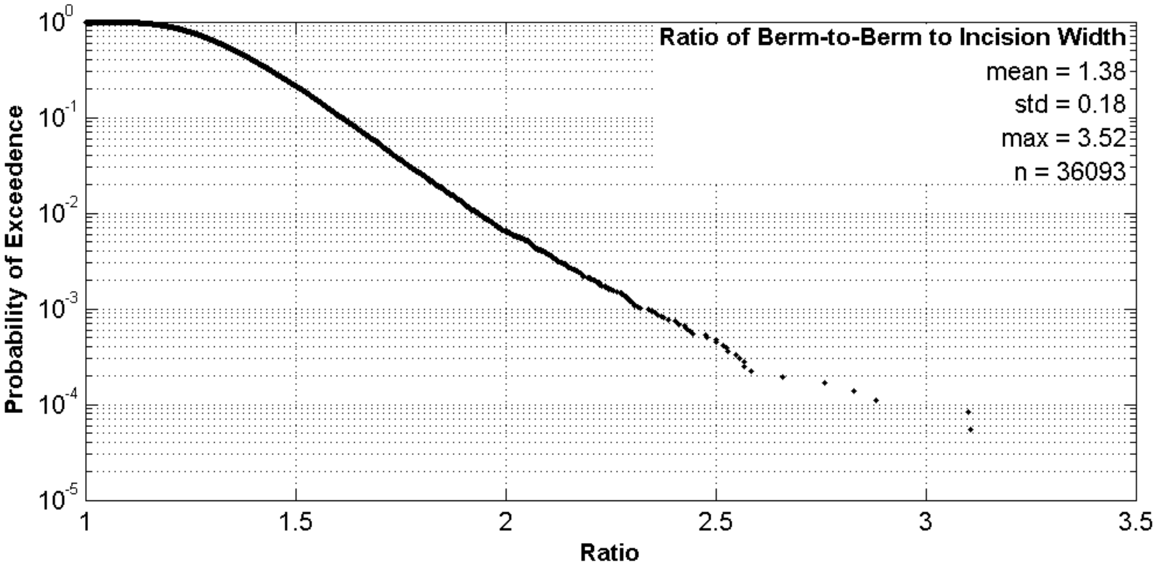

Figure 2-26 Ratio of scour berm-to-berm width to incision width

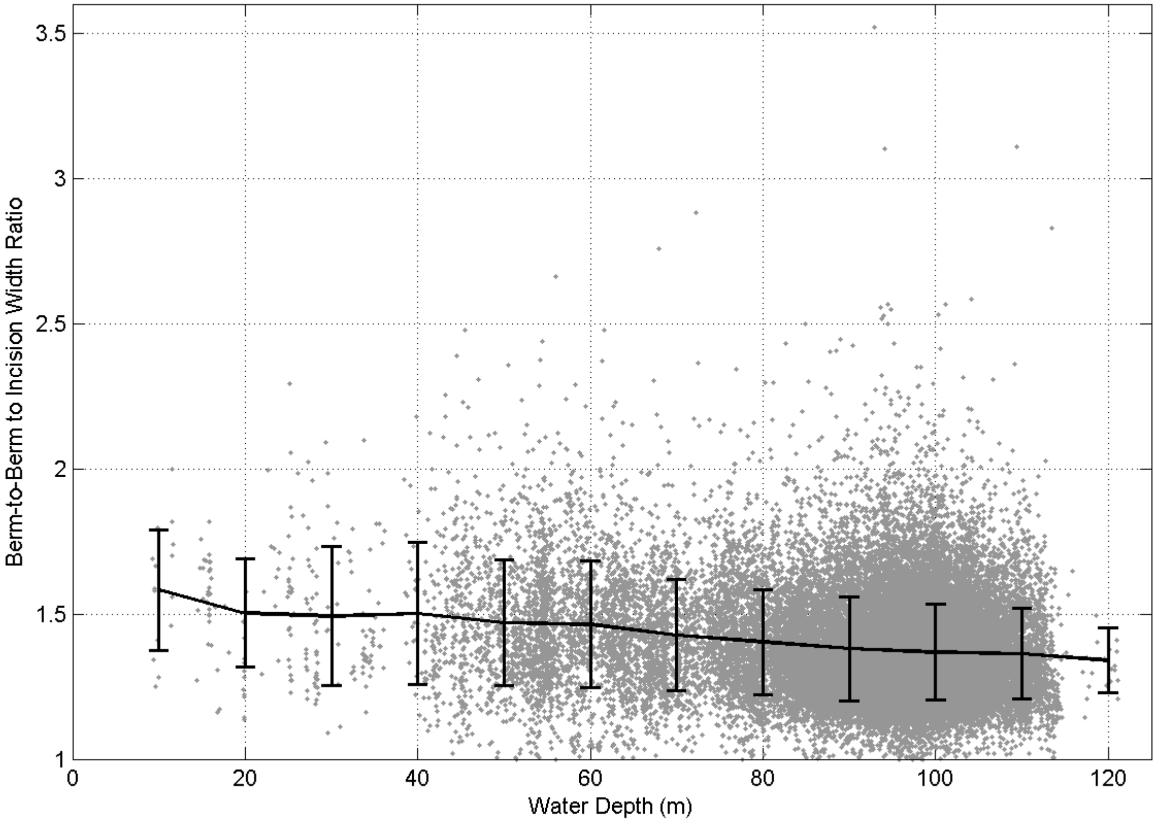

Figure 2-27 Scour berm-to-berm and incision width ratio as a function of water depth

2.3.6 Scour Base Width and Base to Incision Width Ratio

The base width is the width measured at 90% of the furrow depth (10% above its base). The base width to incision width ratio may be used as an indicator of overall scour cross-section shape. Since vertical scour sidewall slopes are unstable, the scour base width to incision ratio must be less than one. A total of 423 scour profiles had ratios of zero. Generally, these were shallower and narrower than average, although some were deep (i.e. 2.2 m) and wide (i.e. 86 m), so the reason(s) for a zero base width to incision width ratio for these features are not clear. Of the remaining 35,570 scour profiles, the mean ratio is 0.19, with a standard deviation of 0.10 and a maximum of 0.71. Figure 2-28 shows a scatter plot of base to incision width ratio and water depth, with means and standard deviations indicated in 10 m water depth intervals. The trend is an increasing ratio with water depth, but no clear transitions that could serve as an indicator of a transition between modern and relict scours.

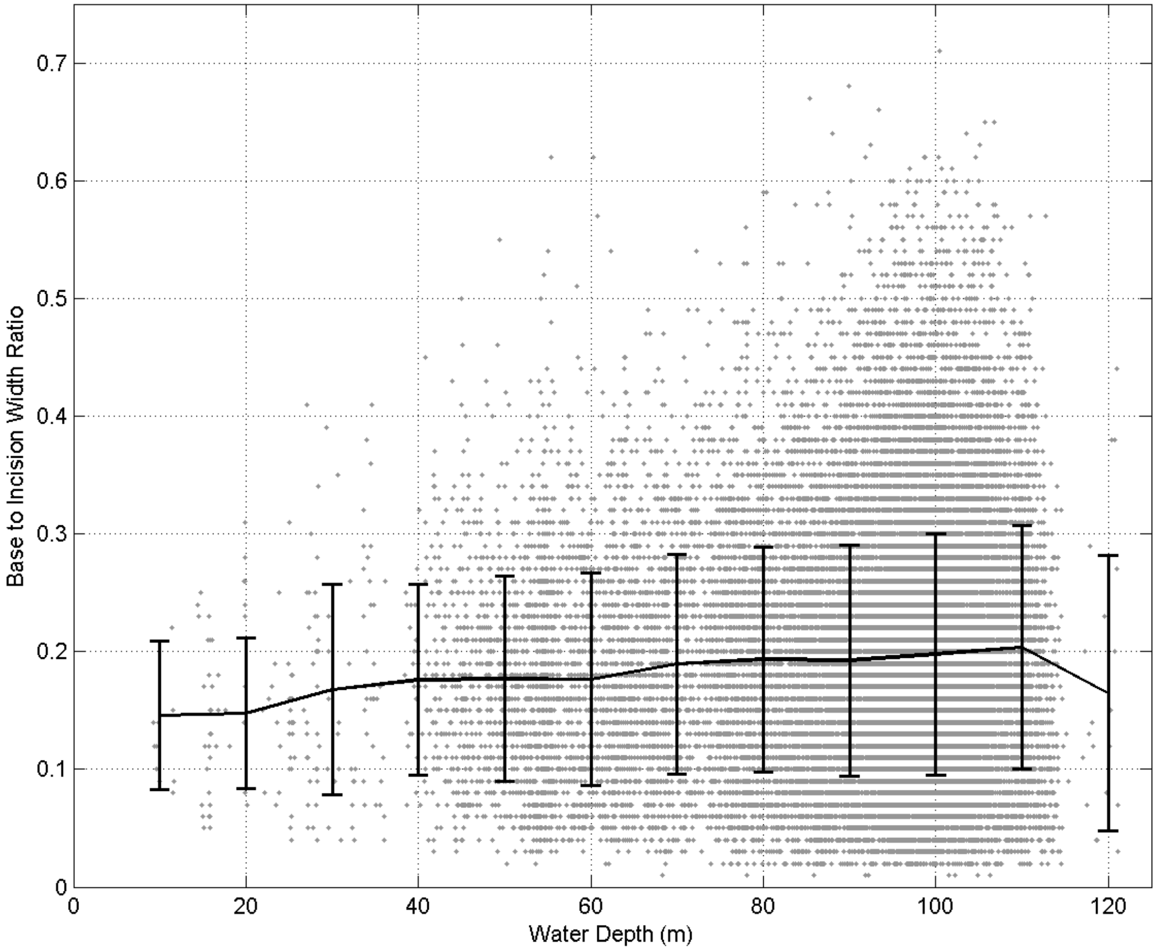

Figure 2-28 Base to incision width ratio as a function of water depth

2.3.7 *Scour Berm Height*

Berms are formed from material displaced during the scour formation process. Each scour profile has two associated berm height measurements (left and right berm heights). Of a total of 72,186 berm height measurements, just over 9% (6,616) had values of zero. The proportion of berm heights with a value of zero was essentially independent of water depth (actually decreasing slightly with increased water depth), and was excluded from any further analysis. Table 2-3 gives berm height statistics in 10 m water depth bins. Figure 2-29 shows a scatter plot of berm height and water depth (excluding zeros), as well as means and standard deviations in 10 m water depth intervals. The distribution of berm heights showed a similar trend as was observed with scour depth, with heights in shallower water following a lognormal distribution (Figure 2-30) and in deeper water following a gamma distribution (Figure 2-31). However, in this case the transition seems to occur in slightly shallower water depth (~ 75 m instead of ~ 85 m observed for scour depths). Figure 2-32 shows the spatial distribution of berm height.

Table 2-3 Scour berm height as a function of water depth

Water Depth (m)	No. Profiles	Excluded (%)	Mean (m)	St. Dev. (m)	Max. (m)
> 5 & ≤ 15	38	0	0.08	0.05	0.21
> 15 & ≤ 25	118	14.4	0.20	0.27	2.06
> 25 & ≤ 35	228	11.0	0.11	0.08	0.48
> 35 & ≤ 45	452	9.7	0.16	0.11	0.85
> 45 & ≤ 55	2,208	10.9	0.21	0.22	2.82
> 55 & ≤ 65	2,692	11.9	0.21	0.21	3.90
> 65 & ≤ 75	2,722	8.2	0.33	0.32	3.50
> 75 & ≤ 85	6,112	9.1	0.37	0.29	2.36
> 85 & ≤ 95	16,818	9.9	0.43	0.32	2.59
> 95 & ≤ 105	32,026	9.1	0.47	0.34	3.76
> 105 & ≤ 115	8,724	7.4	0.45	0.31	2.94
> 115 & ≤ 125	48	10.4	0.39	0.32	1.66
All	72,186	9.2	0.42	0.32	3.90

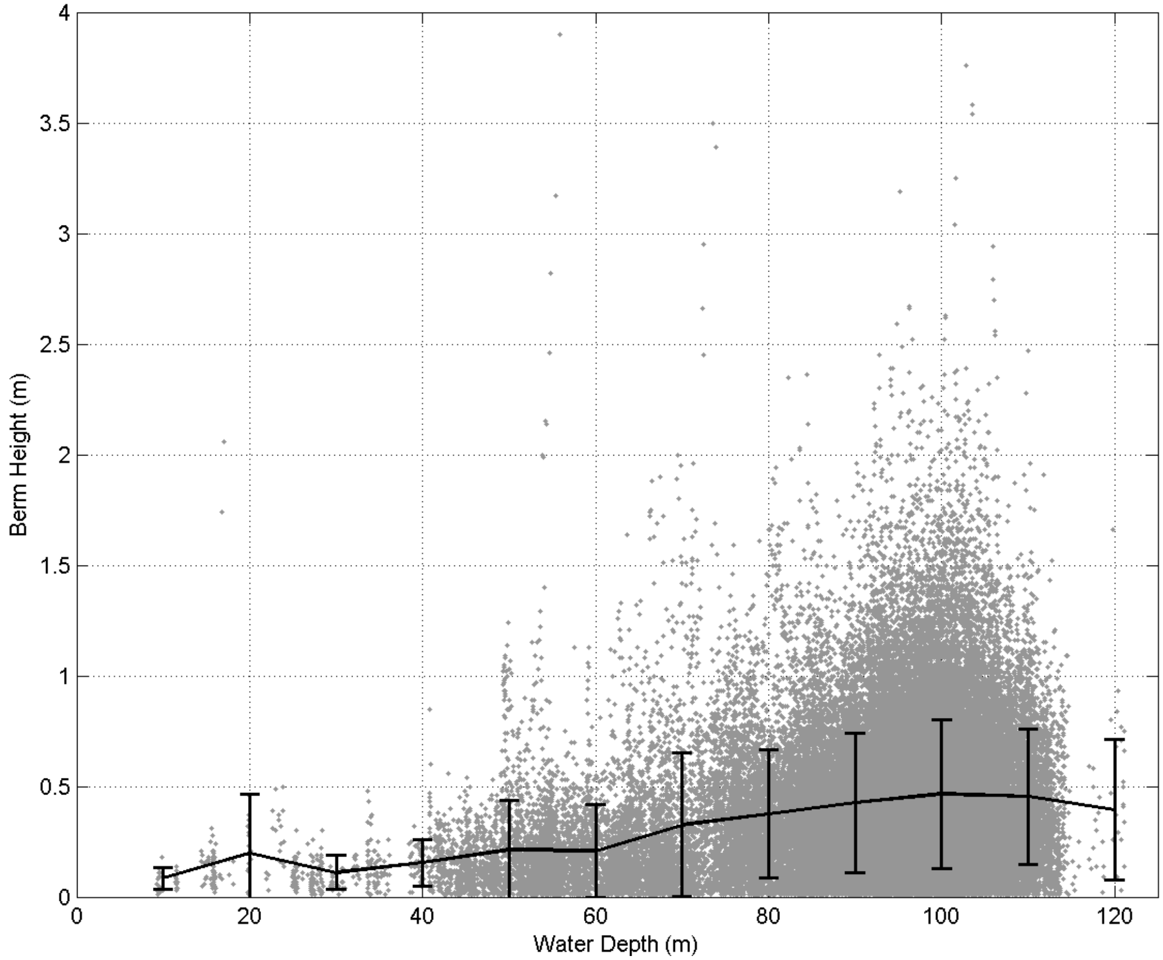

Figure 2-29 Scour berm height as a function of water depth (zeros excluded)

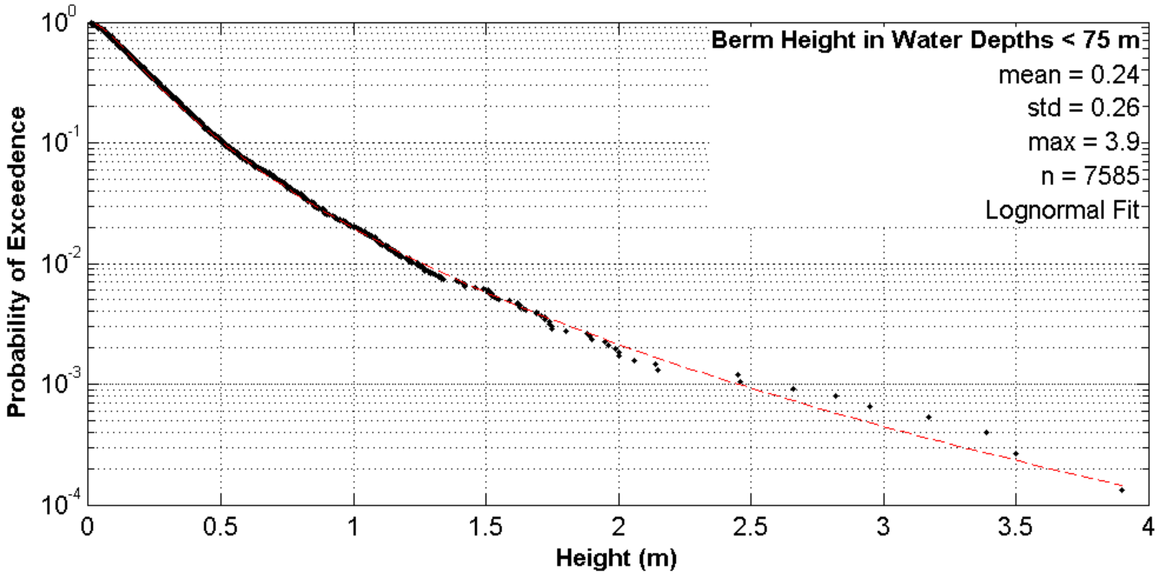

Figure 2-30 Distribution of berm heights (> 0) in less than 75 m water depth

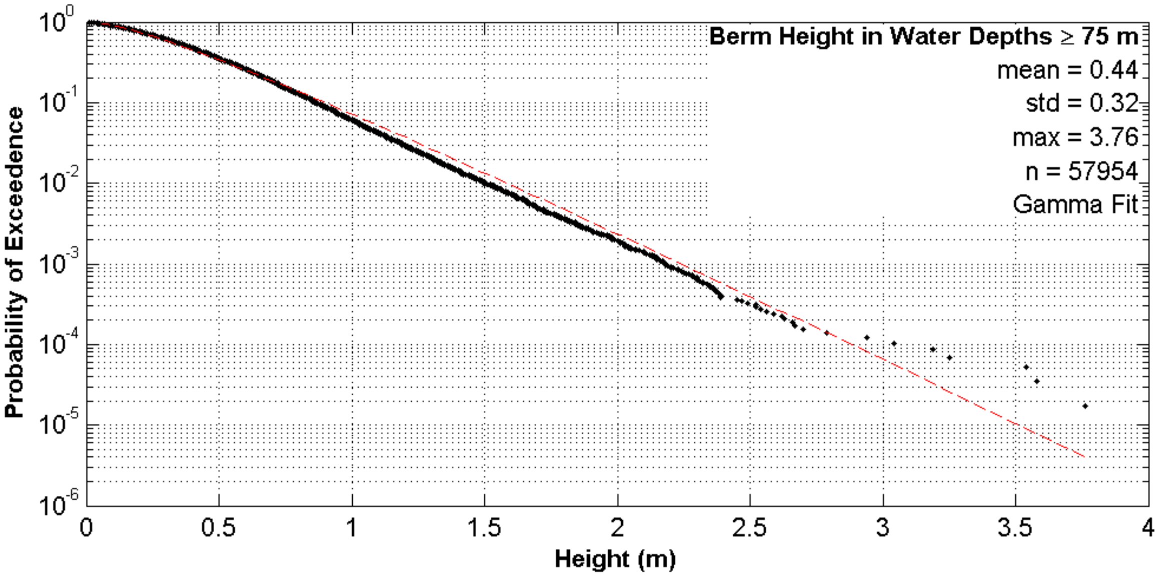

Figure 2-31 Distribution of berm heights (> 0) in more than 75 m water depth

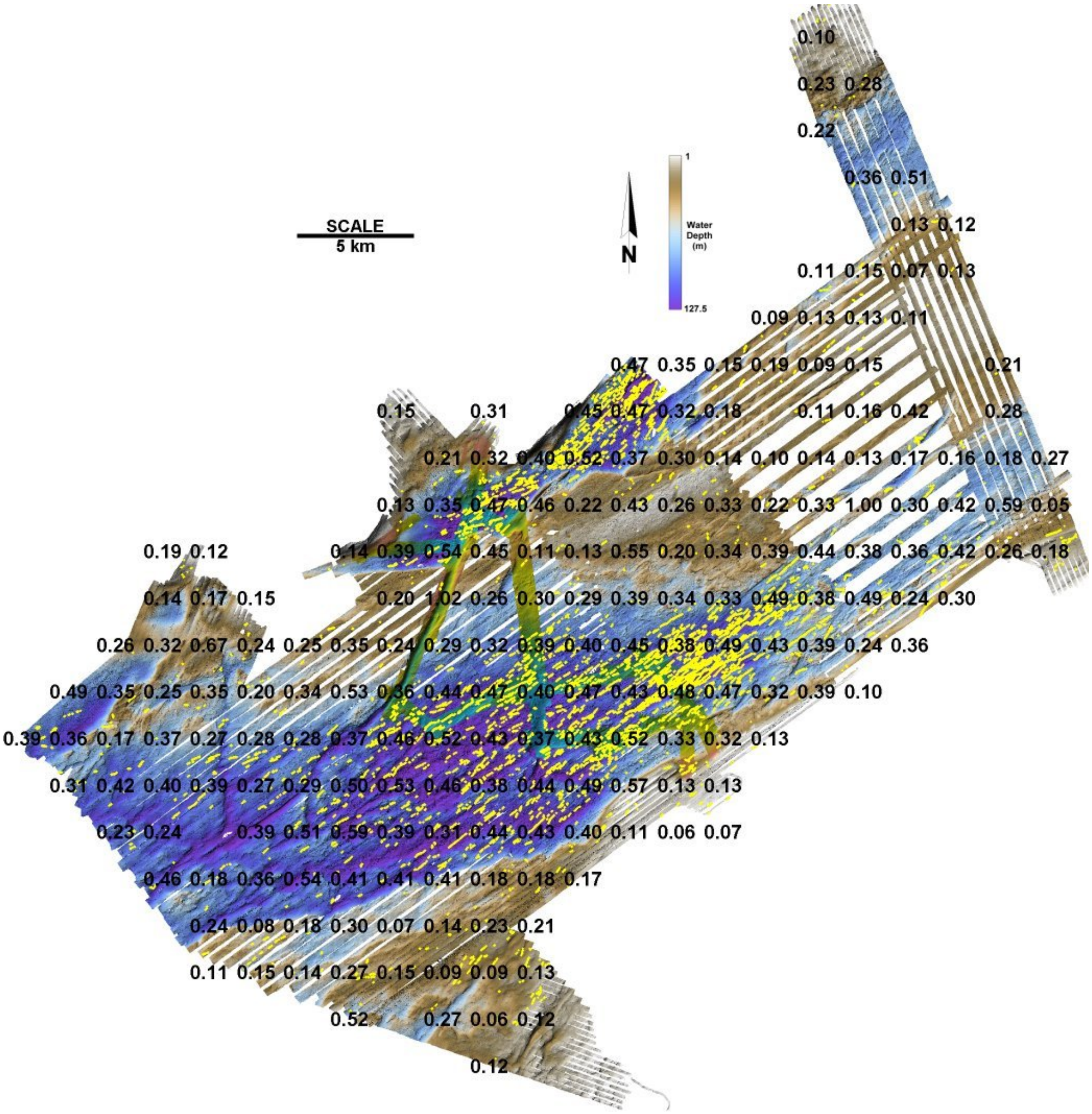

Figure 2-32 Spatial distribution of mean berm height

2.3.8 Scour Depth of Disturbance

Scour depth of disturbance is characterized in the profile database for each scour profile as minimum, average and maximum depth of disturbance. The minimum depth of disturbance is the distance between the top of the shortest of the two berms associated with a profile to the deepest point of the scour. The maximum depth of disturbance is calculated using the tallest berm and the average depth of disturbance is calculated using the mean of the two berm heights. However, it is not possible to reproduce the depth of disturbance by adding the recorded scour depth to the appropriate berm height, or mean of the berm heights. As shown in Figure 2-33 (using maximum depth of disturbance as an example) the values, on average, are comparable. However, on a case by case basis these values vary by a factor of 0.4 to 2.5.

Table 2-4 gives minimum, average and maximum depth of disturbance as a function of water depth. The same information is also given in the form of scatter plots in Figure 2-34 (minimum), Figure 2-35 (average) and Figure 2-36 (maximum). As noted previously with both scour depth and berm height, a noticeable increase in all three parameters is obvious at 70 m water depth. A check of the distributions showed that for minimum and average depth of disturbance the same pattern is seen as observed for scour depth with a transition from a lognormal to a gamma distribution at ~85 m water depth (see Figure 2-37 and Figure 2-38). However, for maximum depth of disturbance the lognormal distribution works equally well in all water depths. The reason for this difference is unknown.

Figure 2-39 shows the spatial distribution of the depth of disturbance using the mean of maximum depth of disturbance on a 2 × 2 m grid.

Table 2-4 Depth of disturbance as a function of water depth

Water Depth (m)	No.	Depth of Disturbance								
		Minimum			Average			Maximum		
		Mean	S.D.	Max.	Mean	S.D.	Max.	Mean	S.D.	Max.
> 5 & ≤ 15	19	0.24	0.13	0.56	0.27	0.13	0.59	0.29	0.14	0.61
> 15 & ≤ 25	59	0.36	0.24	1.14	0.46	0.33	1.72	0.55	0.46	2.75
> 25 & ≤ 35	114	0.27	0.15	0.83	0.32	0.16	0.99	0.36	0.18	1.15
> 35 & ≤ 45	226	0.40	0.20	1.26	0.46	0.21	1.30	0.52	0.24	1.65
> 45 & ≤ 55	1,104	0.52	0.41	3.68	0.61	0.49	4.68	0.70	0.58	5.99
> 55 & ≤ 65	1,346	0.50	0.40	3.32	0.59	0.45	4.28	0.67	0.52	6.23
> 65 & ≤ 75	1,361	0.80	0.71	4.98	0.93	0.79	6.31	1.06	0.89	7.77
> 75 & ≤ 85	3,056	0.89	0.60	5.11	1.05	0.63	5.28	1.21	0.69	5.46
> 85 & ≤ 95	8,409	0.97	0.58	4.19	1.17	0.63	4.55	1.35	0.71	5.06
> 95 & ≤ 105	16,013	1.08	0.60	6.08	1.29	0.65	6.24	1.50	0.74	6.40
> 105 & ≤ 115	4,362	1.10	0.60	3.92	1.29	0.64	5.15	1.47	0.71	6.43
> 115 & ≤ 125	24	0.95	0.55	2.28	1.14	0.65	2.98	1.32	0.76	3.68
All	36,093	0.98	0.61	6.08	1.17	0.66	6.31	1.35	0.75	7.77

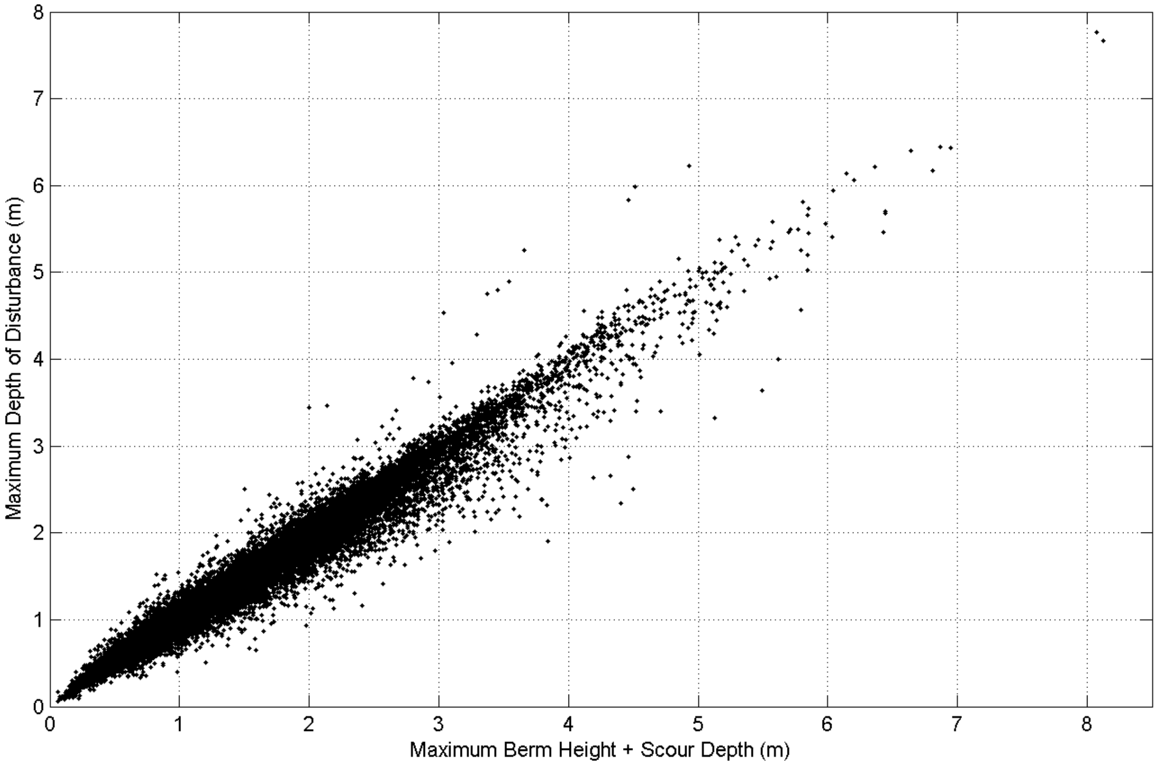

Figure 2-33 Maximum depth of comparison compared with sum of scour depth and maximum berm height

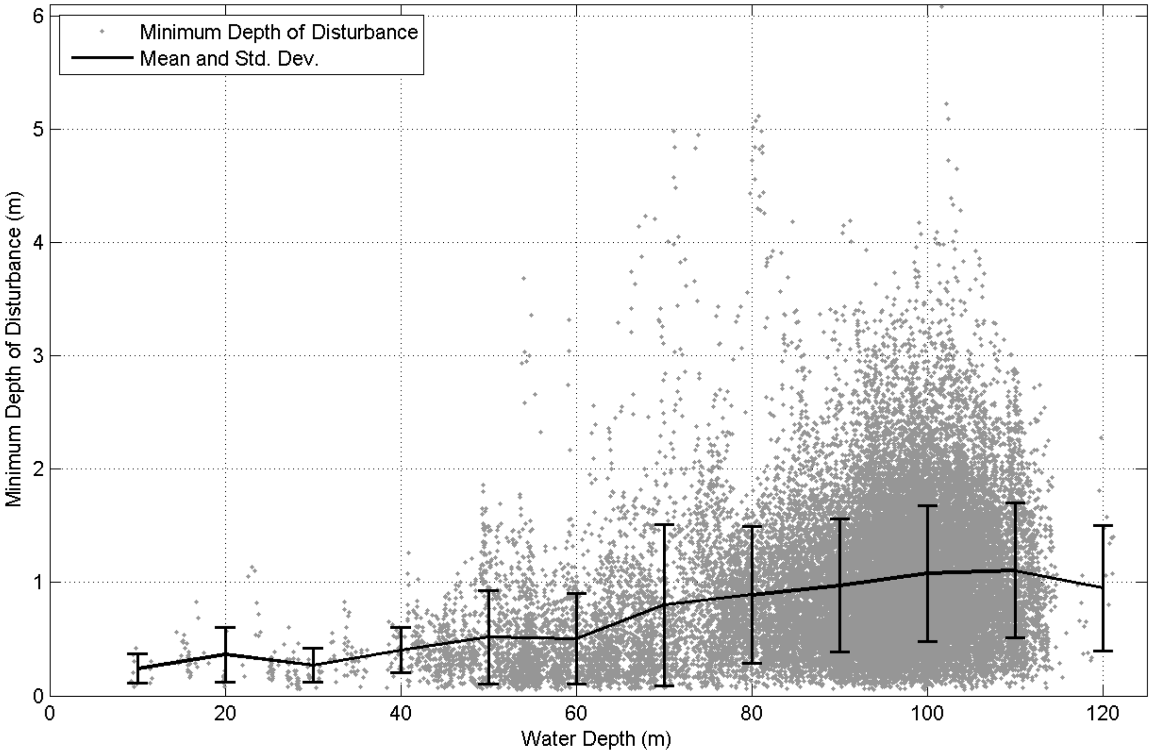

Figure 2-34 Minimum depth of disturbance as a function of water depth

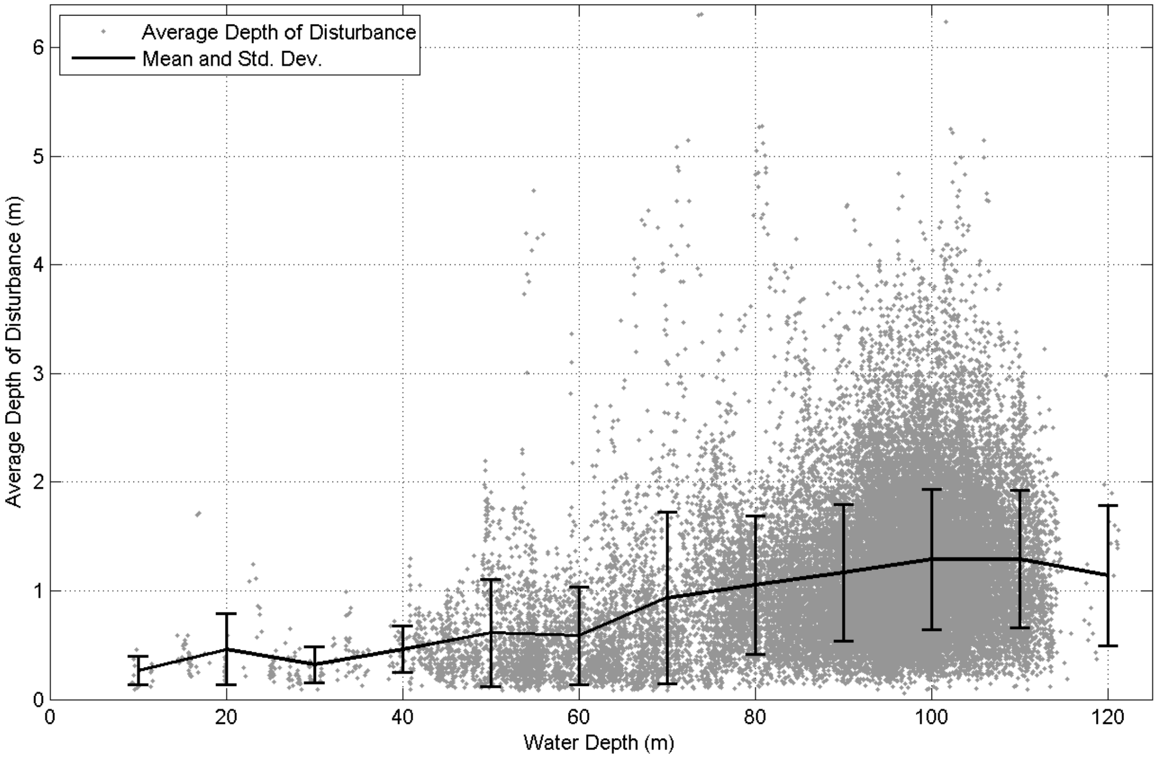

Figure 2-35 Average depth of disturbance as a function of water depth

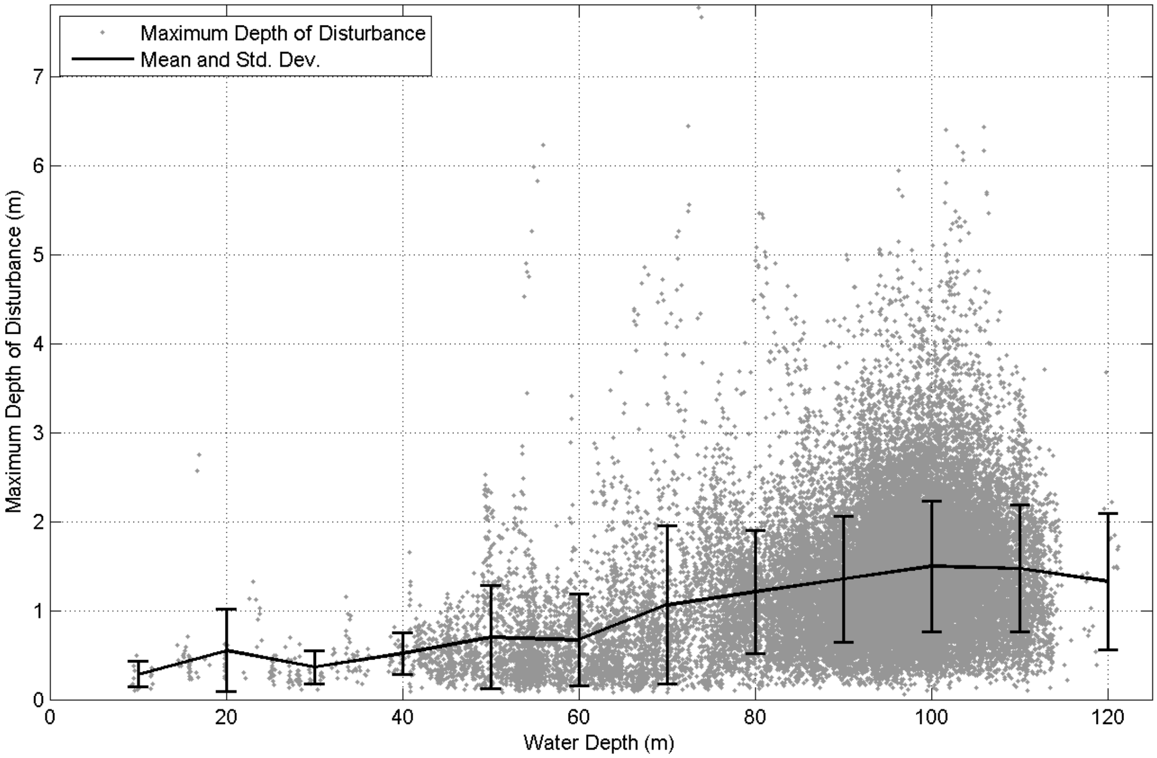

Figure 2-36 Maximum depth of disturbance as a function of water depth

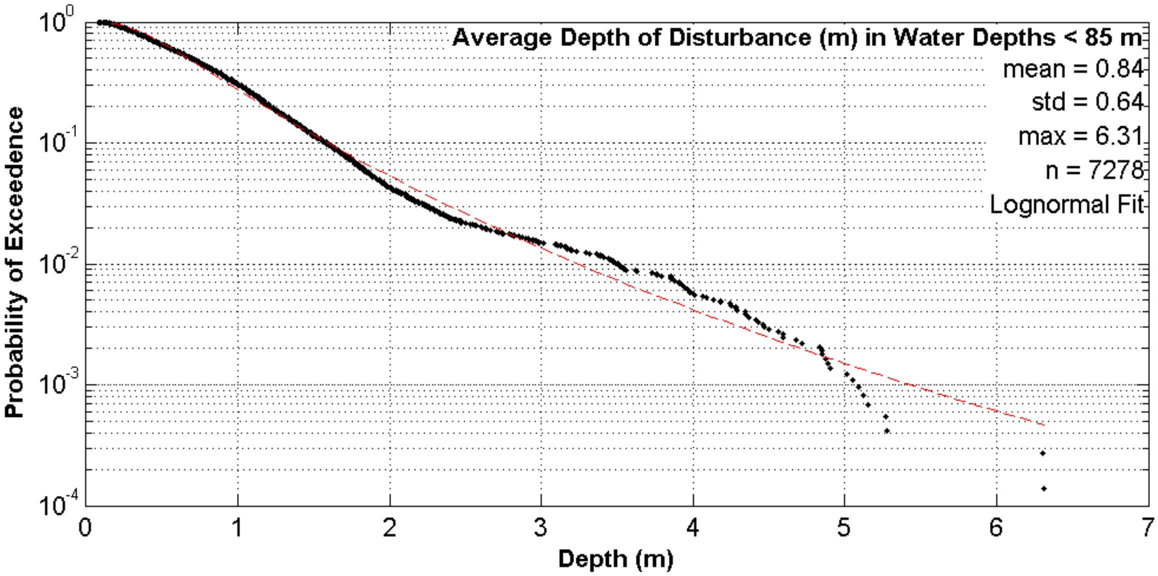

Figure 2-37 Distribution of average depth of disturbance in less than 85 m water depth

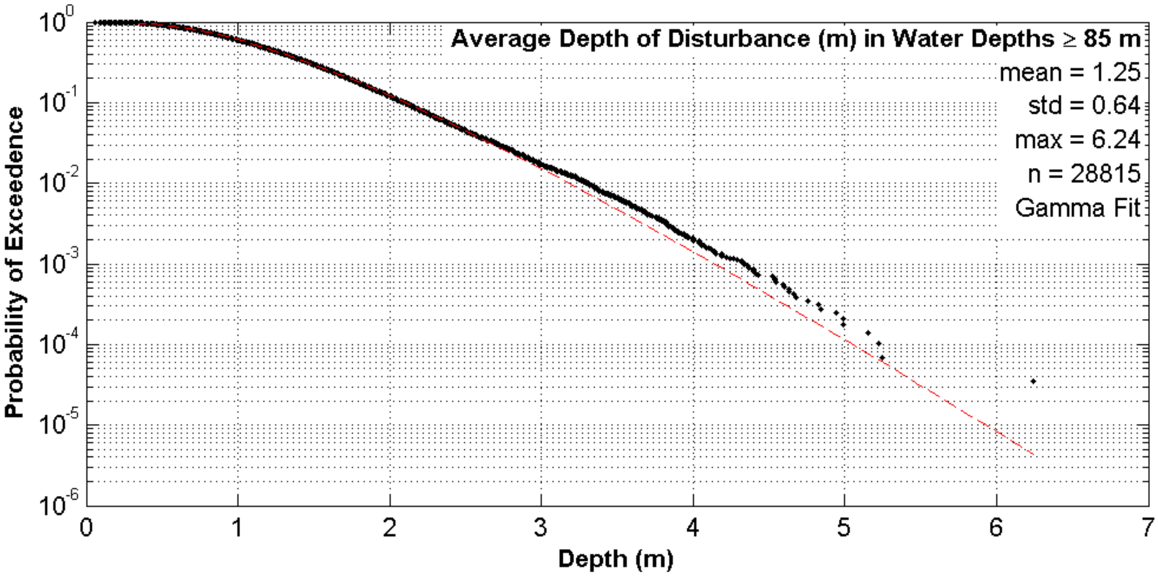

Figure 2-38 Distribution of average depth of disturbance in more than 85 m water depth

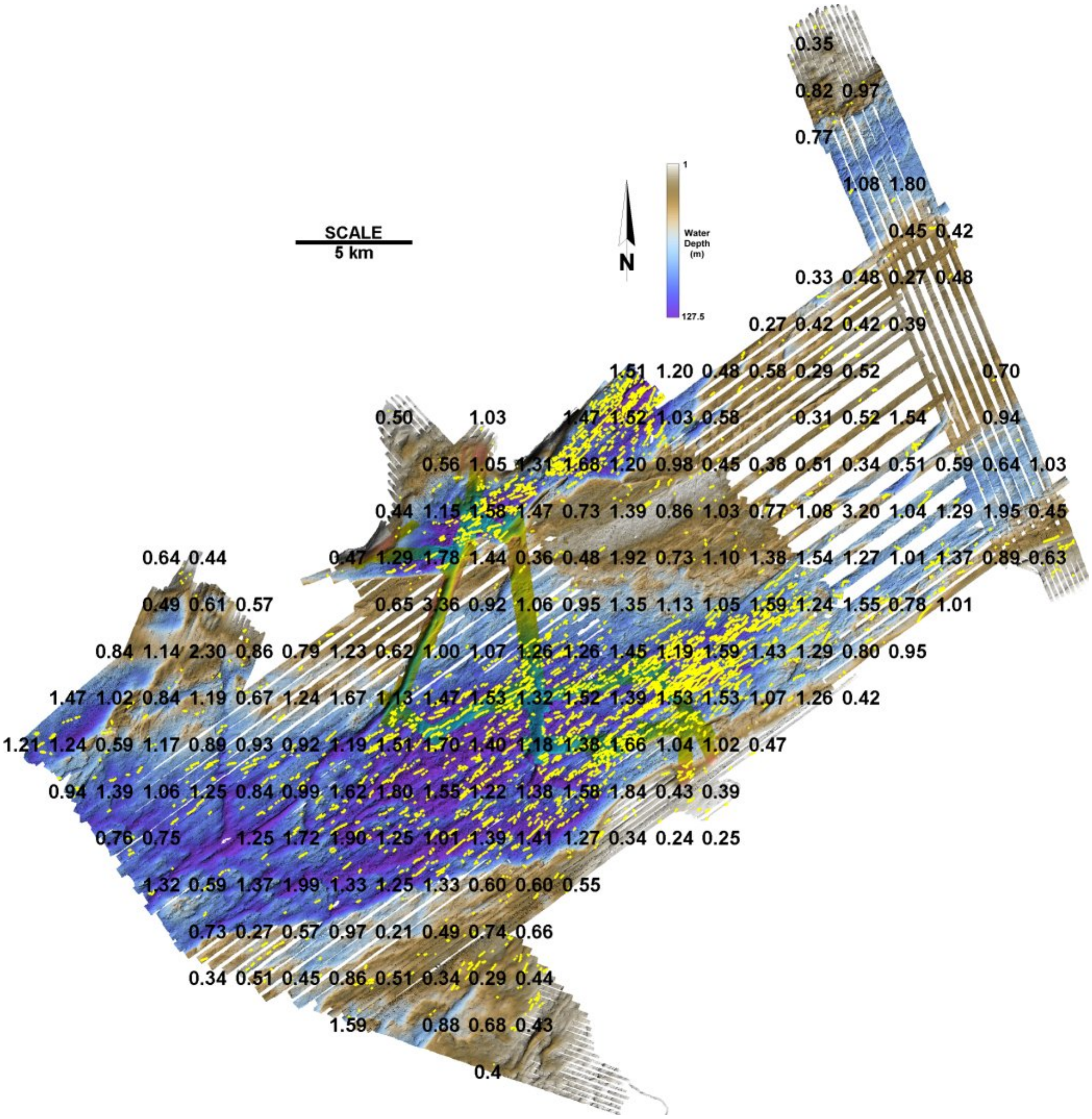

Figure 2-39 Spatial distribution of maximum depth of disturbance (mean in 2×2 km grid)

2.3.9 Scour Sidewall Slopes

Scour sidewall slope parameters given in the profile database are the minimum, average and maximum sidewall slopes, as well as the slope at zero crossing (inside the scour at the elevation corresponding to the original undisturbed seabed). These parameters are given for both the left and right sidewall slopes, and have been combined for the analysis. An initial review of the data indicated 12 null values (coded 999) for minimum, maximum and zero-crossing sidewall slopes, which were excluded from the data analysis. There were no null values in the zero-crossing sidewall slopes.

Table 2-5 gives a breakdown of scour sidewall slope statistics as a function of water depth. These data are also reproduced in Figure 2-40 (minimum slope), Figure 2-41 (average slope), Figure 2-42 (maximum slope), and Figure 2-43 (zero-crossing slope), along with scatter plots of the raw data. Minimum sidewall slopes show little relationship with water depth, with the exception of increased scatter above 70 m water depth. Average sidewall slopes begin to show a trend, with higher slopes initially in shallow water, a minimum around 30 m water depth and then trending towards higher slopes with increasing water depth (with increased scatter above 70 m water depth). This trend is more pronounced with maximum and zero-crossing sidewall slopes (and most pronounced with maximum sidewall slopes). It is possible that higher slopes in shallowest water depth could be the youngest scours which have not had time to infill (and could, in theory, have been formed by pack ice or icebergs). The increase in slope in deeper water may simply be due to the positive correlation between scour depth and sidewall slope (see Figure 2-44) which has been noted in other datasets, although the increase in scatter above 70 m is suggestive of other effects (i.e. possible indicator of relict scours).

The distribution of all scour sidewall slope metrics were best characterized using the lognormal distribution. While the fit was best when considering scour sidewall slopes in 10 m water depth bins, the lognormal distribution also provided a reasonable fit for the combined dataset over all water depths (see Figure 2-45 for maximum sidewall slope distribution). Figure 2-46 shows the spatial distribution of the mean of the maximum scour sidewall slope on a 2 × 2 km grid.

Table 2-5 Scour sidewall slope statistics as a function of water depth (values in brackets are number of zero-crossing slope measurements per 10 m water depth bin)

Water Depth (m)	No.	Sidewall Slope (degrees)							
		Minimum		Average		Maximum		Zero-Crossing	
		Mean	S.D.	Mean	S.D.	Mean	S.D.	Mean	S.D.
> 5 & ≤ 15	38	1.93	1.24	2.57	1.52	3.17	1.87	2.73	1.86
> 15 & ≤ 25	117 (118)	1.32	0.95	1.96	1.18	2.64	1.27	2.00	1.41
> 25 & ≤ 35	228	1.18	1.00	1.66	1.14	2.09	1.30	1.78	1.24
> 35 & ≤ 45	451 (452)	1.50	0.97	2.20	1.23	2.86	1.56	2.37	1.60
> 45 & ≤ 55	2208	1.27	0.88	2.04	1.20	2.78	1.57	2.25	1.53
> 55 & ≤ 65	2692	1.50	1.15	2.30	1.44	3.02	1.82	2.53	1.81
> 65 & ≤ 75	2722	1.69	1.54	2.85	2.29	4.01	3.15	3.50	3.02
> 75 & ≤ 85	6110 (6112)	1.56	1.38	2.90	2.01	4.30	2.70	3.72	2.68
> 85 & ≤ 95	16,814 (16,818)	1.67	1.31	3.19	2.08	4.90	2.97	4.23	3.00
> 95 & ≤ 105	32,023 (32,026)	1.65	1.24	3.33	2.02	5.23	2.97	4.57	3.01
> 105 & ≤ 115	8723 (8,724)	1.52	1.11	3.09	1.69	4.94	2.52	4.41	2.61
> 115 & ≤ 125	48	1.84	1.29	3.28	1.87	4.91	2.60	4.55	2.69
All	72,174 (72,186)	1.61	1.25	3.12	1.99	4.81	2.89	4.18	2.91

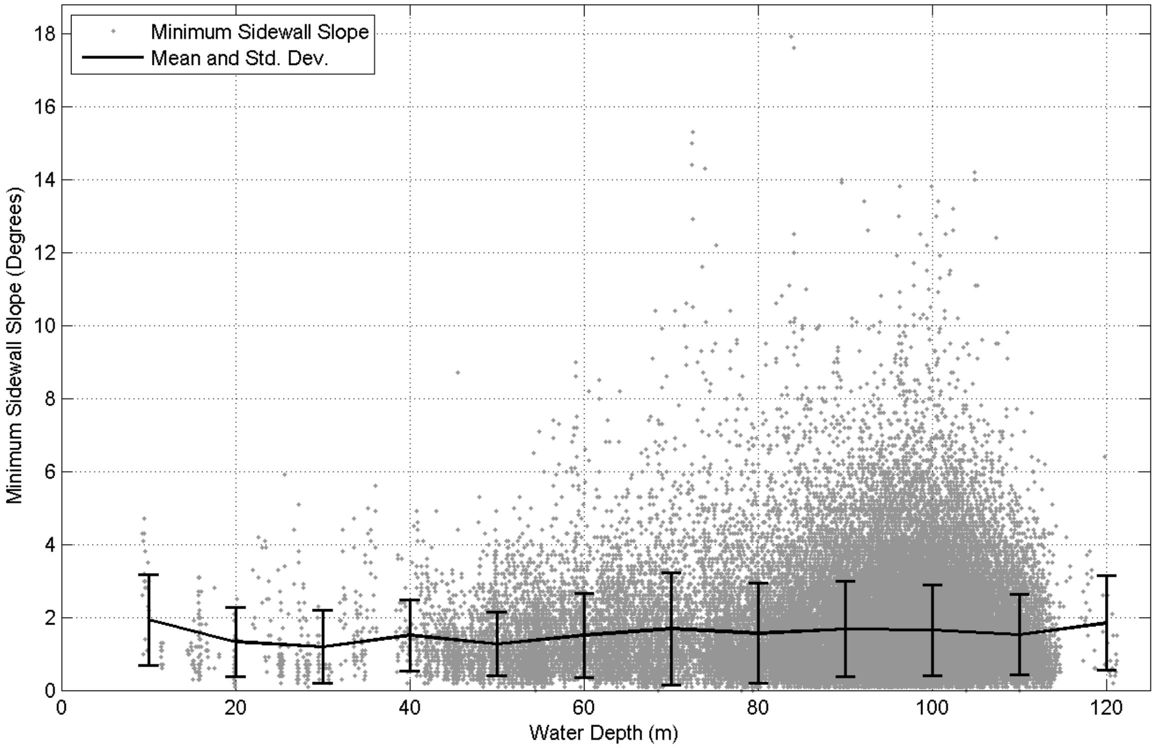

Figure 2-40 Minimum scour sidewall slope as a function of water depth

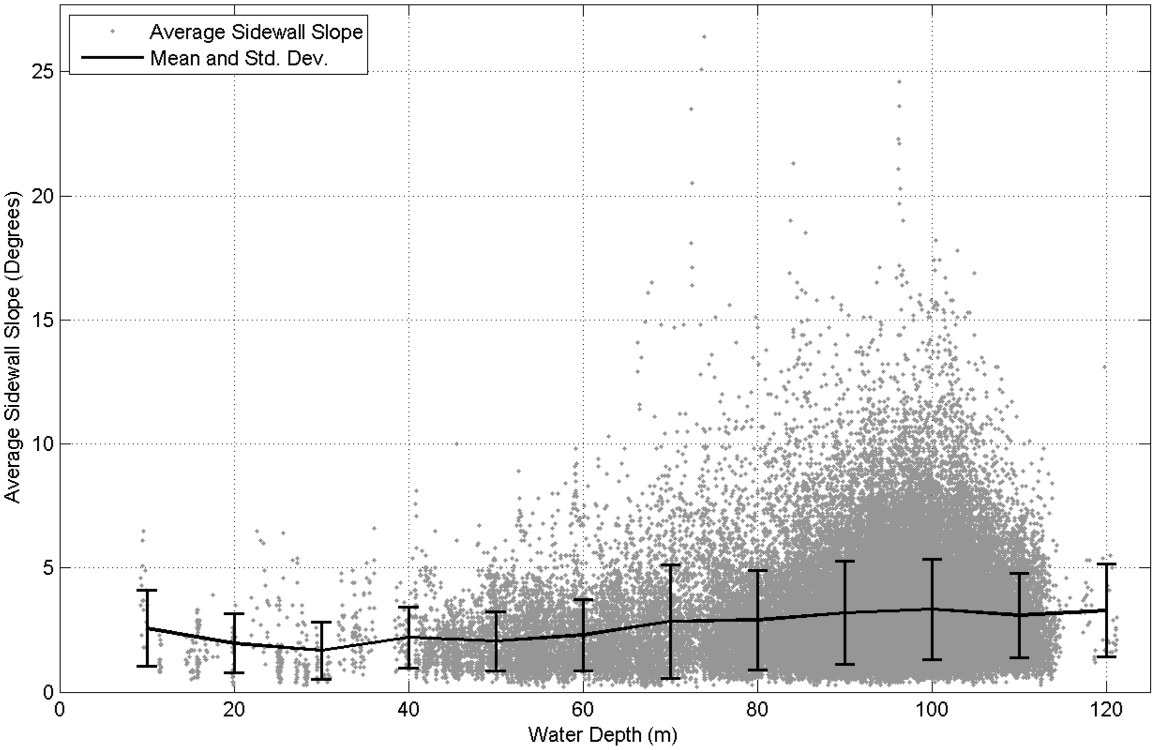

Figure 2-41 Average scour sidewall slope as a function of water depth

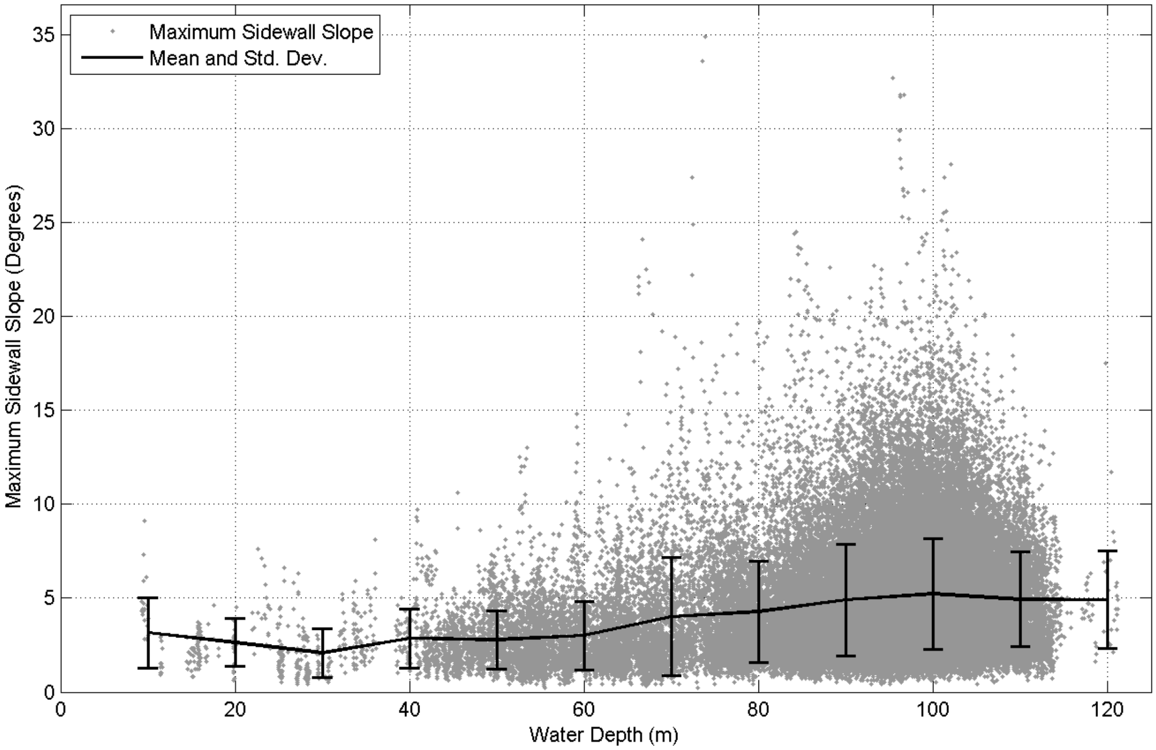

Figure 2-42 Maximum scour sidewall slope as a function of water depth

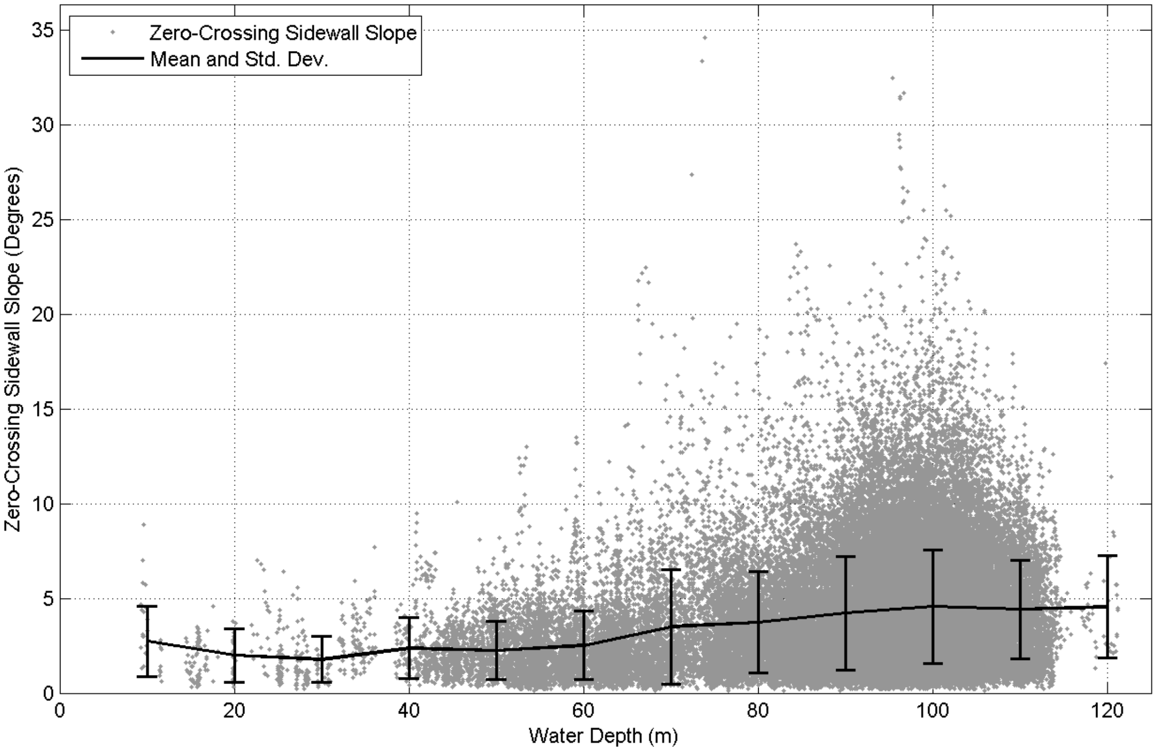

Figure 2-43 Zero-crossing scour sidewall slope as a function of water depth

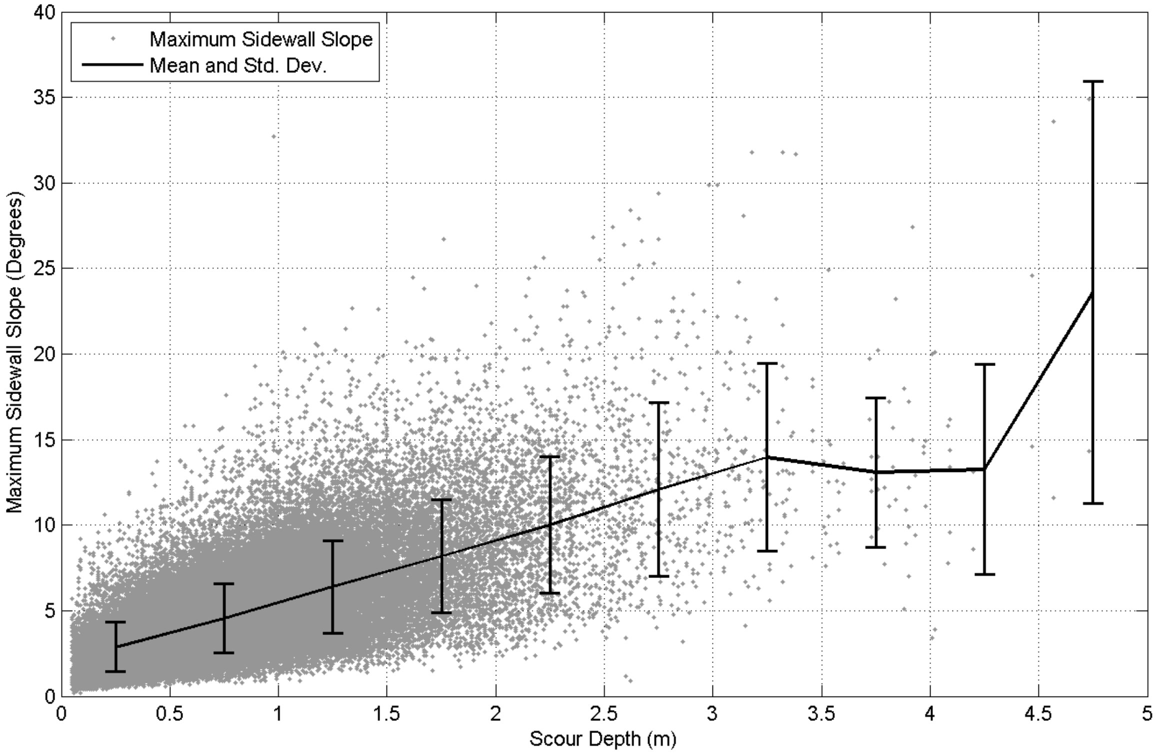

Figure 2-44 Maximum scour sidewall slope as a function of scour depth

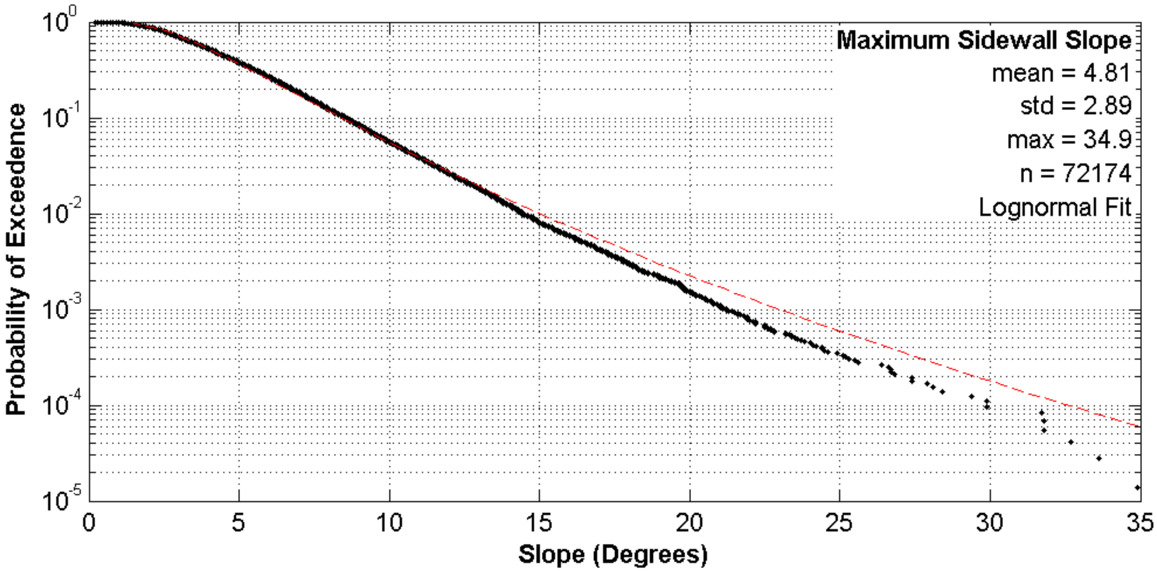

Figure 2-45 Distribution of maximum scour sidewall slope, all water depths

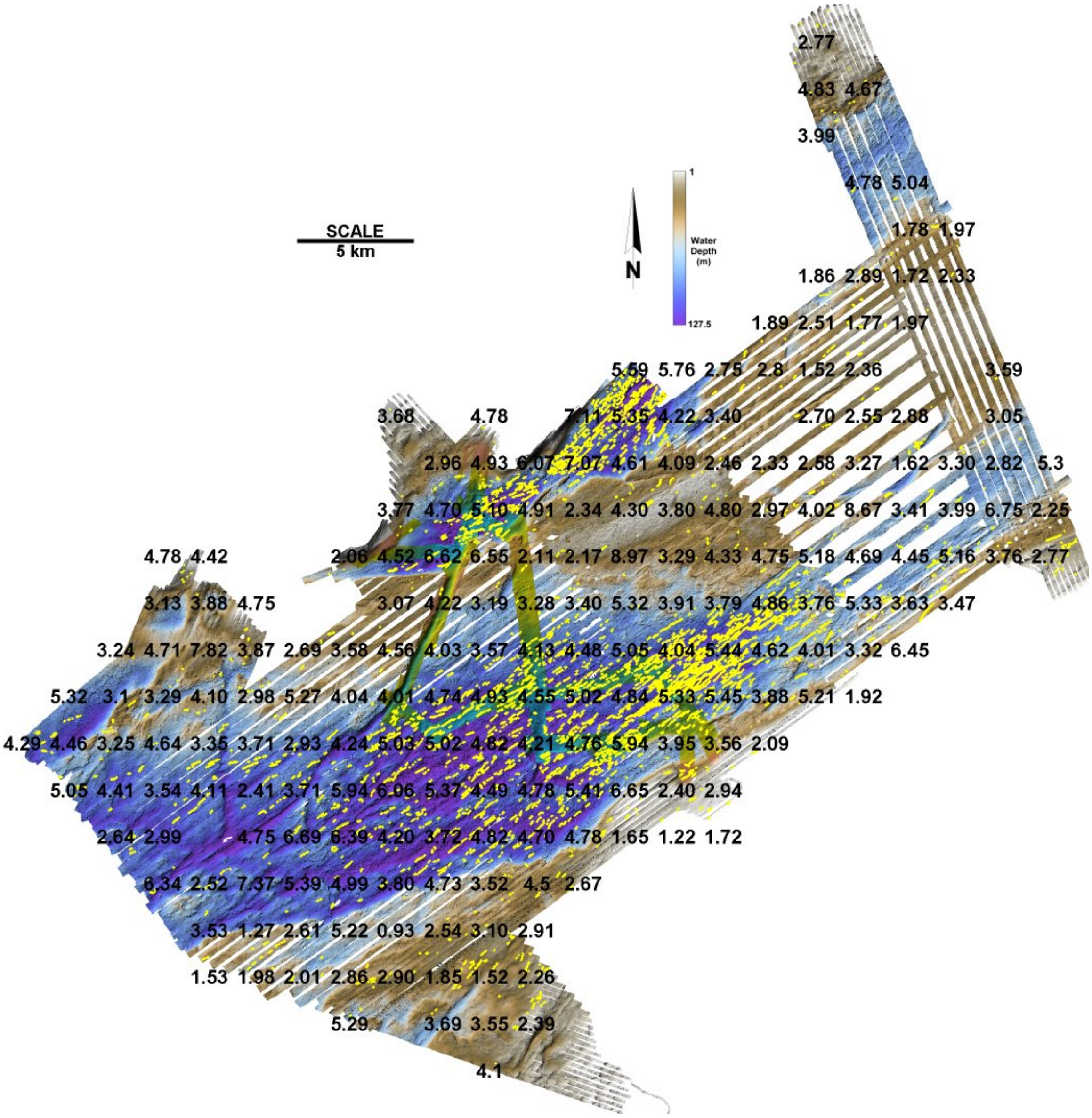

Figure 2-46 Spatial distribution of the mean of the maximum scour sidewall slope

2.3.10 *Scour Orientation*

Often it is not possible to determine the direction a scouring iceberg was traveling based on scour feature morphology. Therefore scour orientations are generally assigned values between 0° (north) and 180° (south) to indicate their overall orientation. Over 99% of 36,093 scour profiles were assigned orientations 0 - 180°. Scour orientations outside this range were reduced by 180° for analysis. An analysis of scour orientation as a function of water depth showed a marked transition of the distribution of scour orientation at 75 m water depth. Figure 2-47 shows a comparison of the distributions, and scour orientations are also given in 10° bins in Table 2-6 for the entire dataset as well as above and below 75 m water depth. Scours are highly aligned in water depths ≥ 75 m, with a peak in the 50 to 60° bin. Scours show a similar overall orientation in < 75 m water depth, but less highly aligned and a peak in the 40 to 50° bin. This difference may be related to conditions during the time of formation (i.e. relict versus modern). Figure 2-48 shows the changes in scour orientation over the survey area using 30º orientation bins.

Table 2-6 Scour orientation (0° = north) for outer and inner portions of the inner shelf

Orientation	Proportion of Profiles (%)		
	All Data	Water Depth < 75m	Water Depth ≥ 75m
0° to 10°	0.8	3.2	0.5
10° to 20°	2.0	4.8	1.6
20° to 30°	4.7	8.8	4.1
30° to 40°	11.3	13.1	11.1
40° to 50°	21.8	15.0	22.7
50° to 60°	28.7	14.4	30.6
60° to 70°	17.5	13.1	18.1
70° to 80°	7.5	7.2	7.5
80° to 90°	2.6	5.9	2.1
90° to 100°	1.2	4.0	0.8
100° to 110°	0.3	1.0	0.2
110° to 120°	0.2	1.0	0.1
120° to 130°	0.2	1.1	0.1
130° to 140°	0.2	1.3	0.1
140° to 150°	0.2	1.0	0.1
150° to 160°	0.2	1.5	0.1
160° to 170°	0.2	1.1	0.1
170° to 180°	0.4	2.5	0.1

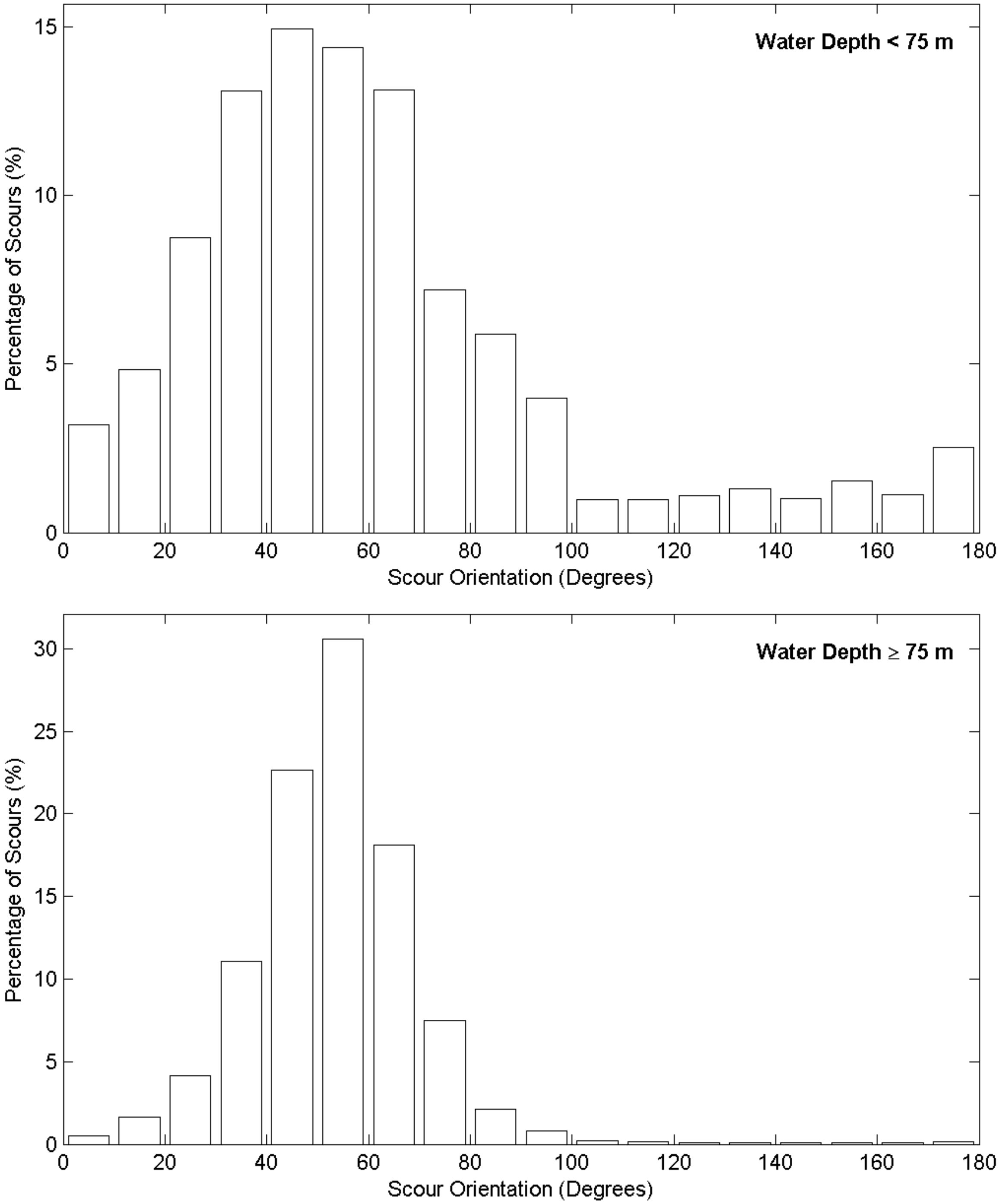

Figure 2-47 Distributions of scour orientation above and below 75 m water depth

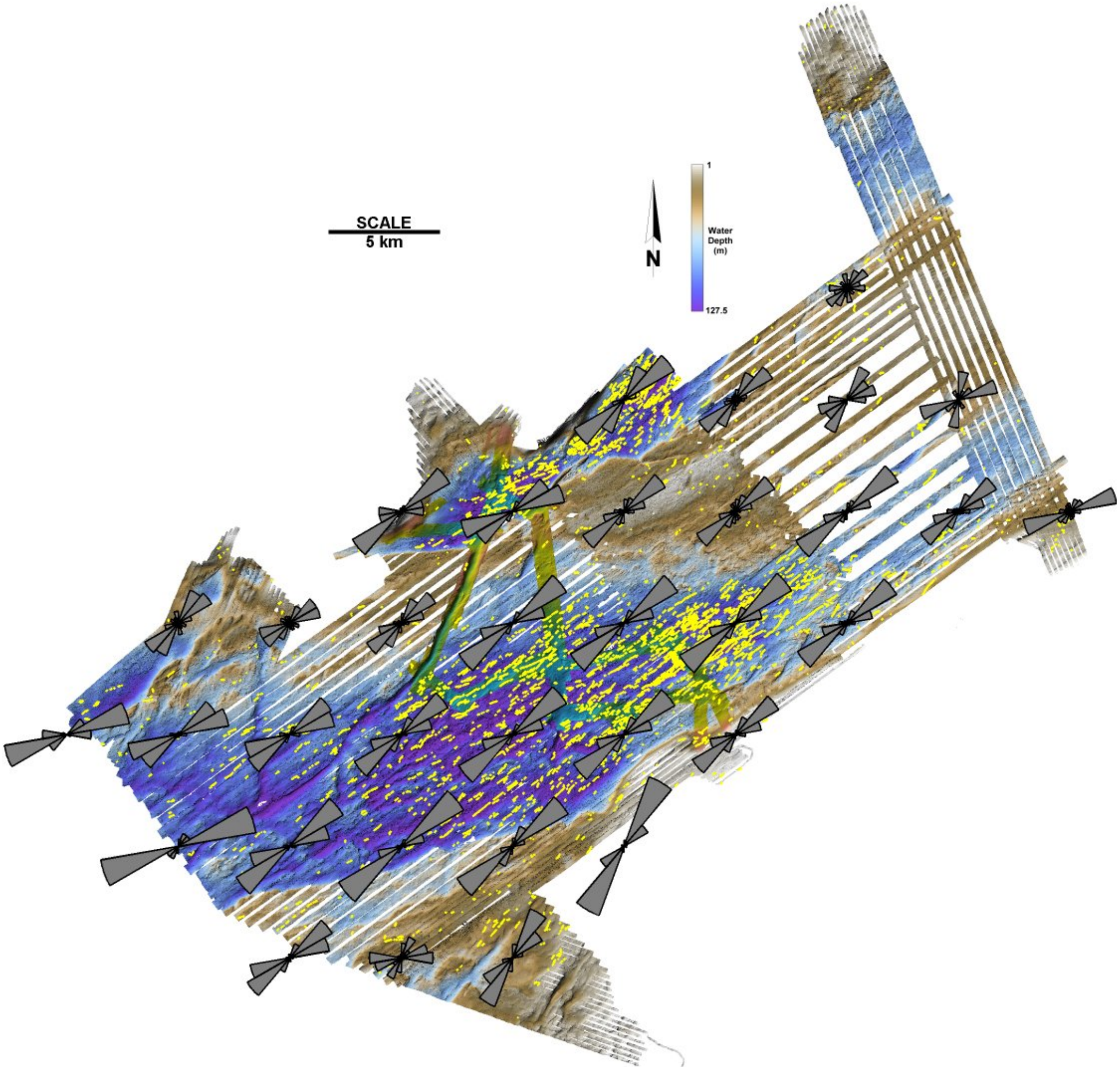

Figure 2-48 Spatial distribution of scour orientation (5 × 5 km bins, 30º orientation bins)

2.3.11 Scour Length

The mean scour length is used to calculate scour crossing rates over subsea structures, pipelines and cables. The algorithm used to calculate scour length uses the cumulative distance between the first and last valid scour profile, which nominally are at 10 m intervals. However, the first and last profiles do not correspond exactly with the end of the scour, therefore using the scour lengths as given in the scour summary database may lead to an underestimation of mean scour length. Since profiles that do not meet the quality checks are not included, the actual mean profile separation is actually greater than 10 m. A check of distances between consecutive profiles shows that the mean separation of profile is 16 m. All scour lengths were increased by 16 m to account for this effect.

Table 2-7 gives a summary of scour length statistics in 10 m water depth bins, and Figure 2-49 shows the same information with a scatter plot of scour length and water depth. Both the mean and standard deviation of scour length increase significantly beyond the 75 m water depth range, which may be indicative of relict scours. Scour lengths follow a lognormal distribution, as shown in Figure 2-50. Figure 2-51 shows the spatial distribution of mean scour length.

Table 2-7 Scour length as a function of water depth

Water Depth (m)	No. Scours	Mean (m)	St. Dev. (m)	Max. (m)
> 5 & ≤ 15	2	145.4	44.8	177.1
> 15 & ≤ 25	10	108.8	89.4	269.5
> 25 & ≤ 35	26	80.2	63.8	226.8
> 35 & ≤ 45	34	143.4	133.9	594.3
> 45 & ≤ 55	113	186.9	185.7	1095.6
> 55 & ≤ 65	156	167.8	238.8	2025.7
> 65 & ≤ 75	136	179.4	163.9	1090.9
> 75 & ≤ 85	184	262.1	301.3	2793.7
> 85 & ≤ 95	440	381.3	342.0	2420.9
> 95 & ≤ 105	653	486.9	483.5	4206.5
> 105 & ≤ 115	153	547.5	792.1	5505.6
> 115 & ≤ 125	3	250.9	105.0	359.1
All	1,910	365.7	439.4	5505.6

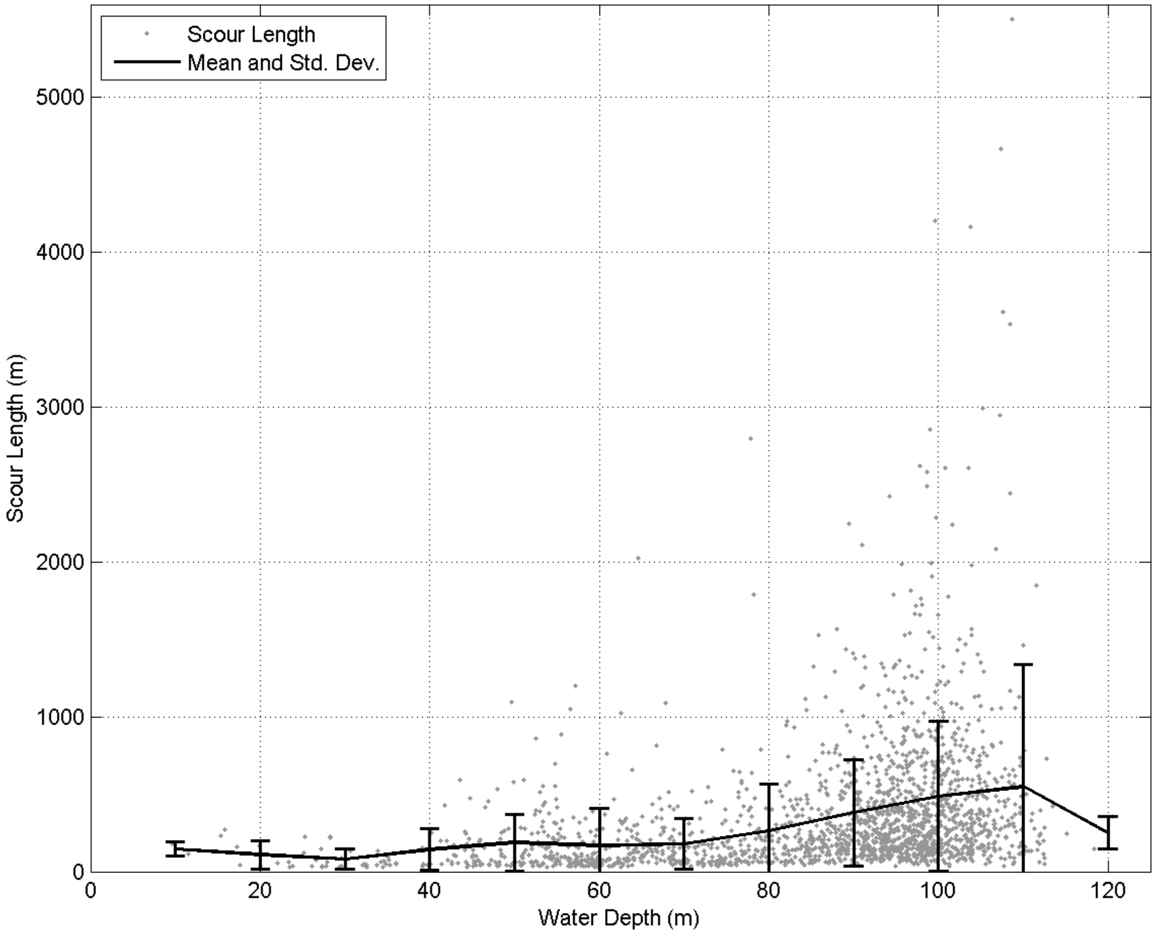

Figure 2-49 Scour length as a function of water depth

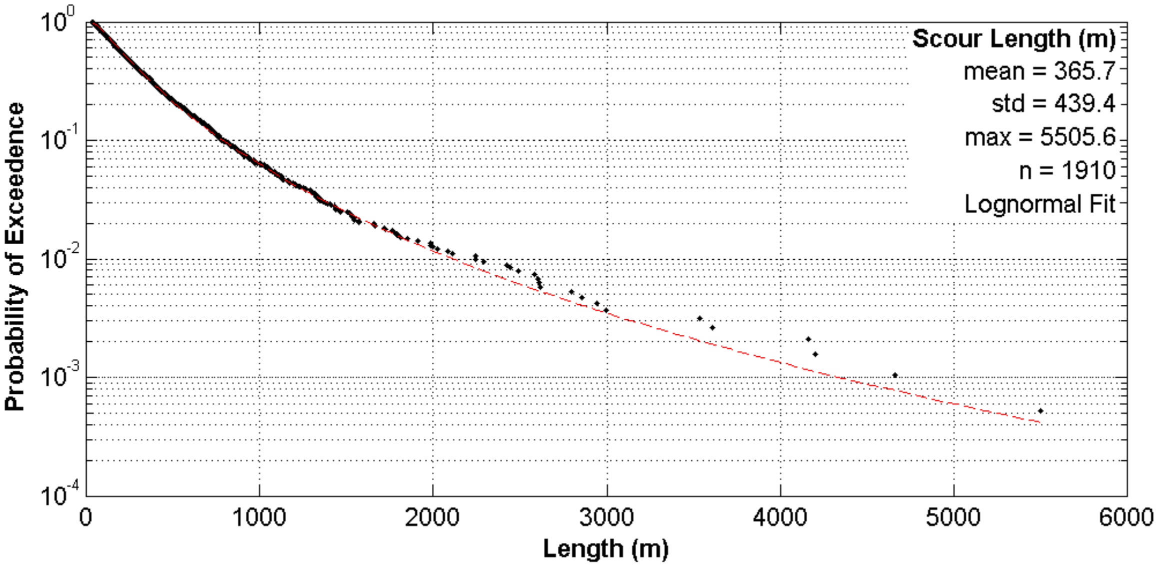

Figure 2-50 Scour length distribution

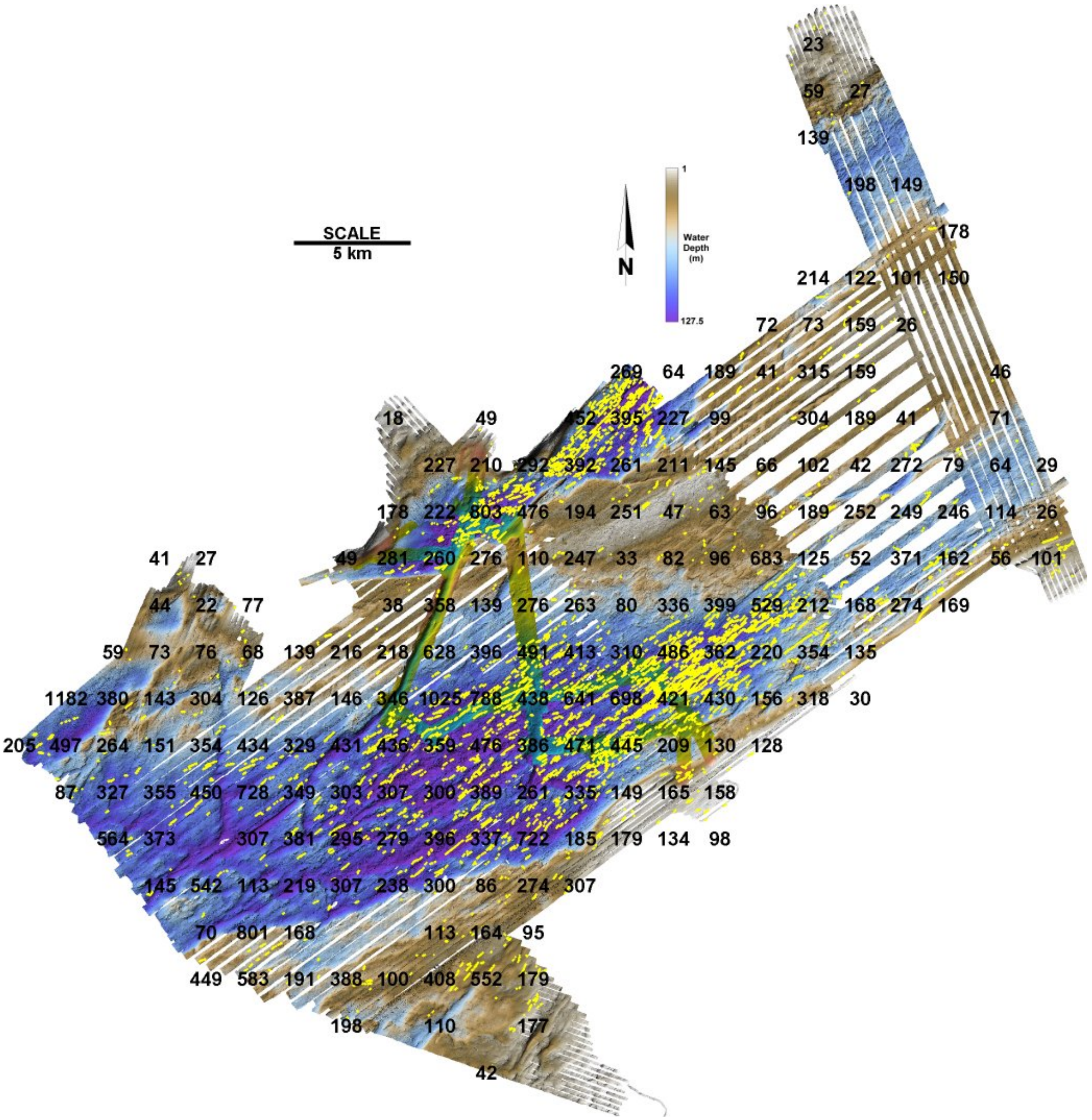

Figure 2-51 Spatial distribution of mean scour length

2.3.12 Scour Rise-Up

Scour rise-up is defined as the change in water depth over the length of the scour. This parameter is of interest in this study as scour rise-up may give an indication of the tendency of icebergs to scour over the shallow bank to the northeast of the cable crossing site and potentially damage the cable.

Table 2-8 gives a summary of scour rise-up statistics in 10 m water depth bins, and Figure 2-52 gives the same information with a scatter plot of scour rise-up and water depth (the mean water depth along the scour). Both the mean and standard deviation of scour rise-up increase significantly beyond the 65 m water depth range, which may be indicative of the presence of relict scours. As shown in Figure 2-53, scour rise-up follows a lognormal distribution.

The spatial distribution of mean scour rise-up over the survey area is shown in Figure 2-54. Figure 2-55 shows the cable crossing site in more detail, and scours with rise-up in excess of 10 m are indicated. While there are a number of scours with rise-ups in excess of 10 m crossing over the cable routes, none appear to have been formed by an iceberg scouring over the shallow bank immediately to the northeast. From this, it can be concluded that this mechanism is not a significant source of risk to the cable(s).

Table 2-8 Scour rise-up as a function of water depth

Water Depth (m)	No. Scours	Mean (m)	St. Dev. (m)	Max. (m)
> 5 & ≤ 15	2	0.52	0.35	0.77
> 15 & ≤ 25	8	0.72	0.77	2.30
> 25 & ≤ 35	17	0.50	0.46	1.77
> 35 & ≤ 45	30	1.20	0.96	3.66
> 45 & ≤ 55	108	0.98	1.05	7.06
> 55 & ≤ 65	143	1.12	1.21	7.07
> 65 & ≤ 75	133	1.74	2.10	13.17
> 75 & ≤ 85	180	1.94	2.04	13.51
> 85 & ≤ 95	434	2.53	2.22	12.41
> 95 & ≤ 105	644	3.06	2.81	20.83
> 105 & ≤ 115	153	3.14	3.07	15.85
> 115 & ≤ 125	3	4.26	5.82	10.98
All	1,855	2.40	2.49	20.83

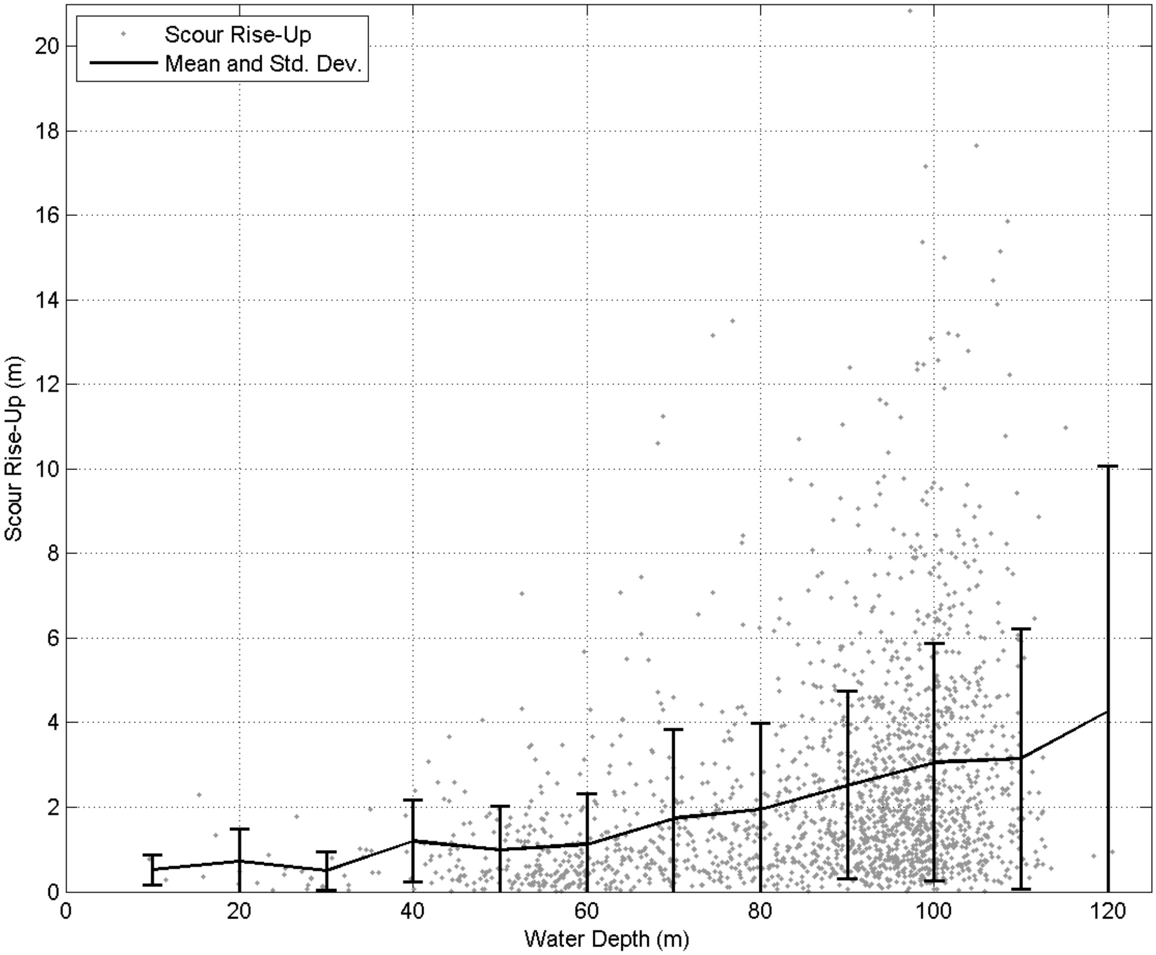

Figure 2-52 Scour rise-up as a function of water depth

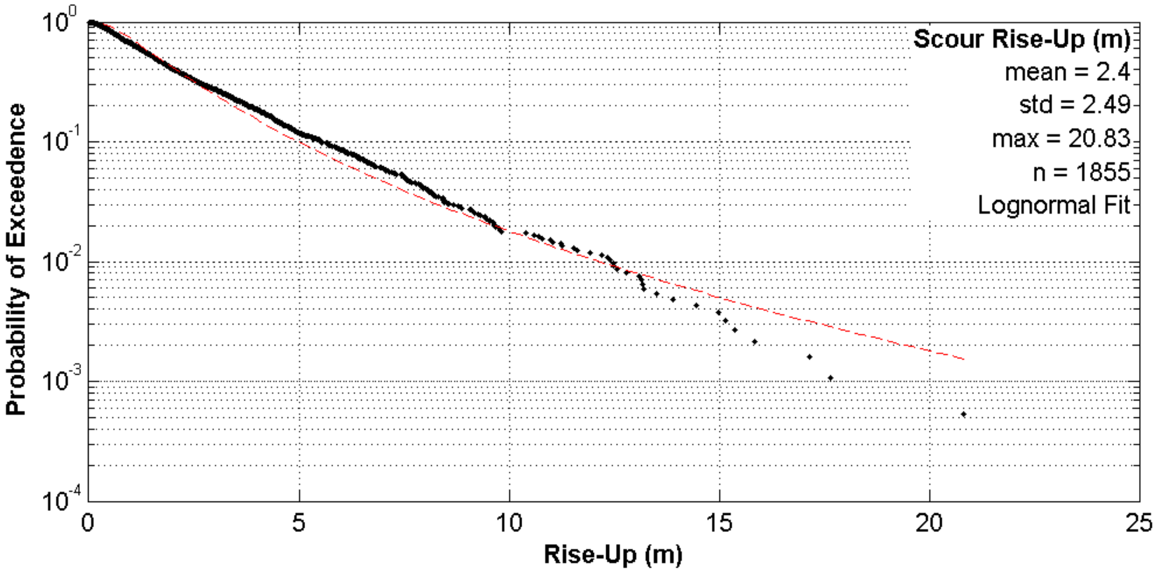

Figure 2-53 Scour rise-up distribution

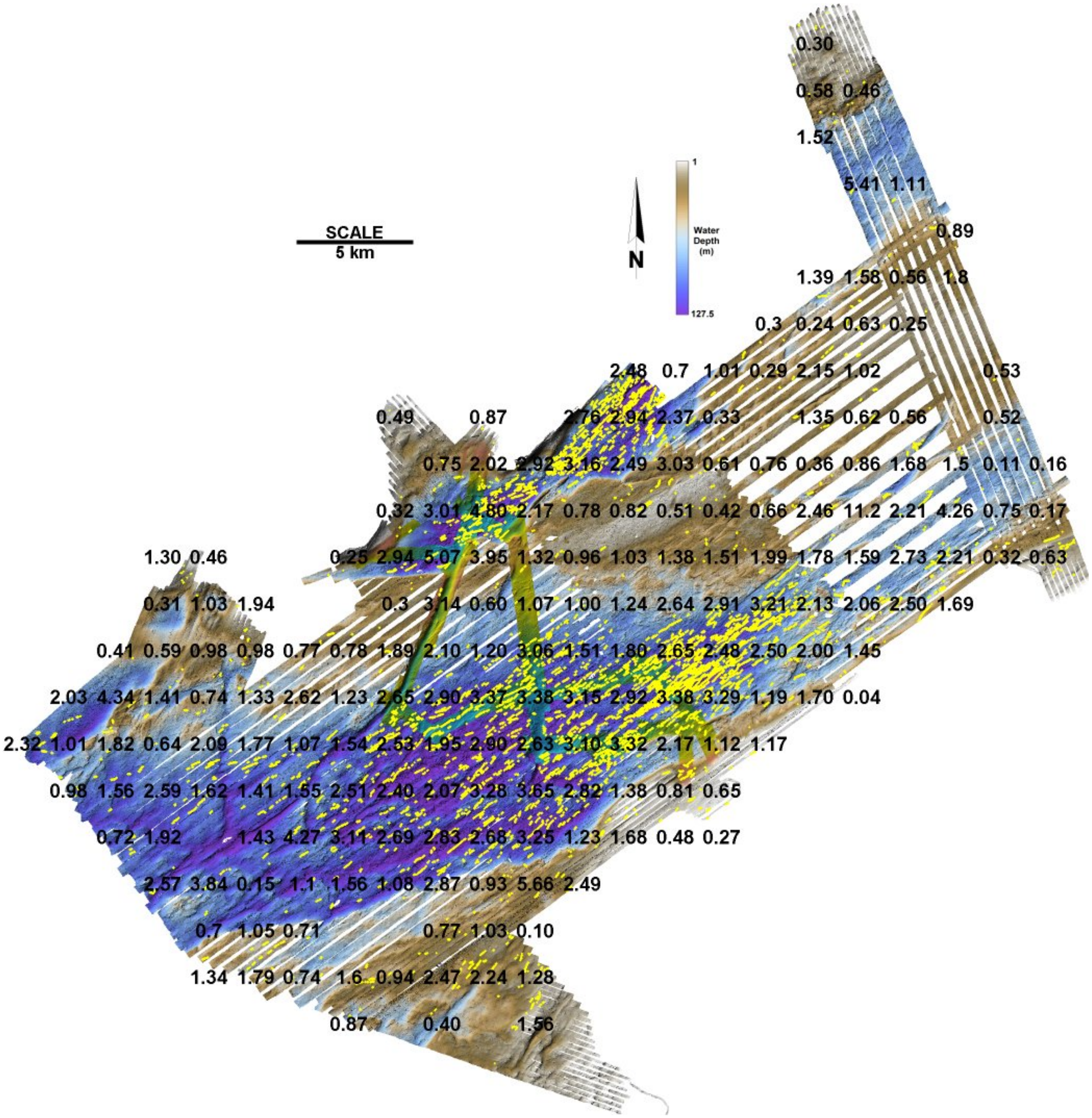

Figure 2-54 Spatial distribution of scour rise-up

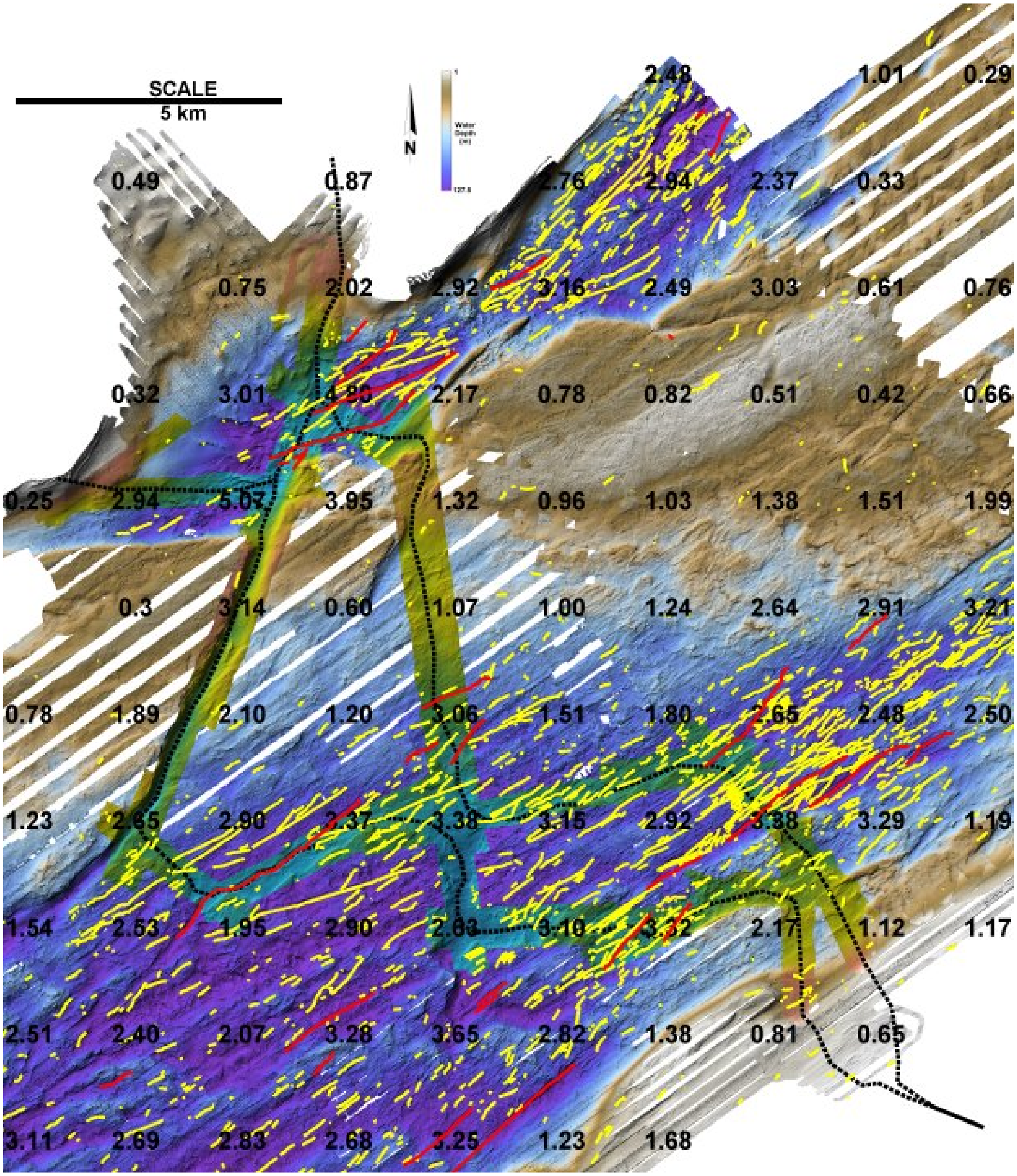

Figure 2-55 Scour rise-up in vicinity of cable crossings (dashed line), scours with rise-ups in excess of 10 m shown in red

2.3.13 Conclusions

The iceberg scour dataset described here is the first systematic assessment of the scour regime in the Strait of Belle Isle. The scour data was derived from ~ 706 km^2 of multibeam data acquired in 2007 and 2009, covering a water depth range of 1 to 128 m. The data population consists of 1,910 measured scours (276 scours were rejected due to scour depth and data limitations) with 36,093 cross-sectional profiles extracted at 10 m intervals along each scour feature. Table 2-9 gives a summary of the scour parameters extracted from the dataset. The scour orientation is highly directional, with a dominant southwest-northeast orientation.

The observed spatial distribution of iceberg scours was unexpected, with the majority of scour features occurring in deeper water in areas thought to be sheltered by bathymetric highs (banks) immediately to the northeast of the cable-crossing site. These features are thought to be predominantly relict features associated with previous glacial events and not indicative of the modern iceberg scour regime. An analysis of the scour data indicated a change, generally in the 70 - 75 m water depth range, characterized by deeper, wider, and longer scours with higher berms, steeper sidewall slopes and increased rise-ups. These changes are characterized by increased mean values, as well as standard deviations. However, it should be noted that criteria have never been established for characterizing relict scours on the basis of geometry, and there is no basis for definitively stating that all scours in deeper water depths in the area of interest are relict features.

Table 2-9 Scour parameter summary

Parameter	Mean	Std. Dev.	Maximum
Density (#/km^2, using 2 × 2 km grid)	2.70	3.64	18.5
Depth (m)	0.81	0.50	4.73
Incision Width (m)	39.1	16.8	132.1
Berm-to-Berm Width (m)	52.8	20.3	155.0
Berm Height (m, excluding 9.2% zeros)	0.42	0.32	3.90
Depth of Disturbance – Max. (m)	1.35	0.75	7.77
Sidewall Slope – Max (°)	4.81	2.89	34.9
Length (m)	365.7	439.4	5,505.8
Rise-Up (m)	2.40	2.49	20.8

3 ICEBERG CONTACT MODEL

3.1 Introduction

A cable laid on the seabed is potentially subject to contact with free-floating and scouring icebergs (see Figure 3-1). Geometric approaches for calculating iceberg risk (i.e. King, 2002) assume a simple, exposed seabed geometry and are not appropriate for the Strait of Belle Isle, where the bathymetry is complex and convoluted, sheltering much of the seabed from icebergs (Figure 3-2). Icebergs in the Strait of Belle Isle drift in from the Labrador Sea and pass over a shoal with an approximate maximum water depth of 70 m before drifting through the cable crossing area. Most of the proposed cable routes are in water depths greater than 70 m where the cables are at least partially sheltered from iceberg interaction (C-CORE, 2007). An assessment of the iceberg contact rate for a cable laid on the seabed must include the sheltering effect of local bathymetry. The approach adopted here is a drift-based Monte Carlo model which incorporates seabed bathymetry and simulates the drift of icebergs over the area of interest, allowing the effect of bathymetry on iceberg interaction with the seabed (or cable on the seabed) to be evaluated. An iceberg contact to a cable in a sheltered area of the seabed may occur when the iceberg scours up over the sheltering bathymetric feature through a process called rise-up, or when the iceberg drifts over the sheltering bathymetric feature, rolls and adopts a deeper draft. Both of these processes have been observed in the field. The Monte Carlo model incorporates the iceberg rolling process, but an assessment of the rise-up phenomena is outside the scope of this report.

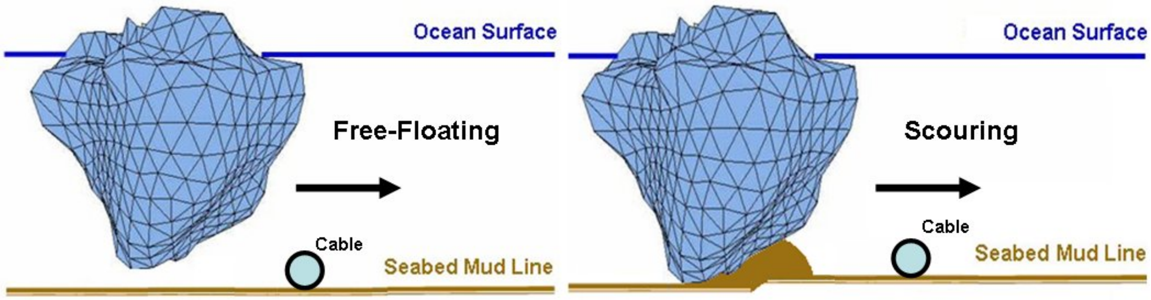

Figure 3-1 Free-floating and scour iceberg impacts with a cable laid on the seabed

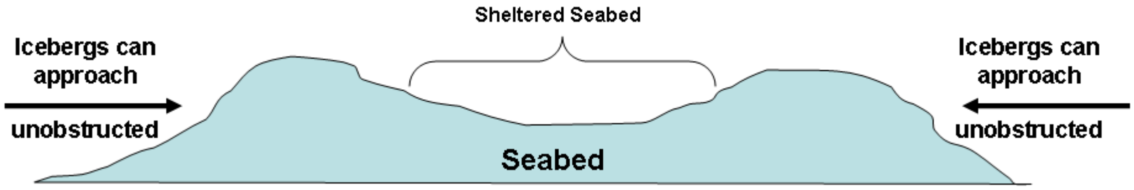

Figure 3-2 Iceberg exposure for sheltered and exposed seabed (C-CORE, 2010)

3.2 Model Overview

The iceberg contact model is a Monte Carlo simulation that models the distribution of iceberg groundings and incidences where iceberg keels are close enough to contact a cable on the seabed (nominally 100 – 120 mm diameter). Figure 3-3 shows a flowchart outlining the operation of the Monte Carlo model. An iceberg is introduced at a defined starting location and assigned an initial waterline length (from an observed size distribution), and a mass and draft (from established length/mass/draft relationships). The iceberg is then moved into the Strait of Bell Isle in 1-hour time steps using a simple autoregressive drift model that incorporates observed iceberg drift data. As the simulation progresses, the mass of the iceberg is reduced to simulate the deterioration (i.e. melting) process and the draft is reduced accordingly. Since icebergs are observed to roll and change drafts, the iceberg draft is occasionally adjusted within the constraints of the mass/draft relationship. During each time increment, the water depth at the iceberg location is checked against the iceberg draft. If the iceberg draft exceeds the water depth, the iceberg is considered grounded and is immobile until its draft decreases sufficiently through melting to refloat. Locations where the draft exceeds the water depth, or the keel is within 1 m of the seabed, are saved. Once the iceberg mass decreased to a defined minimum value (roughly equivalent to a bergy bit) the simulation is terminated. If the iceberg drifts outside the defined model area the simulation is also terminated.

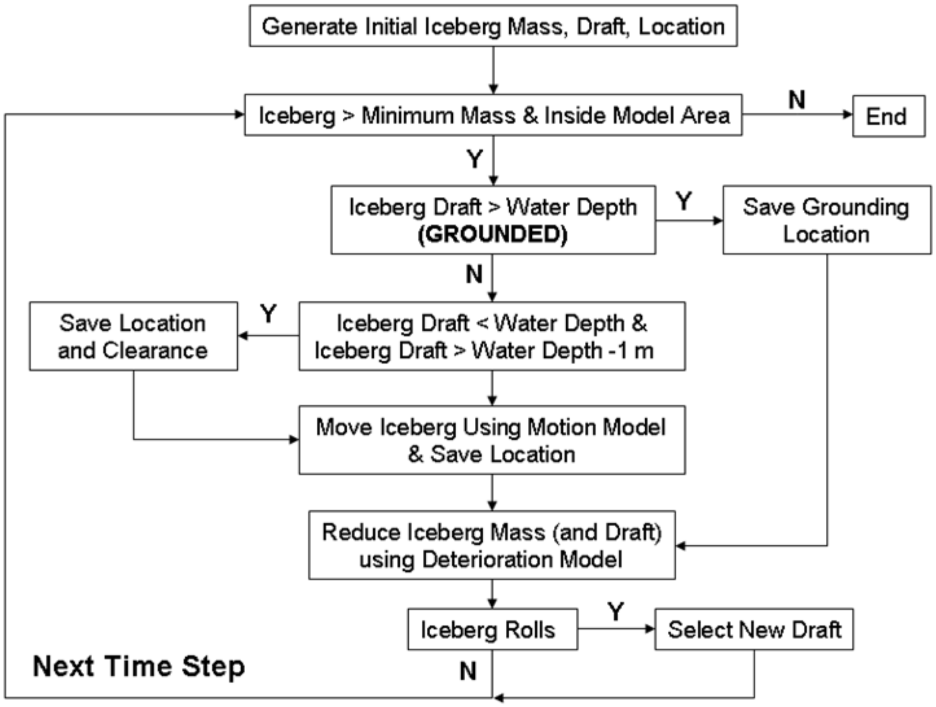

Figure 3-3 Flowchart for Monte Carlo iceberg contact model

3.3 Model Input

The following sections outline the various input parameters used in the Monte Carlo model. These include bathymetry, iceberg size distribution, iceberg size/mass/draft relationships, deterioration rates, draft changes and drift characteristics.

3.3.1 Bathymetry

The bathymetry data used in the model was derived from multibeam surveys of the cable crossings and adjacent areas, as well as regional bathymetric data provided by the Canadian Hydrographic Service (CHS). Multibeam data was collected by Fugro Jacques GeoSurveys Inc. in the Strait of Belle Isle in 2007 (reconnaissance and subsea cable route surveys) and 2009 (tunnel route survey). These data were merged into one data file as shown in Figure 3-4. This dataset consists of 29,529,845 points and covers approximately 700 km^2. Data resolution varies, with 5 m resolution in deeper water and 3 m resolution in shallower water. Also shown in Figure 3-4 are proposed cable routes.

Figure 3-5 shows the regional bathymetric data supplied by the CHS. The resolution of this dataset is 0.0045º latitude and longitude (approximately 500 m north-south and 305 east-west). Also indicated in Figure 3-5 are the coverage of the multibeam data and the proposed cable routes. Some processing of the CHS dataset was required (i.e. to remove null data points) prior to merging with the multibeam data.

The two datasets were combined to create one bathymetry data file for use in the Monte Carlo model. It was necessary to optimize the size of the bathymetry data file to avoid excessive model run times (initial model runs with an unoptimized bathymetry file were in excess of 35 minutes, with a single model run simulating 500 icebergs and thousands of runs required to produce a suitable dataset). The bathymetry data file was optimized by varying the resolution. In the immediate area of the cable crossing a resolution of 0.0005º was used (56 m north-south and 35 m east-west), with decreasing resolutions of 0.005º used where a lower resolution was considered acceptable. A resolution of 0.01º was used on the edge of the model area. The final bathymetry file with resolution of various zones is shown in Figure 3-6. The resulting bathymetry data file is a raster with 596 rows and 791 columns. The shoal responsible for filtering of deep draft icebergs is clearly visible to the northeast of the cable crossing location.

Figure 3-7 (insert) shows the west cable route with markers at 1 km intervals. The water depth profile interpolated from the high-resolution multibeam data is shown as a black line. The red dashed line shows the water depth profile interpolated from the merged bathymetry dataset. The close agreement between the two water depth profiles shows minimal degradation in the accuracy of the bathymetry data in the vicinity of the cable routes.

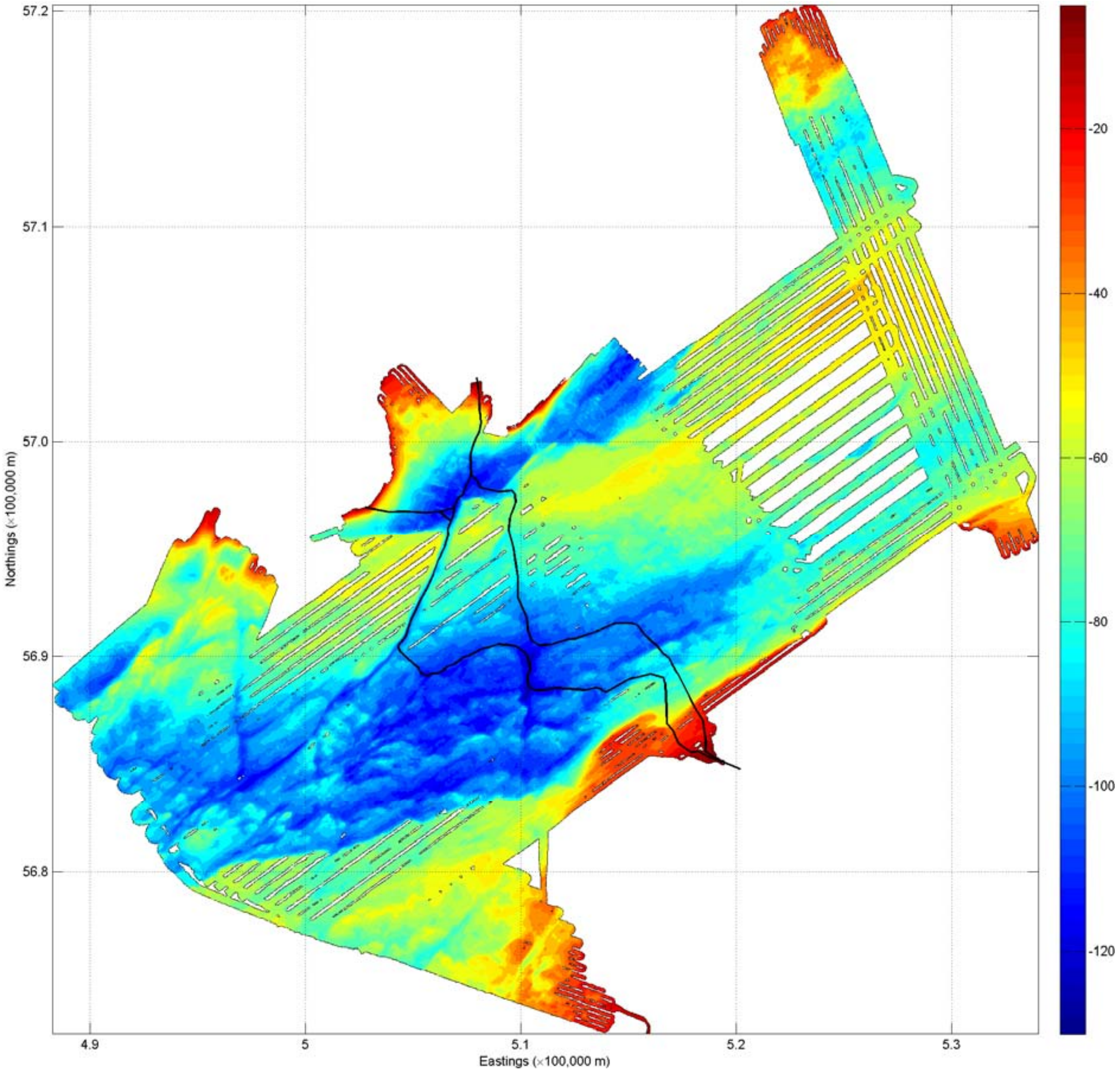

Figure 3-4 Multibeam dataset with proposed cable routes

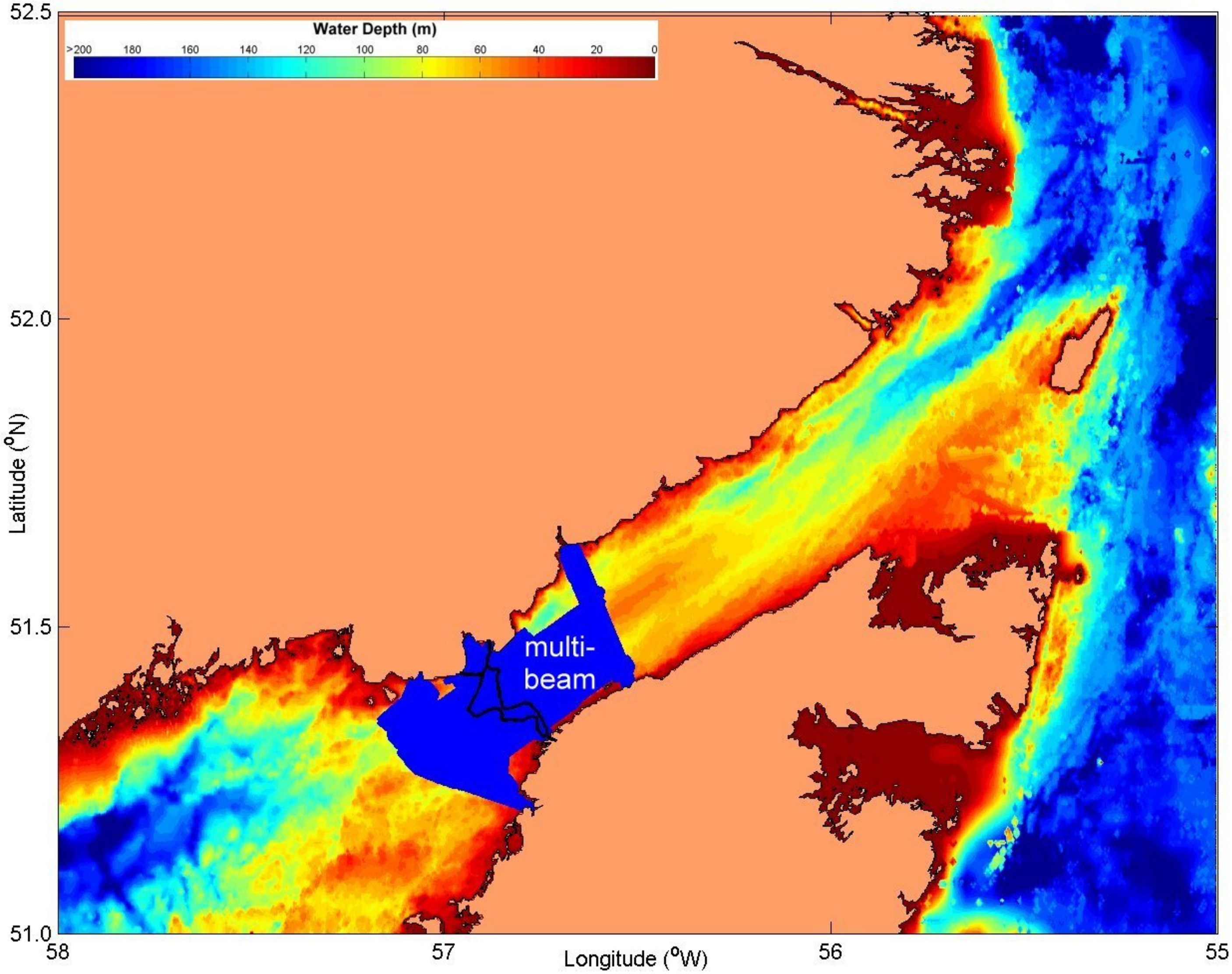

Figure 3-5 Regional CHS bathymetry, along with multibeam coverage and proposed cable routes

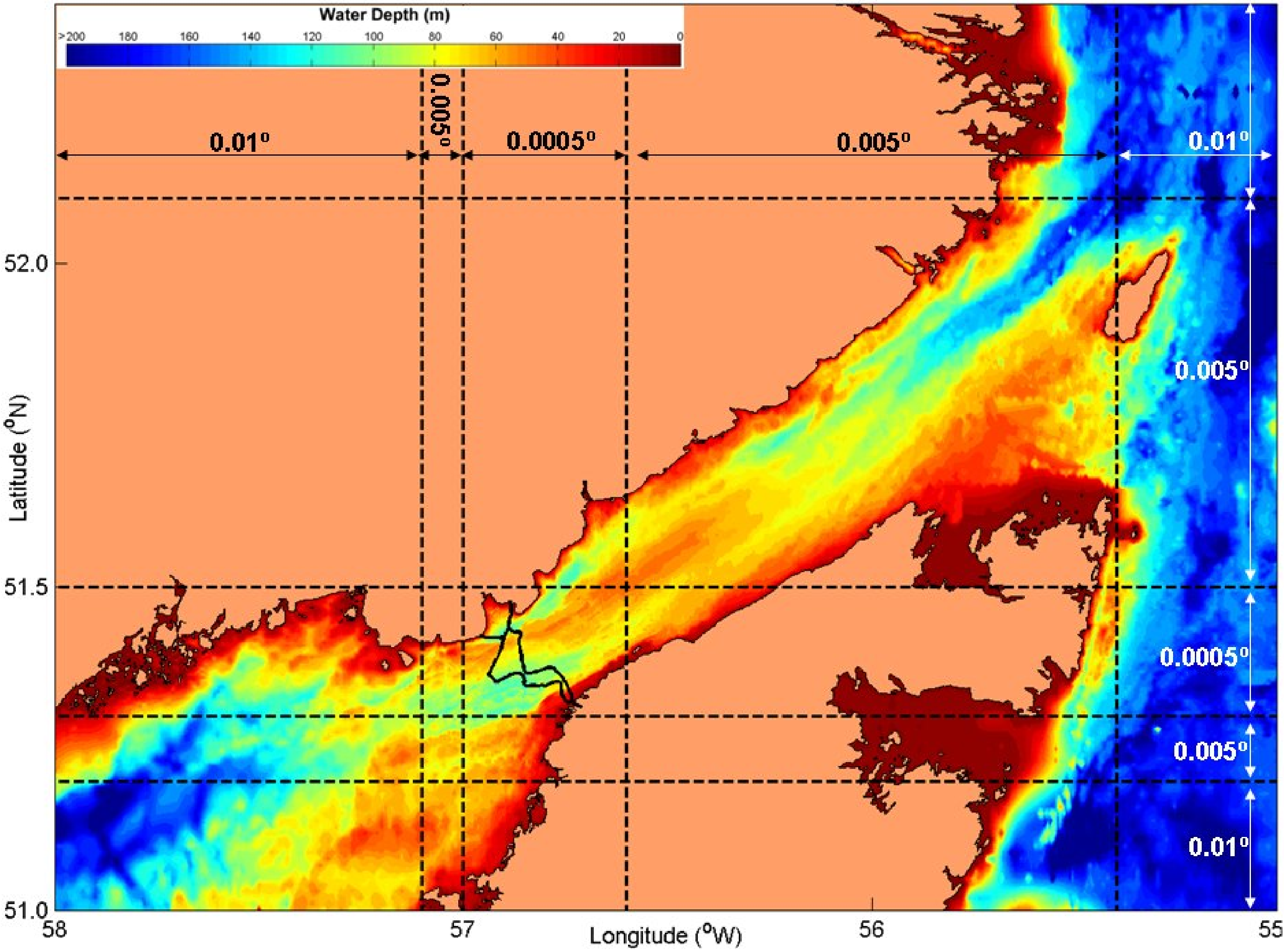

Figure 3-6 Final combined bathymetry dataset with gridding resolution in various zones indicated

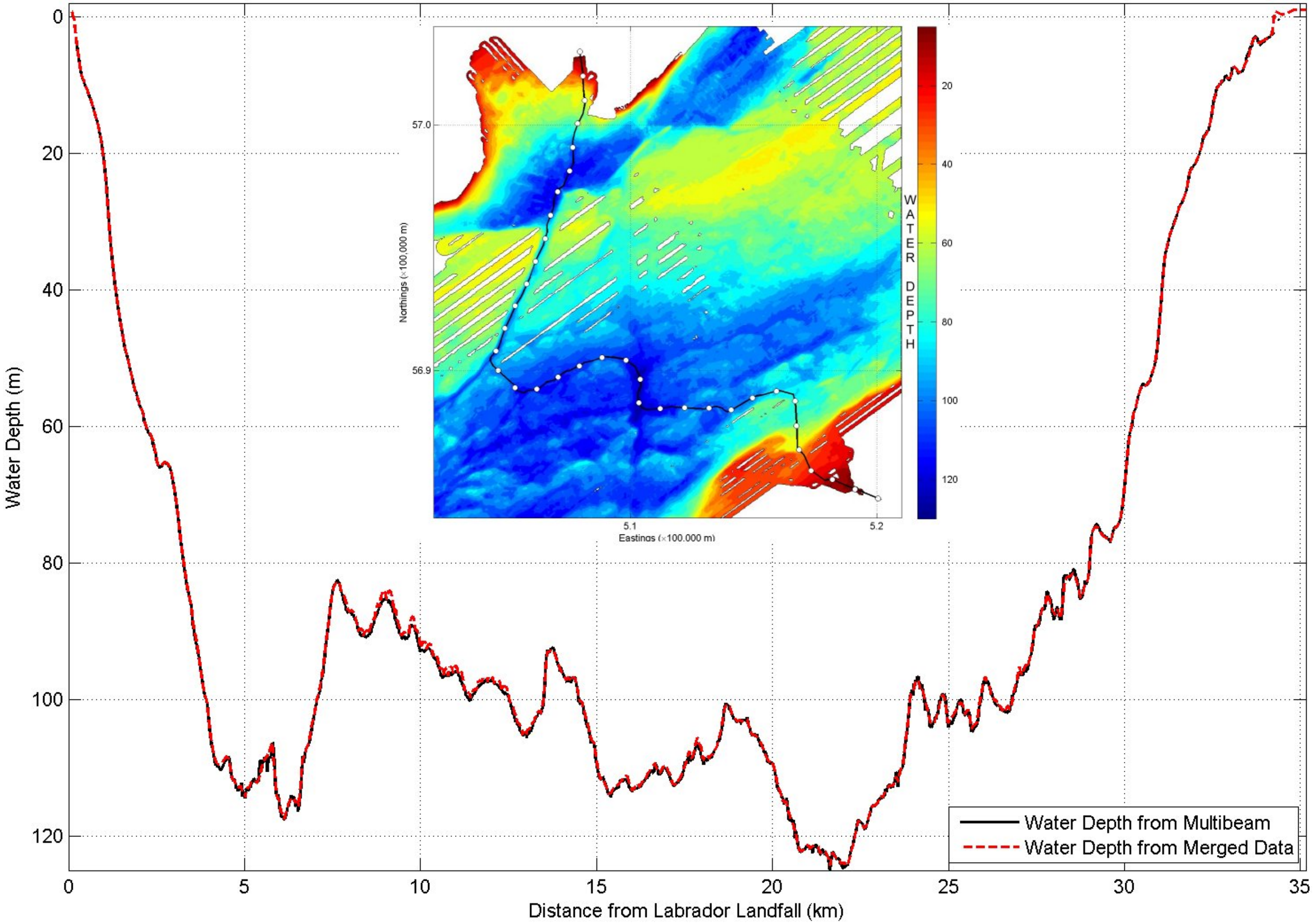

Figure 3-7 Water depth profile along west cable route using multibeam and merged dataset

3.3.2 *Iceberg Waterline Length*

For each model run, a population of icebergs (i.e. typically 500) is generated with an initial waterline length distribution based on iceberg sizes observed in the field. The iceberg waterline length is the maximum horizontal iceberg dimension at its waterline. The initial waterline dimension is used to generate an initial iceberg mass and draft. After this step, the iceberg waterline length is no longer used in the Monte Carlo model (only changes in mass and draft are considered). When selecting a waterline length distribution, care must be exercised to ensure it is not based on a biased dataset. The iceberg waterline length distribution on the Grand Banks follows an exponential distribution with a mean of 59 m (Jordaan et al., 1995). Iceberg waterline length distributions for offshore Labrador have been addressed by King (2002) and King et al. (2009). Substantial variations between datasets have been noted, both in terms of the mean waterline length and the nature of the distribution (see Figure 3-8). However, when combined, the overall distribution is very similar to that inferred for the Grand Banks. A dataset with notably larger waterline lengths was compiled of icebergs towed during management activities on the Labrador Shelf during the 1970s and 1980s (PAL, 2005). This dataset may be biased since waterline lengths for many smaller icebergs were not recorded. The Monte Carlo model uses an exponential waterline length distribution with a mean of 59 m, with waterline lengths less than 15 m excluded.

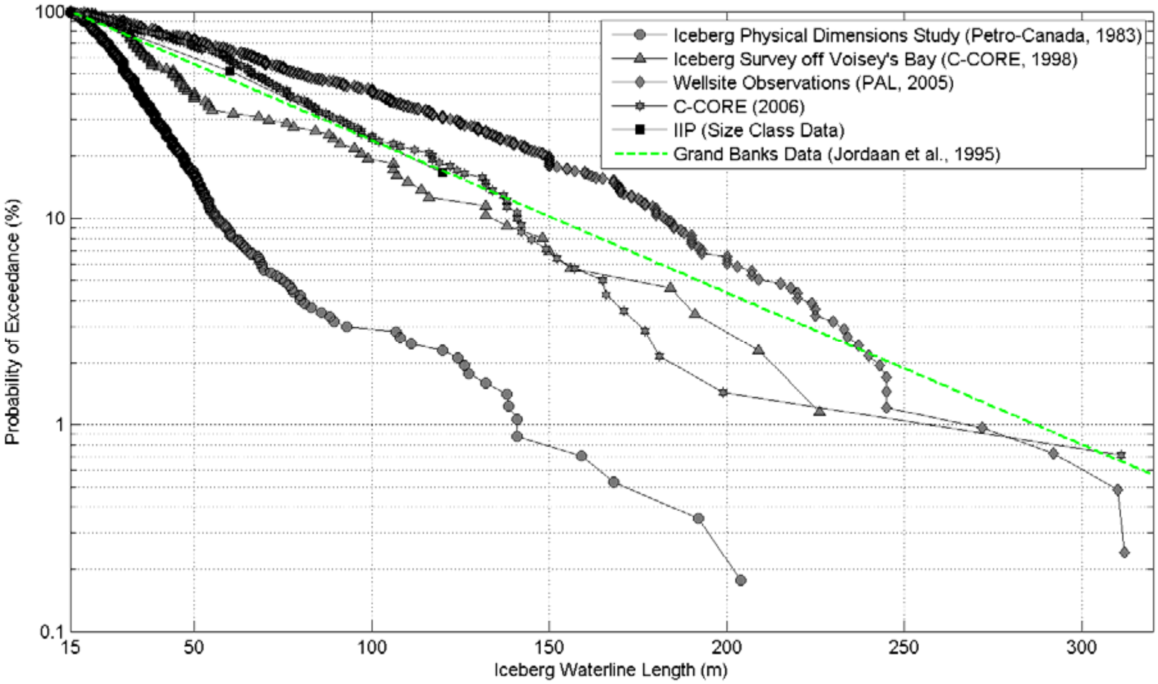

Figure 3-8 Iceberg waterline length distributions, Grand Banks and Labrador Shelf (from King et al., 2009)

3.3.3 Iceberg Mass and Draft

Using the initial iceberg waterline length distribution described in Section 3.3.2, the corresponding iceberg mass for each simulated iceberg was generated using the following relationship:

$$M_i = exp(ln(1.05) + 2.68\ ln(L_i) + N(0,0.607)) \qquad (3.1)$$

where M_i is the iceberg draft, L_i is the waterline length and $N(0,0.607)$ is a normally-distributed random variable with a mean of 0 and a standard deviation of 0.607. The associated iceberg draft, D_i, for each iceberg was then generated from the mass using:

$$D_i = exp(ln(2.05) + 2.68\ ln(M_i) + N(0,0.217)) \qquad (3.2)$$

where $N(0,0.217)$ is a normally-distributed random variable with a mean of 0 and a standard deviation of 0.217. The datasets used to derive these expressions are shown in Figure 3-9, along with best-fit lines, equations and R^2 values.

Icebergs occasionally roll and, as a result, undergo a change in draft. As a result, an iceberg can drift over an obstruction (or an enclosed basin) and then change draft, grounding in an area where it would not otherwise be possible. In order to simulate this process, it was necessary to determine the rate at which icebergs roll and the potential associated variation in draft. While iceberg rolling events are frequently noted during iceberg monitoring or management operations on the Grand Banks, the icebergs must be monitored continuously in order to determine the rolling actual rate. Veitch et al. (2001) described a field program in which two small icebergs grounded off the coast of Newfoundland (≈ 50 – 60 m waterline length) were observed continuously for a period of approximately one week. Based on the number of observed fragmentation and foundering events designated as “significant”, it was estimated that these icebergs rolled (or underwent some sort of draft adjustment) every three days, on average. This likely represents an upper-bound value, particularly for larger icebergs and lower melt rates. This is a very limited dataset, and additional observations are required.

During a rolling event, a new draft was generated using Equation 3.2 for the current mass of the iceberg and by sampling a new random term from a normal distribution with a mean of 0 and a standard deviation of 0.217. For the base case simulation it was assumed that the iceberg rolling rate was once every three days (on average), or a probability of 1/72 (1.4%) of rolling during any 1 hour model time step.

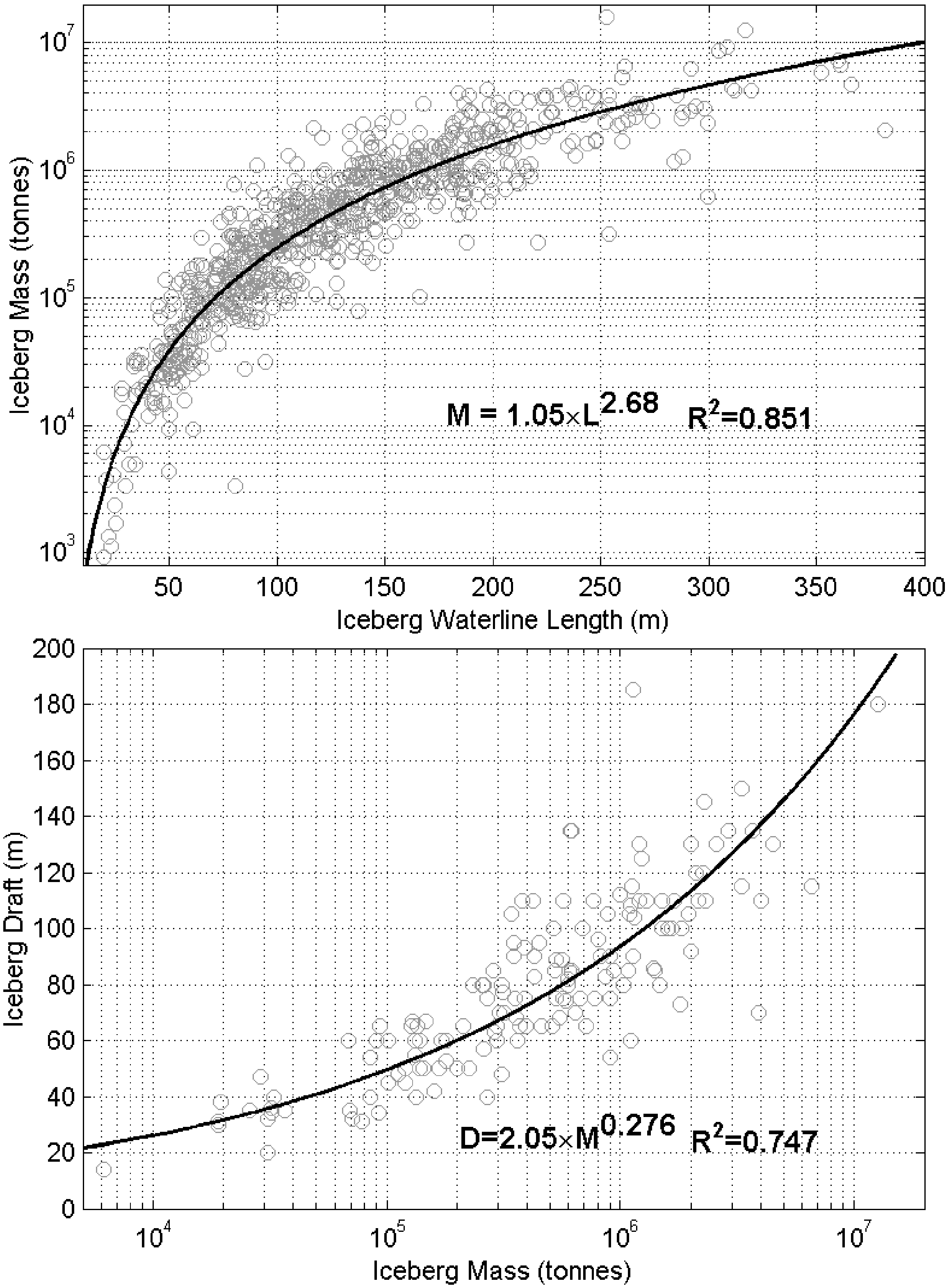

Figure 3-9 Iceberg length/mass data (top) and mass/draft (bottom) relationships

3.3.4 Iceberg Deterioration

Iceberg deterioration rates were based on output from the CIS iceberg drift model (Carrieres et al., 2001). The CIS iceberg drift model allows the initial iceberg size, location and date, to be specified, with the iceberg waterline length updated during each 1-hour time step using a deterioration model and hindcast metocean conditions. Although the CIS iceberg drift model was not accessible during the execution of this project, datasets generated during previous projects (i.e. C-CORE, 2010) were able to be utilized. The CIS model was run for a range of iceberg waterline lengths (15, 50, 100, 150, 200, 250 and 300 m) to model melt rates at monthly intervals between 2000-2006. Figure 3-10 shows sample iceberg tracks generated during a two-day modeling period. A point was not specified in the Strait of Belle Isle, so the closest data (latitude 51 º30' N, longitude 55º W) was used to estimate iceberg deterioration rates for the area of interest.

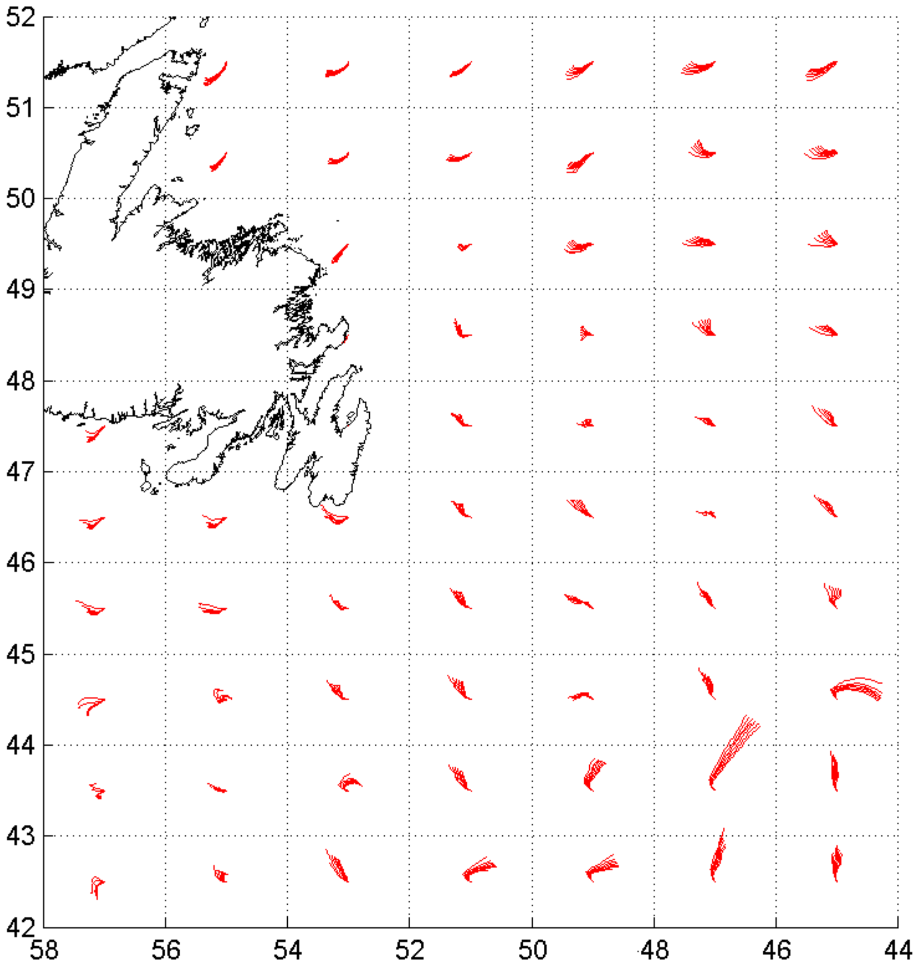

Figure 3-10 Sample trajectories for icebergs of varying initial waterline lengths over two day period

Table 3-1 gives the mean monthly melt rates, in terms of hourly decrease in waterline length, for the specified initial iceberg waterline lengths. A weighted average hourly decrease in waterline length was calculated using the average number of icebergs present per month, derived from Canadian Ice Service iceberg charts (covering the period from May 1988 to October 2010). These mean values, for the degree square covering 51º N to 52º N and 56º W to 57º W, are shown in Figure 3-11. These mean hourly waterline length decreases were used to calculate mean hourly mass decreases using Equation 3.1 (and including a smearing factor of 1.19 to account for the scatter in the original data). Figure 3-12 shows the resulting plot of iceberg mass and corresponding hourly decrease in mass, along with the best fit used in the Monte Carlo model, as follows:

$$\Delta M = 7.24M^{0.36} \tag{3.3}$$

where M is iceberg mass in metric tonnes.

Table 3-1 Mean hourly decrease in iceberg waterline length as a function of month and initial iceberg waterline length in Strait of Belle Isle model area

Waterline Length (m)		15	50	100	150	200	250	300
Month	January	0.23	0.10	0.06	0.04	0.03	0.03	0.02
	February	0.13	0.06	0.03	0.02	0.02	0.02	0.02
	March	0.07	0.03	0.02	0.02	0.02	0.01	0.01
	April	0.10	0.04	0.03	0.02	0.02	0.02	0.01
	May	0.14	0.06	0.04	0.03	0.02	0.02	0.02
	June	0.30	0.13	0.07	0.06	0.05	0.04	0.04
	July	0.53	0.23	0.13	0.09	0.08	0.07	0.06
	August	0.59	0.26	0.15	0.12	0.09	0.08	0.08
	September	0.54	0.24	0.14	0.11	0.09	0.08	0.07
	October	0.75	0.33	0.18	0.13	0.11	0.09	0.08
	November	0.49	0.22	0.12	0.09	0.07	0.06	0.05
	December	0.40	0.18	0.10	0.07	0.05	0.05	0.04
Weighted Annual		0.34	0.15	0.08	0.06	0.05	0.05	0.04
Hourly Mass Decrease (tonnes)		100	350	650	950	1300	1600	2000

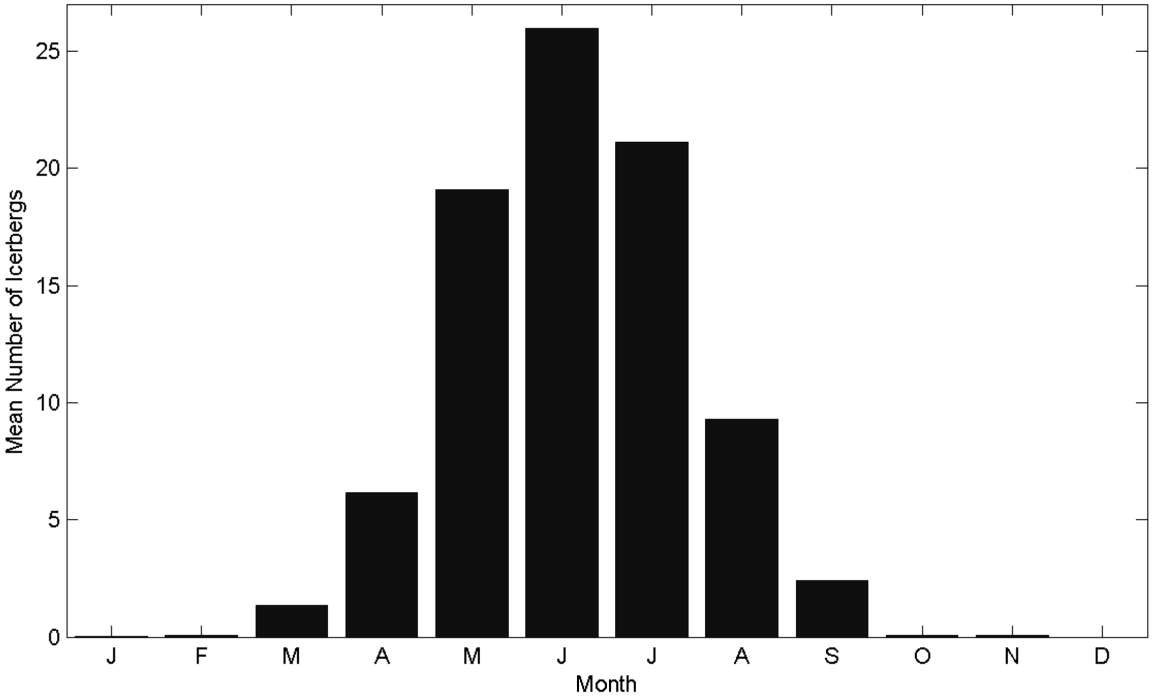

Figure 3-11 Mean monthly number of icebergs in degree square containing cable crossing site according to CIS iceberg charts

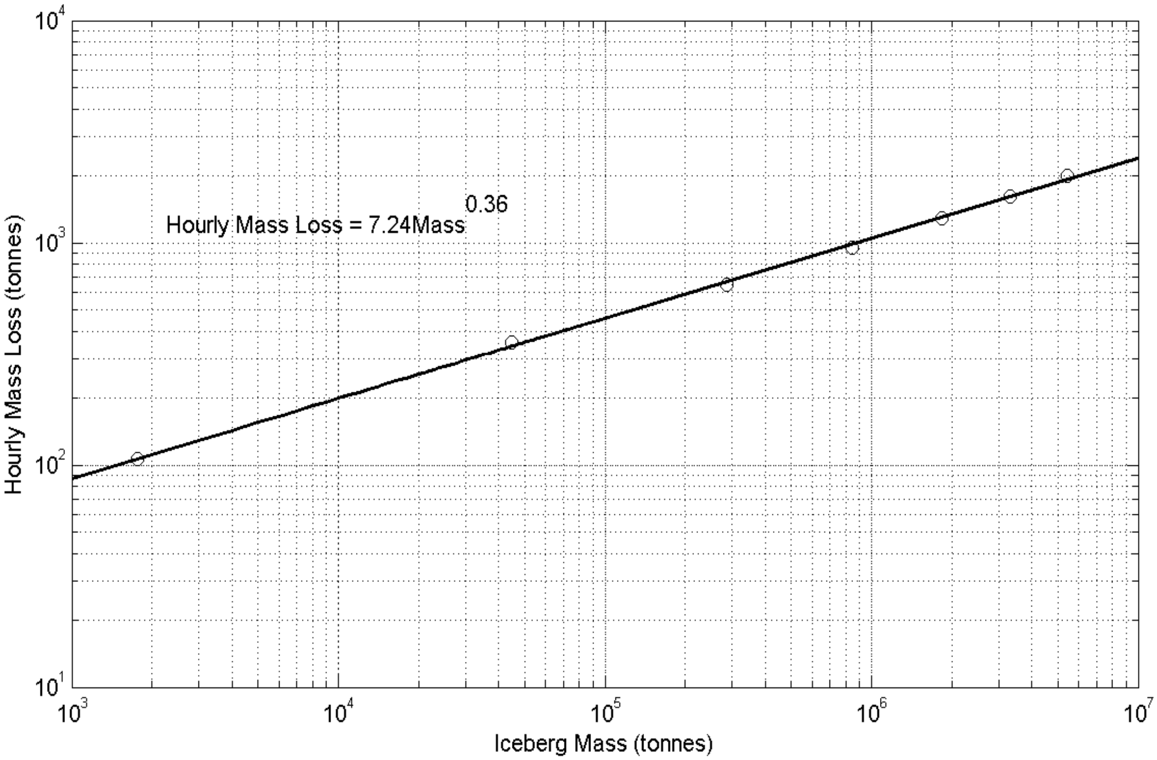

Figure 3-12 Hourly decrease in iceberg mass for Strait of Belle Isle

3.3.5 Iceberg Drift

Two potential sources of data were assessed for use in the iceberg drift component of the Monte Carlo model: iceberg drift tracks produced by the Canadian Ice Service (CIS) iceberg drift model and observed iceberg trajectories. The CIS iceberg drift model (Carrieres et al, 2001) uses forecast wind, waves and currents to calculate an iceberg's expected drift trajectory. The CIS iceberg drift model was used to generate iceberg drift tracks at weekly intervals for the period 2000-2006 (the period for which archived data was available for this exercise). Each model run simulated 2 days of iceberg drift. Initial iceberg locations were spaced at 0.50º longitude and 0.25º latitude and includes the Strait of Belle Isle. Unlike the runs described in Section 3.3.4, a single iceberg size was used for these runs (200 m waterline length).

C-CORE (2004b) assessed the performance of the model on the Grand Banks by comparing observed and modeled iceberg trajectories from 2003 and found that the model provided reasonably accurate predictions on the majority of occasions. However, comparison between observed and modeled iceberg trajectories on the Labrador Shelf has indicated lower levels of accuracy in that region (Luc Desjardins, Canadian Ice Service, personal communication). This exercise cannot be performed for the Strait of Belle Isle, due to the lack of iceberg trajectory data in the time period covered by the CIS model (post-2000). Another consideration is that that the current model used by the CIS iceberg drift model does not include a tidal component, and tides have a significant effect in the Strait of Belle Isle. The mean iceberg drift speed predicted by the CIS model in the cable crossing area was 0.12 m/s, with a standard deviation of 0.07 m/s. A check against observed iceberg trajectories revealed that the CIS model substantially under-estimated iceberg drift speeds in the Strait of Belle Isle and this source was not considered further.

Limited iceberg drift data have been collected in the study area. In 1979 and 1980 iceberg trajectory data were collected for 21 icebergs using an X-band marine radar mounted on the Point Amour lighthouse, at an elevation of approximately 43 m (Roche, 1980). These iceberg tracks are shown in Figure 3-13. It can be observed that iceberg drift is not uniform, with many of the tracks doubling back. When periods of zero drift speed (grounding events) are excluded, the mean drift speed is 0.56 m/s, with a standard deviation of 0.33 m/s and a maximum of 1.53. This is a high mean drift speed compared with the Grand Banks (~0.35 m/s) or the Makkovik Bank (~0.25 m/s). As shown in Figure 3-14, iceberg drift speeds are best characterized by a gamma distribution, which is typical for iceberg drift.

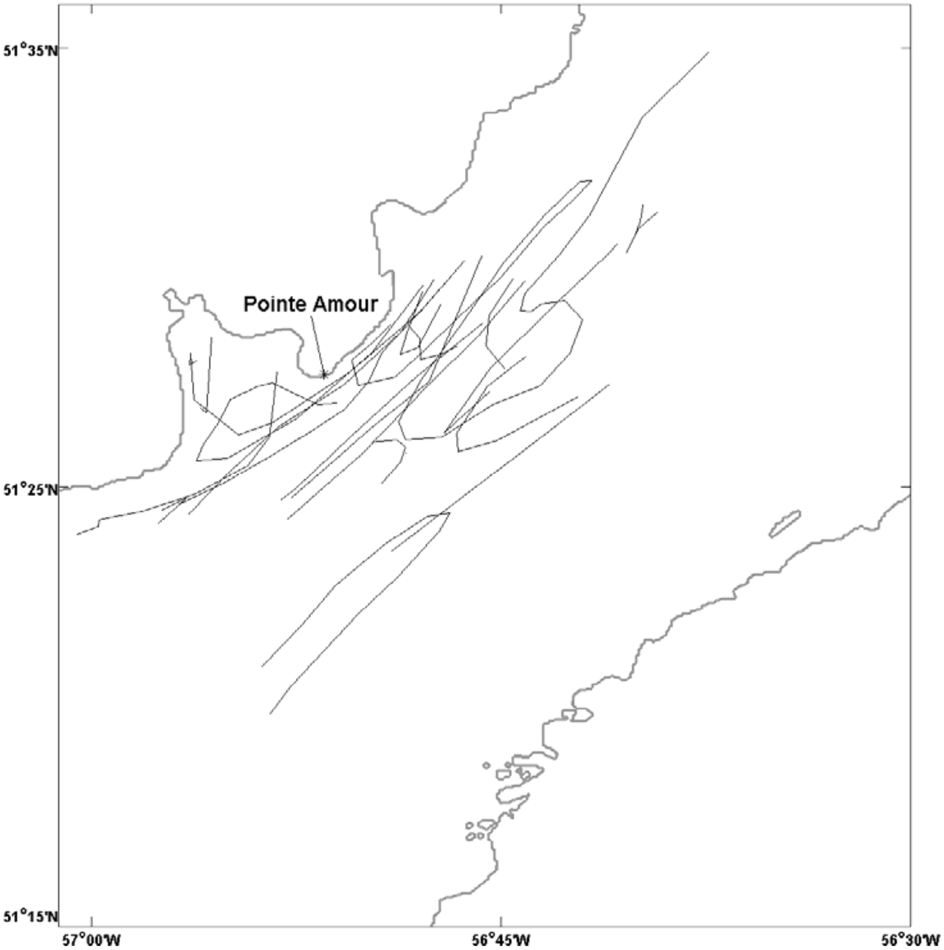

Figure 3-13 Iceberg drift track data from Strait of Belle Isle (Roche, 1980)

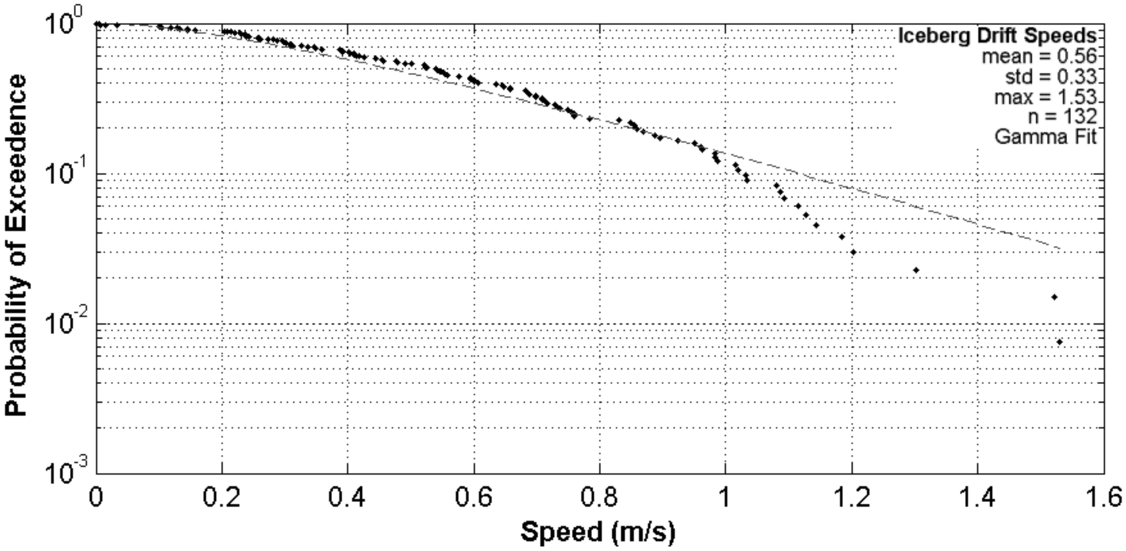

Figure 3-14 Observed iceberg drift speed distribution

Clearly, insufficient data exists in the Strait of Belle Isle to develop and iceberg trajectory model that reproduces the iceberg drift pattern in the region. This may require the development of a local current model that incorporates the complex bathymetry and tidal effects, and both current monitoring and iceberg drift tracking to calibrate and validate the model.

A simplistic approach was adopted for the iceberg grounding model. A uniform mean drift field was used, consisting of a 0.25 m/s westward component and a 0.20 southward component. The resulting mean iceberg drift direction corresponded with the overall orientation of the Strait of Belle Isle. The standard deviation of the north-south and east-west drift was 0.25 m/s. Trial and error indicated that this combination of parameters produced a reasonable representation of the observed drift speed distribution.

The iceberg movement was modeled using a lag-1 autoregressive model, as described by Fiering and Jackson (1971). Iceberg motion in the north-south and east-west directions were modeled independently, as combined to give an overall 2D drift pattern, as follows:

$$\dot{X}_t = \mu_{\dot{X}} + \rho_{\dot{X}}\left(\dot{X}_{t-1} - \mu_{\dot{X}}\right) + \varepsilon\sigma_{\dot{X}}\sqrt{1-\rho_{\dot{X}}^2} \tag{3.4}$$

$$\dot{Y}_t = \mu_{\dot{Y}} + \rho_{\dot{Y}}\left(\dot{Y}_{t-1} - \mu_{\dot{Y}}\right) + \varepsilon\sigma_{\dot{Y}}\sqrt{1-\rho_{\dot{Y}}^2} \tag{3.5}$$

where $\dot{X}_t$ and $\dot{Y}_t$ are the mean eastern and northern components of the drift velocity in the current time step, $\mu_{\dot{X}}$ and $\mu_{\dot{Y}}$ are the mean eastern and northern drift velocity, $\rho_{\dot{X}}$ and $\rho_{\dot{Y}}$ are the correlations between the current eastern and northern drift velocity and the eastern and northern drift velocity one hour previous ($\dot{X}_{t-1}$ and $\dot{Y}_{t-1}$), $\sigma_{\dot{X}}$ and $\sigma_{\dot{Y}}$ are the standard deviations of the eastern and northern components of the drift velocity, and ε is a normally distributed random number with a mean of 0 and a standard deviation of 1. An analysis of larger iceberg drift datasets from the northeast Grand Banks and Makkovik Bank region indicates that a value of 0.98 is appropriate for both $\rho_{\dot{X}}$ and $\rho_{\dot{Y}}$.

3.3.6 Initial Iceberg Starting Location

The starting location for icebergs in the Monte Carlo model was 51.1° N, 55.4°W, at a water depth of ~200 m (see Figure 3-15). This location is immediately north of Belle Isle at the entrance to the Strait of Belle Isle. The water depth at this location is relatively deep compared with most locations in the Strait of Belle Isle and deep draft icebergs placed here will not immediately ground (iceberg draft is capped at 200 m in the Monte Carlo model). Although all icebergs start at a common point, the random component in the drift model ensures sufficient dispersion of icebergs as they drift through the Strait.

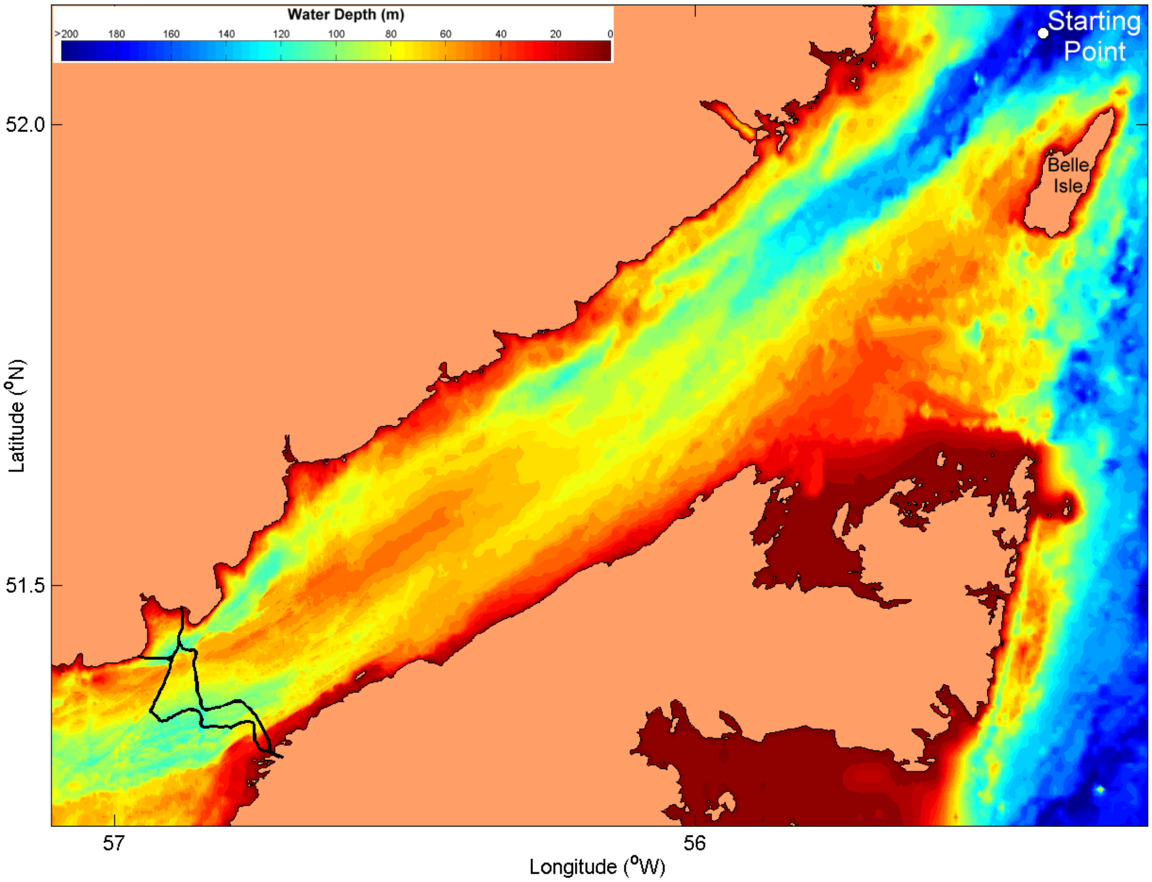

Figure 3-15 Iceberg starting location for Monte Carlo model

3.4 Model Output

3.4.1 *Introduction*

The Monte Carlo model saved two types of data files: RESULTS and GROUNDINGS files. The "RESULTS" output files saved the initial iceberg waterline length, and iceberg mass, draft, latitude, longitude and grounding status for each iceberg and time step (the number of icebergs per model run can be varied, but was usually 500). However, the large size of these data files (~40 MB each) limited the number that was practical to save. However, these output files were useful for assessing model performance and usually 4 were saved from each model run. The "GROUNDINGS" output files saved data primarily for a zone encompassing the cable crossing site (51.3ºN to 51.5ºN and 56.6ºW to 57ºW). The data saved included the number of icebergs modeled, as well as the locations of iceberg groundings, cases where iceberg keels were within 1 m of the seabed, and the all free-floating icebergs within the cable crossing zone. Also saved was the total number of icebergs in the degree square containing the cable crossing site (51ºN to 52ºN and 56ºW to 57ºW) for comparison with iceberg areal density charts. Several thousand datasets were required to get reasonably smooth output from the Monte Carlo model, a process taking a minimum of a week, using multiple copies of MATLAB run on 3 PC's.

3.4.2 *Sample Output*

Figure 3-16 shows modeled iceberg trajectories for one run (500 icebergs), as recorded in a RESULTS output file. The starting point for each iceberg is the location described in Section 3.3.6. Each iceberg then moves on an independent path, based on the autoregressive relationships described in Section 3.3.5. Icebergs that deteriorate to the minimum mass or drift to the defined boundaries of the model area are classified "inactive" (the simulation terminates for that iceberg). Figure 3-17 shows iceberg grounding locations obtained from the same model run. Figure 3-18 (top) shows a sample modeled iceberg trajectory and Figure 3-18 (bottom) shows the water depth and iceberg draft for each hourly time step of the Monte Carlo model. Changes in iceberg draft due to rolling and deterioration are evident.

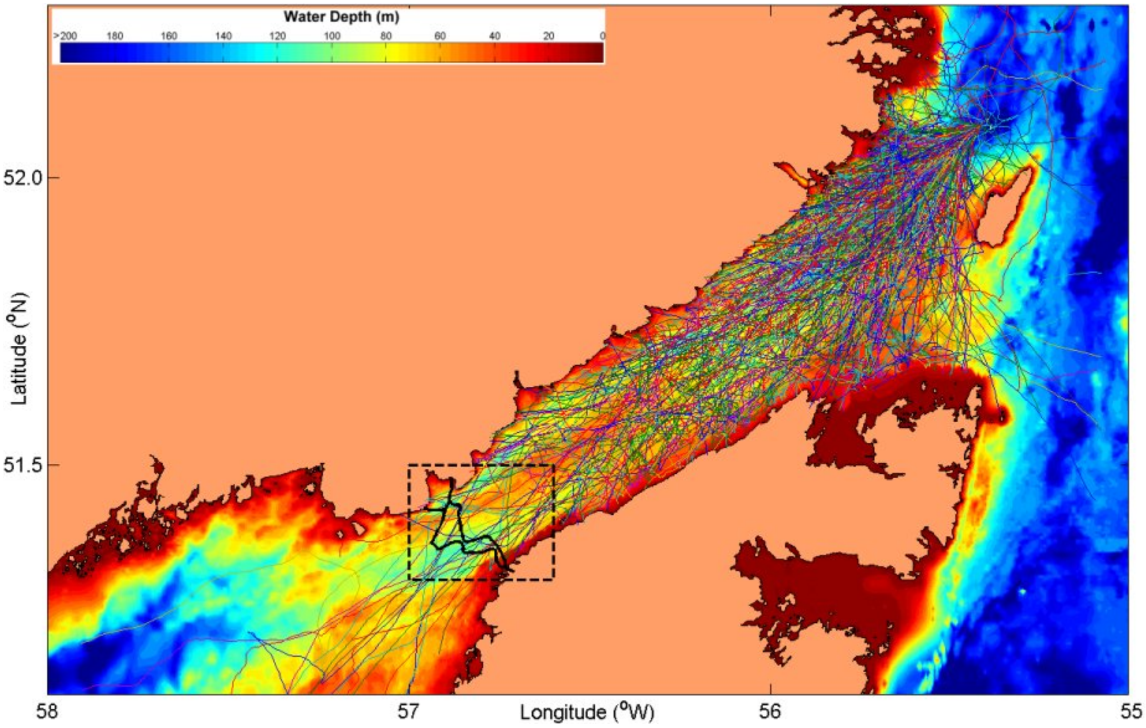

Figure 3-16 Iceberg trajectories (500) generated during a single model run (dashed line indicates cable crossing study area)

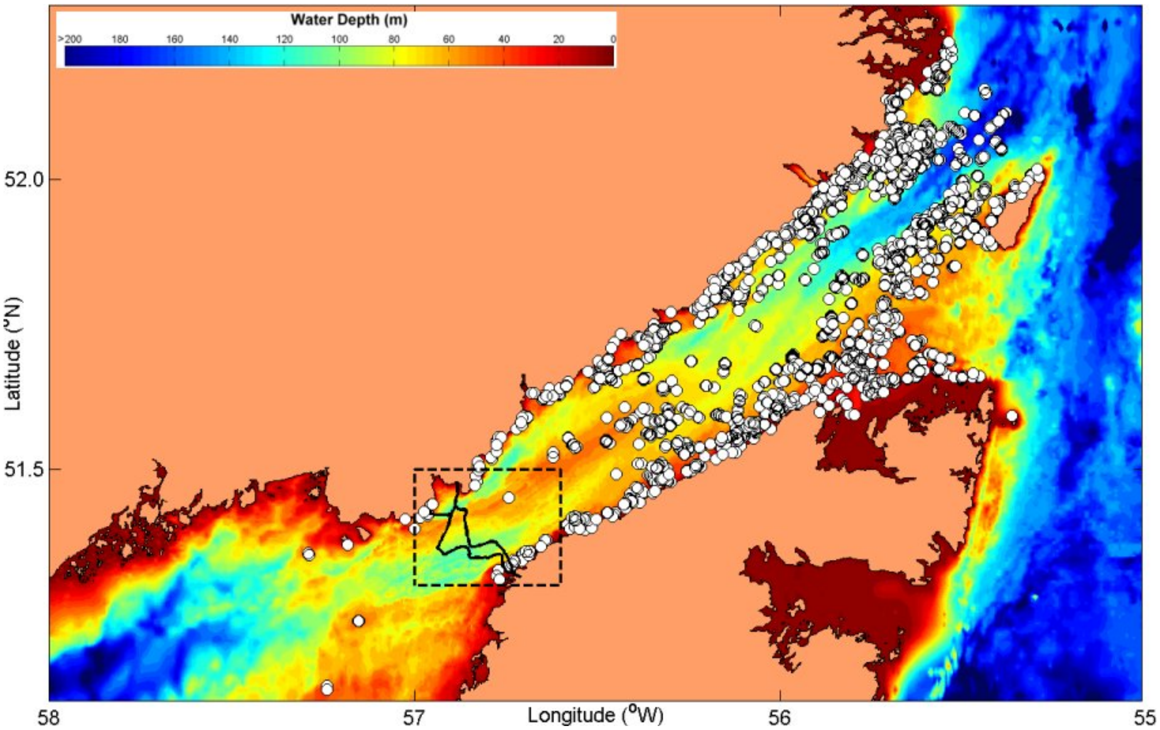

Figure 3-17 Iceberg grounding locations generated during a single model run

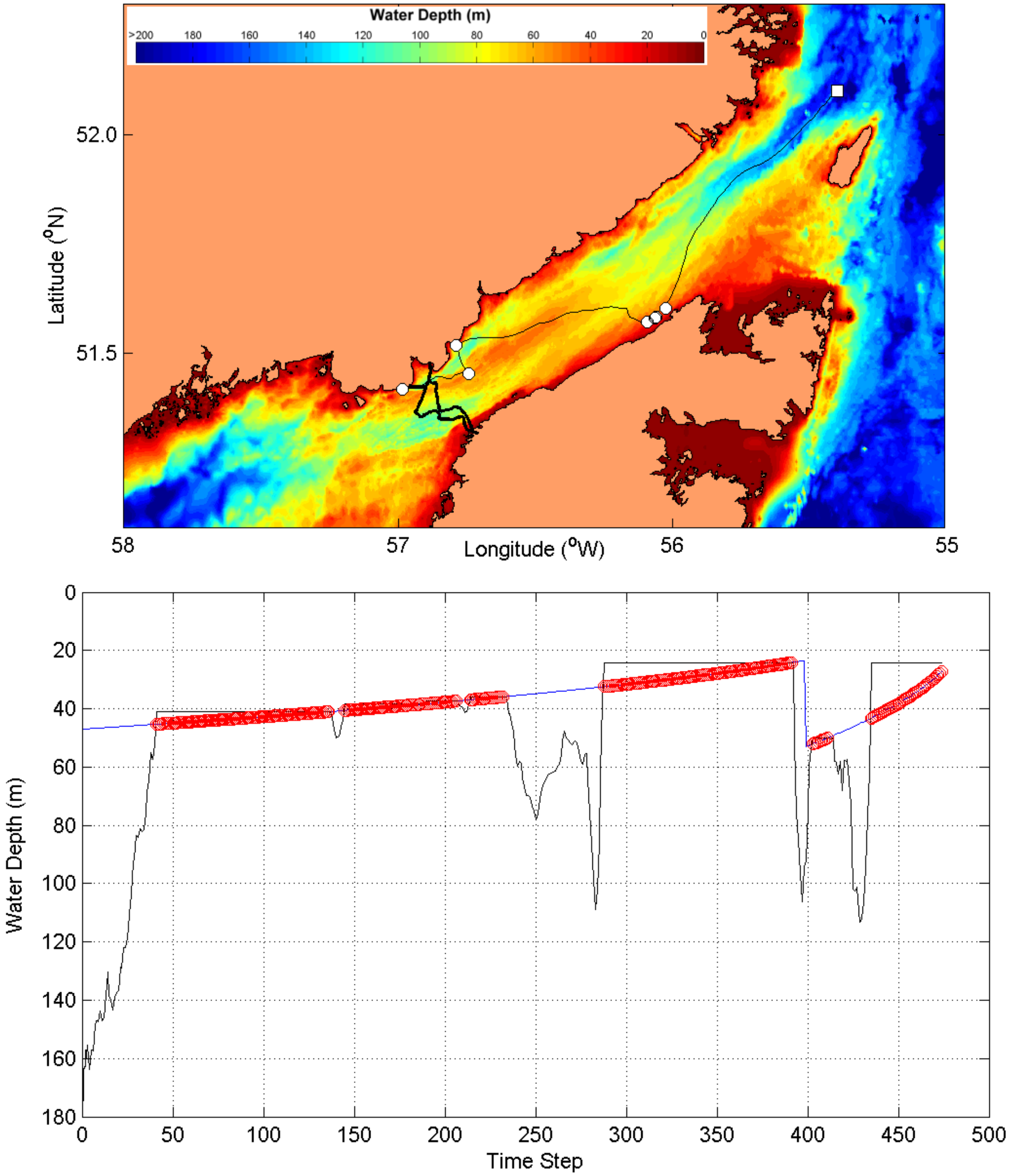

Figure 3-18 Sample iceberg trajectory with grounding locations indicated (top) and corresponding iceberg draft and water depth for each 1-hour time step (bottom, with red circles indicating periods when iceberg is grounded)

3.4.3 Grounding Distribution

Iceberg grounding locations were saved in GROUNDINGS format files for a zone encompassing the cable crossing site (51.3ºN to 51.5ºN and 56.6ºW to 57ºW). As previously discussed in Section 3.3.3, the baseline case uses a mean iceberg rolling rate of once every three days, or a 1/72 probability of rolling during any 1-hour model time step while free-floating. A total of 7,215,500 icebergs were simulated (14,431 datasets of 500 icebergs each), taking approximately 2 weeks to complete using three quad-core PC's with three copies of the Monte Carlo model running on each PC. This resulted in a total of 381,770 modeled iceberg grounding events inside the cable crossing zone, as well as 359,043 cases where the iceberg keel was within 1 m of the seabed (to be addressed further in Section 4).

Figure 3-19 shows the spatial distribution of iceberg grounding events in the cable crossing zone and Figure 3-20 shows the distribution of water depths associated with each grounding event. The maximum water depth for a modeled iceberg grounding event in the cable crossing zone is 114.9 m. It is worthy of note that three of the modeled iceberg grounding events occurred where the cables pass through the sheltered channel between Bank A and Bank B (see Figure 2-3) where no iceberg scours were observed in the multibeam survey data. Low concentrations of groundings are also observed in the Central Trough and the Point Amour Trough, although these are (for the most part) also concentrated on local bathymetric high points. Ideally, additional runs would be completed in order to produce a smoother spatial distribution of grounding events in deeper water; however, given the time required to achieve this (likely on the order of months without substantial model acceleration) some form of spatial averaging will be required to properly assess iceberg risk for cables in these areas.

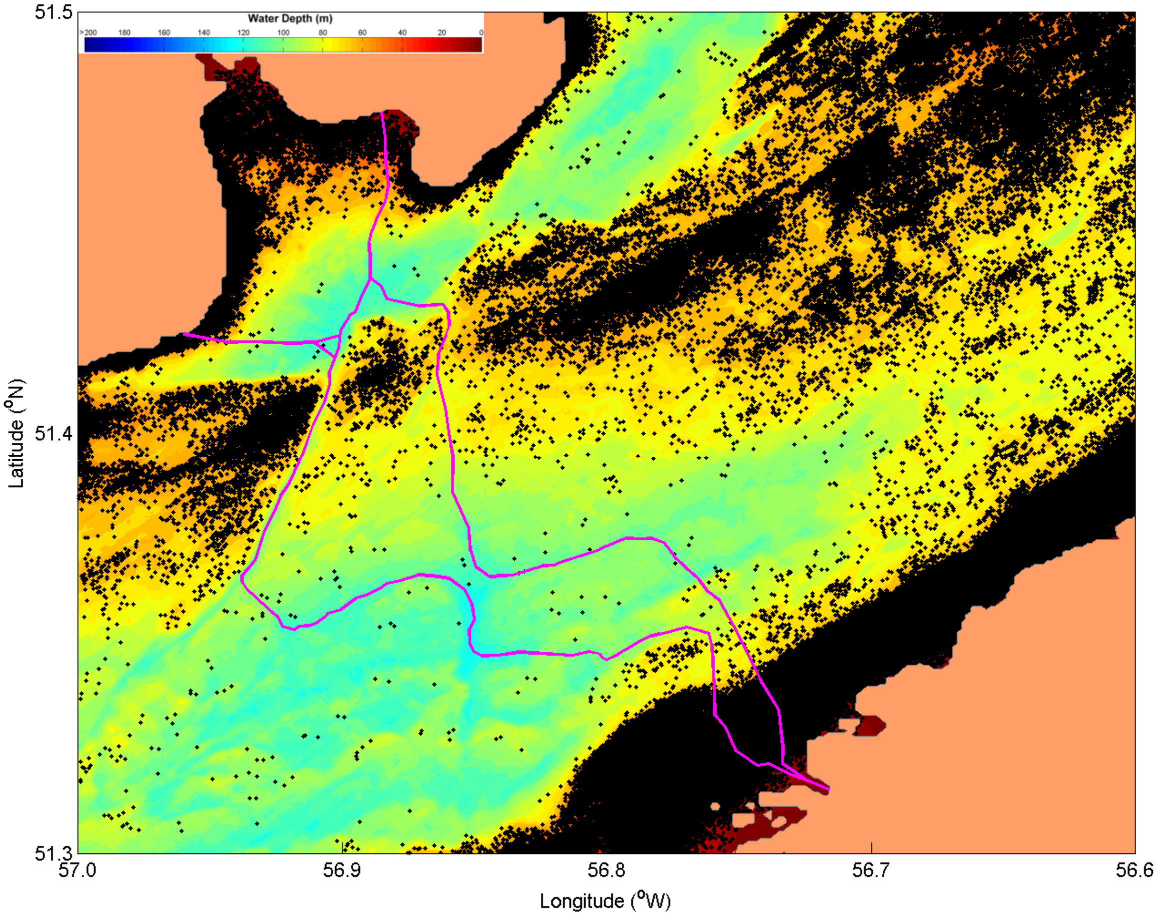

Figure 3-19 Raw groundings in cable crossing area (base case), mean iceberg rolling rate once every three days (7,215,000 simulated icebergs)

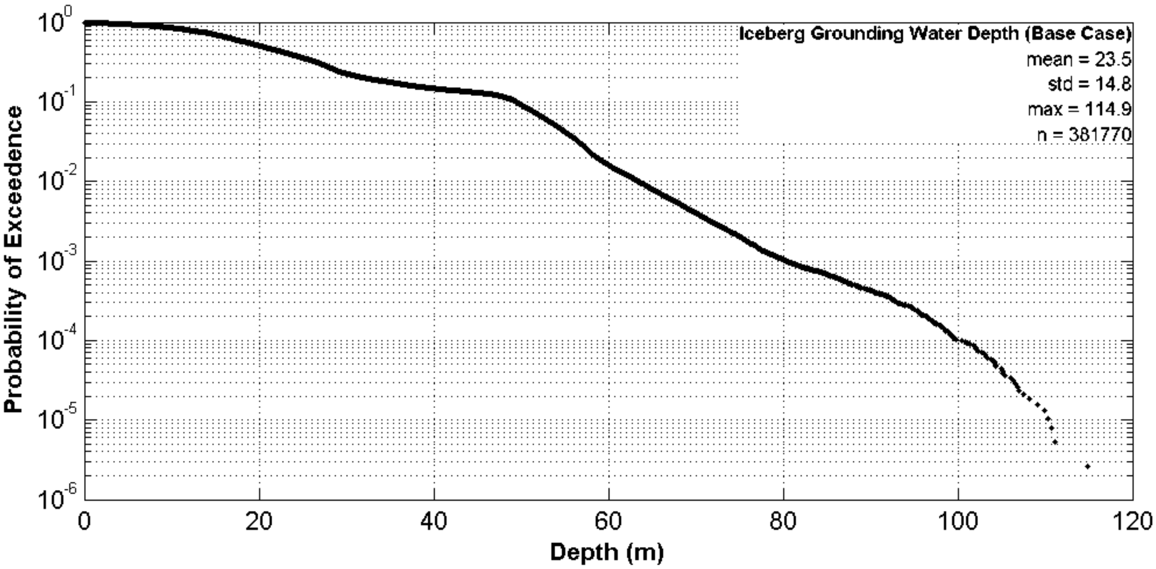

Figure 3-20 Distribution of iceberg grounding water depths (base case), mean iceberg rolling rate once every three days

3.4.4 Sensitivity to Rolling Rates

In order to test the sensitivity of the model to the iceberg rolling rate, a series of sensitivity runs were performed with varying mean iceberg rolling rates: 1 day, 10 days and no rolling, or probabilities of rolling in each 1 hour model time step of 1/24, 1/240 and 0, respectively. The spatial distributions of modeled iceberg grounding events are shown in Figure 3-21, Figure 3-23 and Figure 3-25. The distribution of water depths associated with iceberg grounding events are shown in Figure 3-22, Figure 3-24, and Figure 3-26. Table 3-2 summarizes the results of the sensitivity runs, as well as the base case, including the total number of modeled icebergs and the number of iceberg groundings in the cable crossing zone. In general, decreasing the iceberg rolling rate decreases the modeled iceberg grounding rates in deeper water. Some discrepancies are seen for the 1-day rolling rate and 3-day cases in deeper water depths (> 90 m), but this is likely a random effect (not unusual when using Monte Carlo models). Note that this approach assumes that when an iceberg rolls it can assume any draft as defined by the Equation 3.2, without any correlation with the previous draft or tendency to adopt a deeper or shallower draft when rolling. Of note is the absence of modeled iceberg groundings for the case with no iceberg rolling beyond 70 m water depth.

Table 3-2 Percentage of modeled iceberg grounding events in cable crossing zone exceeding specified water depth as a function of iceberg rolling rate

Rolling Period		1 Day	3 Days (Base Case)	10 Days	No Rolling
Total Icebergs Modeled		2,408,500	7,215,000	2,180,500	8,206,500
Cable Crossing Zone Groundings		114,448	381,770	121,154	463,462
Water Depth (m)	10	84.9	85.0	84.9	84.9
	20	50.9	50.7	50.0	49.5
	30	24.1	22.5	21.1	19.7
	40	16.9	14.7	12.8	11.2
	50	11.6	9.2	7.1	5.4
	60	2.8	1.6	0.81	0.05
	70	0.66	0.40	0.19	0
	80	0.17	0.10	0.05	0
	90	0.05	0.04	0.01	0
	100	0.007	0.01	0.002	0
	110	0	0.001	0	0
	120	0	0	0	0

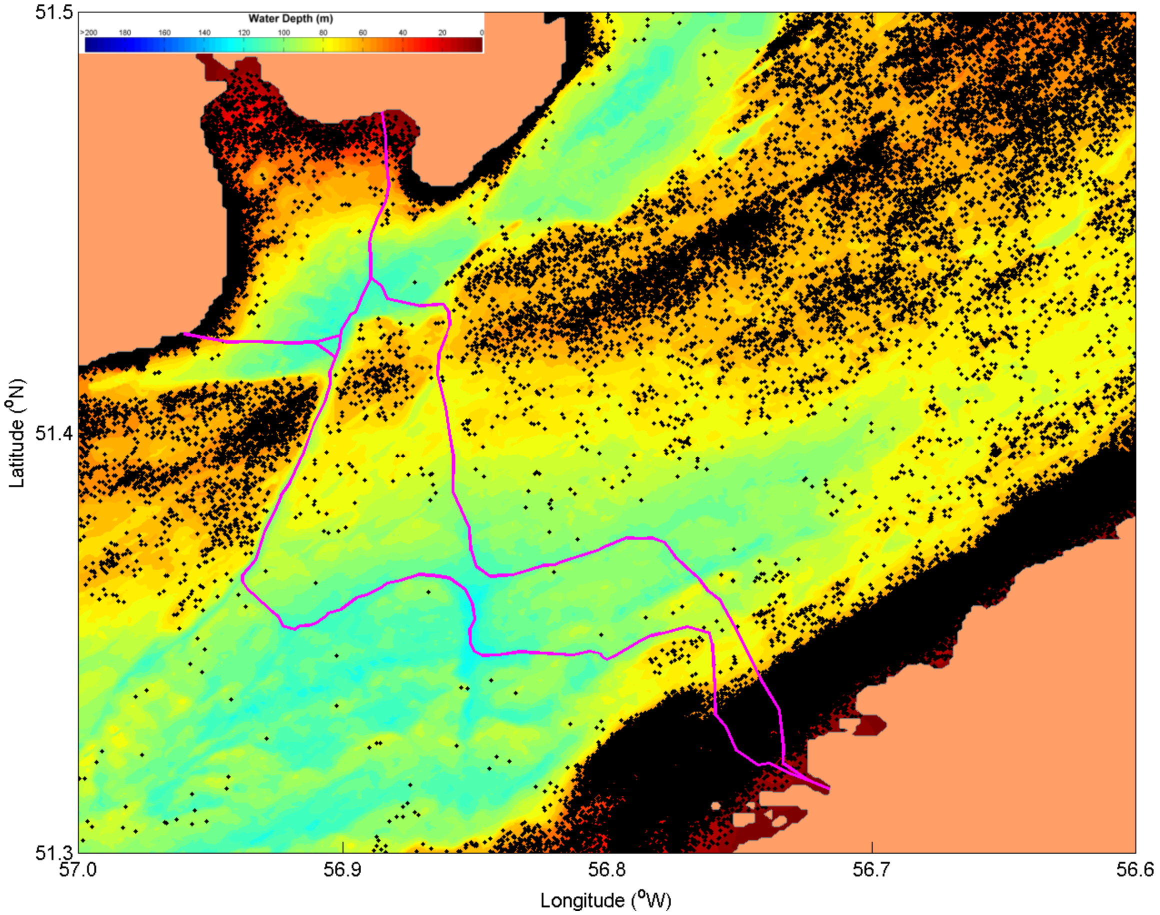

Figure 3-21 Raw groundings in cable crossing area, mean iceberg rolling rate once every day (2,408,500 simulated icebergs)

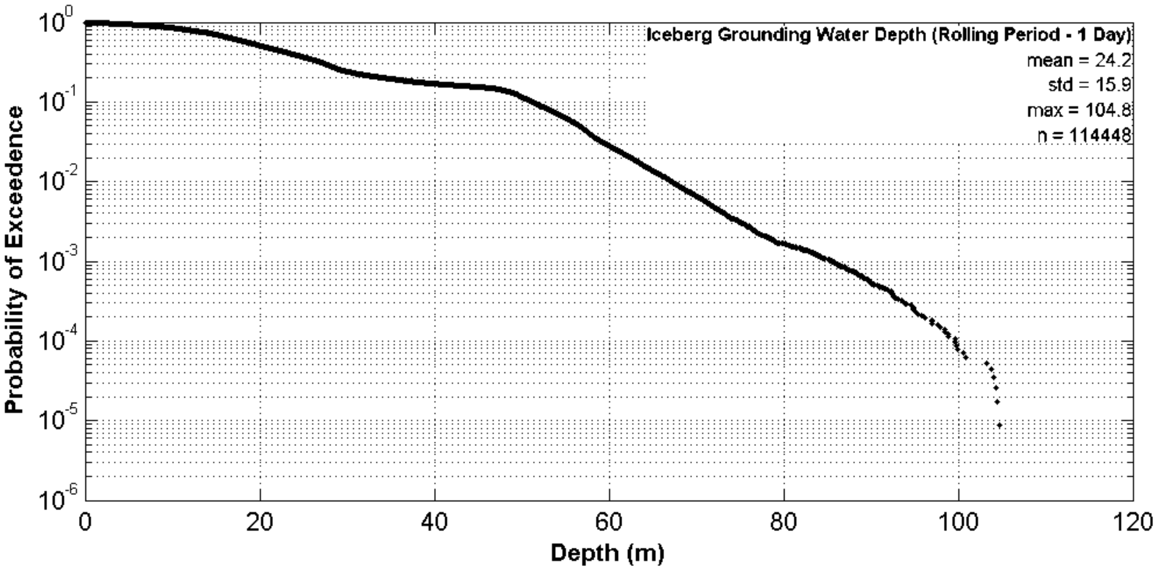

Figure 3-22 Distribution of iceberg grounding water depths, mean iceberg rolling rate once every day

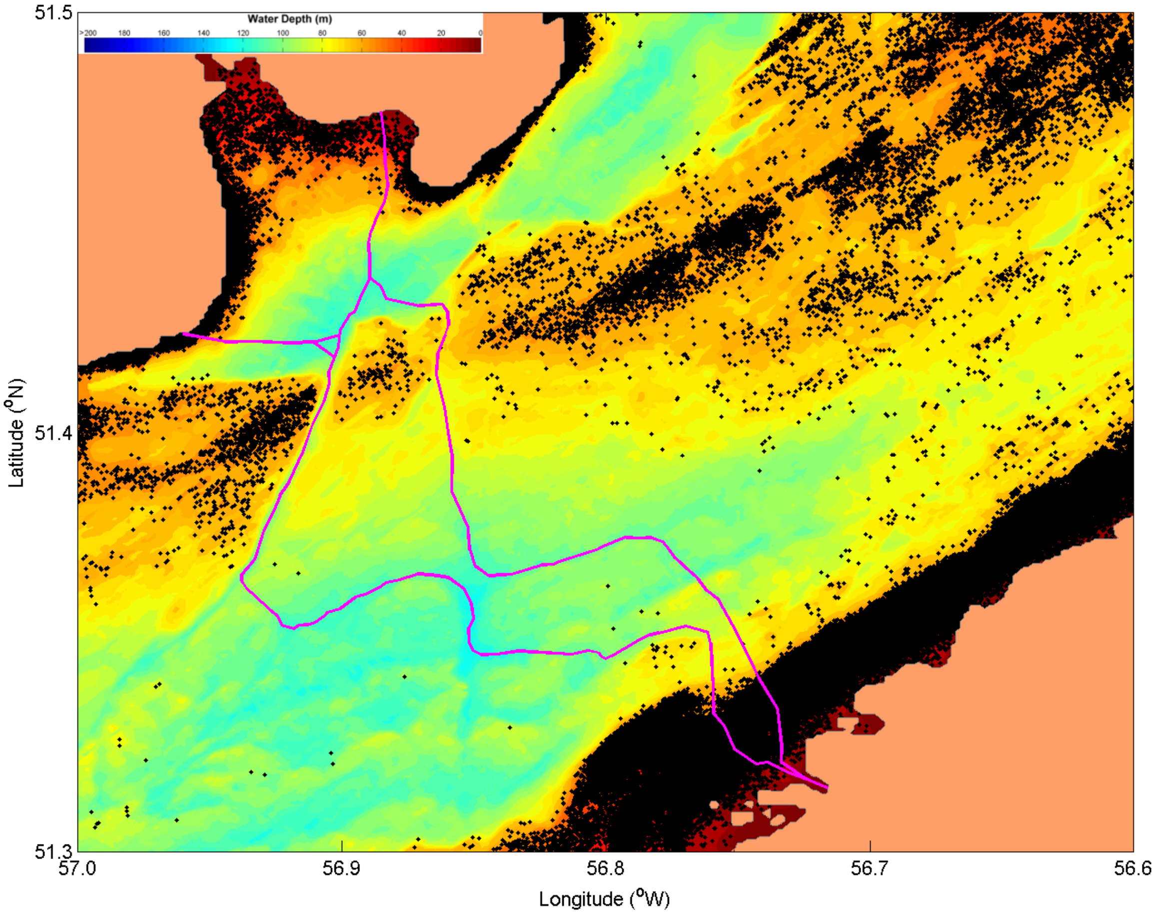

Figure 3-23 Raw groundings in cable crossing area, mean iceberg rolling rate once every ten days (2,180,500 simulated icebergs)

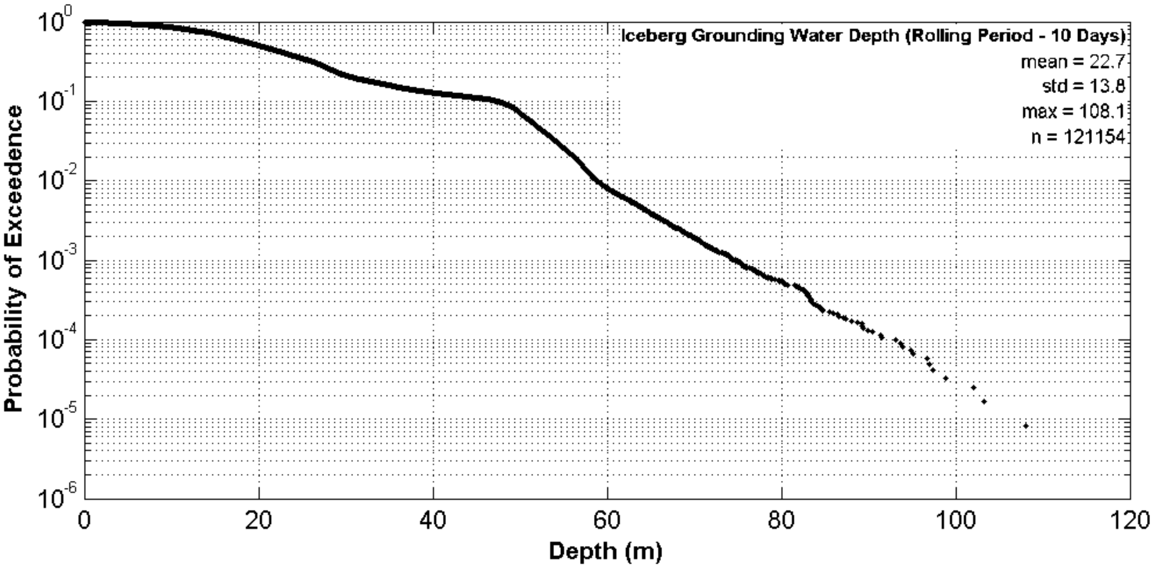

Figure 3-24 Distribution of iceberg grounding water depths, mean iceberg rolling rate once every ten days

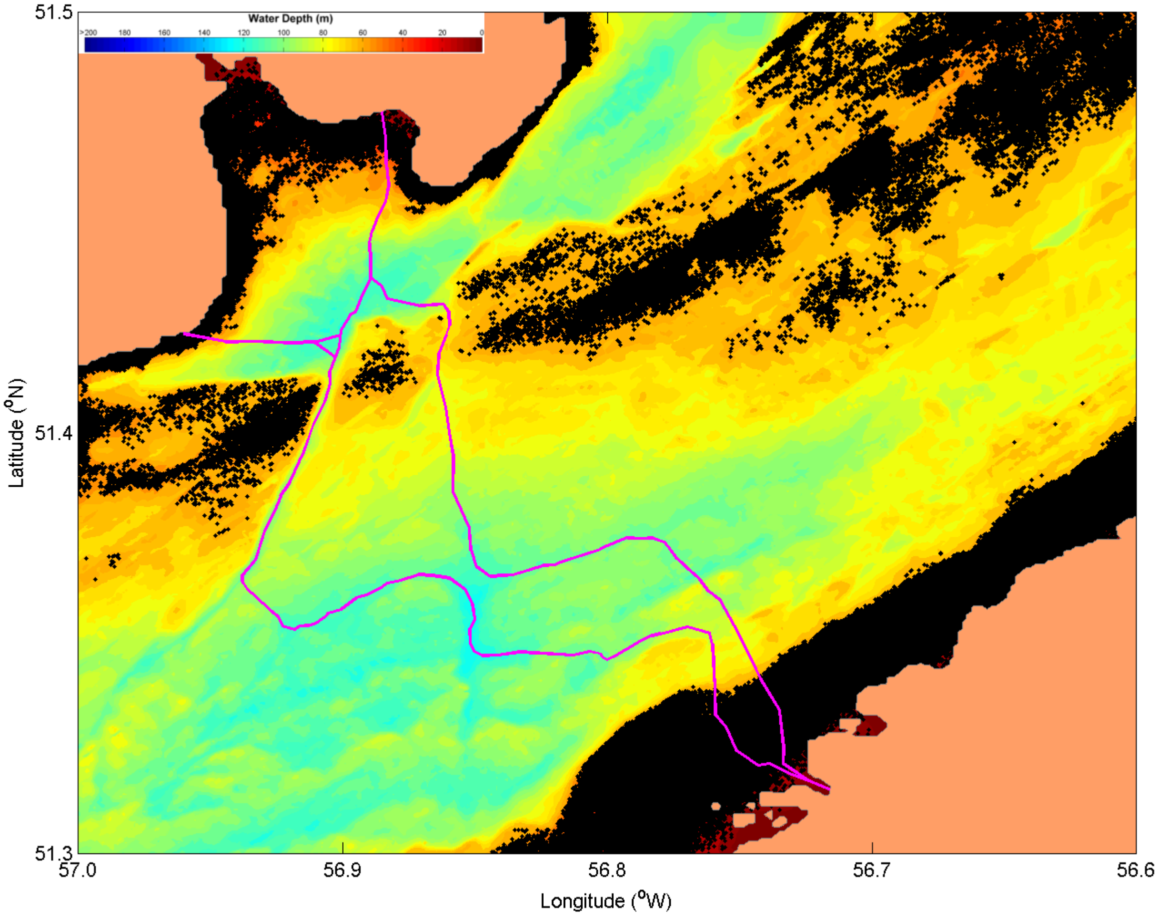

Figure 3-25 Raw groundings in cable crossing area, no iceberg rolling (8,206,500 simulated icebergs)

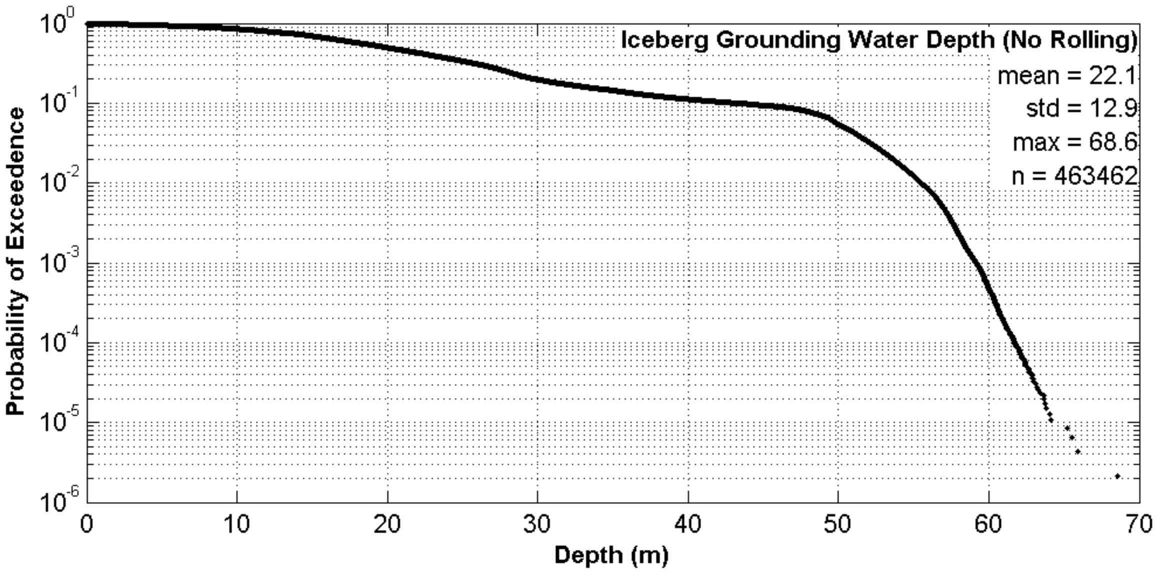

Figure 3-26 Distribution of iceberg grounding water depths, no iceberg rolling

3.4.5 Converting Model Output to Iceberg Grounding Rates

In order to use the Monte Carlo model output to perform an iceberg scour risk analysis for the cable it is necessary to convert modeled grounding events to an iceberg grounding rate (which will be considered equivalent to the iceberg scour formation rate). Typically, this would be performed by comparing the modeled iceberg grounding rate with the observed iceberg scour formation rate determined using repetitive scour mapping (as has been done on the Grand Banks and Makkovik Bank). Unlike the Grand Banks, the annual number of icebergs entering or passing through any arbitrary location in the Strait of Belle Isle is unknown. The only available basis for performing a calibration of model output is iceberg frequency. Figure 3-11 shows the mean monthly number of icebergs in the degree square (51ºN to 52ºN & 56ºW to 57ºW) containing the cable crossing site (51.3ºN to 51.5ºN & 56.6ºW to 57.0ºW), as determined using CIS iceberg charts from May 1988 to October 2010. According to the CIS iceberg charts, the mean annual number of icebergs recorded in the degree square containing the cable crossing site is 7.1.

The maximum number of 1-hour time steps performed during each run of the Monte Carlo model is 4380, which is equivalent to six months. Part of the Monte Carlo model output is the number of cases (per one-hour step) when icebergs drift from the iceberg start point (see Section 3.3.6) into the degree square containing the cable crossing site. The equivalent model time was calculated by dividing the number of "sightings" by the number of time steps, and then by two (to go from a six month rate to an annual rate) and then by 7.1 to match the average annual number of icebergs in the degree square containing the cable crossing site. Equivalent model periods for the various runs are summarized in Table 3-3. Iceberg groundings were gridded into bins measuring 0.001º latitude × 0.001º longitude (111.2 m N-S × 69.4 m E-W, or 7.7×10^{-3} km^2) to get an iceberg grounding density (#/km^2) and then divided by the equivalent model time to get an iceberg grounding rate (km^{-2}yr^{-1}). The resulting iceberg grounding rates are shown in Figure 3-27 (base case), Figure 3-28 (1 day mean rolling period), Figure 3-29 (10 days mean rolling period) and Figure 3-30 (no rolling).

Table 3-3 Equivalent model times for Monte Carlo model runs

Case	Mean Rolling Period	Hourly Iceberg Sightings in Cable Crossing Degree Square	Equivalent Model Time (Years)
Base Case	3 days	682,779,195	10,978
Sensitivity #1	1 day	207,712,569	3,340
Sensitivity #2	10 days	214,198,028	3,444
Sensitivity #3	No rolling	823,074,807	13,234

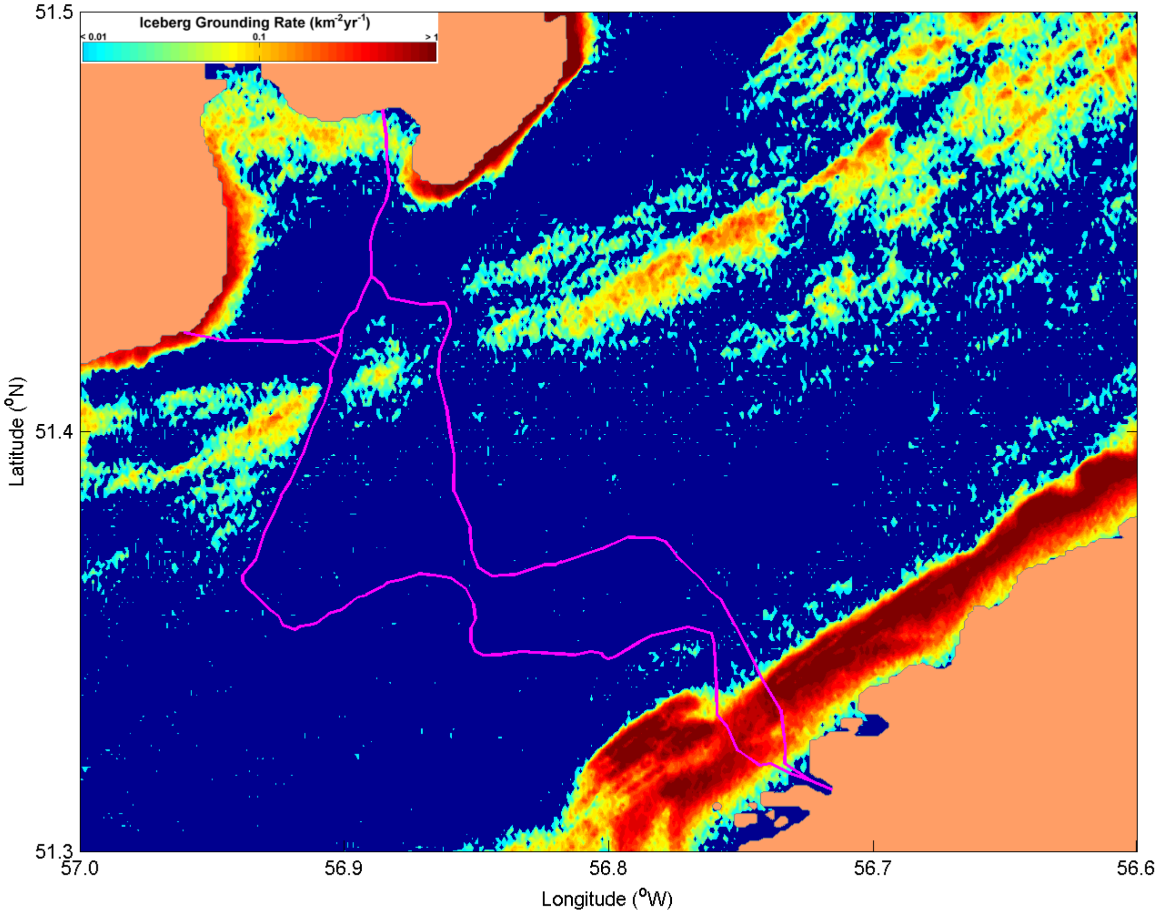

Figure 3-27 Modeled iceberg grounding rate, base case (mean rolling period 3 days)

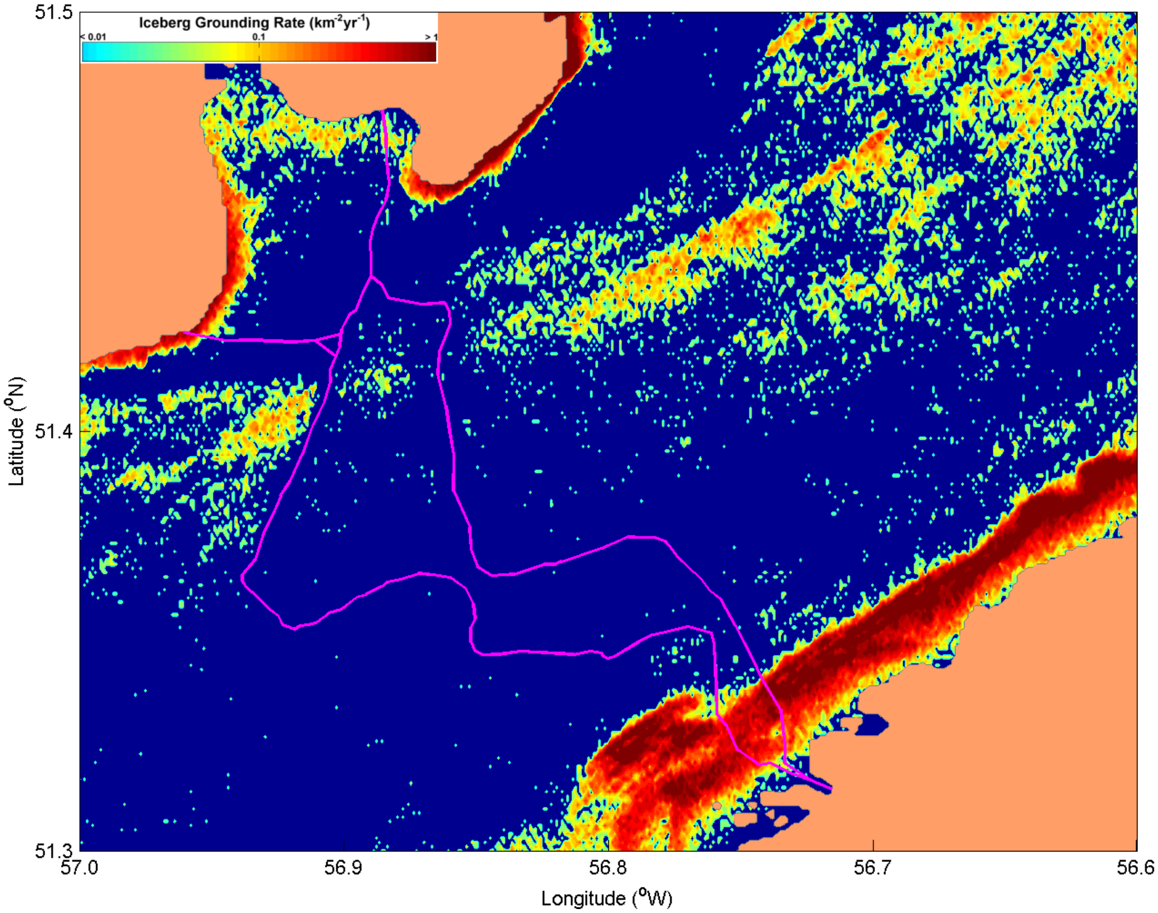

Figure 3-28 Modeled iceberg grounding rate, mean rolling period 1 days

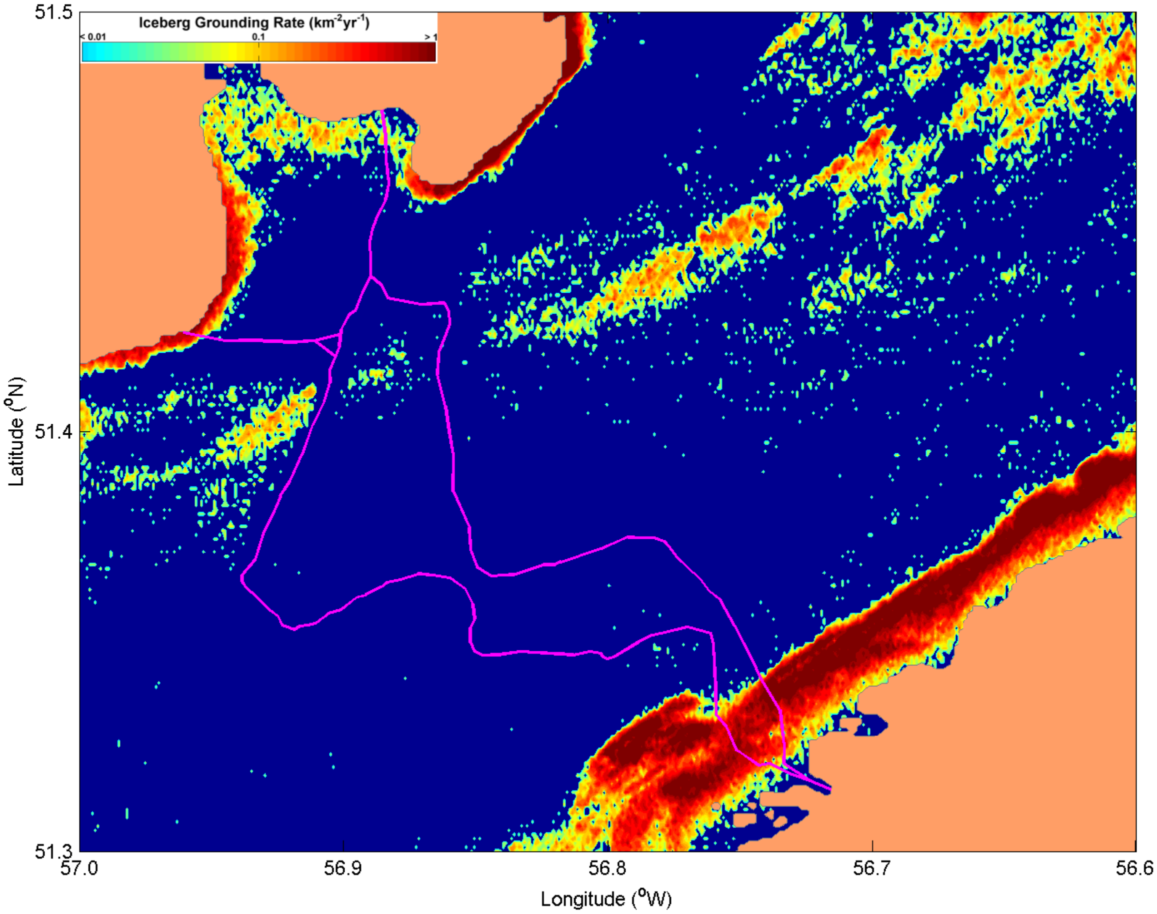

Figure 3-29 Modeled iceberg grounding rate, mean rolling period 10 days

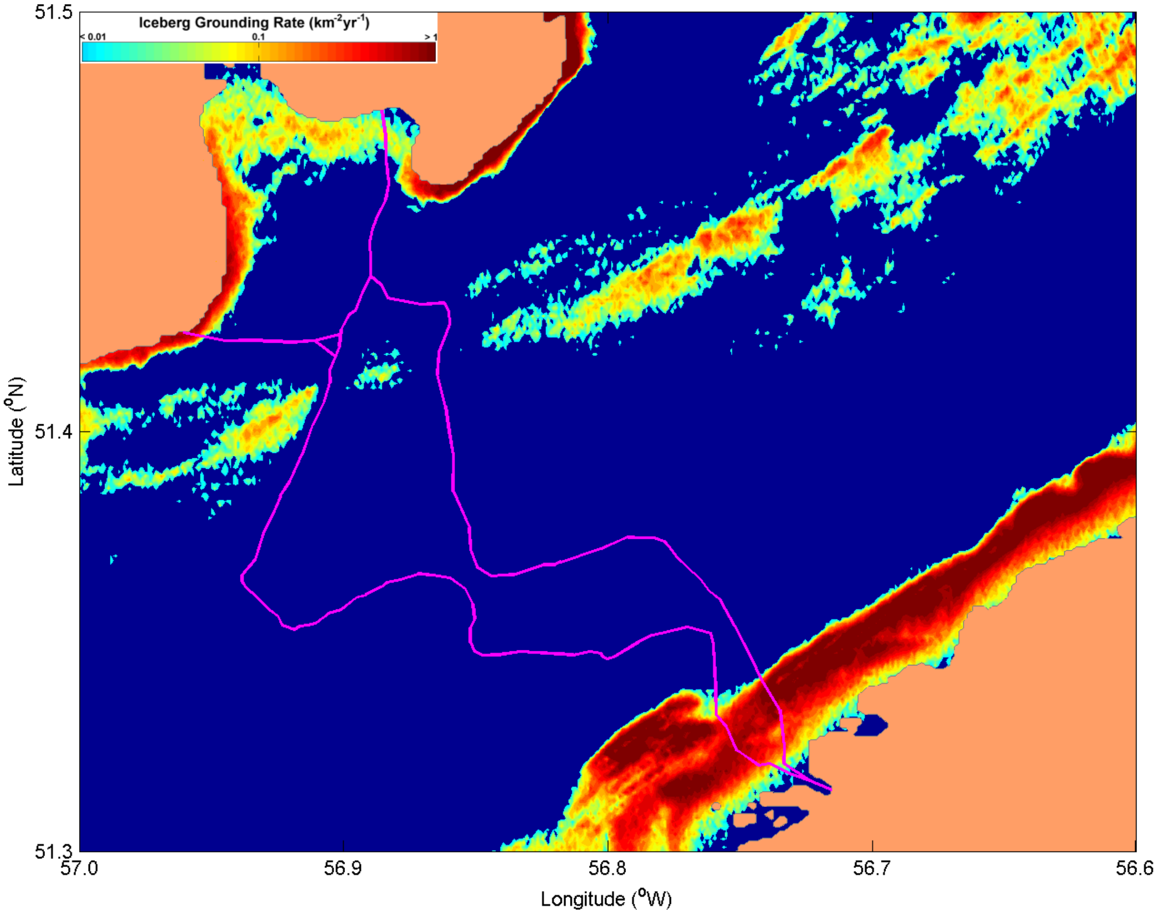

Figure 3-30 Modeled iceberg grounding rate, no rolling

3.4.6 Comparison of Model Output and Field Observations

Figure 3-31 shows modeled iceberg grounding rates (base case), along with mapped iceberg scours and iceberg grounding events inferred from an analysis of iceberg trajectory data collected using a radar installation at Point Amour (Roche, 1980). Iceberg grounding events were defined using the criterion that 6 hours or more of non-motion indicates a grounding event (El-Tahan et al., 1985). The 6 hour criterion is the bottom end of the range used by El-Tahan et al. (1985) and, while not absolute, is considered indicative of iceberg grounding.

Overall, the locations of iceberg grounding events identified from trajectory data agree fairly well with modeled iceberg grounding locations. Most iceberg groundings are clustered near the Labrador side of the Strait, although this may be related to the location of the radar installation. Most iceberg grounding locations are clustered in areas with high modeled iceberg grounding rates. Some iceberg groundings, such as the one in deeper part of the Central Trough, may be cases where the combination of environmental forces caused no movement, or may actually represent an actual grounding event. The degree of positional uncertainty associated with the radar data is unknown, as well as accuracy of the radar locations, and the methodology and the technology of the time of the study. Also, the number of iceberg trajectories available (54) is relatively limited, and many of these trajectories consist of just a few sightings.

The distribution of iceberg scours is essentially opposite of the modeled iceberg grounding locations, which would seem to support the hypothesis that these scour features are likely relict features, especially given the analysis of the trajectory data. Additional collection and analysis of iceberg trajectory data, as well as repetitive seabed mapping, is recommended to clarify this issue further.

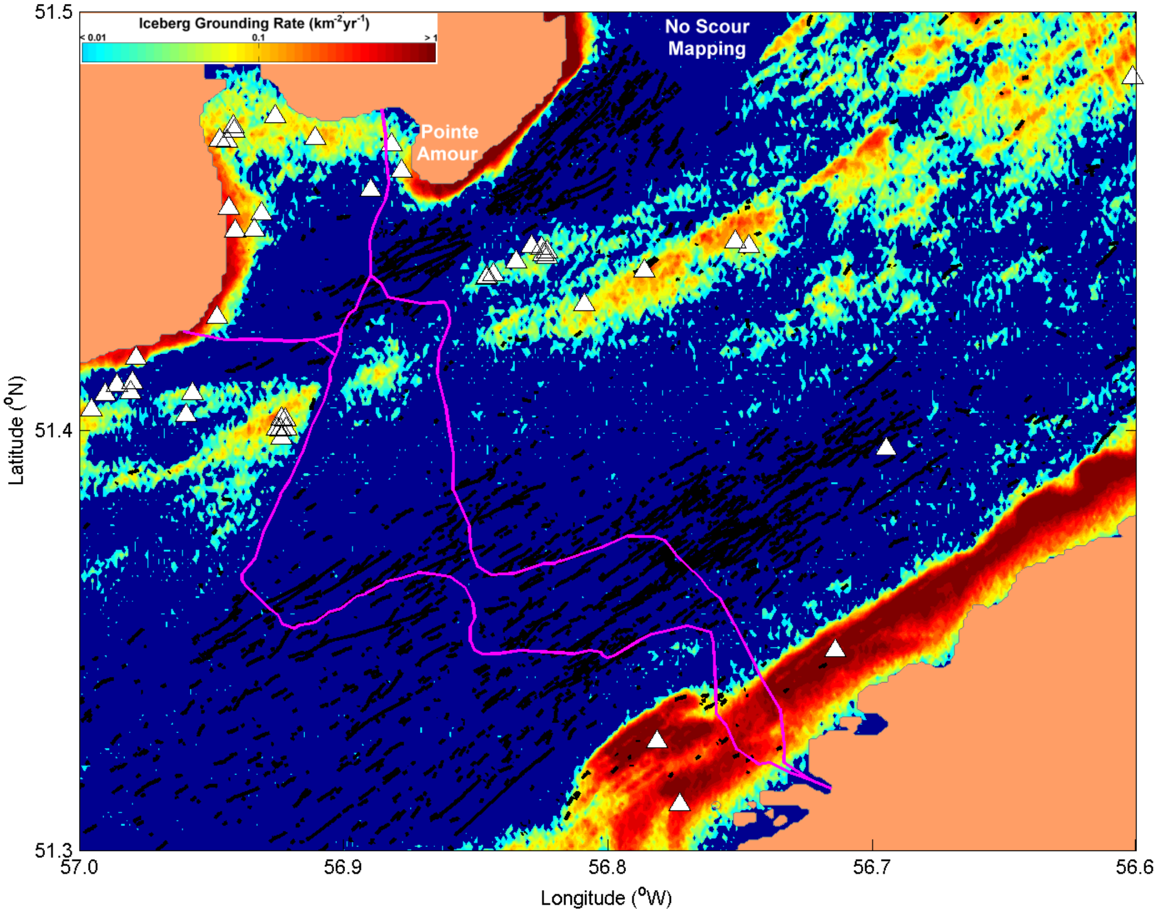

Figure 3-31 Modeled iceberg grounding rates (base case), mapped scours (black) and iceberg grounding events (Δ) inferred from iceberg trajectory data

4 CABLE CONTACT RATE ASSESSMENT

4.1 Introduction

The iceberg contact rate assessment was performed for cables (nominally 120 mm diameter) laid on the seabed in the specified zones, as shown in Figure 4-1. These areas are:

(1) Point Amour Trough and Labrador landfall zone;
(2) Channel zone;
(3) Bank B crossing zone;
(4) Central Trough zone; and
(5) Newfoundland landfall zone.

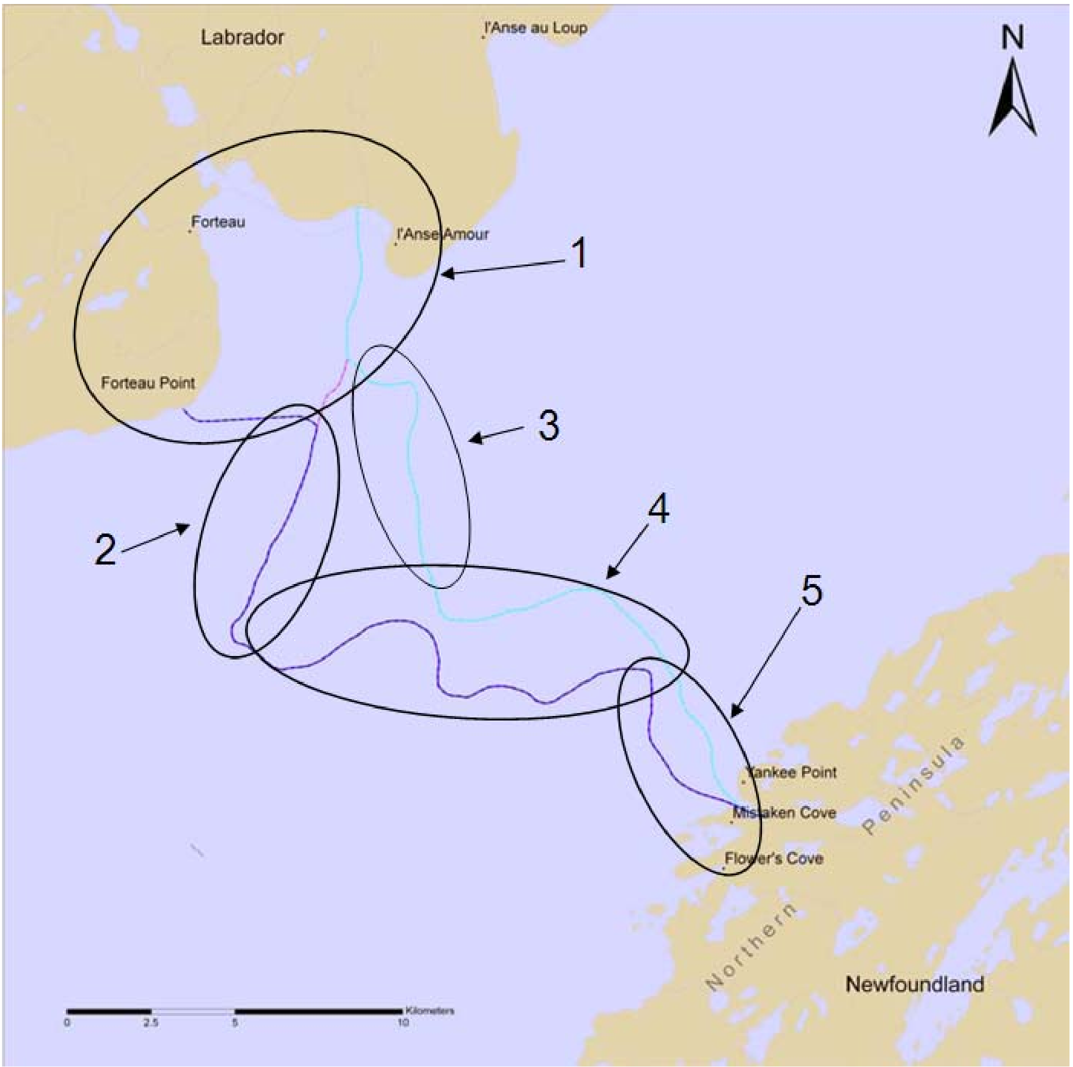

Figure 4-1 Cable sections specified for contact rate assessment

4.2 Methodology

4.2.1 Scouring Iceberg Contact Rates

The contact frequency between scouring icebergs, n_s, and a cable laid on the seabed can be calculated using:

$$n_s = \rho_s L_c \overline{L}_s \tag{4.1}$$

Where:

- ρ_s is the scour formation rate;
- L_c is the cable length, or length of the cable section of interest; and
- $\overline{L}_s$ is the mean scour (or furrow) length;

This relationship assumes that the scours are oriented at right angles to the cable, which is generally the situation observed for the cable crossing site in the Strait of Belle Isle. The scour formation rate will be assumed to be equal to the modeled iceberg grounding rate.

4.2.2 Free-Floating Iceberg Contact Rates

The contact frequency between free-floating icebergs, n_f, and a cable laid on the seabed can be calculated using:

$$n_f = n_o r'_d L_c \overline{U} t \tag{4.2}$$

Where:

- n_o is the annual average areal density of icebergs;
- r'_d is the proportion of icebergs with drafts capable of contacting the cable;
- L_c is the cable length, or length of the cable section of interest;
- $\overline{U}$ is the mean iceberg drift speed; and
- t is time (i.e. number of seconds per year).

As discussed in Section 3.4.5, the average annual iceberg density in the degree square containing the cable crossing site is 7.1. The area covered by a degree square at a 51 - 52ºN latitude is approximately 7,700 km^2, and the degree square containing the cable crossing site is 60% covered by land, giving a density of 2.3×10^{-3} km^{-2}. The average iceberg drift speed, including periods when icebergs are grounded, is 0.12 m/s (Roche, 1980). The number of seconds per year is 3.16×10^7. The proportion of icebergs with drafts capable of contacting the cable (r'_d) is an output of the Monte Carlo model.

4.3 Results

4.3.1 *Point Amour Trough and Labrador Landfall Zone (Zone 1)*

Zone 1 (Figure 4-2) covers the cable landfalls on the Labrador coast and portions of the cable routes in the Point Amour Trough. The total cable length in Zone 1 is 13.41 km, in water depths ranging from 0.3 to 117.5 m. Free-floating iceberg contacts with a 120 mm diameter cable laid on the seabed are approximately 50% higher than contacts with scouring icebergs. Table 4-1 gives a summary of ice keel contact rates for cables in Zone 1 using 2.5 m water depth intervals for the base case (total annual contact rate 0.139). Table 4-2 gives results for a mean iceberg rolling period of 1 day (total annual contact rate 0.144). Table 4-3 gives results for a 10 day mean iceberg rolling period (total annual contact rate 0.143), and Table 4-4 gives results with no rolling (total annual contact rate 0.139). While overall risk levels are consistent, variations in the distribution are readily observed, particularly for the case with no rolling. Note that ice keel contact rates in shallow water (i.e. < 20 m) do not include pack ice, bergy bits or growlers, which are not included in the model.

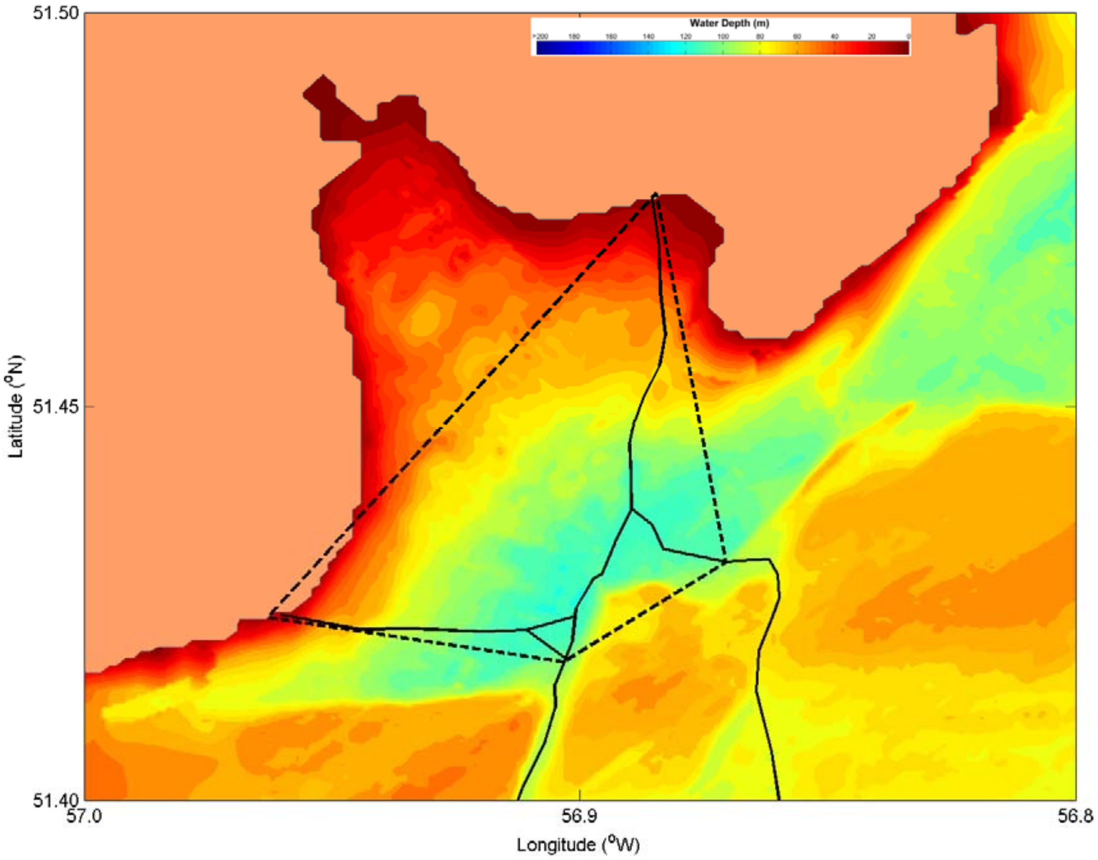

Figure 4-2 Point Amour trough and Labrador landfall (Zone 1)

Table 4-1 Cable contact summary for Zone 1 (base case)

Water Depth (m)		Cable Length (m)	Annual Contact Rate	Water Depth (m)		Cable Length (m)	Annual Contact Rate
Min.	Max.			Min.	Max.		
0.0	2.5	50	3.7×10^{-5}	60.0	62.5	510	8.1×10^{-3}
2.5	5.0	60	1.6×10^{-4}	62.5	65.0	130	8.1×10^{-5}
5.0	7.5	90	9.2×10^{-3}	65.0	67.5	500	1.3×10^{-4}
7.5	10.0	180	1.8×10^{-2}	67.5	70.0	100	3.5×10^{-5}
10.0	12.5	230	2.1×10^{-2}	70.0	72.5	110	2.2×10^{-4}
12.5	15.0	190	1.6×10^{-2}	72.5	75.0	110	3.6×10^{-4}
15.0	17.5	150	1.9×10^{-2}	75.0	77.5	150	4.1×10^{-4}
17.5	20.0	130	1.6×10^{-2}	77.5	80.0	170	0
20.0	22.5	70	5.3×10^{-3}	80.0	82.5	160	0
22.5	25.0	60	4.2×10^{-3}	82.5	85.0	160	0
25.0	27.5	60	3.5×10^{-3}	85.0	87.5	240	0
27.5	30.0	60	2.9×10^{-3}	87.5	90.0	350	0
30.0	32.5	60	2.5×10^{-3}	90.0	92.5	170	0
32.5	35.0	60	2.5×10^{-3}	92.5	95.0	190	0
35.0	37.5	80	3.4×10^{-3}	95.0	97.5	190	0
37.5	40.0	80	2.0×10^{-3}	97.5	100.0	330	0
40.0	42.5	100	2.3×10^{-3}	100.0	102.5	400	0
42.5	45.0	100	2.0×10^{-3}	102.5	105.0	450	0
45.0	47.5	120	1.6×10^{-3}	105.0	107.5	1,060	0
47.5	50.0	150	1.6×10^{-3}	107.5	110.0	1,490	1.4×10^{-5}
50.0	52.5	140	8.1×10^{-4}	110.0	112.5	2,040	9.2×10^{-4}
52.5	55.0	160	8.1×10^{-4}	112.5	115.0	1,240	0
55.0	57.5	200	8.1×10^{-4}	115.0	117.5	370	0
57.5	60.0	200	8.1×10^{-4}	117.5	120.0	10	0

Table 4-2 Cable contact summary for Zone 1 (mean rolling period 1 day)

Water Depth (m)		Cable Length (m)	Annual Contact Rate	Water Depth (m)		Cable Length (m)	Annual Contact Rate
Min.	Max.			Min.	Max.		
0.0	2.5	50	0	60.0	62.5	510	2.3×10^{-3}
2.5	5.0	60	0	62.5	65.0	130	1.1×10^{-3}
5.0	7.5	90	8.2×10^{-3}	65.0	67.5	500	6.7×10^{-4}
7.5	10.0	180	1.7×10^{-2}	67.5	70.0	100	2.4×10^{-5}
10.0	12.5	230	1.9×10^{-2}	70.0	72.5	110	0
12.5	15.0	190	1.3×10^{-2}	72.5	75.0	110	0
15.0	17.5	150	1.6×10^{-2}	75.0	77.5	150	0
17.5	20.0	130	1.7×10^{-2}	77.5	80.0	170	0
20.0	22.5	70	7.0×10^{-3}	80.0	82.5	160	0
22.5	25.0	60	5.8×10^{-3}	82.5	85.0	160	0
25.0	27.5	60	4.9×10^{-3}	85.0	87.5	240	0
27.5	30.0	60	4.0×10^{-3}	87.5	90.0	350	0
30.0	32.5	60	3.5×10^{-3}	90.0	92.5	170	0
32.5	35.0	60	3.5×10^{-3}	92.5	95.0	190	0
35.0	37.5	80	4.6×10^{-3}	95.0	97.5	190	0
37.5	40.0	80	3.1×10^{-3}	97.5	100.0	330	0
40.0	42.5	100	4.0×10^{-3}	100.0	102.5	400	0
42.5	45.0	100	2.7×10^{-3}	102.5	105.0	450	0
45.0	47.5	120	1.3×10^{-3}	105.0	107.5	1,060	0
47.5	50.0	150	1.5×10^{-3}	107.5	110.0	1,490	0
50.0	52.5	140	1.2×10^{-3}	110.0	112.5	2,040	0
52.5	55.0	160	1.2×10^{-3}	112.5	115.0	1,240	0
55.0	57.5	200	6.9×10^{-4}	115.0	117.5	370	0
57.5	60.0	200	2.2×10^{-4}	117.5	120.0	10	0

Table 4-3 Cable contact summary for Zone 1 (mean rolling period 10 days)

Water Depth (m)		Cable Length (m)	Annual Contact Rate	Water Depth (m)		Cable Length (m)	Annual Contact Rate
Min.	Max.			Min.	Max.		
0.0	2.5	50	1.4×10^{-4}	60.0	62.5	510	4.8×10^{-4}
2.5	5.0	60	6.5×10^{-4}	62.5	65.0	130	4.8×10^{-5}
5.0	7.5	90	9.1×10^{-3}	65.0	67.5	500	2.7×10^{-6}
7.5	10.0	180	1.9×10^{-2}	67.5	70.0	100	0
10.0	12.5	230	2.8×10^{-2}	70.0	72.5	110	0
12.5	15.0	190	2.0×10^{-2}	72.5	75.0	110	0
15.0	17.5	150	1.8×10^{-2}	75.0	77.5	150	0
17.5	20.0	130	1.4×10^{-2}	77.5	80.0	170	0
20.0	22.5	70	5.6×10^{-3}	80.0	82.5	160	0
22.5	25.0	60	4.9×10^{-3}	82.5	85.0	160	0
25.0	27.5	60	3.8×10^{-3}	85.0	87.5	240	0
27.5	30.0	60	2.8×10^{-3}	87.5	90.0	350	0
30.0	32.5	60	2.2×10^{-3}	90.0	92.5	170	0
32.5	35.0	60	2.2×10^{-3}	92.5	95.0	190	0
35.0	37.5	80	3.2×10^{-3}	95.0	97.5	190	0
37.5	40.0	80	1.9×10^{-3}	97.5	100.0	330	0
40.0	42.5	100	1.9×10^{-3}	100.0	102.5	400	0
42.5	45.0	100	1.8×10^{-3}	102.5	105.0	450	0
45.0	47.5	120	1.7×10^{-3}	105.0	107.5	1,060	0
47.5	50.0	150	1.5×10^{-3}	107.5	110.0	1,490	0
50.0	52.5	140	7.0×10^{-4}	110.0	112.5	2,040	0
52.5	55.0	160	4.2×10^{-4}	112.5	115.0	1,240	0
55.0	57.5	200	1.6×10^{-5}	115.0	117.5	370	0
57.5	60.0	200	0	117.5	120.0	10	0

Table 4-4 Cable contact summary for Zone 1 (no iceberg rolling)

Water Depth (m)		Cable Length (m)	Annual Contact Rate	Water Depth (m)		Cable Length (m)	Annual Contact Rate
Min.	Max.			Min.	Max.		
0.0	2.5	50	6.9×10^{-4}	60.0	62.5	510	0
2.5	5.0	60	5.1×10^{-4}	62.5	65.0	130	0
5.0	7.5	90	7.3×10^{-3}	65.0	67.5	500	0
7.5	10.0	180	1.6×10^{-2}	67.5	70.0	100	0
10.0	12.5	230	2.1×10^{-2}	70.0	72.5	110	0
12.5	15.0	190	1.8×10^{-2}	72.5	75.0	110	0
15.0	17.5	150	1.9×10^{-2}	75.0	77.5	150	0
17.5	20.0	130	1.5×10^{-2}	77.5	80.0	170	0
20.0	22.5	70	4.9×10^{-3}	80.0	82.5	160	0
22.5	25.0	60	4.0×10^{-3}	82.5	85.0	160	0
25.0	27.5	60	3.7×10^{-3}	85.0	87.5	240	0
27.5	30.0	60	3.4×10^{-3}	87.5	90.0	350	0
30.0	32.5	60	3.4×10^{-3}	90.0	92.5	170	0
32.5	35.0	60	3.5×10^{-3}	92.5	95.0	190	0
35.0	37.5	80	4.8×10^{-3}	95.0	97.5	190	0
37.5	40.0	80	3.0×10^{-3}	97.5	100.0	330	0
40.0	42.5	100	3.7×10^{-3}	100.0	102.5	400	0
42.5	45.0	100	2.8×10^{-3}	102.5	105.0	450	0
45.0	47.5	120	2.0×10^{-3}	105.0	107.5	1,060	0
47.5	50.0	150	1.7×10^{-3}	107.5	110.0	1,490	0
50.0	52.5	140	7.3×10^{-4}	110.0	112.5	2,040	0
52.5	55.0	160	4.1×10^{-4}	112.5	115.0	1,240	0
55.0	57.5	200	1.6×10^{-5}	115.0	117.5	370	0
57.5	60.0	200	0	117.5	120.0	10	0

4.3.2 Channel Zone (Zone 2)

Zone 2 (Figure 4-3) covers a sheltered channel which runs between Banks A & B. The total cable length in Zone 2 is 7.44 km, with water depths ranging from 82.6 m to 105.1 m. The total annual contact rate for all cable segments in Zone 2 is 2.0×10^{-4}. Table 4-5 gives a summary of ice keel contact rates for cables in Zone 2 using 2.5 m water depth intervals (base case). Table 4-6, Table 4-7 and Table 4-8 give results for the cases 1 and 10 days rolling and no rolling, respectively. In none of these additional runs was an iceberg grounding produced over the cable route in Zone 2.

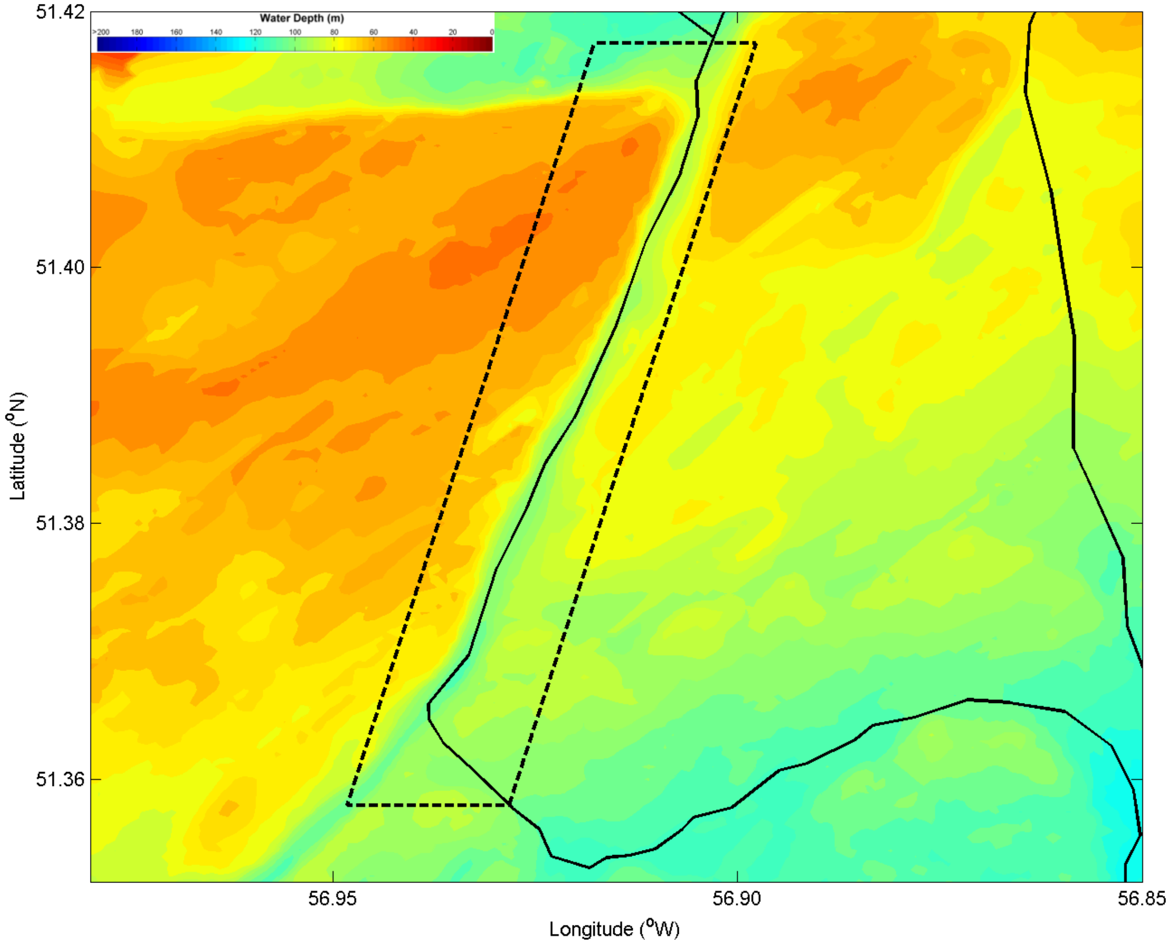

Figure 4-3 Channel zone (Zone 2)

Table 4-5 Cable contact summary for Zone 2 (base case)

Water Depth (m)		Cable Length (m)	Annual Contact Rate	Water Depth (m)		Cable Length (m)	Annual Contact Rate
Min.	Max.			Min.	Max.		
82.5	85.0	620	0	95.0	97.5	1,890	0
85.0	87.5	670	0	97.5	100.0	960	0
87.5	90.0	830	0	100.0	102.5	390	0
90.0	92.5	870	2.0×10^{-4}	102.5	105.0	560	0
92.5	95.0	630	0	105.0	107.5	20	0

Table 4-6 Cable contact summary for Zone 2 (mean rolling period 1 day)

Water Depth (m)		Cable Length (m)	Annual Contact Rate	Water Depth (m)		Cable Length (m)	Annual Contact Rate
Min.	Max.			Min.	Max.		
82.5	85.0	620	0	95.0	97.5	1,890	0
85.0	87.5	670	0	97.5	100.0	960	0
87.5	90.0	830	0	100.0	102.5	390	0
90.0	92.5	870	0	102.5	105.0	560	0
92.5	95.0	630	0	105.0	107.5	20	0

Table 4-7 Cable contact summary for Zone 2 (mean rolling period 10 days)

Water Depth (m)		Cable Length (m)	Annual Contact Rate	Water Depth (m)		Cable Length (m)	Annual Contact Rate
Min.	Max.			Min.	Max.		
82.5	85.0	620	0	95.0	97.5	1,890	0
85.0	87.5	670	0	97.5	100.0	960	0
87.5	90.0	830	0	100.0	102.5	390	0
90.0	92.5	870	0	102.5	105.0	560	0
92.5	95.0	630	0	105.0	107.5	20	0

Table 4-8 Cable contact summary for Zone 2 (no iceberg rolling)

Water Depth (m)		Cable Length (m)	Annual Contact Rate	Water Depth (m)		Cable Length (m)	Annual Contact Rate
Min.	Max.			Min.	Max.		
82.5	85.0	620	0	95.0	97.5	1,890	0
85.0	87.5	670	0	97.5	100.0	960	0
87.5	90.0	830	0	100.0	102.5	390	0
90.0	92.5	870	0	102.5	105.0	560	0
92.5	95.0	630	0	105.0	107.5	20	0

4.3.3 Bank B Crossing Zone (Zone 3)

Zone 3 (Figure 4-4) covers a relatively sheltered portion of Bank B. The total cable length in Zone 3 is 6.42 km, with water depths ranging from 66.9 m to 100.1 m. The total annual contact rate for all cable segments in Zone 2 is 5.8×10^{-4}. Table 4-9 gives a summary of ice keel contact rates for cables in Zone 3 using 2.5 m water depth intervals. Table 4-10 gives results for a 1 day rolling period, with no grounding events over the cable. However, grounding events did occur over the cable with a 10 day rolling period (Table 4-11), for an annual contact rate of 1.3×10^{-3}. Table 4-12 gives results for no rolling (no groundings occur over the cable).

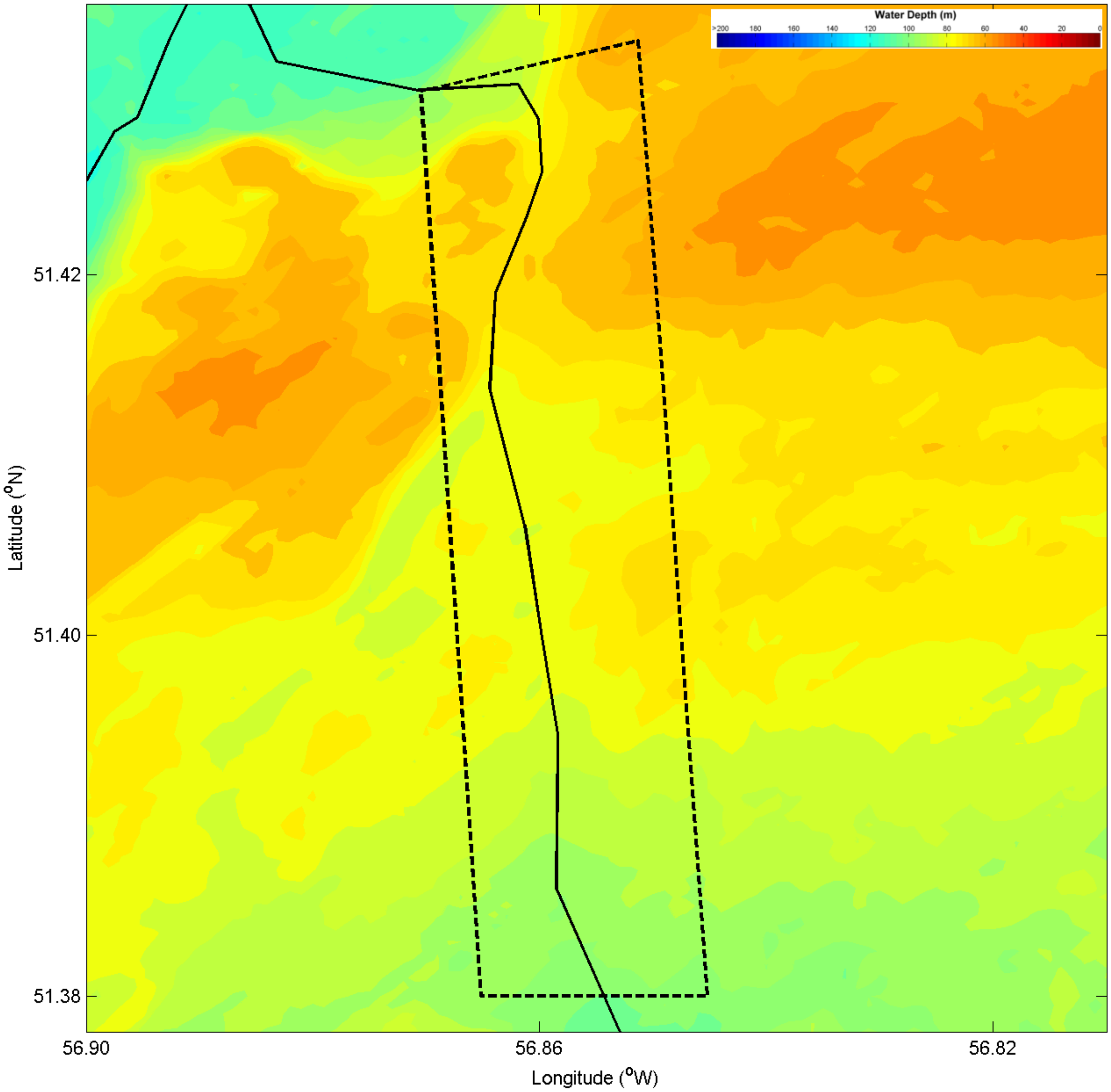

Figure 4-4 Bank B crossing zone (Zone 3)

Table 4-9 Cable contact summary for Zone 3 (base case)

Water Depth (m)		Cable Length (m)	Annual Contact Rate	Water Depth (m)		Cable Length (m)	Annual Contact Rate
Min.	Max.			Min.	Max.		
65.0	67.5	220	4.4×10^{-4}	85.0	87.5	260	0
67.5	70.0	650	1.4×10^{-4}	87.5	90.0	620	0
70.0	72.5	290	0	90.0	92.5	290	0
72.5	75.0	280	0	92.5	95.0	400	0
75.0	77.5	630	0	95.0	97.5	430	0
77.5	80.0	1,590	0	97.5	100.0	90	0
80.0	82.5	310	0	100.0	102.5	10	0
82.5	85.0	350	0				

Table 4-10 Cable contact summary for Zone 3 (mean rolling period 1 day)

Water Depth (m)		Cable Length (m)	Annual Contact Rate	Water Depth (m)		Cable Length (m)	Annual Contact Rate
Min.	Max.			Min.	Max.		
65.0	67.5	220	0	85.0	87.5	260	0
67.5	70.0	650	0	87.5	90.0	620	0
70.0	72.5	290	0	90.0	92.5	290	0
72.5	75.0	280	0	92.5	95.0	400	0
75.0	77.5	630	0	95.0	97.5	430	0
77.5	80.0	1,590	0	97.5	100.0	90	0
80.0	82.5	310	0	100.0	102.5	10	0
82.5	85.0	350	0				

Table 4-11 Cable contact summary for Zone 3 (mean rolling period 10 days)

Water Depth (m)		Cable Length (m)	Annual Contact Rate	Water Depth (m)		Cable Length (m)	Annual Contact Rate
Min.	Max.			Min.	Max.		
65.0	67.5	220	1.1×10^{-3}	85.0	87.5	260	0
67.5	70.0	650	1.9×10^{-4}	87.5	90.0	620	0
70.0	72.5	290	0	90.0	92.5	290	0
72.5	75.0	280	0	92.5	95.0	400	0
75.0	77.5	630	0	95.0	97.5	430	0
77.5	80.0	1,590	0	97.5	100.0	90	0
80.0	82.5	310	0	100.0	102.5	10	0
82.5	85.0	350	0				

Table 4-12 Cable contact summary for Zone 3 (no rolling)

Water Depth (m)		Cable Length (m)	Annual Contact Rate	Water Depth (m)		Cable Length (m)	Annual Contact Rate
Min.	Max.			Min.	Max.		
65.0	67.5	220	0	85.0	87.5	260	0
67.5	70.0	650	0	87.5	90.0	620	0
70.0	72.5	290	0	90.0	92.5	290	0
72.5	75.0	280	0	92.5	95.0	400	0
75.0	77.5	630	0	95.0	97.5	430	0
77.5	80.0	1,590	0	97.5	100.0	90	0
80.0	82.5	310	0	100.0	102.5	10	0
82.5	85.0	350	0				

4.3.4 Central Trough Zone (Zone 4)

Zone 4 (Figure 4-5) covers the relatively well-sheltered Central Trough. The total cable length in Zone 4 is 23.93 km, with water depths ranging from 76.2 m to 124.4 m. Table 4-13 gives a summary of ice keel contact rates for cables in Zone 4 using 2.5 m water depth intervals (base case), with a total annual iceberg contact rate of 2.7×10^{-3}. A one day rolling period (Table 4-14) gives a total annual iceberg contact rate of 4.7×10^{-4}, while a ten day rolling period (Table 4-15) gives a total annual iceberg contact rate of 0. The no rolling case (Table 4-16) also gives a total annual iceberg contact rate of 0.

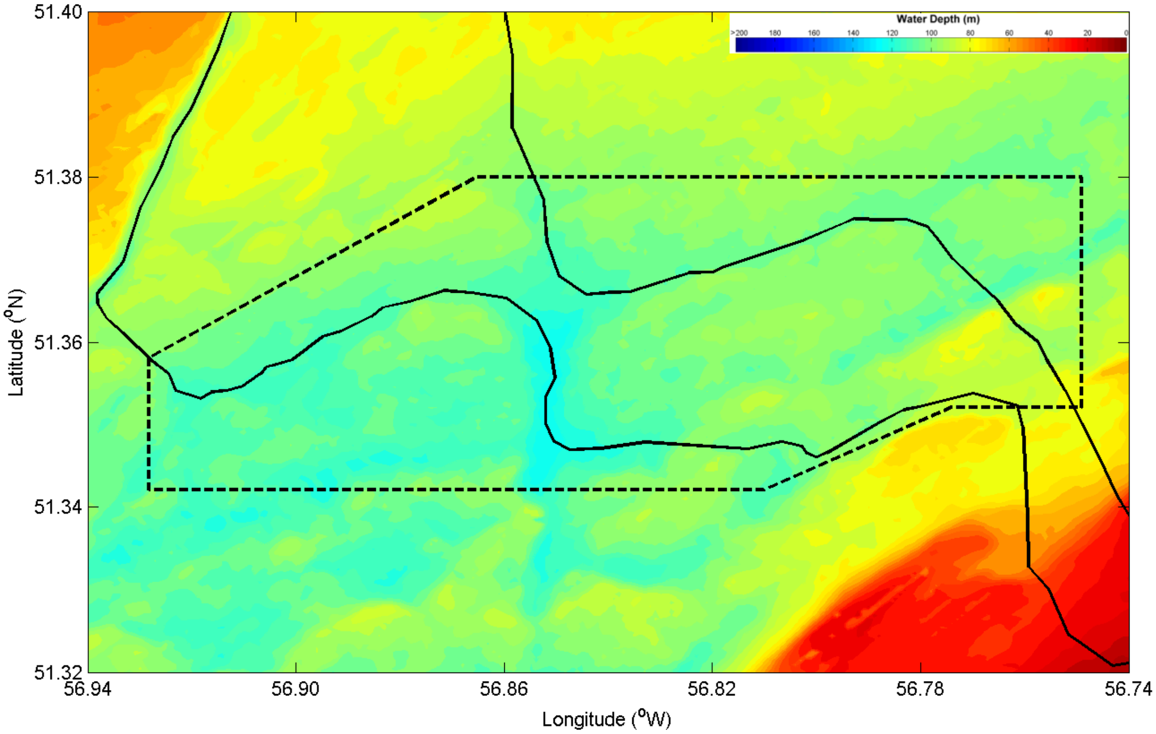

Figure 4-5 Central trough zone (Zone 4)

Table 4-13 Cable contact summary for Zone 4 (base case)

Water Depth (m)		Cable Length (m)	Annual Contact Rate	Water Depth (m)		Cable Length (m)	Annual Contact Rate
Min.	Max.			Min.	Max.		
75.0	77.5	210	5.0×10^{-6}	100.0	102.5	4,390	4.3×10^{-4}
77.5	80.0	290	2.6×10^{-4}	102.5	105.0	4,320	2.0×10^{-3}
80.0	82.5	350	0	105.0	107.5	1,550	0
82.5	85.0	270	0	107.5	110.0	1,820	0
85.0	87.5	580	0	110.0	112.5	2,700	0
87.5	90.0	490	0	112.5	115.0	1,500	0
90.0	92.5	820	0	115.0	117.5	440	0
92.5	95.0	210	0	117.5	120.0	530	0
95.0	97.5	550	0	120.0	122.5	980	0
97.5	100.0	1,240	0	122.5	125.0	690	0

Table 4-14 Cable contact summary for Zone 4 (mean rolling period 1 day)

Water Depth (m)		Cable Length (m)	Annual Contact Rate	Water Depth (m)		Cable Length (m)	Annual Contact Rate
Min.	Max.			Min.	Max.		
75.0	77.5	210	1.4×10^{-4}	100.0	102.5	4,390	0
77.5	80.0	290	0	102.5	105.0	4,320	0
80.0	82.5	350	3.3×10^{-4}	105.0	107.5	1,550	0
82.5	85.0	270	0	107.5	110.0	1,820	0
85.0	87.5	580	0	110.0	112.5	2,700	0
87.5	90.0	490	0	112.5	115.0	1,500	0
90.0	92.5	820	0	115.0	117.5	440	0
92.5	95.0	210	0	117.5	120.0	530	0
95.0	97.5	550	0	120.0	122.5	980	0
97.5	100.0	1,240	0	122.5	125.0	690	0

Table 4-15 Cable contact summary for Zone 4 (mean rolling period 10 days)

Water Depth (m)		Cable Length (m)	Annual Contact Rate	Water Depth (m)		Cable Length (m)	Annual Contact Rate
Min.	Max.			Min.	Max.		
75.0	77.5	210	0	100.0	102.5	4,390	0
77.5	80.0	290	0	102.5	105.0	4,320	0
80.0	82.5	350	0	105.0	107.5	1,550	0
82.5	85.0	270	0	107.5	110.0	1,820	0
85.0	87.5	580	0	110.0	112.5	2,700	0
87.5	90.0	490	0	112.5	115.0	1,500	0
90.0	92.5	820	0	115.0	117.5	440	0
92.5	95.0	210	0	117.5	120.0	530	0
95.0	97.5	550	0	120.0	122.5	980	0
97.5	100.0	1,240	0	122.5	125.0	690	0

Table 4-16 Cable contact summary for Zone 4 (no rolling)

Water Depth (m)		Cable Length (m)	Annual Contact Rate	Water Depth (m)		Cable Length (m)	Annual Contact Rate
Min.	Max.			Min.	Max.		
75.0	77.5	210	0	100.0	102.5	4,390	0
77.5	80.0	290	0	102.5	105.0	4,320	0
80.0	82.5	350	0	105.0	107.5	1,550	0
82.5	85.0	270	0	107.5	110.0	1,820	0
85.0	87.5	580	0	110.0	112.5	2,700	0
87.5	90.0	490	0	112.5	115.0	1,500	0
90.0	92.5	820	0	115.0	117.5	440	0
92.5	95.0	210	0	117.5	120.0	530	0
95.0	97.5	550	0	120.0	122.5	980	0
97.5	100.0	1,240	0	122.5	125.0	690	0

4.3.5 Newfoundland Landfall Zone (Zone 5)

Zone 5 (Figure 4-6) covers the Newfoundland cable landfall site. There is a total of 10.04 km of cable in Zone 5, in water depths ranging from 0.16 to 85 m. The base case scenario (Table 4-17) gives a total annual iceberg contact rate of 0.751. The other mean rolling periods considered: 1 day (Table 4-18), 10 days (Table 4-19) and no rolling (Table 4-20) gave total annual iceberg contact rates of 0.732, 0.885 and 0.843, respectively. With the exception of the no rolling scenario, iceberg contacts were modeled in the 70-80 m water depth range.

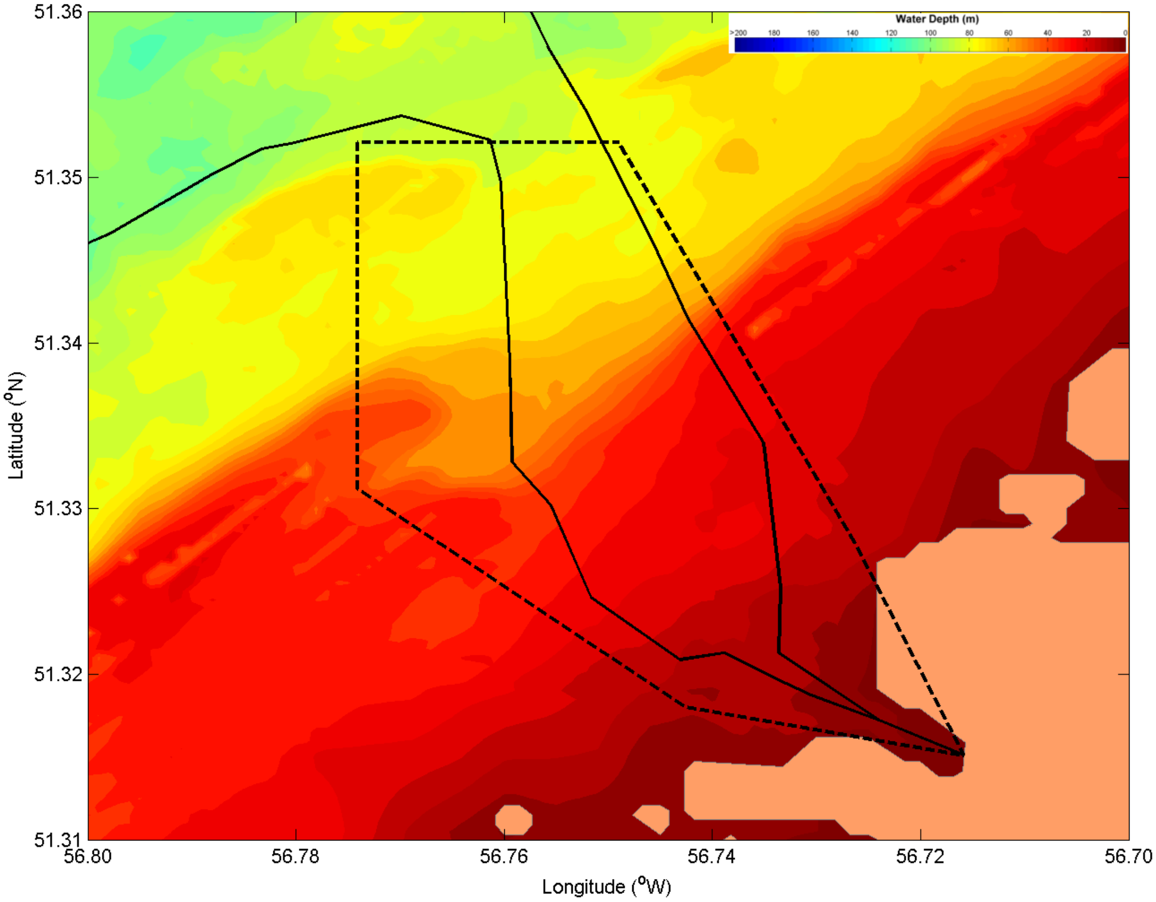

Figure 4-6 Newfoundland landfall zone (Zone 5)

Table 4-17 Cable contact summary for Zone 5 (base case)

Water Depth (m)		Cable Length (m)	Annual Contact Rate	Water Depth (m)		Cable Length (m)	Annual Contact Rate
Min.	Max.			Min.	Max.		
0.0	2.5	80	5.2×10^{-5}	45.0	47.5	60	6.0×10^{-3}
2.5	5.0	1130	2.0×10^{-3}	47.5	50.0	90	7.0×10^{-3}
5.0	7.5	310	3.2×10^{-3}	50.0	52.5	150	7.4×10^{-3}
7.5	10.0	1310	6.1×10^{-2}	52.5	55.0	370	1.2×10^{-2}
10.0	12.5	190	2.5×10^{-2}	55.0	57.5	180	3.2×10^{-3}
12.5	15.0	200	2.8×10^{-2}	57.5	60.0	150	1.9×10^{-3}
15.0	17.5	320	4.3×10^{-2}	60.0	62.5	160	2.0×10^{-3}
17.5	20.0	850	1.2×10^{-1}	62.5	65.0	120	7.9×10^{-4}
20.0	22.5	720	1.9×10^{-1}	65.0	67.5	100	1.6×10^{-4}
22.5	25.0	270	7.4×10^{-2}	67.5	70.0	100	1.9×10^{-4}
25.0	27.5	250	5.3×10^{-2}	70.0	72.5	130	3.1×10^{-4}
27.5	30.0	240	3.5×10^{-2}	72.5	75.0	530	3.3×10^{-4}
30.0	32.5	190	2.6×10^{-2}	75.0	77.5	930	1.1×10^{-3}
32.5	35.0	130	2.1×10^{-2}	77.5	80.0	270	0
35.0	37.5	70	1.1×10^{-2}	80.0	82.5	60	0
37.5	40.0	50	7.4×10^{-3}	82.5	85.0	190	0
40.0	42.5	60	7.9×10^{-3}	85.0	87.5	20	0
42.5	45.0	60	6.8×10^{-3}				

Table 4-18 Cable contact summary for Zone 5 (mean rolling period 1 day)

Water Depth (m)		Cable Length (m)	Annual Contact Rate	Water Depth (m)		Cable Length (m)	Annual Contact Rate
Min.	Max.			Min.	Max.		
0.0	2.5	80	1.7×10^{-4}	45.0	47.5	60	6.5×10^{-3}
2.5	5.0	1130	4.3×10^{-3}	47.5	50.0	90	6.6×10^{-3}
5.0	7.5	310	4.4×10^{-3}	50.0	52.5	150	5.6×10^{-3}
7.5	10.0	1310	5.4×10^{-2}	52.5	55.0	370	1.1×10^{-2}
10.0	12.5	190	3.0×10^{-2}	55.0	57.5	180	4.8×10^{-3}
12.5	15.0	200	2.7×10^{-2}	57.5	60.0	150	2.9×10^{-4}
15.0	17.5	320	4.8×10^{-2}	60.0	62.5	160	1.5×10^{-5}
17.5	20.0	850	1.2×10^{-1}	62.5	65.0	120	0
20.0	22.5	720	1.9×10^{-1}	65.0	67.5	100	8.9×10^{-7}
22.5	25.0	270	7.1×10^{-2}	67.5	70.0	100	0
25.0	27.5	250	4.3×10^{-2}	70.0	72.5	130	0
27.5	30.0	240	3.2×10^{-2}	72.5	75.0	530	0
30.0	32.5	190	2.5×10^{-2}	75.0	77.5	930	1.8×10^{-3}
32.5	35.0	130	2.1×10^{-2}	77.5	80.0	270	0
35.0	37.5	70	9.1×10^{-3}	80.0	82.5	60	0
37.5	40.0	50	5.8×10^{-3}	82.5	85.0	190	0
40.0	42.5	60	7.0×10^{-3}	85.0	87.5	20	0
42.5	45.0	60	7.3×10^{-3}				

Table 4-19 Cable contact summary for Zone 5 (mean rolling period 10 days)

Water Depth (m)		Cable Length (m)	Annual Contact Rate	Water Depth (m)		Cable Length (m)	Annual Contact Rate
Min.	Max.			Min.	Max.		
0.0	2.5	80	0	45.0	47.5	60	6.5×10^{-3}
2.5	5.0	1130	6.0×10^{-4}	47.5	50.0	90	6.1×10^{-3}
5.0	7.5	310	3.4×10^{-3}	50.0	52.5	150	6.5×10^{-3}
7.5	10.0	1310	6.9×10^{-2}	52.5	55.0	370	1.5×10^{-2}
10.0	12.5	190	3.3×10^{-2}	55.0	57.5	180	3.8×10^{-3}
12.5	15.0	200	4.2×10^{-2}	57.5	60.0	150	1.8×10^{-3}
15.0	17.5	320	6.3×10^{-2}	60.0	62.5	160	2.4×10^{-4}
17.5	20.0	850	1.4×10^{-1}	62.5	65.0	120	0
20.0	22.5	720	2.0×10^{-1}	65.0	67.5	100	0
22.5	25.0	270	9.6×10^{-2}	67.5	70.0	100	0
25.0	27.5	250	6.7×10^{-2}	70.0	72.5	130	0
27.5	30.0	240	4.0×10^{-2}	72.5	75.0	530	0
30.0	32.5	190	2.9×10^{-2}	75.0	77.5	930	2.2×10^{-3}
32.5	35.0	130	2.4×10^{-2}	77.5	80.0	270	2.5×10^{-4}
35.0	37.5	70	1.1×10^{-2}	80.0	82.5	60	0
37.5	40.0	50	7.4×10^{-3}	82.5	85.0	190	0
40.0	42.5	60	8.4×10^{-3}	85.0	87.5	20	0
42.5	45.0	60	8.1×10^{-3}				

Table 4-20 Cable contact summary for Zone 5 (no rolling)

Water Depth (m)		Cable Length (m)	Annual Contact Rate	Water Depth (m)		Cable Length (m)	Annual Contact Rate
Min.	Max.			Min.	Max.		
0.0	2.5	80	7.5×10^{-5}	45.0	47.5	60	5.6×10^{-3}
2.5	5.0	1130	2.0×10^{-3}	47.5	50.0	90	5.3×10^{-3}
5.0	7.5	310	3.2×10^{-3}	50.0	52.5	150	6.1×10^{-3}
7.5	10.0	1310	6.6×10^{-2}	52.5	55.0	370	8.8×10^{-3}
10.0	12.5	190	2.6×10^{-2}	55.0	57.5	180	1.5×10^{-3}
12.5	15.0	200	3.1×10^{-2}	57.5	60.0	150	5.7×10^{-4}
15.0	17.5	320	5.5×10^{-2}	60.0	62.5	160	3.8×10^{-4}
17.5	20.0	850	1.2×10^{-1}	62.5	65.0	120	1.2×10^{-4}
20.0	22.5	720	2.3×10^{-1}	65.0	67.5	100	2.2×10^{-5}
22.5	25.0	270	9.1×10^{-2}	67.5	70.0	100	0
25.0	27.5	250	5.9×10^{-2}	70.0	72.5	130	0
27.5	30.0	240	4.2×10^{-2}	72.5	75.0	530	0
30.0	32.5	190	2.9×10^{-2}	75.0	77.5	930	0
32.5	35.0	130	2.2×10^{-2}	77.5	80.0	270	0
35.0	37.5	70	1.1×10^{-2}	80.0	82.5	60	0
37.5	40.0	50	7.8×10^{-3}	82.5	85.0	190	0
40.0	42.5	60	8.7×10^{-3}	85.0	87.5	20	0
42.5	45.0	60	7.5×10^{-3}				

4.3.6 Probability of Multiple Contact Events

Up to this point, the cable has been treated as a single entity. However, multiple cables will be required and the probability that an iceberg contact event will involve more than one of the cables is a consideration. Three subsea cables are being considered for the strait crossing, and will be used here for the analysis.

As indicated in Section 4.3, cable contacts are dominated by free-floating icebergs. However, a methodology based on free-floating contacts was not apparent, therefore scouring icebergs were used as the basis of the analysis. It will be assumed that the observed scour parameters (specifically the length distribution) derived from seabed mapping reflect modern scour parameters and are representative, should a scour form (which may be a very low probability in deeper water depths). Since the scour orientation is highly directional and aligned with the Strait of Belle Isle, and the cables cross the Strait of Belle Isle, scours will be assumed to be oriented at right angles to the cables. It is also assumed that the cables are laid parallel on the seabed with a constant distance between them.

A Monte Carlo model was used for the analysis. Large samples of iceberg scours were generated using lognormal distributions based on iceberg scour length parameters given in Table 2-7. The spacing between the cables was varied from 0 m to 1 km in 50 m increments. Given that a scouring iceberg crosses over and contacts any of the three cables, the proportion of cases with one, two or three “simultaneous” iceberg contacts per scour-crossing event were determined for a range of cable configurations and water depths.

The results of the analysis are shown in Figure 4-7 to Figure 4-18 for varying water depth ranges. Each figure shows the proportion of cases with one, two and three cables contacted, given that a contact event occurs (cases where no contact event occurred were omitted from the analysis). For the case of zero distance between cables, all contact events always involve all three cables. As the distance increases, the proportion of cases involving three cables decreases and the proportion of cases involving just one cable increases. Table 4-21 summarizes the results of the analysis, giving the required cable separation such that the probability of just one cable (out of three) is contacted during a scour crossing event equals 50% and 90%. It is assumed here that, given contact occurs, that a high probability of contact with just one cable (arbitrarily 90%) is desired. The distances required between cables to achieve this target vary from 120 m (25 to 35 m water depth range) to 1,400 m (105 to 115 m water depth range).

Table 4-21 Required distance between cables (3) so that probability of one cable contacted during an iceberg interaction event equals 50% and 90%

Water Depth (m)	Scour Length Parameters		Distance (m) Required for 50% Probability of One Cable Contact	Distance (m) Required for 90% Probability of One Cable Contact
	Mean (m)	St. Dev. (m)		
> 5 & ≤ 15	145.4	44.8	60	140
> 15 & ≤ 25	108.8	89.4	45	160
> 25 & ≤ 35	80.2	63.8	35	120
> 35 & ≤ 45	143.4	133.9	55	235
> 45 & ≤ 55	186.9	185.7	75	325
> 55 & ≤ 65	167.8	238.8	70	420
> 65 & ≤ 75	179.4	163.9	70	295
> 75 & ≤ 85	262.1	301.3	105	520
> 85 & ≤ 95	381.3	342.0	150	610
> 95 & ≤ 105	486.9	483.5	195	850
> 105 & ≤ 115	547.5	792.1	230	1,400
> 115 & ≤ 125	250.9	105.0	100	260

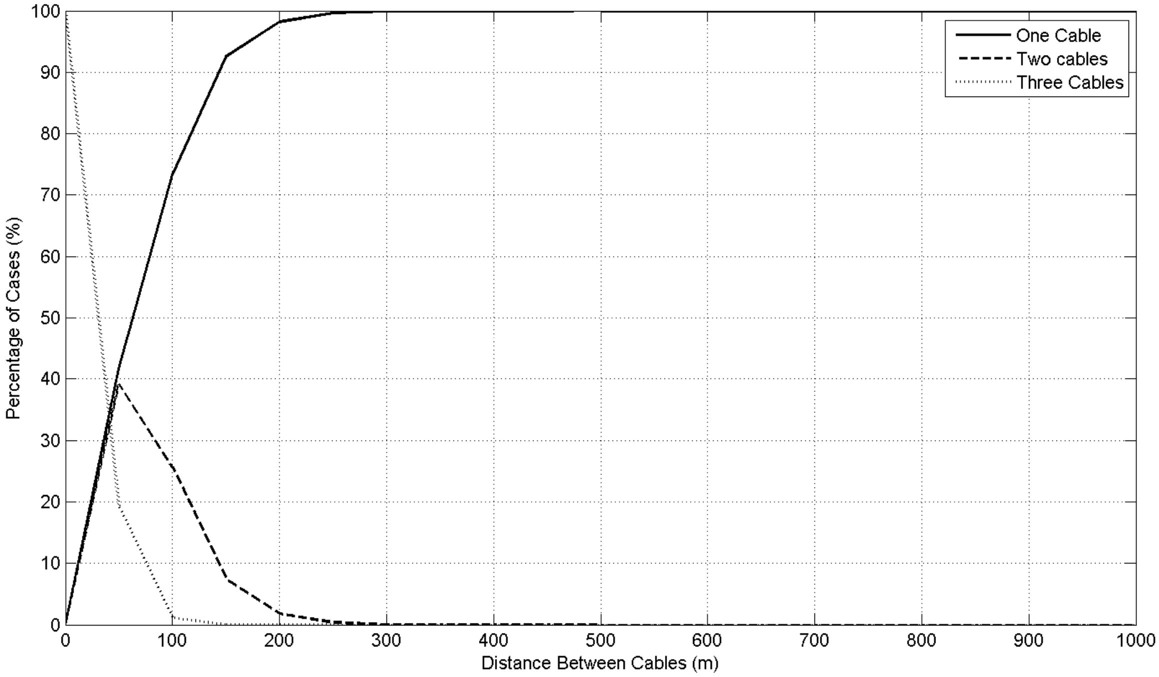

Figure 4-7 Percentage of events involving 1 to 3 cables, 5 to 15 m water depth

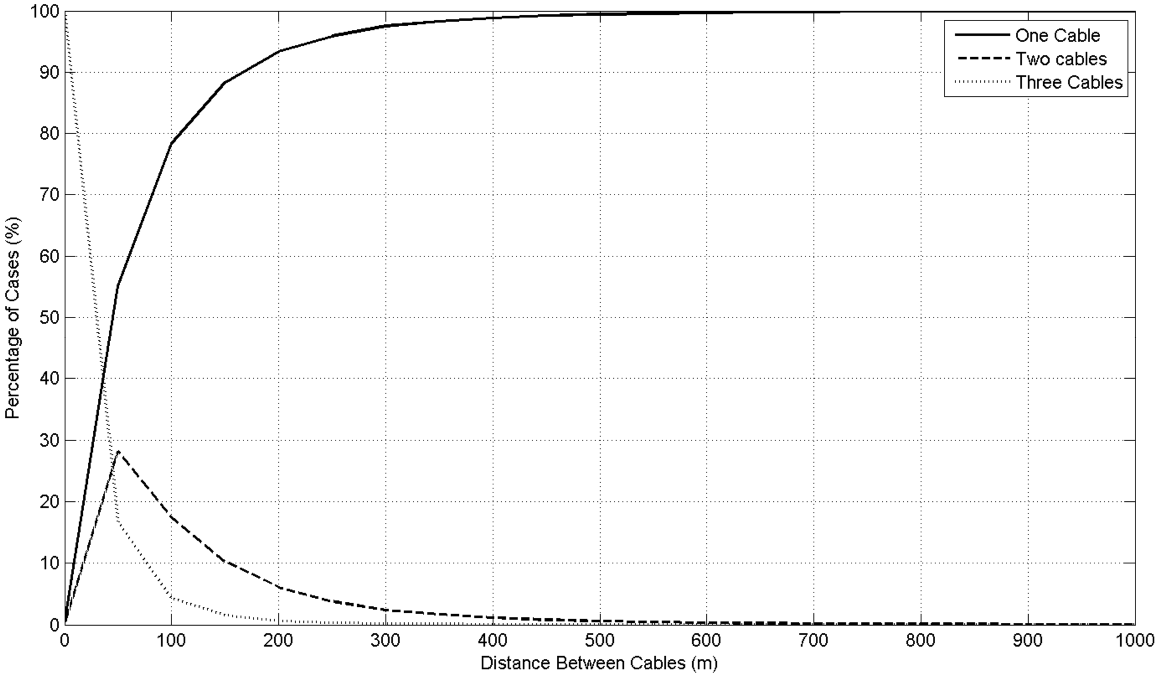

Figure 4-8 Percentage of events involving 1 to 3 cables, 15 to 25 m water depth

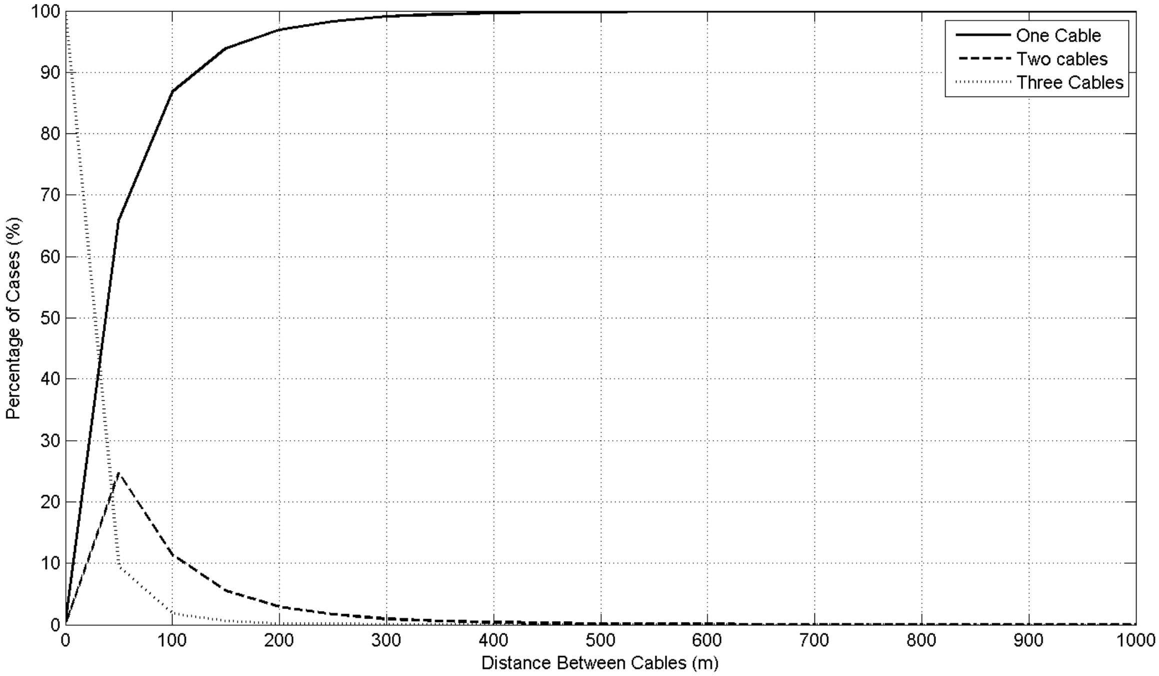

Figure 4-9 Percentage of events involving 1 to 3 cables, 25 to 35 m water depth

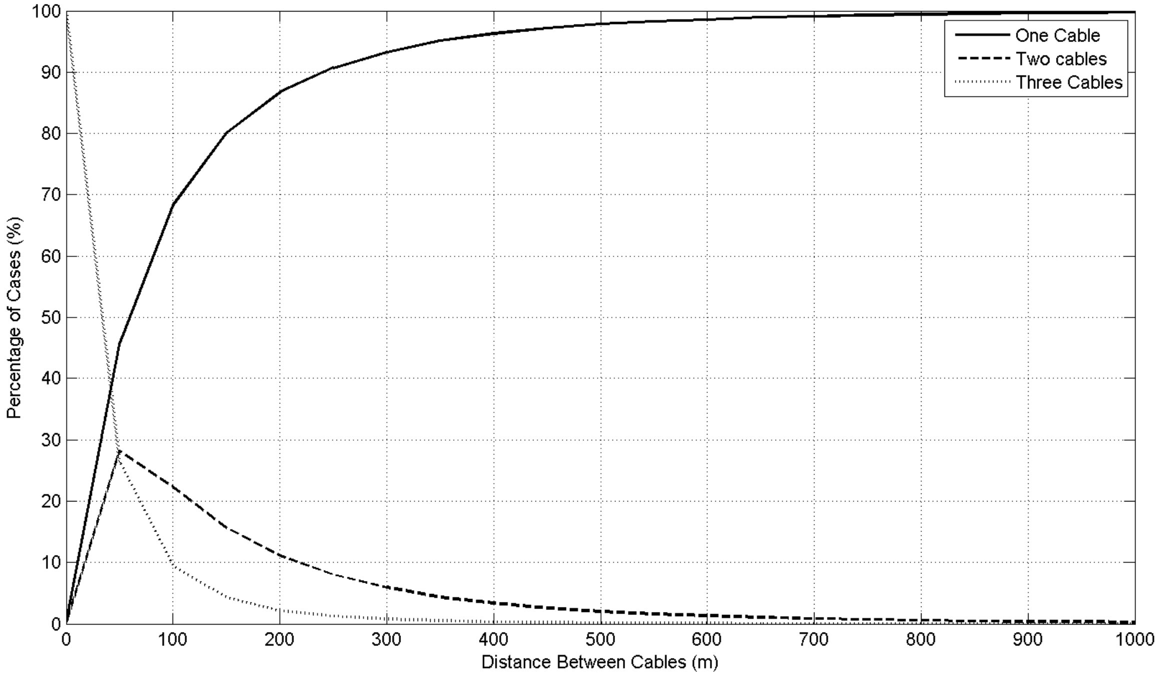

Figure 4-10 Percentage of events involving 1 to 3 cables, 35 to 45 m water depth

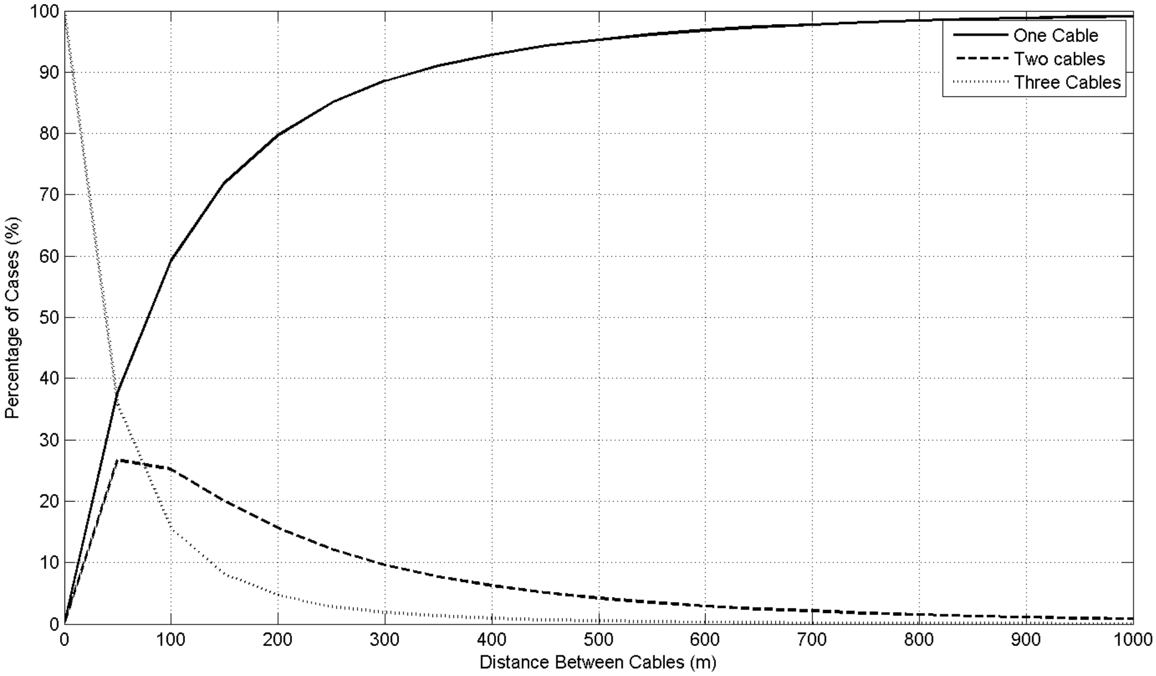

Figure 4-11 Percentage of events involving 1 to 4 cables, 45 to 55 m water depth

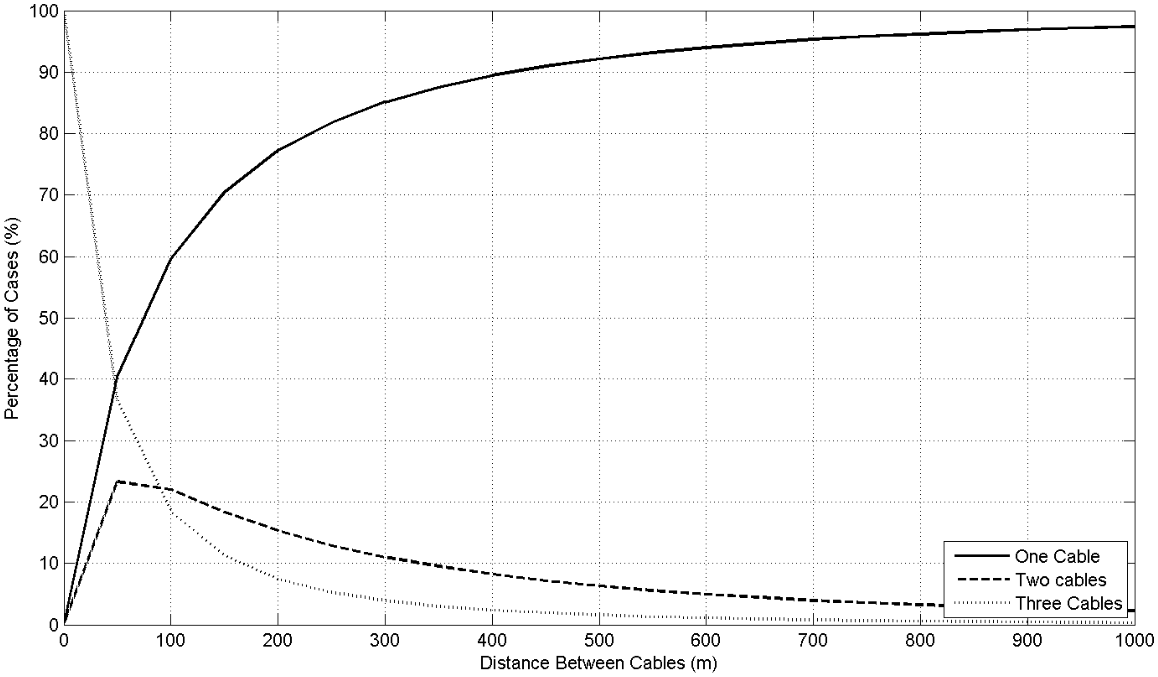

Figure 4-12 Percentage of events involving 1 to 3 cables, 55 to 65 m water depth

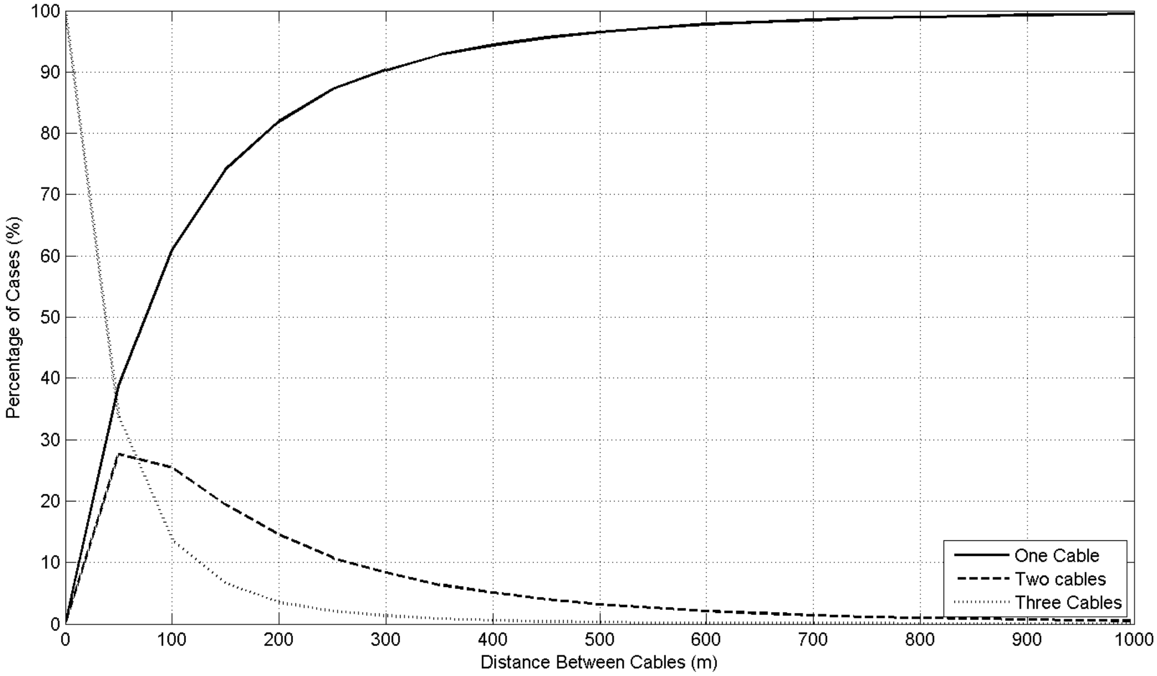

Figure 4-13 Percentage of events involving 1 to 3 cables, 65 to 75 m water depth

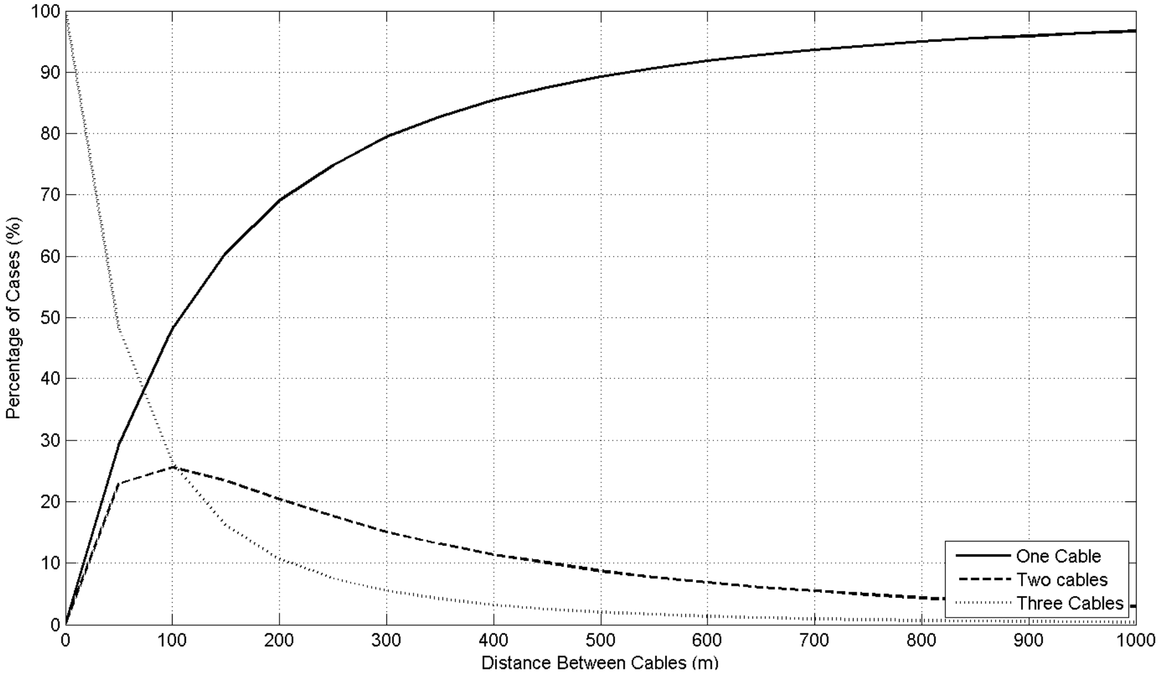

Figure 4-14 Percentage of events involving 1 to 3 cables, 75 to 85 m water depth

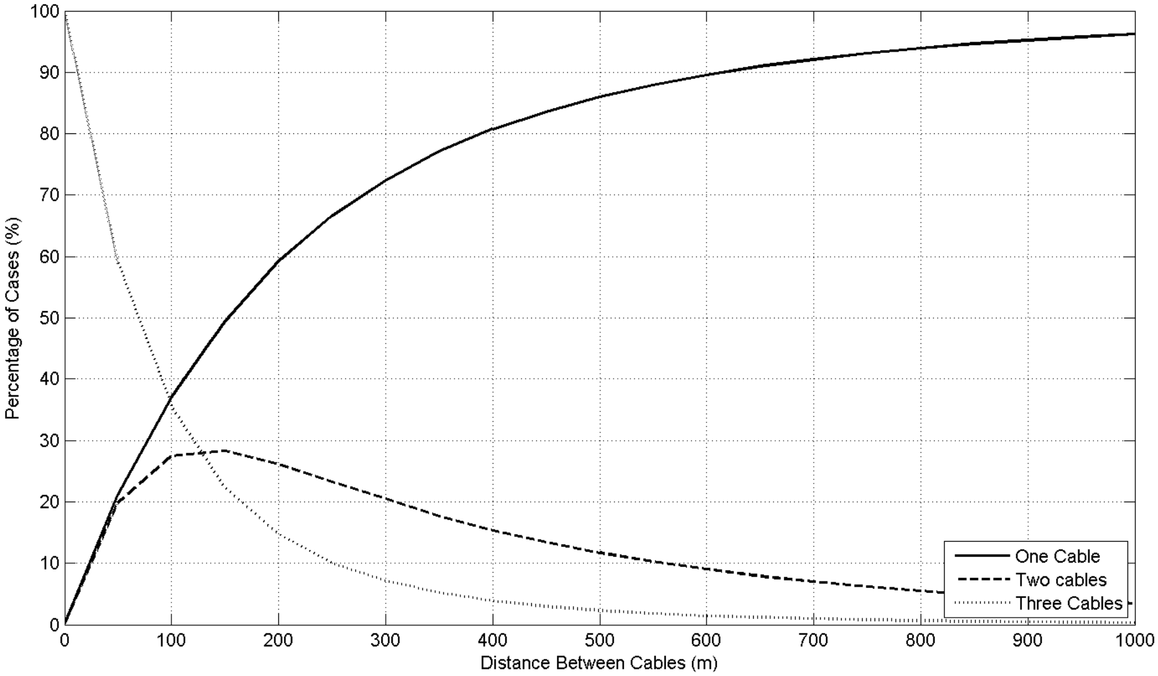

Figure 4-15 Percentage of events involving 1 to 3 cables, 85 to 95 m water depth

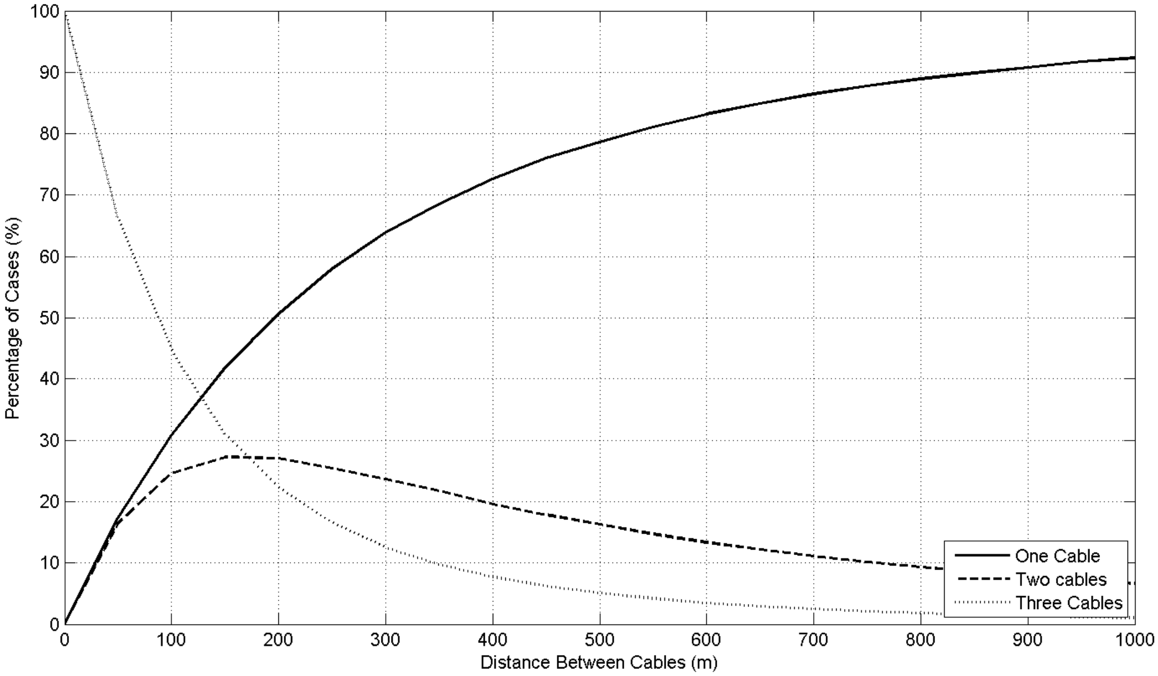

Figure 4-16 Percentage of events involving 1 to 3 cables, 95 to 105 m water depth

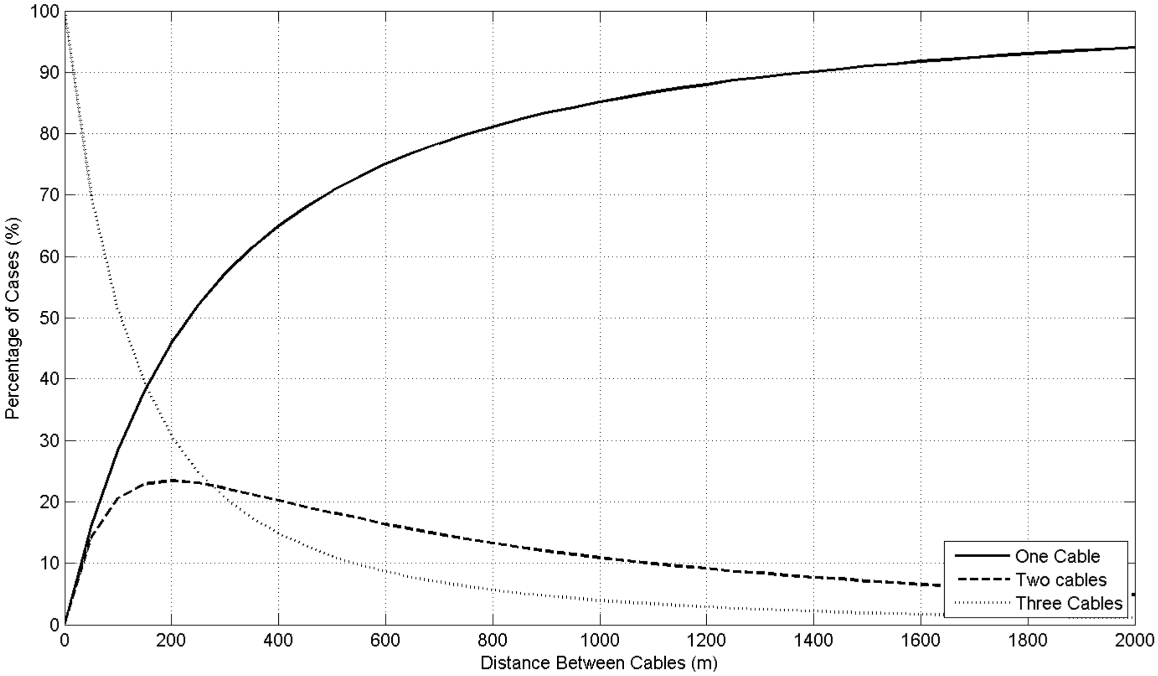

Figure 4-17 Percentage of events involving 1 to 3 cables, 105 to 115 m water depth

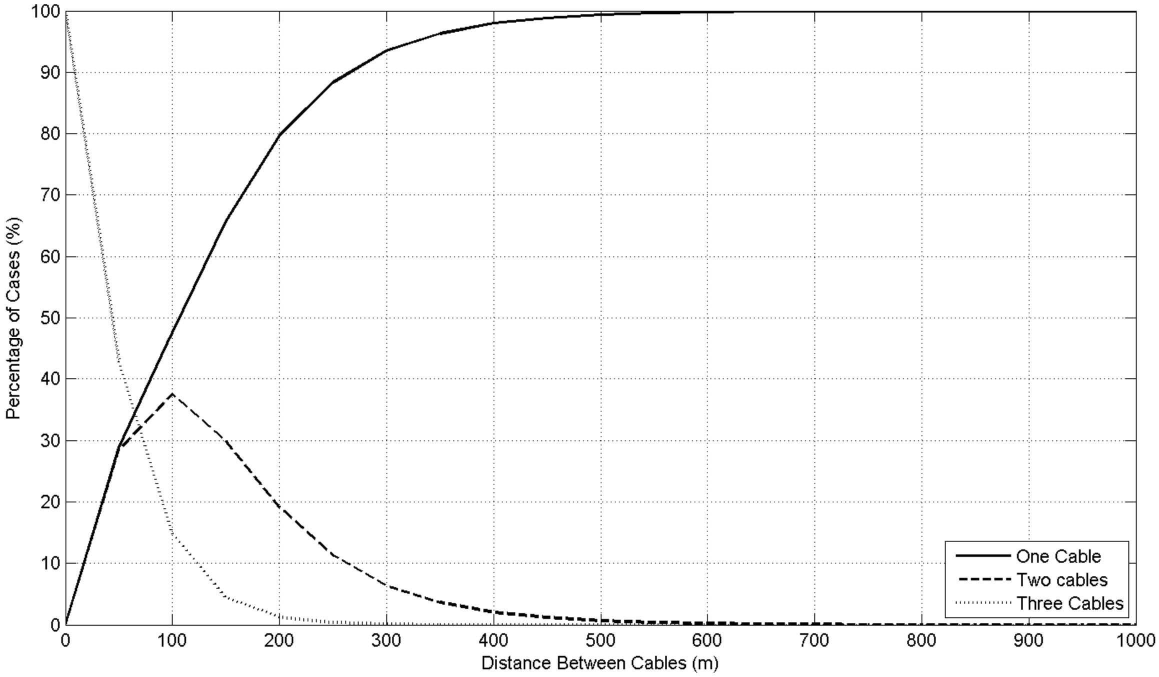

Figure 4-18 Percentage of events involving 1 to 3 cables, 115 to 125 m water depth

4.4 Results for Alternate Cable Route

4.4.1 Introduction

Subsequent to the analyses of the cable routes shown in Figure 4-1, an alternate cable route was specified, as shown in Figure 4-19. This route (shown as a cross-hatched zone) encompasses an area which actually contains three cables (150 m spacing) which, for the analysis presented here, are to be installed on the seabed within the cross-hatched zone and pass from the areas labeled “Transition Compound Target Zone” to the areas designated “Seabed Piercing Target Zone” via directional drilling.

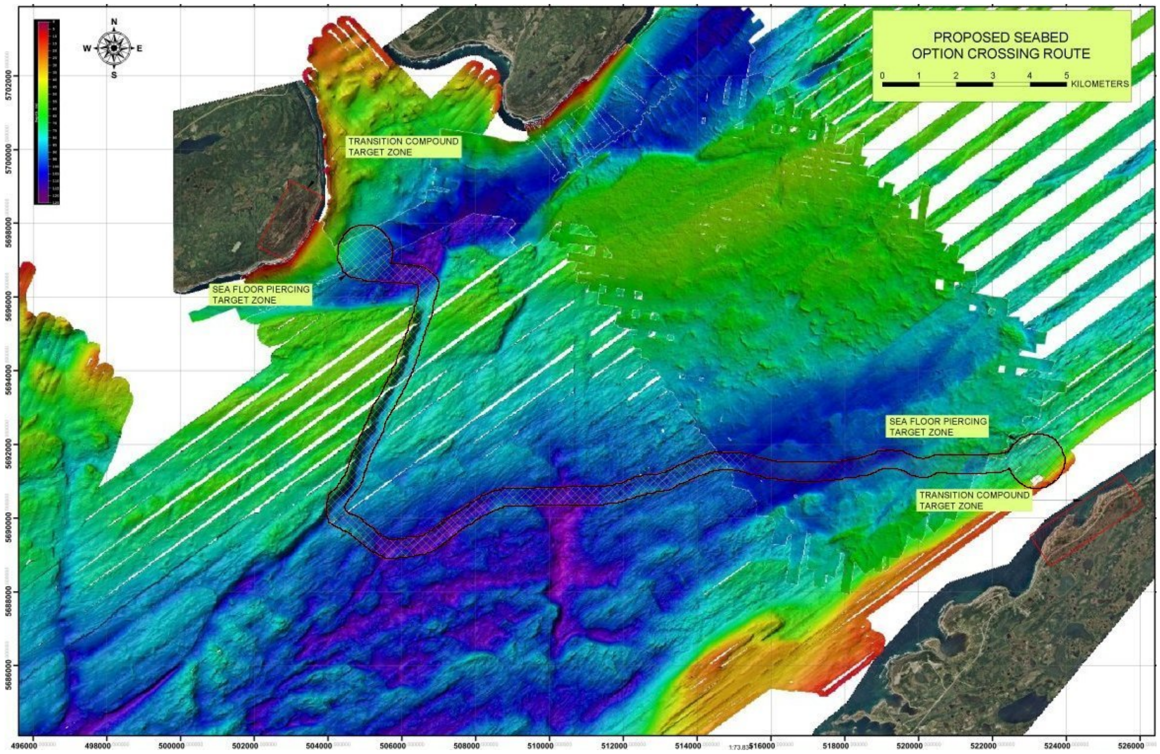

Figure 4-19 Alternate cable route

The precise water depth where the directional drilling pierces the seabed was unspecified, thus the decision was made to extend the cable routes to shore and treat the transition from directional drilling to cable lay on the seabed as a variable. The resulting cable routing is shown in Figure 4-20. Also shown in Figure 4-20 are zones 1 through 5, which were redefined to allow for changes in the cable routes. The numbering of zones is consistent with the previous analysis, and zone 3 (Bank 3 crossing) is not shown as the cables do not pass that zone. Figure 4-21 shows water depth along each of the cable routes which, despite a spacing of only 120 m, differ somewhat. In particular, between 4 and 10 km (zone 2, the Channel zone) the north and south cables differ by as much as 30 m from the central cable, which highlights the limited width of the channel feature.

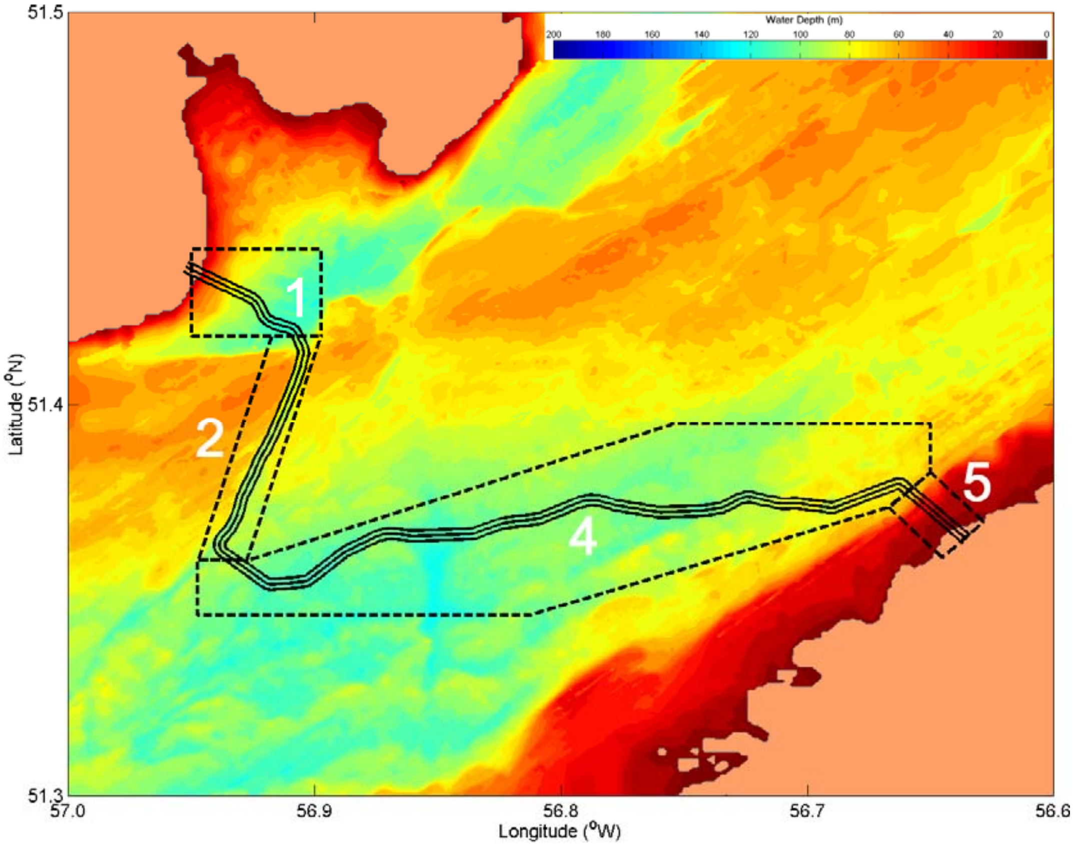

Figure 4-20 Revised cable routes and redefined zones

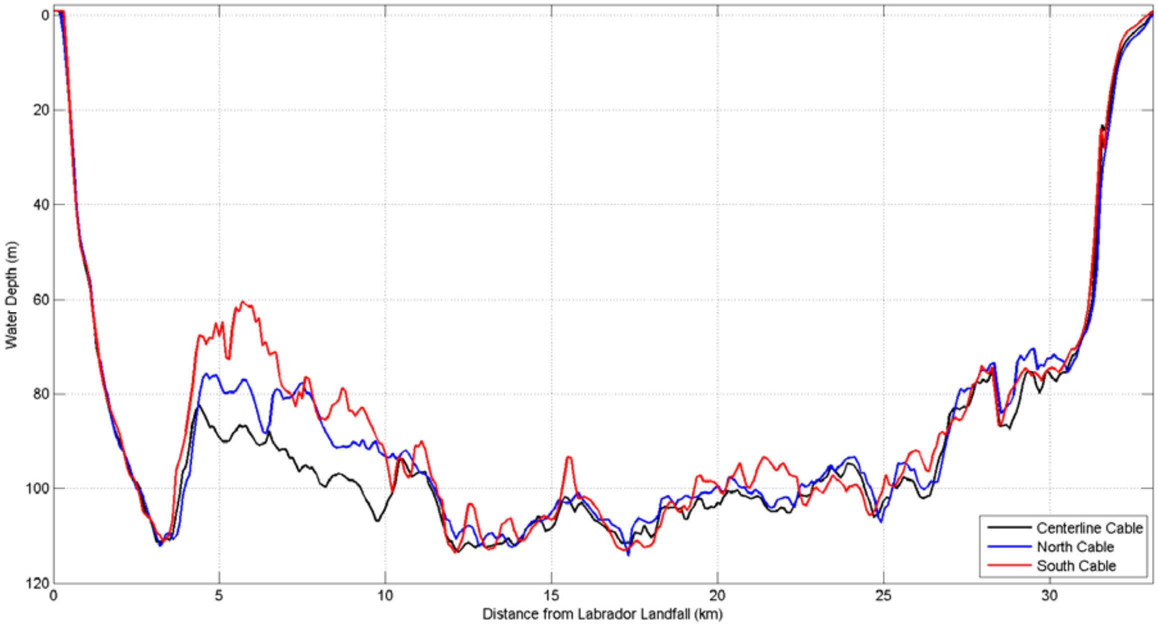

Figure 4-21 Water depths along cable routes

Additional Monte Carlo model runs were performed to reduce the random scatter evident in the iceberg cable contact assessments presented in Section 4.3. The total number of modeled iceberg for the base case was increased to 26,516,000 (53,032 model runs), equivalent to a model period of 40,368 years. The distribution of modeled iceberg grounding locations is shown in Figure 4-22. Additional runs were also performed for sensitivity cases #1 and #2 (1 day and 10 days mean rolling period) so that all sensitivity cases represent approximately the same equivalent model time.

Table 4-22 Summary of Monte Carlo data sets used in assessing revised cable routes

Case	Mean Rolling Period	Equivalent Model Period (years)
Base Case	3 days	40,368
Sensitivity Case #1	1 day	10,313
Sensitivity Case #2	10 days	11,123
Sensitivity Case #3	No rolling	13,243

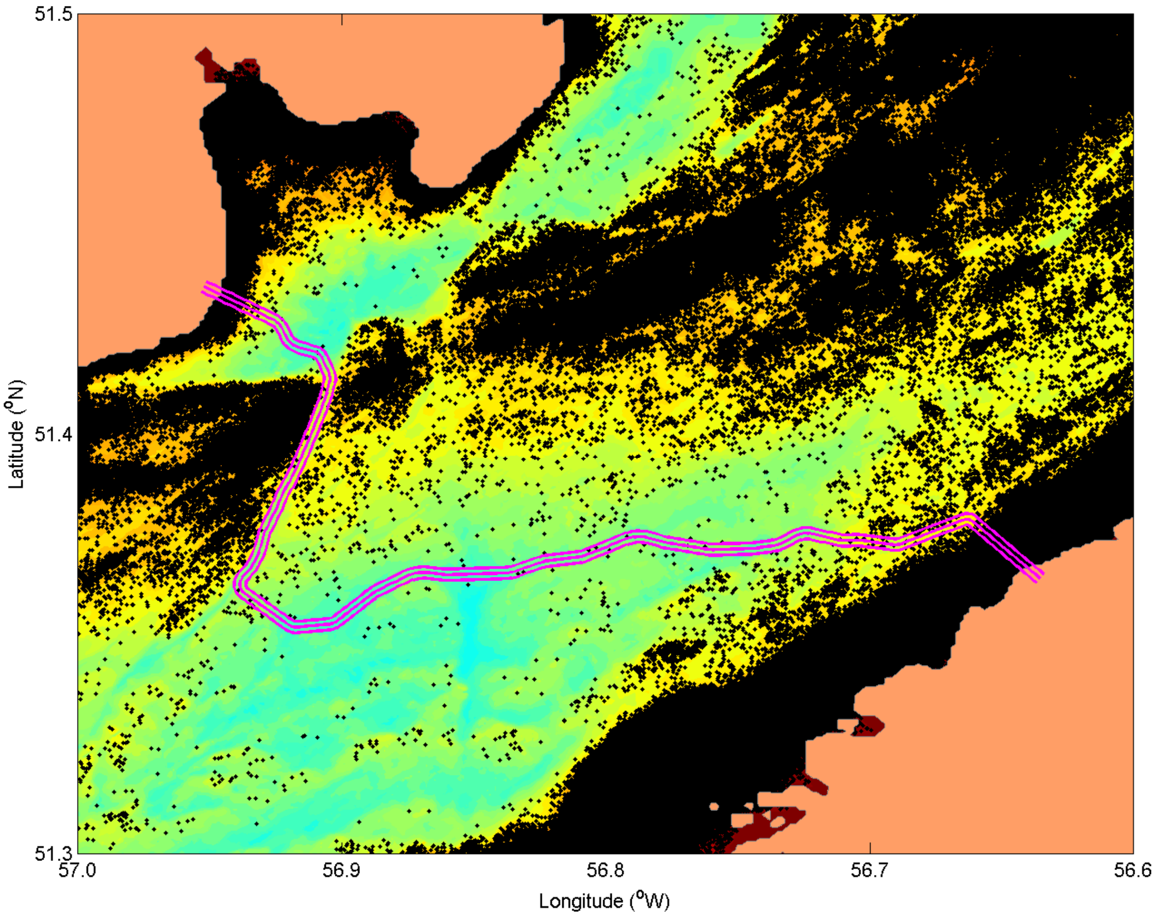

Figure 4-22 Raw groundings in cable crossing area (base case) used expanded model data set

4.4.2 Contact Rates in Zone 1 (Point Amour Trough& Labrador Landfall)

Iceberg contact rates in Zone 1 for the central, north and south cables are given in Table 4-24 to Table 4-31, broken down in 2.5 m water depth intervals. Table 4-23 gives a summary of the water depth ranges and scenarios summarized by each table. The overall patterns noted previously are repeated in the cases considered here. For the base case, iceberg contacts persist up to 80 m water depth, with isolated contacts in deeper water depths. Results from the 1 day mean rolling period case are similar. The 10 day mean iceberg rolling period gives no iceberg contacts beyond 65 m water depth, and the no rolling case gives similar results.

Table 4-23 Summary of results tables for zone 1 revised cable iceberg contact analysis

Table Number	Water Depth Range (m)	Scenario
Table 4-24	0 to 60	Base Case (3 day mean iceberg rolling period)
Table 4-25	60 to 120	Base Case (3 day mean iceberg rolling period)
Table 4-26	0 to 60	1 day mean iceberg rolling period
Table 4-27	60 to 120	1 day mean iceberg rolling period
Table 4-28	0 to 60	10 day mean iceberg rolling period
Table 4-29	60 to 120	10 day mean iceberg rolling period
Table 4-30	0 to 60	No iceberg rolling
Table 4-31	60 to 120	No iceberg rolling

Table 4-24 Revised cables contact rates for Zone 1, base case (0 - 60 m water depth)

Water Depth (m)		Central Cable		North Cable		South Cable	
Min.	Max.	Cable Length (m)	Annual Contact Rate	Cable Length (m)	Annual Contact Rate	Cable Length (m)	Annual Contact Rate
0.0	2.5	60	1.8×10^{-2}	60	1.5×10^{-2}	20	5.1×10^{-3}
2.5	5.0	20	6.5×10^{-3}	40	1.2×10^{-2}	20	6.7×10^{-3}
5.0	7.5	20	6.6×10^{-3}	30	9.7×10^{-3}	10	3.5×10^{-3}
7.5	10.0	20	6.7×10^{-3}	30	1.0×10^{-2}	20	7.1×10^{-3}
10.0	12.5	20	6.7×10^{-3}	30	1.0×10^{-2}	10	3.5×10^{-3}
12.5	15.0	30	9.7×10^{-3}	30	1.0×10^{-2}	30	9.8×10^{-3}
15.0	17.5	20	6.0×10^{-3}	30	9.3×10^{-3}	20	5.9×10^{-3}
17.5	20.0	20	5.3×10^{-3}	30	8.1×10^{-3}	20	5.1×10^{-3}
20.0	22.5	30	6.7×10^{-3}	20	4.7×10^{-3}	20	4.5×10^{-3}
22.5	25.0	20	3.8×10^{-3}	30	6.1×10^{-3}	20	3.8×10^{-3}
25.0	27.5	20	3.2×10^{-3}	20	3.2×10^{-3}	20	3.2×10^{-3}
27.5	30.0	30	3.8×10^{-3}	30	3.6×10^{-3}	30	3.7×10^{-3}
30.0	32.5	20	2.2×10^{-3}	20	2.0×10^{-3}	20	2.2×10^{-3}
32.5	35.0	20	2.2×10^{-3}	20	2.0×10^{-3}	20	2.1×10^{-3}
35.0	37.5	30	3.1×10^{-3}	30	3.1×10^{-3}	30	2.9×10^{-3}
37.5	40.0	30	2.6×10^{-3}	30	3.0×10^{-3}	30	2.4×10^{-3}
40.0	42.5	30	2.1×10^{-3}	30	2.6×10^{-3}	30	2.0×10^{-3}
42.5	45.0	40	2.2×10^{-3}	40	2.6×10^{-3}	40	2.3×10^{-3}
45.0	47.5	50	2.1×10^{-3}	50	2.3×10^{-3}	30	1.4×10^{-3}
47.5	50.0	50	1.9×10^{-3}	70	2.1×10^{-3}	70	2.6×10^{-3}
50.0	52.5	80	2.1×10^{-3}	90	2.2×10^{-3}	130	3.0×10^{-3}
52.5	55.0	90	9.2×10^{-4}	90	1.1×10^{-3}	80	9.8×10^{-4}
55.0	57.5	70	6.1×10^{-4}	60	2.7×10^{-4}	40	1.9×10^{-4}
57.5	60.0	40	2.1×10^{-4}	30	1.2×10^{-4}	40	1.4×10^{-4}

Table 4-25 Revised cables contact rates for Zone 1, base case (60 - 120 m water depth)

Water Depth (m)		Central Cable		North Cable		South Cable	
Min.	Max.	Cable Length (m)	Annual Contact Rate	Cable Length (m)	Annual Contact Rate	Cable Length (m)	Annual Contact Rate
60.0	62.5	40	1.3×10^{-4}	40	9.4×10^{-5}	40	1.1×10^{-4}
62.5	65.0	40	1.1×10^{-4}	30	2.0×10^{-5}	50	1.2×10^{-4}
65.0	67.5	30	7.0×10^{-5}	30	1.0×10^{-5}	50	6.9×10^{-5}
67.5	70.0	50	9.2×10^{-5}	60	1.2×10^{-5}	50	3.6×10^{-6}
70.0	72.5	60	7.7×10^{-5}	70	5.1×10^{-5}	40	6.4×10^{-7}
72.5	75.0	90	1.7×10^{-4}	70	2.0×10^{-4}	50	9.6×10^{-6}
75.0	77.5	70	6.8×10^{-5}	70	2.2×10^{-4}	80	3.2×10^{-6}
77.5	80.0	50	9.2×10^{-7}	80	6.9×10^{-5}	70	2.5×10^{-5}
80.0	82.5	90	0.0	70	0.0	110	1.6×10^{-4}
82.5	85.0	90	0.0	70	0.0	120	0.0
85.0	87.5	90	0.0	80	0.0	140	0.0
87.5	90.0	150	0.0	100	5.4×10^{-5}	110	0.0
90.0	92.5	150	0.0	200	1.9×10^{-5}	70	8.7×10^{-7}
92.5	95.0	90	0.0	150	2.2×10^{-4}	70	4.7×10^{-6}
95.0	97.5	100	0.0	100	3.3×10^{-5}	120	0.0
97.5	100.0	260	0.0	150	0.0	230	0.0
100.0	102.5	100	0.0	310	0.0	100	0.0
102.5	105.0	170	0.0	130	0.0	80	5.1×10^{-7}
105.0	107.5	250	0.0	190	0.0	350	3.3×10^{-5}
107.5	110.0	160	2.9×10^{-5}	400	3.0×10^{-6}	250	1.7×10^{-4}
110.0	112.5	540	2.9×10^{-4}	420	2.4×10^{-4}	310	1.3×10^{-5}
112.5	115.0	0	0.0	0	0.0	0	0.0
115.0	117.5	0	0.0	0	0.0	0	0.0
117.5	120.0	0	0.0	0	0.0	0	0.0

Table 4-26 Revised cables contact rates for Zone 1, mean rolling period 1 day (0 - 60 m water depth)

Water Depth (m)		Central Cable		North Cable		South Cable	
Min.	Max.	Cable Length (m)	Annual Contact Rate	Cable Length (m)	Annual Contact Rate	Cable Length (m)	Annual Contact Rate
0.0	2.5	60	1.7×10^{-2}	60	1.6×10^{-2}	20	5.5×10^{-3}
2.5	5.0	20	5.8×10^{-3}	40	1.1×10^{-2}	20	7.1×10^{-3}
5.0	7.5	20	6.0×10^{-3}	30	9.4×10^{-3}	10	3.6×10^{-3}
7.5	10.0	20	6.4×10^{-3}	30	1.1×10^{-2}	20	7.1×10^{-3}
10.0	12.5	20	6.8×10^{-3}	30	1.2×10^{-2}	10	3.3×10^{-3}
12.5	15.0	30	1.0×10^{-2}	30	1.1×10^{-2}	30	9.0×10^{-3}
15.0	17.5	20	6.4×10^{-3}	30	9.4×10^{-3}	20	5.2×10^{-3}
17.5	20.0	20	5.6×10^{-3}	30	7.3×10^{-3}	20	4.5×10^{-3}
20.0	22.5	30	7.1×10^{-3}	20	3.8×10^{-3}	20	3.9×10^{-3}
22.5	25.0	20	3.9×10^{-3}	30	4.3×10^{-3}	20	3.3×10^{-3}
25.0	27.5	20	3.1×10^{-3}	20	2.5×10^{-3}	20	2.8×10^{-3}
27.5	30.0	30	3.2×10^{-3}	30	3.2×10^{-3}	30	3.3×10^{-3}
30.0	32.5	20	1.4×10^{-3}	20	2.2×10^{-3}	20	2.1×10^{-3}
32.5	35.0	20	1.3×10^{-3}	20	2.2×10^{-3}	20	2.1×10^{-3}
35.0	37.5	30	1.8×10^{-3}	30	3.2×10^{-3}	30	3.0×10^{-3}
37.5	40.0	30	1.7×10^{-3}	30	2.7×10^{-3}	30	2.7×10^{-3}
40.0	42.5	30	1.7×10^{-3}	30	2.3×10^{-3}	30	2.3×10^{-3}
42.5	45.0	40	2.2×10^{-3}	40	2.3×10^{-3}	40	2.6×10^{-3}
45.0	47.5	50	2.4×10^{-3}	50	2.3×10^{-3}	30	1.7×10^{-3}
47.5	50.0	50	2.4×10^{-3}	70	2.0×10^{-3}	70	2.6×10^{-3}
50.0	52.5	80	1.6×10^{-3}	90	8.2×10^{-4}	130	3.0×10^{-3}
52.5	55.0	90	1.2×10^{-3}	90	4.5×10^{-4}	80	6.9×10^{-4}
55.0	57.5	70	4.0×10^{-4}	60	2.5×10^{-4}	40	2.5×10^{-4}
57.5	60.0	40	7.3×10^{-5}	30	1.8×10^{-4}	40	6.5×10^{-5}

Table 4-27 Revised cables contact rates for Zone 1, mean rolling period 1 day (60 - 120 m water depth)

Water Depth (m)		Central Cable		North Cable		South Cable	
Min.	Max.	Cable Length (m)	Annual Contact Rate	Cable Length (m)	Annual Contact Rate	Cable Length (m)	Annual Contact Rate
60.0	62.5	40	6.4×10^{-7}	40	1.8×10^{-4}	40	1.7×10^{-5}
62.5	65.0	40	0	30	3.4×10^{-5}	50	1.1×10^{-4}
65.0	67.5	30	0	30	0	50	9.9×10^{-5}
67.5	70.0	50	0	60	0	50	5.3×10^{-5}
70.0	72.5	60	0	70	2.1×10^{-6}	40	2.0×10^{-4}
72.5	75.0	90	2.3×10^{-5}	70	2.8×10^{-4}	50	3.4×10^{-4}
75.0	77.5	70	9.0×10^{-5}	70	3.0×10^{-4}	80	4.2×10^{-4}
77.5	80.0	50	2.8×10^{-6}	80	5.0×10^{-7}	70	2.7×10^{-4}
80.0	82.5	90	3.5×10^{-4}	70	0	110	6.1×10^{-4}
82.5	85.0	90	1.2×10^{-3}	70	0	120	0
85.0	87.5	90	1.3×10^{-5}	80	0	140	0
87.5	90.0	150	0	100	0	110	2.3×10^{-4}
90.0	92.5	150	0	200	0	70	6.5×10^{-4}
92.5	95.0	90	0	150	0	70	9.1×10^{-5}
95.0	97.5	100	0	100	0	120	0
97.5	100.0	260	1.4×10^{-3}	150	0	230	0
100.0	102.5	100	3.0×10^{-4}	310	0	100	0
102.5	105.0	170	0	130	0	80	0
105.0	107.5	250	0	190	0	350	0
107.5	110.0	160	0	400	0	250	0
110.0	112.5	540	0	420	0	310	0
112.5	115.0	0	0	0	0	0	0
115.0	117.5	0	0	0	0	0	0
117.5	120.0	0	0	0	0	0	0

Table 4-28 Revised cables contact rates for Zone 1, mean rolling period 10 days (0 - 60 m water depth)

Water Depth (m)		Central Cable		North Cable		South Cable	
Min.	Max.	Cable Length (m)	Annual Contact Rate	Cable Length (m)	Annual Contact Rate	Cable Length (m)	Annual Contact Rate
0.0	2.5	60	2.0×10^{-2}	60	1.4×10^{-2}	20	5.4×10^{-3}
2.5	5.0	20	6.7×10^{-3}	40	1.0×10^{-2}	20	6.9×10^{-3}
5.0	7.5	20	6.4×10^{-3}	30	8.5×10^{-3}	10	3.6×10^{-3}
7.5	10.0	20	6.5×10^{-3}	30	9.8×10^{-3}	20	7.2×10^{-3}
10.0	12.5	20	6.7×10^{-3}	30	1.1×10^{-2}	10	3.5×10^{-3}
12.5	15.0	30	9.7×10^{-3}	30	9.9×10^{-3}	30	1.0×10^{-2}
15.0	17.5	20	6.1×10^{-3}	30	8.7×10^{-3}	20	6.2×10^{-3}
17.5	20.0	20	5.6×10^{-3}	30	7.2×10^{-3}	20	5.4×10^{-3}
20.0	22.5	30	7.4×10^{-3}	20	4.1×10^{-3}	20	4.6×10^{-3}
22.5	25.0	20	4.4×10^{-3}	30	5.2×10^{-3}	20	3.9×10^{-3}
25.0	27.5	20	3.8×10^{-3}	20	2.9×10^{-3}	20	3.2×10^{-3}
27.5	30.0	30	4.4×10^{-3}	30	3.6×10^{-3}	30	3.6×10^{-3}
30.0	32.5	20	2.4×10^{-3}	20	2.2×10^{-3}	20	2.0×10^{-3}
32.5	35.0	20	2.3×10^{-3}	20	2.4×10^{-3}	20	1.9×10^{-3}
35.0	37.5	30	3.1×10^{-3}	30	4.1×10^{-3}	30	2.8×10^{-3}
37.5	40.0	30	2.5×10^{-3}	30	4.4×10^{-3}	30	2.5×10^{-3}
40.0	42.5	30	2.3×10^{-3}	30	3.5×10^{-3}	30	2.1×10^{-3}
42.5	45.0	40	2.9×10^{-3}	40	2.8×10^{-3}	40	2.2×10^{-3}
45.0	47.5	50	2.8×10^{-3}	50	2.0×10^{-3}	30	1.3×10^{-3}
47.5	50.0	50	1.6×10^{-3}	70	1.9×10^{-3}	70	2.5×10^{-3}
50.0	52.5	80	9.9×10^{-4}	90	2.6×10^{-3}	130	2.5×10^{-3}
52.5	55.0	90	7.0×10^{-4}	90	1.2×10^{-3}	80	7.9×10^{-4}
55.0	57.5	70	1.3×10^{-4}	60	2.8×10^{-4}	40	8.2×10^{-5}
57.5	60.0	40	1.6×10^{-4}	30	1.3×10^{-4}	40	1.6×10^{-4}

Table 4-29 Revised cables contact rates for Zone 1, mean rolling period 10 days (60 - 120 m water depth)

Water Depth (m)		Central Cable		North Cable		South Cable	
Min.	Max.	Cable Length (m)	Annual Contact Rate	Cable Length (m)	Annual Contact Rate	Cable Length (m)	Annual Contact Rate
60.0	62.5	40	1.9×10^{-4}	40	5.7×10^{-5}	40	1.4×10^{-4}
62.5	65.0	40	6.0×10^{-5}	30	1.2×10^{-6}	50	3.5×10^{-5}
65.0	67.5	30	0	30	0	50	0
67.5	70.0	50	0	60	0	50	0
70.0	72.5	60	0	70	0	40	0
72.5	75.0	90	0	70	0	50	0
75.0	77.5	70	0	70	0	80	0
77.5	80.0	50	0	80	0	70	0
80.0	82.5	90	0	70	0	110	0
82.5	85.0	90	0	70	0	120	0
85.0	87.5	90	0	80	0	140	0
87.5	90.0	150	0	100	0	110	0
90.0	92.5	150	0	200	0	70	0
92.5	95.0	90	0	150	0	70	0
95.0	97.5	100	0	100	0	120	0
97.5	100.0	260	0	150	0	230	0
100.0	102.5	100	0	310	0	100	0
102.5	105.0	170	0	130	0	80	0
105.0	107.5	250	0	190	0	350	0
107.5	110.0	160	0	400	0	250	0
110.0	112.5	540	0	420	0	310	0
112.5	115.0	0	0	0	0	0	0
115.0	117.5	0	0	0	0	0	0
117.5	120.0	0	0	0	0	0	0

Table 4-30 Revised cables contact rates for Zone 1, no rolling (0 - 60 m water depth)

Water Depth (m)		Central Cable		North Cable		South Cable	
Min.	Max.	Cable Length (m)	Annual Contact Rate	Cable Length (m)	Annual Contact Rate	Cable Length (m)	Annual Contact Rate
0.0	2.5	60	1.8×10^{-2}	60	1.7×10^{-2}	20	5.4×10^{-3}
2.5	5.0	20	7.1×10^{-3}	40	1.1×10^{-2}	20	7.0×10^{-3}
5.0	7.5	20	7.7×10^{-3}	30	9.0×10^{-3}	10	3.7×10^{-3}
7.5	10.0	20	7.8×10^{-3}	30	9.4×10^{-3}	20	7.7×10^{-3}
10.0	12.5	20	7.2×10^{-3}	30	9.7×10^{-3}	10	3.8×10^{-3}
12.5	15.0	30	9.4×10^{-3}	30	9.8×10^{-3}	30	1.1×10^{-2}
15.0	17.5	20	5.4×10^{-3}	30	9.6×10^{-3}	20	6.2×10^{-3}
17.5	20.0	20	5.1×10^{-3}	30	7.6×10^{-3}	20	5.3×10^{-3}
20.0	22.5	30	6.8×10^{-3}	20	4.0×10^{-3}	20	4.6×10^{-3}
22.5	25.0	20	4.0×10^{-3}	30	4.6×10^{-3}	20	4.0×10^{-3}
25.0	27.5	20	3.3×10^{-3}	20	2.8×10^{-3}	20	3.5×10^{-3}
27.5	30.0	30	3.9×10^{-3}	30	3.8×10^{-3}	30	4.3×10^{-3}
30.0	32.5	20	2.3×10^{-3}	20	2.7×10^{-3}	20	2.7×10^{-3}
32.5	35.0	20	2.3×10^{-3}	20	2.8×10^{-3}	20	2.7×10^{-3}
35.0	37.5	30	3.5×10^{-3}	30	3.7×10^{-3}	30	3.9×10^{-3}
37.5	40.0	30	3.3×10^{-3}	30	2.7×10^{-3}	30	3.5×10^{-3}
40.0	42.5	30	2.8×10^{-3}	30	2.5×10^{-3}	30	3.0×10^{-3}
42.5	45.0	40	2.5×10^{-3}	40	3.4×10^{-3}	40	3.6×10^{-3}
45.0	47.5	50	2.0×10^{-3}	50	3.4×10^{-3}	30	2.2×10^{-3}
47.5	50.0	50	1.6×10^{-3}	70	2.6×10^{-3}	70	3.5×10^{-3}
50.0	52.5	80	1.4×10^{-3}	90	8.5×10^{-4}	130	2.4×10^{-3}
52.5	55.0	90	4.5×10^{-4}	90	3.5×10^{-4}	80	9.0×10^{-5}
55.0	57.5	70	2.2×10^{-5}	60	9.3×10^{-5}	40	4.1×10^{-5}
57.5	60.0	40	0	30	4.1×10^{-6}	40	1.3×10^{-4}

Table 4-31 Revised cables contact rates for Zone 1, no rolling (60 - 120 m water depth)

Water Depth (m)		Central Cable		North Cable		South Cable	
Min.	Max.	Cable Length (m)	Annual Contact Rate	Cable Length (m)	Annual Contact Rate	Cable Length (m)	Annual Contact Rate
60.0	62.5	40	0	40	0	40	1.1×10^{-4}
62.5	65.0	40	0	30	0	50	2.9×10^{-5}
65.0	67.5	30	0	30	0	50	0
67.5	70.0	50	0	60	0	50	0
70.0	72.5	60	0	70	0	40	0
72.5	75.0	90	0	70	0	50	0
75.0	77.5	70	0	70	0	80	0
77.5	80.0	50	0	80	0	70	0
80.0	82.5	90	0	70	0	110	0
82.5	85.0	90	0	70	0	120	0
85.0	87.5	90	0	80	0	140	0
87.5	90.0	150	0	100	0	110	0
90.0	92.5	150	0	200	0	70	0
92.5	95.0	90	0	150	0	70	0
95.0	97.5	100	0	100	0	120	0
97.5	100.0	260	0	150	0	230	0
100.0	102.5	100	0	310	0	100	0
102.5	105.0	170	0	130	0	80	0
105.0	107.5	250	0	190	0	350	0
107.5	110.0	160	0	400	0	250	0
110.0	112.5	540	0	420	0	310	0
112.5	115.0	0	0	0	0	0	0
115.0	117.5	0	0	0	0	0	0
117.5	120.0	0	0	0	0	0	0

4.4.3 Contact Rates in Zone 2 (Channel)

Iceberg contact rates with the cables in Zone 2 are given in Table 4-32 (base case, 3 day mean rolling period), Table 4-33 (1 day mean rolling period), Table 4-34 (10 day mean rolling period), and Table 4-35 (no iceberg rolling). The base case and 1 day mean rolling period case give similar results, while in the 10 day and no rolling cases the iceberg contacts are limited to the south cable, which climbs up the side of the channel to shallower water. This issue is addressed in Section 4.4.6 by reducing the spacing between cables to 50 m in Zone 2.

Table 4-32 Revised cables contact rates for Zone 2, base case

Water Depth (m)		Central Cable		North Cable		South Cable	
Min.	Max.	Cable Length (m)	Annual Contact Rate	Cable Length (m)	Annual Contact Rate	Cable Length (m)	Annual Contact Rate
57.5	60.0	0	0	0	0	20	4.1×10^{-5}
60.0	62.5	0	0	0	0	510	1.4×10^{-3}
62.5	65.0	0	0	0	0	260	8.0×10^{-4}
65.0	67.5	0	0	0	0	450	8.8×10^{-4}
67.5	70.0	0	0	0	0	590	8.8×10^{-4}
70.0	72.5	0	0	0	0	470	4.8×10^{-4}
72.5	75.0	0	0	0	0	230	3.1×10^{-4}
75.0	77.5	0	0	720	1.9×10^{-4}	240	1.1×10^{-4}
77.5	80.0	0	0	1450	4.5×10^{-4}	740	3.4×10^{-4}
80.0	82.5	0	0	870	2.7×10^{-5}	690	3.9×10^{-4}
82.5	85.0	350	4.4×10^{-5}	300	0	900	3.6×10^{-4}
85.0	87.5	660	2.6×10^{-4}	340	0	570	3.6×10^{-4}
87.5	90.0	880	4.2×10^{-5}	570	0	160	3.6×10^{-4}
90.0	92.5	1090	2.2×10^{-4}	1690	0	310	2.3×10^{-4}
92.5	95.0	510	2.6×10^{-6}	810	0	370	1.0×10^{-4}
95.0	97.5	1530	2.7×10^{-5}	350	1.0×10^{-4}	270	6.9×10^{-8}
97.5	100.0	1110	2.6×10^{-4}	120	0	200	0
100.0	102.5	390	0	0	0	110	0
102.5	105.0	320	0	0	0	10	0

Table 4-33 Revised cables contact rates for Zone 2, mean rolling period 1 day

Water Depth (m)		Central Cable		North Cable		South Cable	
Min.	Max.	Cable Length (m)	Annual Contact Rate	Cable Length (m)	Annual Contact Rate	Cable Length (m)	Annual Contact Rate
57.5	60.0	0	0	0	0	20	2.1×10^{-4}
60.0	62.5	0	0	0	0	510	4.3×10^{-3}
62.5	65.0	0	0	0	0	260	2.4×10^{-3}
65.0	67.5	0	0	0	0	450	8.4×10^{-4}
67.5	70.0	0	0	0	0	590	6.0×10^{-4}
70.0	72.5	0	0	0	0	470	3.4×10^{-4}
72.5	75.0	0	0	0	0	230	2.6×10^{-4}
75.0	77.5	0	0	720	5.0×10^{-4}	240	2.0×10^{-4}
77.5	80.0	0	0	1450	5.8×10^{-4}	740	4.0×10^{-4}
80.0	82.5	0	0	870	1.7×10^{-4}	690	7.1×10^{-4}
82.5	85.0	350	0	300	1.7×10^{-4}	900	8.9×10^{-4}
85.0	87.5	660	0	340	7.1×10^{-4}	570	6.1×10^{-4}
87.5	90.0	880	5.8×10^{-5}	570	1.8×10^{-5}	160	0
90.0	92.5	1090	1.1×10^{-5}	1690	0	310	0
92.5	95.0	510	0	810	0	370	1.3×10^{-3}
95.0	97.5	1530	0	350	0	270	0
97.5	100.0	1110	0	120	0	200	0
100.0	102.5	390	0	0	0	110	0
102.5	105.0	320	0	0	0	10	0

Table 4-34 Revised cables contact rates for Zone 2, mean rolling period 10 days

Water Depth (m)		Central Cable		North Cable		South Cable	
Min.	Max.	Cable Length (m)	Annual Contact Rate	Cable Length (m)	Annual Contact Rate	Cable Length (m)	Annual Contact Rate
57.5	60.0	0	0	0	0	20	3.0×10^{-5}
60.0	62.5	0	0	0	0	510	2.7×10^{-4}
62.5	65.0	0	0	0	0	260	7.3×10^{-4}
65.0	67.5	0	0	0	0	450	6.0×10^{-4}
67.5	70.0	0	0	0	0	590	2.6×10^{-4}
70.0	72.5	0	0	0	0	470	2.3×10^{-5}
72.5	75.0	0	0	0	0	230	5.2×10^{-5}
75.0	77.5	0	0	720	0	240	0
77.5	80.0	0	0	1450	0	740	0
80.0	82.5	0	0	870	0	690	0
82.5	85.0	350	0	300	0	900	0
85.0	87.5	660	0	340	0	570	0
87.5	90.0	880	0	570	0	160	0
90.0	92.5	1090	0	1690	0	310	0
92.5	95.0	510	0	810	0	370	0
95.0	97.5	1530	0	350	0	270	0
97.5	100.0	1110	0	120	0	200	0
100.0	102.5	390	0	0	0	110	0
102.5	105.0	320	0	0	0	10	0

Table 4-35 Revised cables contact rates for Zone 2, no rolling

Water Depth (m)		Central Cable		North Cable		South Cable	
Min.	Max.	Cable Length (m)	Annual Contact Rate	Cable Length (m)	Annual Contact Rate	Cable Length (m)	Annual Contact Rate
57.5	60.0	0	0	0	0	20	1.2×10^{-5}
60.0	62.5	0	0	0	0	510	1.9×10^{-4}
62.5	65.0	0	0	0	0	260	8.8×10^{-5}
65.0	67.5	0	0	0	0	450	1.2×10^{-4}
67.5	70.0	0	0	0	0	590	3.7×10^{-5}
70.0	72.5	0	0	0	0	470	0
72.5	75.0	0	0	0	0	230	0
75.0	77.5	0	0	720	0	240	0
77.5	80.0	0	0	1450	0	740	0
80.0	82.5	0	0	870	0	690	0
82.5	85.0	350	0	300	0	900	0
85.0	87.5	660	0	340	0	570	0
87.5	90.0	880	0	570	0	160	0
90.0	92.5	1090	0	1690	0	310	0
92.5	95.0	510	0	810	0	370	0
95.0	97.5	1530	0	350	0	270	0
97.5	100.0	1110	0	120	0	200	0
100.0	102.5	390	0	0	0	110	0
102.5	105.0	320	0	0	0	10	0

4.4.4 *Contact Rates in Zone 4 (Central Trough)*

Iceberg contact rates with the cables in Zone 4 are given in Table 4-36 (base case, 3 day mean iceberg rolling period), Table 4-37 (1 day mean iceberg rolling period), Table 4-38 (10 day mean iceberg rolling period) and Table 4-39 (no iceberg rolling). Iceberg contact rates in Zone 4 are relatively low as this area is sheltered by the bathymetric high point to the northeast. Iceberg groundings in this zone are due to icebergs drifting over this high point and then rolling and adopting a deeper draft. Some iceberg contacts are observed in the base case and 1 day rolling scenarios, with fewer using 10 days mean rolling period and no contacts with no rolling.

Table 4-36 Revised cables contact rates for Zone 4, base case

Water Depth (m)		Central Cable		North Cable		South Cable	
Min.	Max.	Cable Length (m)	Annual Contact Rate	Cable Length (m)	Annual Contact Rate	Cable Length (m)	Annual Contact Rate
65.0	67.5	10	2.6×10^{-5}	140	2.8×10^{-4}	20	9.0×10^{-5}
67.5	70.0	170	3.8×10^{-4}	90	1.8×10^{-4}	200	1.9×10^{-4}
70.0	72.5	240	0	880	1.2×10^{-3}	270	8.9×10^{-5}
72.5	75.0	190	1.5×10^{-5}	1210	1.7×10^{-3}	820	7.7×10^{-4}
75.0	77.5	1410	6.6×10^{-4}	450	4.3×10^{-4}	1200	9.9×10^{-4}
77.5	80.0	600	1.5×10^{-4}	620	3.1×10^{-4}	450	3.4×10^{-4}
80.0	82.5	240	7.3×10^{-5}	290	4.8×10^{-5}	220	4.4×10^{-5}
82.5	85.0	720	6.0×10^{-4}	370	8.8×10^{-5}	270	1.2×10^{-5}
85.0	87.5	570	3.6×10^{-4}	100	0	550	2.5×10^{-4}
87.5	90.0	70	0	80	0	450	0
90.0	92.5	90	0	80	0	680	5.0×10^{-4}
92.5	95.0	350	0	890	5.4×10^{-5}	1250	2.7×10^{-4}
95.0	97.5	1050	3.0×10^{-4}	1340	8.1×10^{-5}	1770	2.6×10^{-4}
97.5	100.0	1470	1.9×10^{-4}	2430	3.5×10^{-4}	2860	3.3×10^{-4}
100.0	102.5	3100	2.5×10^{-4}	3340	1.8×10^{-4}	1920	7.4×10^{-5}
102.5	105.0	3390	4.4×10^{-4}	2200	2.7×10^{-5}	1930	1.5×10^{-5}
105.0	107.5	1670	0	2370	2.1×10^{-5}	1620	0
107.5	110.0	1780	0	1640	2.0×10^{-4}	1070	0
110.0	112.5	2620	0	1280	0	1820	0
112.5	115.0	360	0	130	0	900	0

Table 4-37 Revised cables contact rates for Zone 4, mean rolling period 1 day

Water Depth (m)		Central Cable		North Cable		South Cable	
Min.	Max.	Cable Length (m)	Annual Contact Rate	Cable Length (m)	Annual Contact Rate	Cable Length (m)	Annual Contact Rate
65.0	67.5	10	3.0×10^{-5}	140	1.1×10^{-3}	20	1.1×10^{-4}
67.5	70.0	170	5.6×10^{-4}	90	6.0×10^{-4}	200	4.3×10^{-4}
70.0	72.5	240	1.8×10^{-4}	880	1.7×10^{-4}	270	1.1×10^{-3}
72.5	75.0	190	8.4×10^{-5}	1210	6.8×10^{-5}	820	9.6×10^{-4}
75.0	77.5	1410	1.1×10^{-3}	450	9.5×10^{-5}	1200	9.4×10^{-4}
77.5	80.0	600	5.0×10^{-4}	620	6.5×10^{-4}	450	4.5×10^{-4}
80.0	82.5	240	1.8×10^{-4}	290	6.3×10^{-5}	220	0
82.5	85.0	720	0	370	4.1×10^{-4}	270	0
85.0	87.5	570	2.9×10^{-5}	100	0	550	0
87.5	90.0	70	0	80	0	450	0
90.0	92.5	90	0	80	0	680	0
92.5	95.0	350	0	890	0	1250	0
95.0	97.5	1050	8.0×10^{-4}	1340	2.2×10^{-4}	1770	0
97.5	100.0	1470	3.0×10^{-4}	2430	7.5×10^{-4}	2860	0
100.0	102.5	3100	0	3340	0	1920	0
102.5	105.0	3390	0	2200	0	1930	0
105.0	107.5	1670	0	2370	0	1620	0
107.5	110.0	1780	0	1640	0	1070	0
110.0	112.5	2620	0	1280	0	1820	0
112.5	115.0	360	0	130	0	900	0

Table 4-38 Revised cables contact rates for Zone 4, mean rolling period 10 days

Water Depth (m)		Central Cable		North Cable		South Cable	
Min.	Max.	Cable Length (m)	Annual Contact Rate	Cable Length (m)	Annual Contact Rate	Cable Length (m)	Annual Contact Rate
65.0	67.5	10	8.8×10^{-6}	140	1.2×10^{-7}	20	5.3×10^{-5}
67.5	70.0	170	3.7×10^{-4}	90	0	200	8.9×10^{-5}
70.0	72.5	240	3.8×10^{-6}	880	0	270	2.3×10^{-4}
72.5	75.0	190	7.5×10^{-6}	1210	1.7×10^{-4}	820	0
75.0	77.5	1410	1.8×10^{-4}	450	7.4×10^{-4}	1200	0
77.5	80.0	600	1.3×10^{-4}	620	2.1×10^{-5}	450	9.7×10^{-7}
80.0	82.5	240	6.6×10^{-5}	290	0	220	5.2×10^{-6}
82.5	85.0	720	3.4×10^{-6}	370	0	270	2.2×10^{-6}
85.0	87.5	570	0	100	0	550	0
87.5	90.0	70	0	80	0	450	0
90.0	92.5	90	0	80	0	680	0
92.5	95.0	350	0	890	0	1250	0
95.0	97.5	1050	0	1340	0	1770	8.2×10^{-4}
97.5	100.0	1470	0	2430	0	2860	9.2×10^{-5}
100.0	102.5	3100	0	3340	1.2×10^{-5}	1920	0
102.5	105.0	3390	8.2×10^{-4}	2200	8.7×10^{-6}	1930	0
105.0	107.5	1670	0	2370	0	1620	0
107.5	110.0	1780	0	1640	0	1070	0
110.0	112.5	2620	0	1280	0	1820	0
112.5	115.0	360	0	130	0	900	0

Table 4-39 Revised cables contact rates for Zone 4, no rolling

Water Depth (m)		Central Cable		North Cable		South Cable	
Min.	Max.	Cable Length (m)	Annual Contact Rate	Cable Length (m)	Annual Contact Rate	Cable Length (m)	Annual Contact Rate
65.0	67.5	10	0	140	0	20	0
67.5	70.0	170	0	90	0	200	0
70.0	72.5	240	0	880	0	270	0
72.5	75.0	190	0	1210	0	820	0
75.0	77.5	1410	0	450	0	1200	0
77.5	80.0	600	0	620	0	450	0
80.0	82.5	240	0	290	0	220	0
82.5	85.0	720	0	370	0	270	0
85.0	87.5	570	0	100	0	550	0
87.5	90.0	70	0	80	0	450	0
90.0	92.5	90	0	80	0	680	0
92.5	95.0	350	0	890	0	1250	0
95.0	97.5	1050	0	1340	0	1770	0
97.5	100.0	1470	0	2430	0	2860	0
100.0	102.5	3100	0	3340	0	1920	0
102.5	105.0	3390	0	2200	0	1930	0
105.0	107.5	1670	0	2370	0	1620	0
107.5	110.0	1780	0	1640	0	1070	0
110.0	112.5	2620	0	1280	0	1820	0
112.5	115.0	360	0	130	0	900	0

4.4.5 Contact Rates in Zone 5 (Newfoundland Landfall)

Iceberg contact rates with the cables in Zone 5 (Newfoundland landfall) are given in Table 4-40 (base case, 3 day mean iceberg rolling period), Table 4-41 (1 day mean iceberg rolling period), Table 4-42 (10 day mean iceberg rolling period) and Table 4-43 (no iceberg rolling). The water depth cut-off for Zone 5 is less than 70 m, thus iceberg contacts rates are relatively high for all cases. The exception is the no iceberg rolling case, where no iceberg keel contacts are seen in water depths greater than 65 m.

Table 4-40 Revised cables contact rates for Zone 5, base case

Water Depth (m)		Central Cable		North Cable		South Cable	
Min.	Max.	Cable Length (m)	Annual Contact Rate	Cable Length (m)	Annual Contact Rate	Cable Length (m)	Annual Contact Rate
0.0	2.5	340	1.1×10^{-2}	220	7.3×10^{-3}	430	1.5×10^{-2}
2.5	5.0	390	3.5×10^{-2}	380	3.2×10^{-2}	340	4.2×10^{-2}
5.0	7.5	200	4.7×10^{-2}	250	4.9×10^{-2}	120	3.1×10^{-2}
7.5	10.0	100	3.9×10^{-2}	150	6.1×10^{-2}	90	3.5×10^{-2}
10.0	12.5	80	4.2×10^{-2}	80	4.5×10^{-2}	70	3.4×10^{-2}
12.5	15.0	60	3.3×10^{-2}	50	2.9×10^{-2}	70	3.6×10^{-2}
15.0	17.5	60	3.4×10^{-2}	40	2.1×10^{-2}	60	2.9×10^{-2}
17.5	20.0	60	3.1×10^{-2}	50	2.4×10^{-2}	40	1.8×10^{-2}
20.0	22.5	100	4.4×10^{-2}	50	2.2×10^{-2}	30	1.2×10^{-2}
22.5	25.0	120	4.7×10^{-2}	60	2.3×10^{-2}	90	2.9×10^{-2}
25.0	27.5	10	3.1×10^{-3}	50	1.6×10^{-2}	50	1.4×10^{-2}
27.5	30.0	20	5.2×10^{-3}	60	1.6×10^{-2}	70	1.7×10^{-2}
30.0	32.5	10	2.4×10^{-3}	60	1.5×10^{-2}	40	1.0×10^{-2}
32.5	35.0	20	4.9×10^{-3}	40	1.0×10^{-2}	20	4.4×10^{-3}
35.0	37.5	20	4.6×10^{-3}	30	7.5×10^{-3}	10	2.1×10^{-3}
37.5	40.0	20	3.9×10^{-3}	20	4.6×10^{-3}	20	4.0×10^{-3}
40.0	42.5	20	3.2×10^{-3}	20	4.2×10^{-3}	20	3.6×10^{-3}
42.5	45.0	20	2.9×10^{-3}	20	3.6×10^{-3}	30	4.7×10^{-3}
45.0	47.5	20	2.6×10^{-3}	10	1.6×10^{-3}	20	2.5×10^{-3}
47.5	50.0	20	2.2×10^{-3}	10	1.4×10^{-3}	20	2.1×10^{-3}
50.0	52.5	20	1.8×10^{-3}	20	2.3×10^{-3}	30	2.2×10^{-3}
52.5	55.0	20	1.3×10^{-3}	20	1.5×10^{-3}	40	1.6×10^{-3}
55.0	57.5	30	1.1×10^{-3}	30	1.1×10^{-3}	30	7.0×10^{-4}
57.5	60.0	40	4.6×10^{-4}	50	4.9×10^{-4}	40	5.7×10^{-4}
60.0	62.5	60	2.6×10^{-4}	50	9.9×10^{-5}	50	3.7×10^{-4}
62.5	65.0	80	2.4×10^{-4}	80	3.3×10^{-4}	70	2.6×10^{-4}
65.0	67.5	70	1.4×10^{-4}	60	3.8×10^{-4}	70	3.2×10^{-4}

Table 4-41 Revised cables contact rates for Zone 5, mean rolling period 1 day

Water Depth (m)		Central Cable		North Cable		South Cable	
Min.	Max.	Cable Length (m)	Annual Contact Rate	Cable Length (m)	Annual Contact Rate	Cable Length (m)	Annual Contact Rate
0.0	2.5	340	1.1×10^{-2}	220	7.3×10^{-3}	430	1.6×10^{-2}
2.5	5.0	390	3.9×10^{-2}	380	3.2×10^{-2}	340	4.0×10^{-2}
5.0	7.5	200	4.2×10^{-2}	250	5.0×10^{-2}	120	2.7×10^{-2}
7.5	10.0	100	3.5×10^{-2}	150	5.8×10^{-2}	90	3.3×10^{-2}
10.0	12.5	80	3.9×10^{-2}	80	4.3×10^{-2}	70	3.3×10^{-2}
12.5	15.0	60	3.3×10^{-2}	50	2.9×10^{-2}	70	3.6×10^{-2}
15.0	17.5	60	3.2×10^{-2}	40	2.1×10^{-2}	60	3.0×10^{-2}
17.5	20.0	60	2.9×10^{-2}	50	2.3×10^{-2}	40	1.7×10^{-2}
20.0	22.5	100	4.0×10^{-2}	50	2.0×10^{-2}	30	1.1×10^{-2}
22.5	25.0	120	4.2×10^{-2}	60	2.0×10^{-2}	90	2.7×10^{-2}
25.0	27.5	10	3.3×10^{-3}	50	1.4×10^{-2}	50	1.4×10^{-2}
27.5	30.0	20	5.6×10^{-3}	60	1.3×10^{-2}	70	1.7×10^{-2}
30.0	32.5	10	2.6×10^{-3}	60	1.2×10^{-2}	40	1.0×10^{-2}
32.5	35.0	20	5.0×10^{-3}	40	8.2×10^{-3}	20	4.5×10^{-3}
35.0	37.5	20	4.6×10^{-3}	30	6.1×10^{-3}	10	2.2×10^{-3}
37.5	40.0	20	3.9×10^{-3}	20	3.7×10^{-3}	20	4.2×10^{-3}
40.0	42.5	20	3.3×10^{-3}	20	3.5×10^{-3}	20	3.7×10^{-3}
42.5	45.0	20	2.8×10^{-3}	20	3.0×10^{-3}	30	4.8×10^{-3}
45.0	47.5	20	2.4×10^{-3}	10	1.4×10^{-3}	20	2.7×10^{-3}
47.5	50.0	20	2.0×10^{-3}	10	1.3×10^{-3}	20	2.2×10^{-3}
50.0	52.5	20	1.5×10^{-3}	20	2.1×10^{-3}	30	2.3×10^{-3}
52.5	55.0	20	1.2×10^{-3}	20	1.5×10^{-3}	40	1.6×10^{-3}
55.0	57.5	30	1.2×10^{-3}	30	1.4×10^{-3}	30	6.5×10^{-4}
57.5	60.0	40	6.5×10^{-4}	50	1.2×10^{-3}	40	5.3×10^{-4}
60.0	62.5	60	5.8×10^{-4}	50	5.5×10^{-4}	50	3.9×10^{-4}
62.5	65.0	80	4.7×10^{-4}	80	7.6×10^{-4}	70	7.9×10^{-4}
65.0	67.5	70	1.7×10^{-4}	60	3.0×10^{-4}	70	6.9×10^{-4}

Table 4-42 Revised cables contact rates for Zone 5, mean rolling period 10 days

Water Depth (m)		Central Cable		North Cable		South Cable	
Min.	Max.	Cable Length (m)	Annual Contact Rate	Cable Length (m)	Annual Contact Rate	Cable Length (m)	Annual Contact Rate
0.0	2.5	340	1.1×10^{-2}	220	6.9×10^{-3}	430	1.5×10^{-2}
2.5	5.0	390	3.3×10^{-2}	380	3.0×10^{-2}	340	3.5×10^{-2}
5.0	7.5	200	4.4×10^{-2}	250	4.6×10^{-2}	120	2.8×10^{-2}
7.5	10.0	100	3.7×10^{-2}	150	6.2×10^{-2}	90	3.7×10^{-2}
10.0	12.5	80	4.0×10^{-2}	80	4.2×10^{-2}	70	3.3×10^{-2}
12.5	15.0	60	3.1×10^{-2}	50	2.7×10^{-2}	70	3.4×10^{-2}
15.0	17.5	60	3.3×10^{-2}	40	2.1×10^{-2}	60	3.0×10^{-2}
17.5	20.0	60	3.4×10^{-2}	50	2.3×10^{-2}	40	1.9×10^{-2}
20.0	22.5	100	4.7×10^{-2}	50	1.9×10^{-2}	30	1.3×10^{-2}
22.5	25.0	120	4.8×10^{-2}	60	2.2×10^{-2}	90	3.2×10^{-2}
25.0	27.5	10	3.9×10^{-3}	50	1.7×10^{-2}	50	1.6×10^{-2}
27.5	30.0	20	6.8×10^{-3}	60	1.6×10^{-2}	70	1.9×10^{-2}
30.0	32.5	10	3.1×10^{-3}	60	1.5×10^{-2}	40	1.1×10^{-2}
32.5	35.0	20	6.3×10^{-3}	40	1.1×10^{-2}	20	4.7×10^{-3}
35.0	37.5	20	5.6×10^{-3}	30	8.3×10^{-3}	10	2.2×10^{-3}
37.5	40.0	20	4.4×10^{-3}	20	5.2×10^{-3}	20	4.0×10^{-3}
40.0	42.5	20	3.1×10^{-3}	20	4.8×10^{-3}	20	3.5×10^{-3}
42.5	45.0	20	2.7×10^{-3}	20	4.1×10^{-3}	30	4.3×10^{-3}
45.0	47.5	20	2.2×10^{-3}	10	1.8×10^{-3}	20	2.2×10^{-3}
47.5	50.0	20	1.8×10^{-3}	10	1.6×10^{-3}	20	1.7×10^{-3}
50.0	52.5	20	1.3×10^{-3}	20	2.4×10^{-3}	30	1.7×10^{-3}
52.5	55.0	20	8.7×10^{-4}	20	1.5×10^{-3}	40	7.8×10^{-4}
55.0	57.5	30	7.7×10^{-4}	30	1.1×10^{-3}	30	2.6×10^{-4}
57.5	60.0	40	3.8×10^{-4}	50	7.6×10^{-4}	40	3.5×10^{-4}
60.0	62.5	60	4.6×10^{-4}	50	2.9×10^{-4}	50	2.7×10^{-4}
62.5	65.0	80	6.1×10^{-4}	80	8.8×10^{-5}	70	1.0×10^{-4}
65.0	67.5	70	6.2×10^{-5}	60	7.6×10^{-7}	70	1.9×10^{-4}

Table 4-43 Revised cables contact rates for Zone 5, no rolling

Water Depth (m)		Central Cable		North Cable		South Cable	
Min.	Max.	Cable Length (m)	Annual Contact Rate	Cable Length (m)	Annual Contact Rate	Cable Length (m)	Annual Contact Rate
0.0	2.5	340	1.1×10^{-2}	220	7.0×10^{-3}	430	1.7×10^{-2}
2.5	5.0	390	3.5×10^{-2}	380	3.4×10^{-2}	340	3.9×10^{-2}
5.0	7.5	200	4.2×10^{-2}	250	5.1×10^{-2}	120	3.1×10^{-2}
7.5	10.0	100	3.9×10^{-2}	150	5.6×10^{-2}	90	3.3×10^{-2}
10.0	12.5	80	4.2×10^{-2}	80	4.2×10^{-2}	70	3.4×10^{-2}
12.5	15.0	60	3.4×10^{-2}	50	2.6×10^{-2}	70	3.8×10^{-2}
15.0	17.5	60	3.5×10^{-2}	40	2.1×10^{-2}	60	3.2×10^{-2}
17.5	20.0	60	3.5×10^{-2}	50	2.5×10^{-2}	40	1.9×10^{-2}
20.0	22.5	100	4.8×10^{-2}	50	2.3×10^{-2}	30	1.3×10^{-2}
22.5	25.0	120	4.9×10^{-2}	60	2.3×10^{-2}	90	3.2×10^{-2}
25.0	27.5	10	3.7×10^{-3}	50	1.5×10^{-2}	50	1.6×10^{-2}
27.5	30.0	20	6.1×10^{-3}	60	1.5×10^{-2}	70	2.0×10^{-2}
30.0	32.5	10	2.8×10^{-3}	60	1.4×10^{-2}	40	1.2×10^{-2}
32.5	35.0	20	5.7×10^{-3}	40	1.0×10^{-2}	20	5.2×10^{-3}
35.0	37.5	20	5.4×10^{-3}	30	7.3×10^{-3}	10	2.5×10^{-3}
37.5	40.0	20	4.7×10^{-3}	20	4.4×10^{-3}	20	4.6×10^{-3}
40.0	42.5	20	4.1×10^{-3}	20	4.1×10^{-3}	20	4.1×10^{-3}
42.5	45.0	20	3.6×10^{-3}	20	3.5×10^{-3}	30	5.0×10^{-3}
45.0	47.5	20	3.1×10^{-3}	10	1.6×10^{-3}	20	2.6×10^{-3}
47.5	50.0	20	2.5×10^{-3}	10	1.5×10^{-3}	20	2.2×10^{-3}
50.0	52.5	20	1.7×10^{-3}	20	2.5×10^{-3}	30	2.6×10^{-3}
52.5	55.0	20	1.1×10^{-3}	20	1.8×10^{-3}	40	1.9×10^{-3}
55.0	57.5	30	9.1×10^{-4}	30	1.3×10^{-3}	30	6.2×10^{-4}
57.5	60.0	40	2.2×10^{-4}	50	3.8×10^{-4}	40	2.8×10^{-4}
60.0	62.5	60	0	50	3.7×10^{-5}	50	2.6×10^{-5}
62.5	65.0	80	0	80	0	70	3.8×10^{-5}
65.0	67.5	70	0	60	0	70	0

4.4.6 *Modifications to Cable Routes*

The spacing of the cables was modified in Zone 2 in order to address the issue noted in Section 4.4.3 regarding the relatively high contact rates with the north and south cables in the channel. In Zone 2 the spacing between the cables was reduced from 150 m to 50 m to keep the north and south cables in deeper water. Slight modifications were also made to the central cable route. The modifications to the cable routes are shown in Figure 4-23.

Revised contact rates based on the cable routes shown in Figure 4-23 are given in Table 4-44 (base case), Table 4-45 (mean rolling period 1 day), Table 4-46 (mean rolling period 10 days) and Table 4-47 (no iceberg rolling). In all cases, the iceberg keel contacts have been reduced substantially, and in the cases of 10 days mean rolling period and no rolling have been reduced to zero.

Any further analyses of iceberg contact rates for cable routes will use these revised routes in Zone 2.

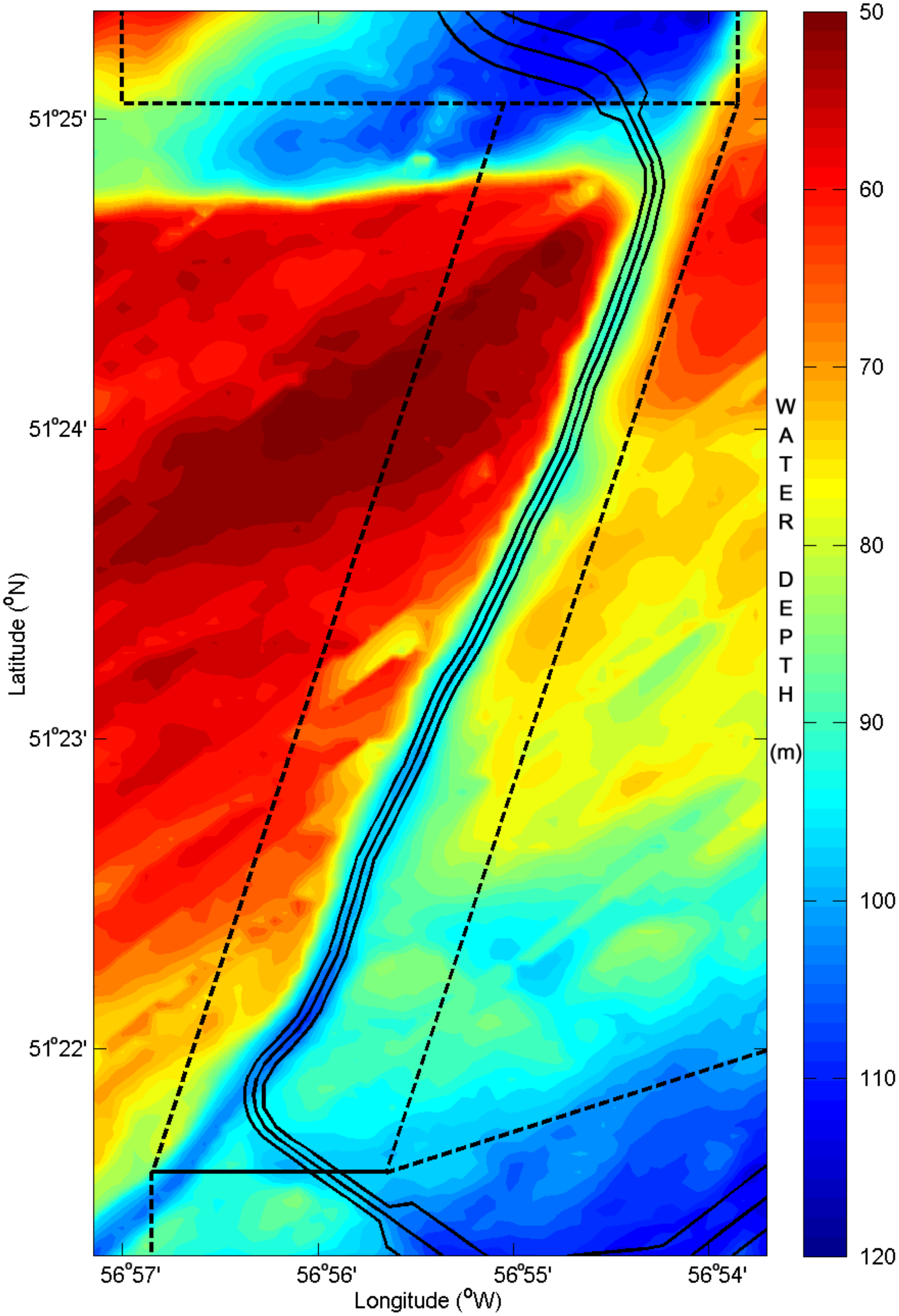

Figure 4-23 Modified cable routes (spacing reduced from 150 to 50 m)

Table 4-44 Contact rates for modified cable rates for Zone 2, base case

Water Depth (m)		Central Cable		North Cable		South Cable	
Min.	Max.	Cable Length (m)	Annual Contact Rate	Cable Length (m)	Annual Contact Rate	Cable Length (m)	Annual Contact Rate
80.0	82.5	0	0	160	0	210	6.2×10^{-6}
82.5	85.0	350	4.4×10^{-5}	520	1.0×10^{-4}	380	5.4×10^{-5}
85.0	87.5	660	2.6×10^{-4}	840	1.6×10^{-6}	1090	9.1×10^{-5}
87.5	90.0	800	0	1180	3.8×10^{-8}	1000	6.4×10^{-4}
90.0	92.5	1180	8.6×10^{-5}	740	0	490	1.0×10^{-4}
92.5	95.0	500	3.3×10^{-6}	790	0	1230	4.6×10^{-4}
95.0	97.5	1530	2.0×10^{-5}	1670	5.7×10^{-5}	1290	9.5×10^{-5}
97.5	100.0	1110	2.6×10^{-4}	430	0	570	2.4×10^{-5}
100.0	102.5	390	0	420	0	730	0
102.5	105.0	330	0	430	0	240	0
105.0	107.5	310	0	0	0	0	0

Table 4-45 Contact rates for modified cable rates for Zone 2, mean rolling period 1 day

Water Depth (m)		Central Cable		North Cable		South Cable	
Min.	Max.	Cable Length (m)	Annual Contact Rate	Cable Length (m)	Annual Contact Rate	Cable Length (m)	Annual Contact Rate
80.0	82.5	0	0	160	0	210	0
82.5	85.0	350	0	520	0	380	0
85.0	87.5	660	0	840	0	1090	7.5×10^{-5}
87.5	90.0	800	0	1180	0	1000	1.8×10^{-4}
90.0	92.5	1180	0	740	0	490	2.8×10^{-4}
92.5	95.0	500	0	790	0	1230	8.4×10^{-6}
95.0	97.5	1530	0	1670	0	1290	1.5×10^{-4}
97.5	100.0	1110	0	430	0	570	7.4×10^{-5}
100.0	102.5	390	0	420	0	730	0
102.5	105.0	330	0	430	0	240	0
105.0	107.5	310	0	0	0	0	0

Table 4-46 Contact rates for modified cable rates for Zone 2, mean rolling period 10 days

Water Depth (m)		Central Cable		North Cable		South Cable	
Min.	Max.	Cable Length (m)	Annual Contact Rate	Cable Length (m)	Annual Contact Rate	Cable Length (m)	Annual Contact Rate
80.0	82.5	0	0	160	0	210	0
82.5	85.0	350	0	520	0	380	0
85.0	87.5	660	0	840	0	1090	0
87.5	90.0	800	0	1180	0	1000	0
90.0	92.5	1180	0	740	0	490	0
92.5	95.0	500	0	790	0	1230	0
95.0	97.5	1530	0	1670	0	1290	0
97.5	100.0	1110	0	430	0	570	0
100.0	102.5	390	0	420	0	730	0
102.5	105.0	330	0	430	0	240	0
105.0	107.5	310	0	0	0	0	0

Table 4-47 Contact rates for modified cable rates for Zone 2, no rolling

Water Depth (m)		Central Cable		North Cable		South Cable	
Min.	Max.	Cable Length (m)	Annual Contact Rate	Cable Length (m)	Annual Contact Rate	Cable Length (m)	Annual Contact Rate
80.0	82.5	0	0	160	0	210	0
82.5	85.0	350	0	520	0	380	0
85.0	87.5	660	0	840	0	1090	0
87.5	90.0	800	0	1180	0	1000	0
90.0	92.5	1180	0	740	0	490	0
92.5	95.0	500	0	790	0	1230	0
95.0	97.5	1530	0	1670	0	1290	0
97.5	100.0	1110	0	430	0	570	0
100.0	102.5	390	0	420	0	730	0
102.5	105.0	330	0	430	0	240	0
105.0	107.5	310	0	0	0	0	0

4.4.7 Contact Rates as a Function of Transition Depth

Water depth profiles along the cable routes and iceberg contact rates are shown for the various scenarios in Figure 4-24 (base case, 3 day mean iceberg rolling period), Figure 4-26 (1 day mean iceberg rolling period), Figure 4-28 (10 day mean iceberg rolling period) and Figure 4-30 (no iceberg rolling).

Shown in Figure 4-25, Figure 4-27, Figure 4-29 and Figure 4-31 are corresponding figures showing annual iceberg contacts as a function of directional drilling seabed piercing water depth. In all cases, seabed piercing water depths of 60 m give iceberg contact frequencies less than 0.01 yr^{-1}, or mean return periods in excess of 100 years. The relationship between iceberg rolling frequency and contact rate is evident, as outlined in Table 4-48.

Table 4-48 Iceberg contact frequency as a function of directional drilling seabed piercing water depth for various scenarios (mean return period in brackets)

Mean Iceberg Rolling Frequency	Seabed Piercing Water Depth (m)		
	50 m	60 m	70 m
3 days (Base Case)	0.015 yr^{-1} (67 years)	0.007 yr^{-1} (140 years)	0.005 yr^{-1} (200 years)
1 Day	0.016 yr^{-1} (63 years)	0.008 yr^{-1} (125 years)	0.005 yr^{-1} (200 years)
10 Days	0.009 yr^{-1} (110 years)	0.002 yr^{-1} (500 years)	0.001 yr^{-1} (1,000 years)
No rolling	0.006 yr^{-1} (160 years)	0.0001 yr^{-1} (10,000 years)	N.A.

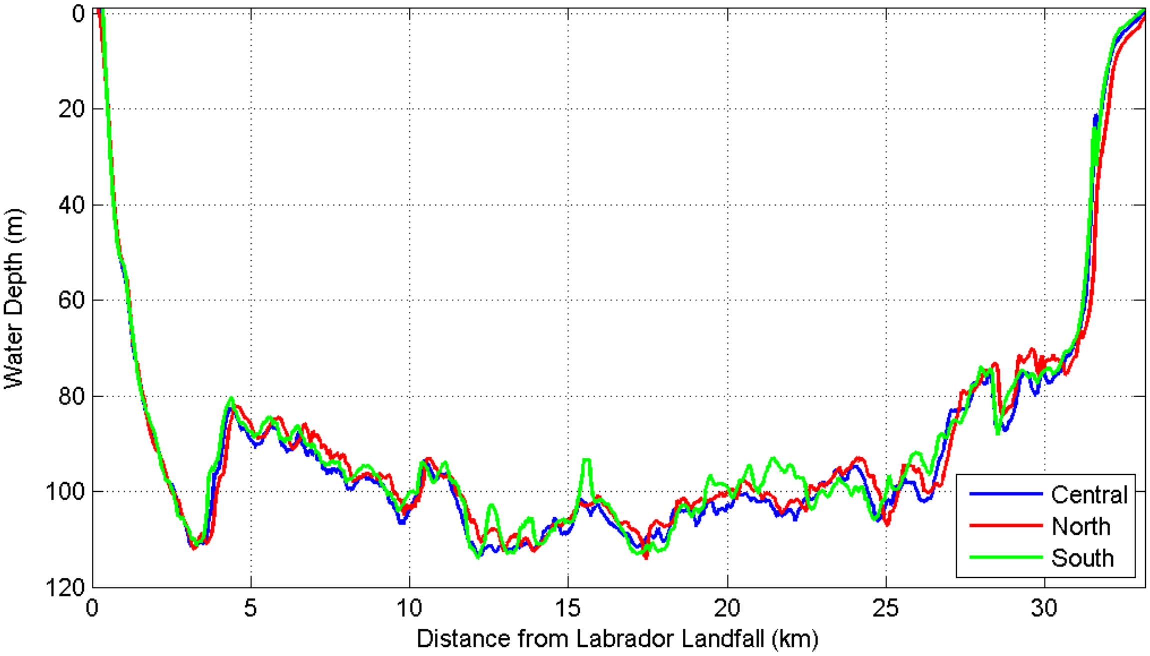

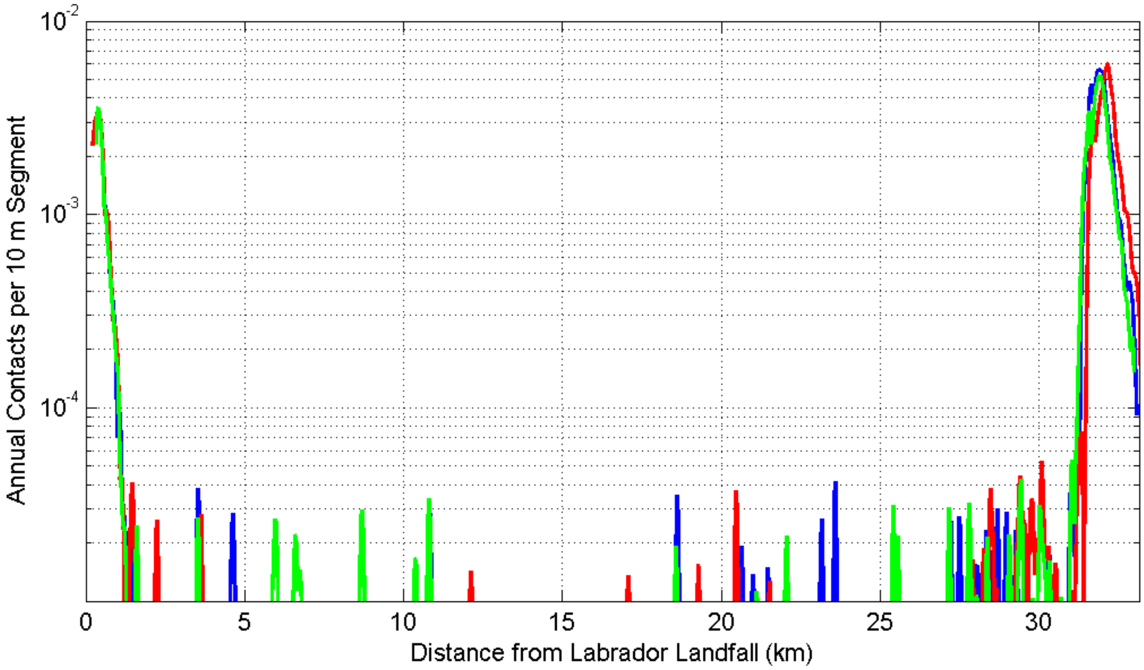

Figure 4-24 Water depth along cable routes (top) and iceberg keel contacts (bottom) using base case scenario (mean iceberg rolling period 3 days)

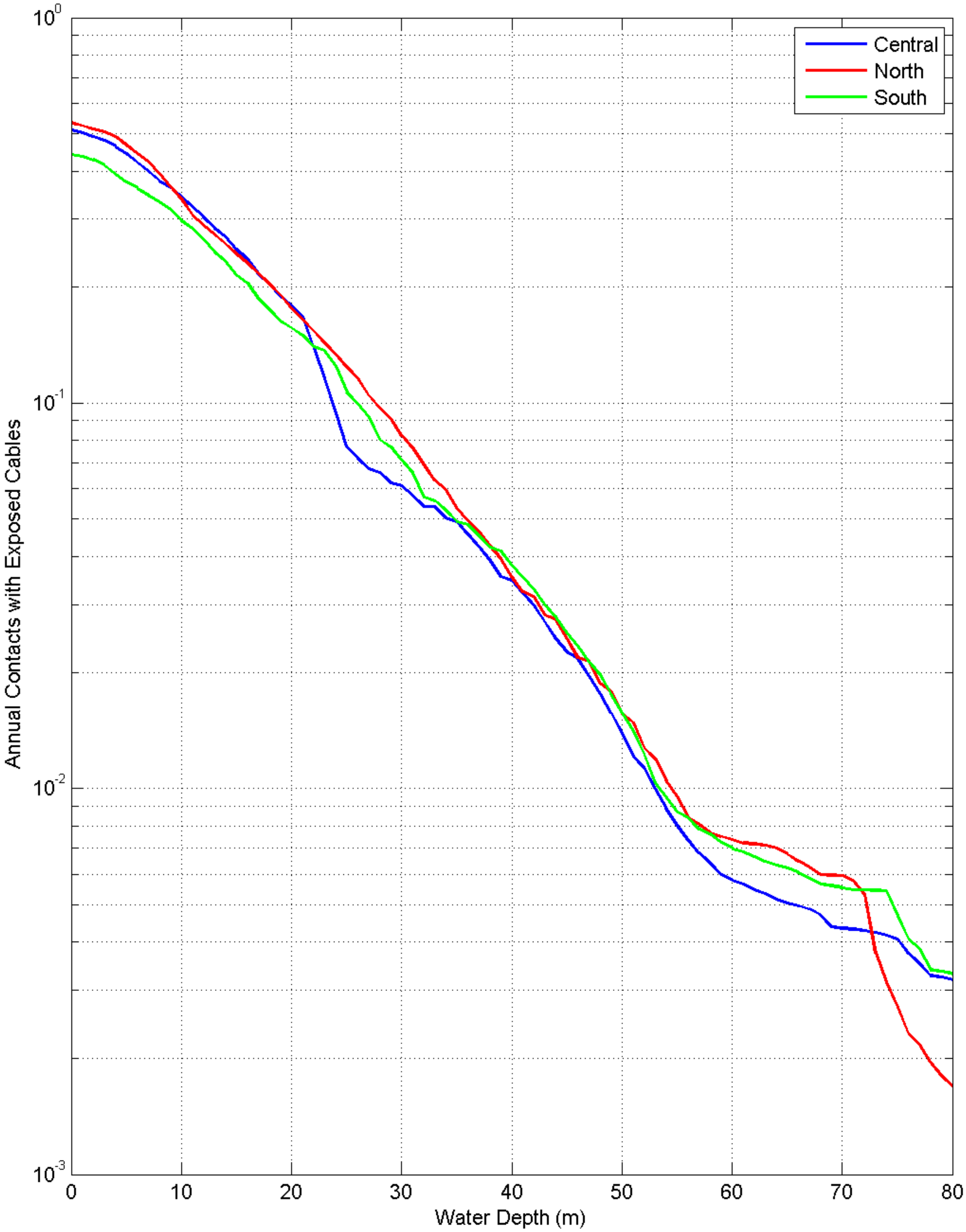

Figure 4-25 Annual cable contacts as a function of directional drilling seabed piercing water depth using base case scenario (mean iceberg rolling period 3 days)

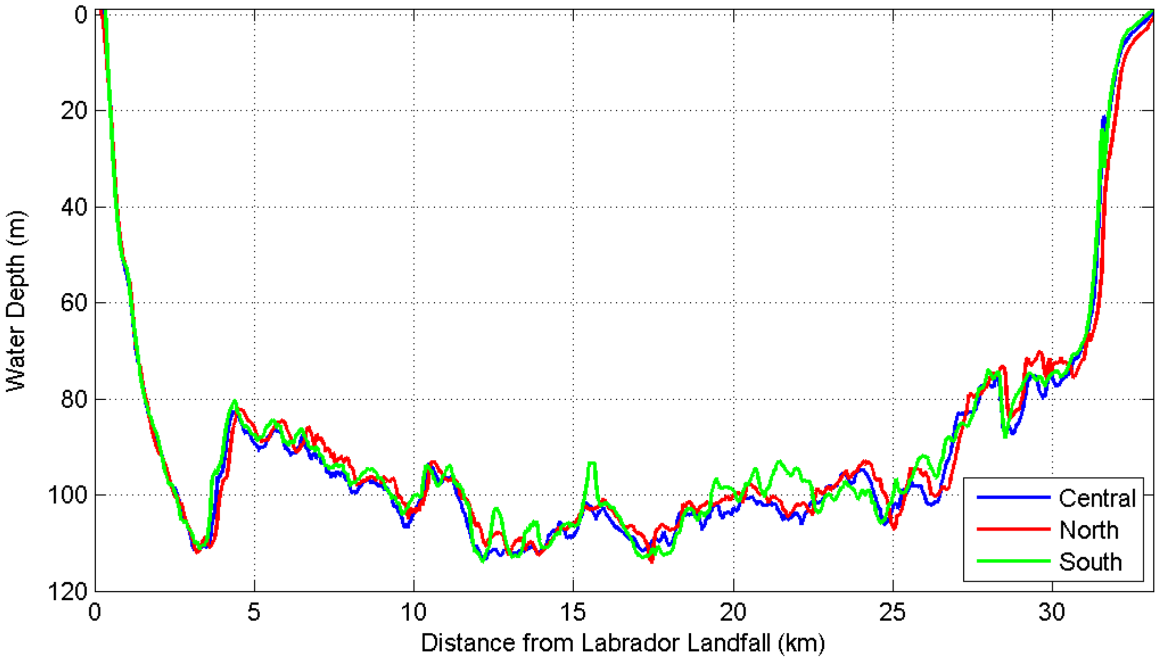

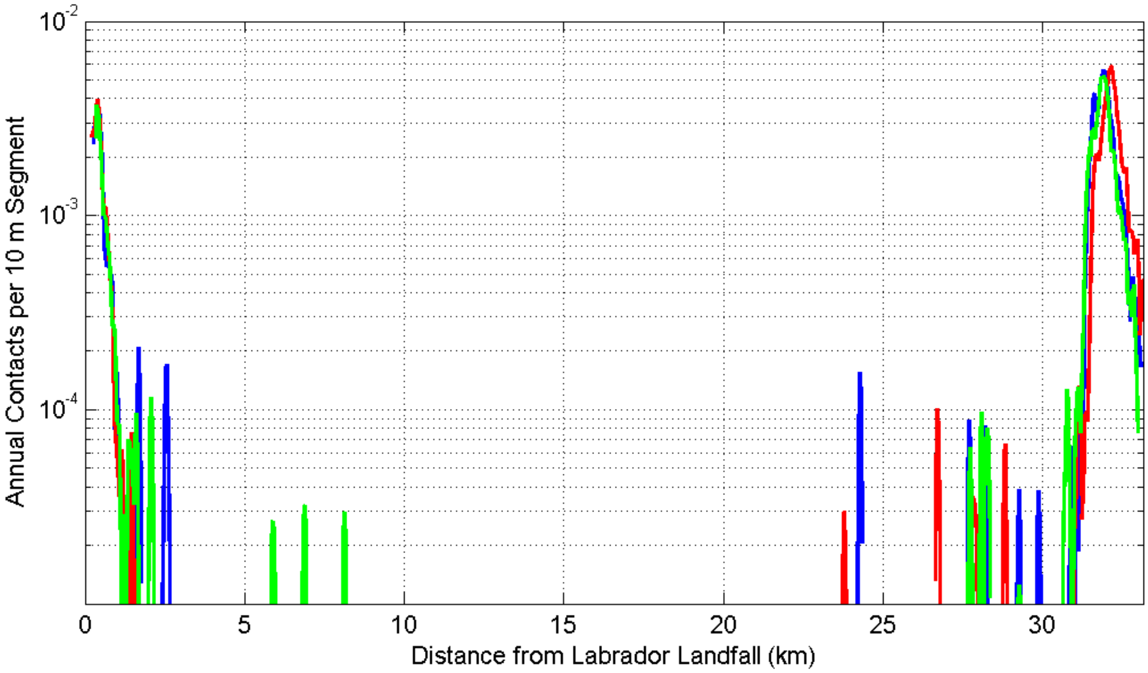

Figure 4-26 Water depth along cable routes (top) and iceberg keel contacts (bottom) using mean iceberg rolling period of 1 day

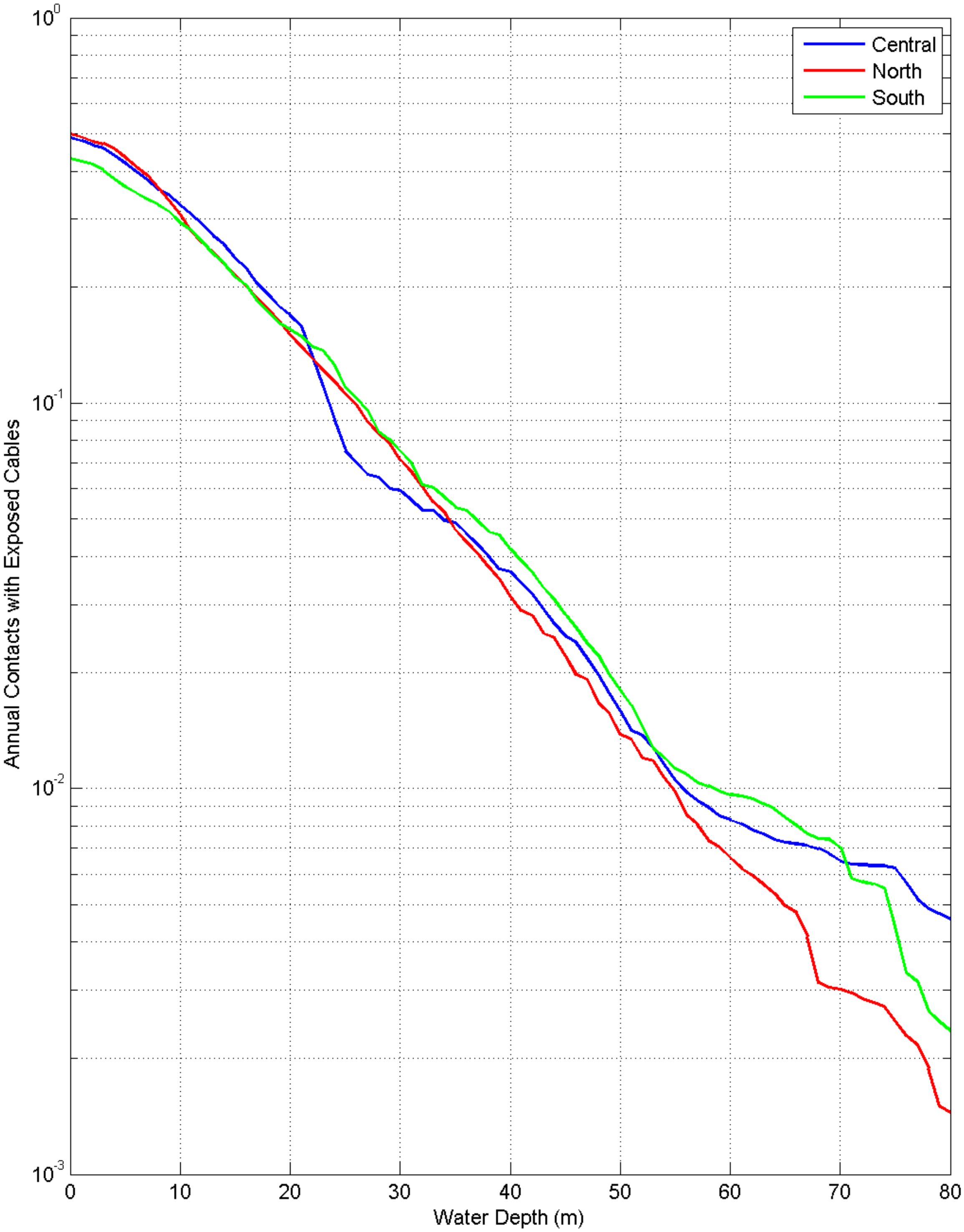

Figure 4-27 Annual cable contacts as a function of directional drilling seabed piercing water depth using mean iceberg rolling period of 1 day

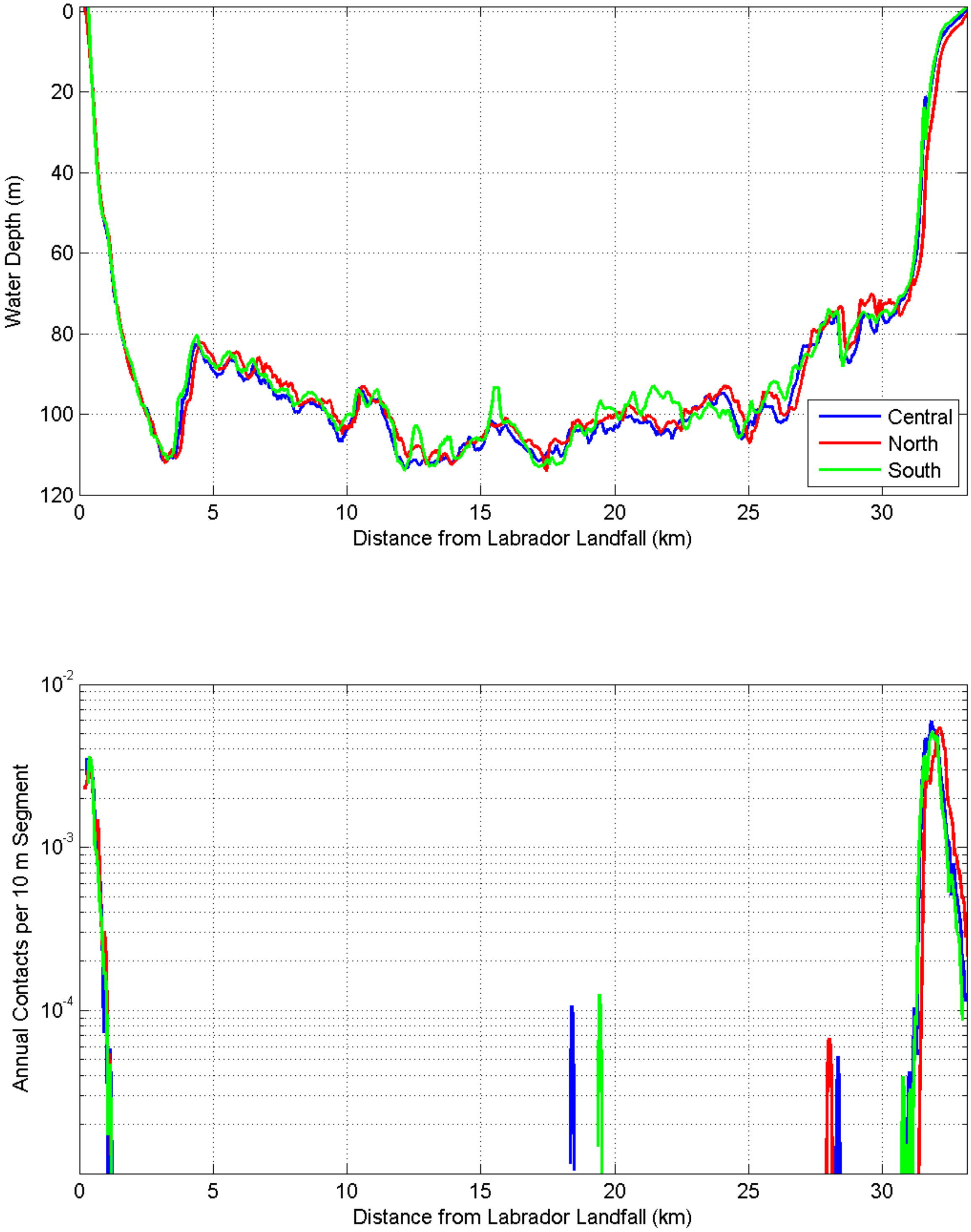

Figure 4-28 Water depth along cable routes (top) and iceberg keel contacts (bottom) using mean iceberg rolling period of 10 days

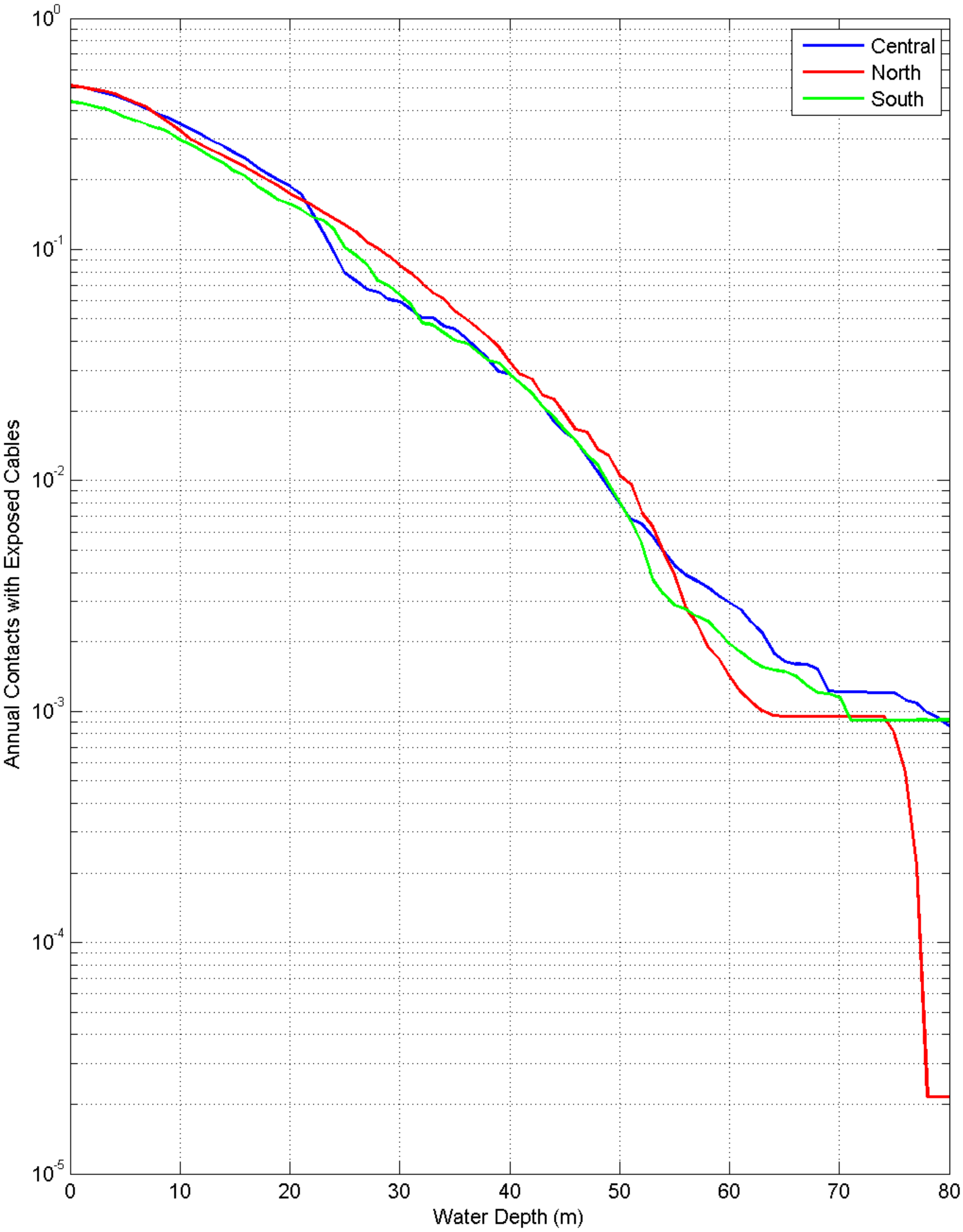

Figure 4-29 Annual cable contacts as a function of directional drilling seabed piercing water depth using mean iceberg rolling period of 10 days

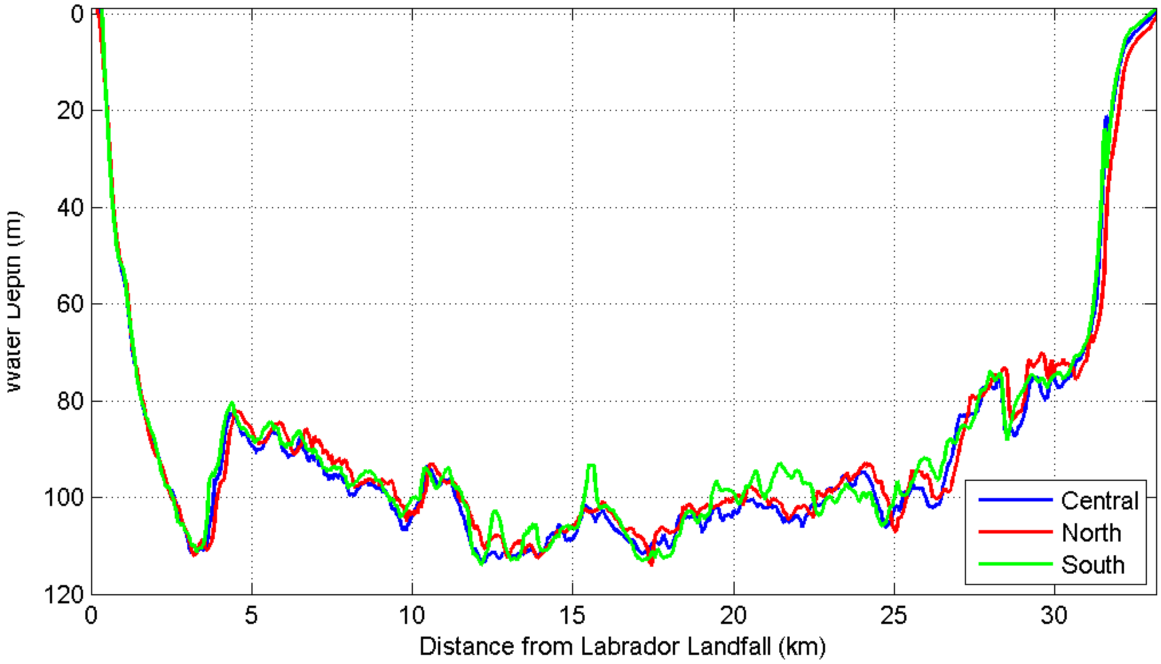

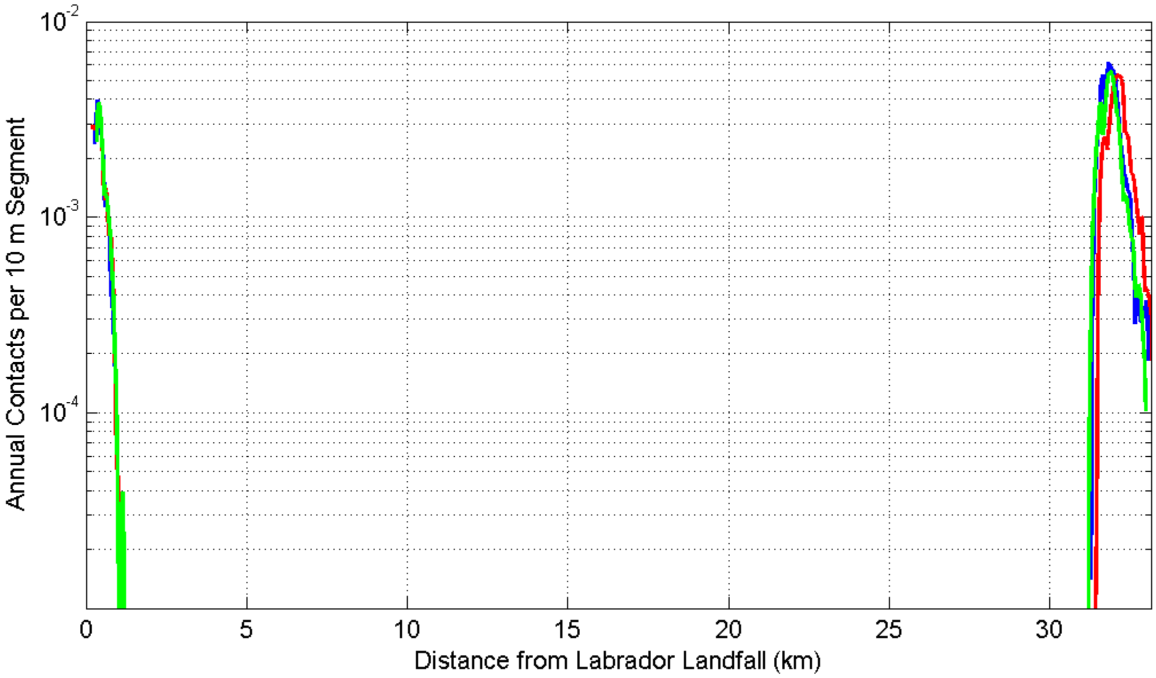

Figure 4-30 Water depth along cable routes (top) and iceberg keel contacts (bottom) using no iceberg rolling

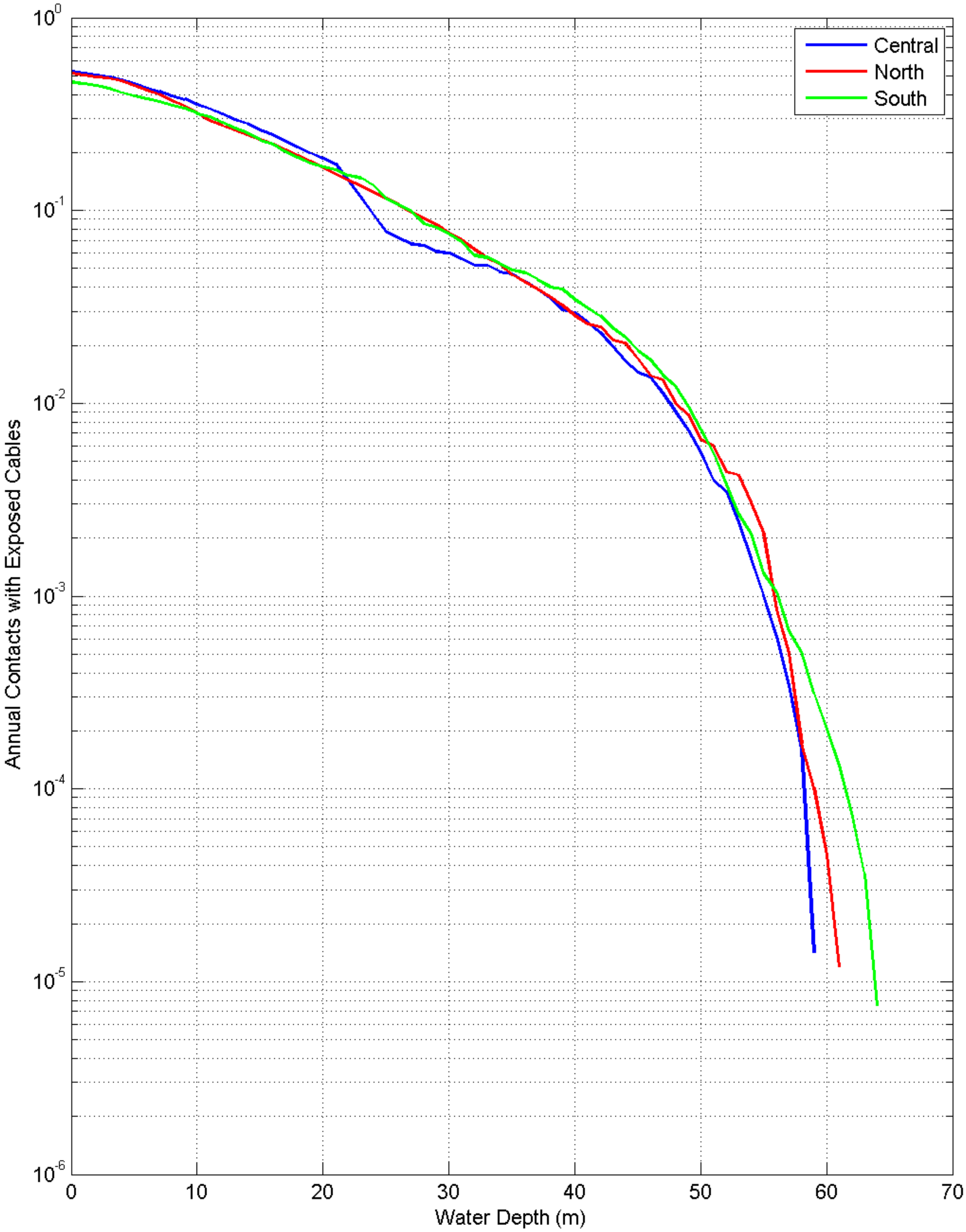

Figure 4-31 Annual cable contacts as a function of directional drilling seabed piercing water depth using no iceberg rolling

5 CONCLUSIONS AND RECOMMENDATIONS

5.1 Conclusions

The multibeam data processing, scour analysis, numerical modeling and risk analysis presented in this report represent a significant effort. While much has been learned, there still remain many unanswered questions and issues. The iceberg scour dataset produced as part of this project is unique. The Strait of Belle Isle is a challenging environment, and additional data collection and analysis is required to ensure adequate understanding for engineering and design.

The multibeam data analysis revealed a significant population of iceberg scours at the site, most in deeper water in locations thought to be sheltered from iceberg by local bathymetric features. While it is considered highly likely that most (if not all) of the scours at these site are relict (evidence of past glaciations), there is currently no basis for excluding all of these features as indications of potential threats to subsea cables placed on the seabed. However, there is no evidence in the scour dataset of icebergs scouring over the local bathymetric features thought to shelter the site.

The Monte Carlo model used to simulate iceberg movement and grounding at the site indicated that iceberg rolling and associated draft adjustments provide a mechanism for icebergs to drift over bathymetric highs and ground on the seabed in areas otherwise considered sheltered from iceberg keels. Further data, in particular iceberg rolling frequencies and magnitudes of the associated changes in draft, is vital in order to properly characterize this phenomenon. The Monte Carlo model itself is computationally intensive, slow and exhibits significant scatter in the results. These types of problems are not unusual with Monte Carlo models, however further refinement of the model or the application of additional computing resources may be required in the future.

Multiple cables will be required at the site, and additional analysis was performed to address the issue of “simultaneous” contact with more than one cable. The separation distance between cables was compared to the observed scour length distributions and it was noted that the probability of contacting multiple cables is reduced with increased separation distance. It should be noted these results may be influenced by the presence of relict scours, particularly in deeper water depths.

5.2 Recommendations

Further data collection and analysis are recommended to better characterize conditions at the Strait of Belle Isle and refine the iceberg risk assessment for the cable crossing. These primarily fall into two categories: characterization of icebergs and related parameters, and improved understanding of the iceberg scour record on the seabed.

Unlike the Grand Banks, where ongoing data collection is performed as part of offshore operations, there has been relatively little systematic collection of iceberg data in the Strait of Belle Isle. A summary of required data are given below.

- Iceberg frequency, which at present is crudely defined in terms of "average number per degree square", could be better understood by analyzing archived satellite imagery and ongoing collection/analysis of new imagery.
- Expanding the limited existing iceberg drift dataset would provide a basis for modeling iceberg drift in the Monte Carlo model and can also give important information regarding iceberg grounding frequencies and locations. These data could be collected using either temporary or permanent radar installations. The data itself would consist of iceberg locations on a regular time interval (i.e. hourly, or less), and could be supplemented with current and wind data, as well as above-waterline dimensions and draft measurements.
- Site specific iceberg size (length, mass) and deterioration rates would give site specific values for parameters that are currently estimated using data from other regions. Iceberg above-waterline dimensions are typically based on visual inspection and/or analysis of photographs, and overall iceberg mass is based on above-waterline mass (estimated from dimensions) and the ratio of ice/seawater densities (which governs the portion of the iceberg below the waterline). Approaches have also been developed for assessing iceberg above-waterline mass using stereo photography. Deterioration rates would be assessed by performing these measurements on a periodic basis and determining the decrease in mass.
- Iceberg rolling rates and associated draft changes have a significant effect on iceberg grounding rates in areas otherwise sheltered by local seabed bathymetry, and currently very limited data are available on either of these factors. Rolling rates can be established through direct observation. Draft changes could be established through pre and post-rolling draft measurements. A number of systems exist for measuring iceberg drafts.
- The collection of current data and the development of a current model for the site would provide a basis for understanding and modeling iceberg drift patterns at the cable crossing site. This could be accomplished using a number of technologies,

such as moored current meters, bottom-mounted ADCP or beacons equipped with drogues.

The recommended investigations of iceberg scour include analyses based on existing information, as extensions of the current work, and also potential future studies involving acquisition and analysis of new datasets. These are summarized below:

- Assessment of the relative age of ice scour populations using cross-cut analysis methods. Involves a review and classification of all scour features in the existing database, with scours separated into relative age classes based on visual interpretation of cross-cut relationships. Limited to areas of continuous data coverage with intersecting scour features.
- Generation of scour statistics for relative age classes, demonstrating their relationship with water depth, location, and seabed geology (where known).
- Characterization of metrics for “recent” scour populations to assist with subsea engineering design.
- Repetitive mapping analysis of iceberg scour populations to identify “new” scours and estimate the frequency of seabed-ice contact events. The analysis would be based on existing time-lapse data (2007-2009), and potential future survey work. Includes depth-differencing of digital terrain data for seabed change detection, as well as a systematic visual comparison of shaded relief bathymetry images.
- Characterization of scour geometries relative to interpreted seabed geology and soil types; based on existing geophysical-geotechnical datasets and potential future survey work. Contributes to understanding of ice keel – soil interaction mechanics and substrate controls on penetration depth.
- Quantitative age dating of selected scour features, with data collection guided by results of the cross-cut analysis. Involves physical sampling and potential radiocarbon and/or optical luminesence dating methods. Successful execution would provide calibration of cross-cut age classification, and identify scour relict populations.

In addition to the items outlined above, additional development of the Monte Carlo iceberg contact model is recommended to improve the speed and performance of the simulation.

6 REFERENCES

Amec Earth and Environmental (2009). Labrador – Island Transmission Link: Marine Flora, Fauna and Habitat Survey - Strait of Belle Isle Subsea Cable Crossing Corridors. Interim (Draft) Report for Nalcor Energy, August 2009.

C-CORE (1998). Analysis of Pack Ice and Iceberg data from the 1997 CCGS Henry Larson Probe to Voisey's Bay. Contract Report prepared for Canadian Coast Guard, Fisheries and Oceans Canada, June, C-CORE Publication 98-C7.

C-CORE (2004a). Assessment of a Direct Pipeline Route for Transport of Grand Banks Natural Gas. C-CORE Report R-03-092-261, June 2004.

C-CORE (2004b). Iceberg Management JIP, Year 2003. "Chapter 6 – Iceberg Drift Prediction". C-CORE Report R-03-059-226.

C-CORE (2006). Dual-Polarization Evaluation for RADARSAT-2 – Field Report. Prepared for DRDC. C-CORE Publication No. R-06-047-453, October.

C-CORE (2007). C-CORE (2007). Ice Scour Risk in Strait of Belle Isle and Cabot Strait. Prepared for Fugro Jacques GeoSurveys Inc., C-CORE Report R-07-032-552 V1.1 (DRAFT), August 2007

C-CORE (2010). SIRAM – Iceberg Contact Frequency, Volume 3 of 9. C-CORE Report R-10-003-480 v1 (Draft). Prepared for SIRAM JIP Participants, April 2010.

Carrieres, T., Sayed, M., Savage, S. and Crocker, G. (2001). Preliminary verification of an operational iceberg drift model. Proceedings of 16th International Conference on Port and Ocean Engineering under Arctic Conditions (POAC 01), August 12-17, Ottawa, Canada.

Davis, L., Ralph, T., Cumming, E., Sonnichsen, G. and King, T. (2005). Morphometric Analysis of Iceberg Scours using Multibeam Sonar Bathymetry Data, Eastern Canadian Continental Shelf. POAC '05 Conference Proceedings, Potsdam, NY, June, 2005.

El-Tahan, M., El-Tahan, H. and Courage, D. (1985). Documentation of Iceberg Groundings. Report prepared by Fenco Newfoundland Limited, ESRF Report 007.

Fiering, Myron B. and Jackson, Barbra B. (1971). Synthetic Streamflows. American Geophysical Union, Washington, 98 pp.

FGI (Fugro Geosurveys, Inc.), (2010). Strait of Belle Isle ice Scour Analysis, 2007 & 2009 Survey Data. Report Prepared by Fugro GeoSurveys Inc. for C-CORE, Report Document No. 10056SGN-001-RPT-001 Rev0., December.

FJGI (Fugro Jacques Geosurveys, Inc.), (2010a). Labrador – Island Transmission Link Marine Habitats in the Strait of Belle Isle: Interpretation of 2007 Geophysical (Sonar) Survey Information for the Subsea Cable Crossing Corridors. FJGI Project # 9056SG.

FJGI (Fugro Jacques Geosurveys, Inc.), (2010b). Lower Churchill Hudro Development Bedrock Tunnel Route Survey, Strait of Belle Isle, Newfoundland and Labrador. FJGI Document No. 9093SGN-001 RPT-001 Rev 0.

FJGI (Fugro Jacques Geosurveys, Inc.), (2008). Lower Churchill Hydro Development Subsea Cable Route Survey Strait of Belle Isle, Newfoundland and Labrador. Volume I – Survey Results. Report Document No. 7045SGN-DC1131-RPT-001 Rev1.

FJGI (Fugro Jacques Geosurveys, Inc.), (2007). Lower Churchill Hydro Development Proposed Subsea hvDC Cable Route, Strait of Belle Isle, Newfoundland and Labrador, Data Compilation Desk Study. Report Document No. 7045SGN-DC1132-DKSD-001 Rev 0.

Grant, D.R. (1992). Quaternary geology of St. Anthony – Blanc Sablon area, Newfoundland and Quebec. Geological Survey of Canada, Memoir 427: 60 pages.

Jordaan, I.J., Fuglem, M., Crocker, G., and Olsen, C. (1995). Canadian Offshore Design for Ice Environments, Volume 1, Environment and Routes, September, 1995.

King, A.D. (2002). Iceberg Scour Risk Analysis for Pipelines on the Labrador Shelf. M.Eng. Thesis, Memorial University of Newfoundland, St. John's, Newfoundland, Canada, 212 p.

King, T., Phillips, R., Barrett, J. and Sonnichsen, G. (2009). Probabilistic pipeline burial analysis for protection against ice scour, Cold Regions Science and Technology, Vol. 59, No. 1, October, pp. 58-64.

King, T. and Sonnichsen, G. (2010). Seabed and iceberg scour conditions affecting a potential pipeline landfall offshore Labrador, ICETECH 2010, Anchorage, Alaska.

King, T., Howekk, C., Youden, J. and Lynch, M. (2009). 2006 Labrador iceberg survey. Proceedings of 20th International Conference on Port and Ocean Engineering under Arctic Conditions (POAC 09), June 9-12, Lulea, Sweden.

Nalcor Energy (2009). Labrador – Island Transmission Link: Environmental Assessment Registration and Project Description, Submitted by Nalcor Energy, January 29, 2009.

PAL (2005). Comprehensive Iceberg Management Database. PERD/CHC Report 20-72, March.

Petro-Canada (1983). Bjarni/North Bjarni Production Perspectives Study. Prepared by Petro-Canada Resources – Frontier Development Group for The Labrador Group of Companies. 10 volumes.

Roche, C. (1980). Iceberg Tracking Program, Pointe Amour, Labrador. Report Prepared for SNC-Lavalin Newfoundland Limited. Report Number 80-15. 71 p.

Veitch, B., Williams, M., Gardner, A. and Liang, B. (2001). Field Observations of Iceberg Deterioration. PERD/CHC Report 20-64.

Appendix A

Seabed Datum Quality Flags

Appendix A: Seabed Datum Quality Flags

Table A-1 Quality flags for cross-sectional scour profiles

Flag Name	Bit No.	Condition	Set Method
Deepest Point Not Negative	0	Set if deepest point detected is shallower than the seabed datum.	Auto detected
No Zero Crossing Left	1	Set if the seabed datum does not intersect the scour profile on the left of the deepest point	Auto detected
No Zero Crossing Right	2	Set if the seabed datum does not intersect the scour profile on the right of the deepest point	Auto detected
No Peak Left	3	Set if no berm top is detected on the left side of the scour profile	Auto detected
No Peak Right	4	Set if no berm top is detected on the right side of the scour profile	Auto detected
User Modified Seabed	5	Set if the user modified the seabed datum in the profile viewer	Auto detected
Cross Cut Area	6	Set by the user if the profile is observed to be in a cross cut area	User
Rejected by User	7	Set by user if the profile/datum pick is deemed to be inadequate	User
Flagged For Editing	8	Set by user to indicate that the profile should be modified to improve its quality	User
Multiple Scour Area	9	Set if more than one scour vector resides between the detected datum (zero) crossings	Auto detected
Depth< System Resolution	10	Set if scour depth is less than 5cm	Auto detected
Unbalanced Datum	11	Set if all datum picks are on one side of the scour center point	Auto detected

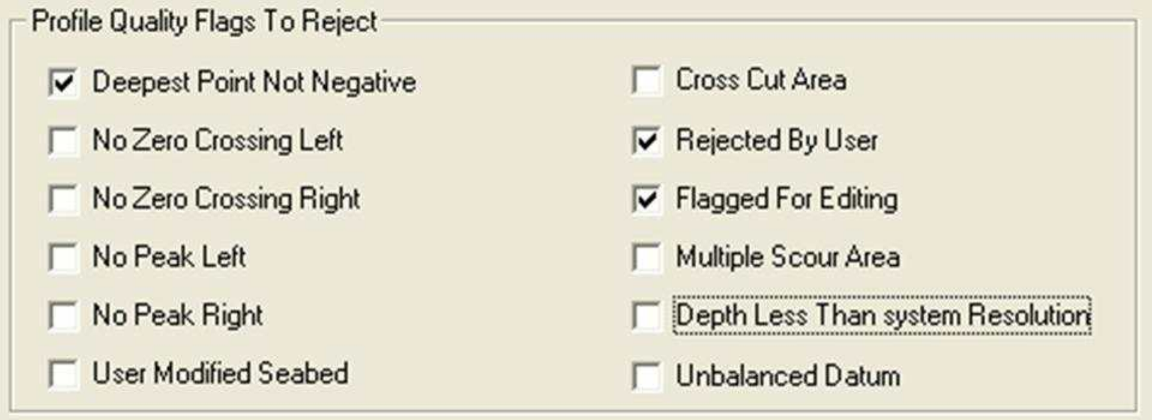

Profile Quality Flags To Reject

☑ Deepest Point Not Negative
☐ No Zero Crossing Left
☐ No Zero Crossing Right
☐ No Peak Left
☐ No Peak Right
☐ User Modified Seabed
☐ Cross Cut Area
☑ Rejected By User
☑ Flagged For Editing
☐ Multiple Scour Area
☐ Depth Less Than system Resolution
☐ Unbalanced Datum

Figure A-1 Selection menu for filtering profiles based on quality flags

Appendix B

List of Scour Cross-Sectional Parameters

Appendix B: List of Scour Cross-Sectional Parameters

Table B-1 Cross-sectional scour metrics

Profile Parameter	Description	Comments
ScourID	Four character sequential number	e.g. SIV1_0095
ProfileNumber	Sequential profile number along the scour	
DeepestPoint.Easting	Easting of profile deepest point	UTM06N, NAD83
DeepestPoint.Northing	Northing of profile deepest point	UTM06N, NAD83
DeepestPoint.ScourDepth	Depth of scour	Scour depth (m) is calculated as elevation difference between deepest point and coincident datum point.
DeepestPoint.DatumDepth	Pre-scour water depth	Water depth (m) is the depth at seabed datum point coincident with the location of the deepest point for any given profile
TotalWaterDepth	Water depth	Water depth at deepest part of profile (datum depth + scour depth)
IncisionWidth	Scour width	Incision width is calculated as the distance between two datum (zero) crossing points
BaseWidth	Base width	A point on the scour profile is considered to be part of the scour base if it is between the datum (zero) crossings and not more than 10% shallower than the deepest point
BaseToIncisionRatio	Ratio of Base width to Incision width	Calculated as the BaseWidth / IncisionWidth. This is an indicator of the shape of the scour profile
BTBWidth	Berm to Berm Width	Width of scour as measured from left berm top to right berm top
BermLeft.Height	Height of left berm	Berm height is calculated as the vertical distance from berm top to the coincident datum point
BermRight.Height	Height of right berm	

Table B-1(continued) Cross-sectional scour metrics

Profile Parameter	**Description**	**Comments**
MinDepthDisturbance	Minimum depth difference between berm top and scour base (on either left or right side of scour profile)	Depth differences are calculated between berm tops (left and right) and base of scour (DeepestPoint). Minimum value is the lesser of the right and left measurements.
MaxDepthDisturbance	Maximum depth difference between berm top and scour base (on either left or right side of scour profile)	Depth differences are calculated between berm tops (left and right) and base of scour (DeepestPoint). Maximum value is the greater of the right and left measurements.
AvgDepthDisturbance	Average depth difference between berm top and scour base (on left and right sides of scour profile)	Depth differences are calculated between berm tops (left and right) and base of scour (DeepestPoint). Left and right side measurements are averaged..
LeftSideWall.minSlope	minimum slope on left sidewall	Between datum (zero) crossing & deepest point
LeftSideWall.maxSlope	maximum slope on left sidewall	Between datum (zero) crossing & deepest point
LeftSideWall.avgSlope	average slope on left sidewall	Between datum (zero) crossing & deepest point
LeftSideWall.slopeAtZeroCrossing	slope on left sidewall at datum (zero) crossing	Between datum (zero) crossing & deepest point
RightSideWall.minSlope	minimum slope on right sidewall	Between datum (zero) crossing & deepest point
RightSideWall.maxSlope	maximum slope on right sidewall	Between datum (zero) crossing & deepest point
RightSideWall.avgSlope	average slope on right sidewall	Between datum (zero) crossing & deepest point
RightSideWall.slopeAtZeroCrossing	slope on right sidewall at datum (zero) crossing	
ScourOrientation	Orientation of scour at profile crossing	
Quality Flag	Numerical value of status bits	

Appendix C

Summary Scour Statistics

Appendix C: Summary Scour Statistics

Table C-1 Summary scour statistics

Scour Parameter	Parameter Description	Comments
ScourID	Four character description_scour sequential number	e.g. SOBI_0095
SurveyID	FJG_project number	e.g. 10056SGN
SurveyDate	Month and year of survey	mm/yyyy
SYS_TYPE	Survey system type as defined in GBSC_huskyregion-final.dbf	sss sss/swath swath sss/huntec
Start_E	Easting of the digitized vector start point. Uses digitized vector data and is irrespective of quality flags	UTM22N, NAD83
Start_N	Northing of the digitized vector start point. Uses digitized vector data and is irrespective of quality flags	UTM22N, NAD83
End_E	Easting of the digitized vector end point. Uses digitized vector data and is irrespective of quality flags	UTM22N, NAD83
End_N	Northing of the digitized vector end point. Uses digitized vector data and is irrespective of quality flags	UTM22N, NAD83

Table C-1(continued) Summary scour statistics

Scour Parameter	**Parameter Description**	**Comments**
ScourDepthMin	minimum scour depth derived from accepted points along the scour	scour depth is calculated as difference in elevation between deepest point and coincident datum point
ScourDepthMax	maximum scour depth derived from accepted points along the scour	meters
ScourDepthAvg	average scour depth derived from accepted points along the scour	meters
DatumDepthMin	minimum datum depth derived from accepted points along the scour	Depth at seabed datum point coincident with the location of the deepest point for any given profile
DatumDepthMax	maximum datum depth derived from accepted points along the scour	meters
DatumDepthAvg	average datum depth derived from accepted points along the scour	meters
WaterDepthMin	minimum water depth derived from accepted points along the scour	Depth at seabed at the location of the deepest point for any given profile
WaterDepthMax	maximum water depth derived from accepted points along the scour	meters
WaterDepthAvg	average water depth derived from accepted points along the scour	meters
RiseUp	water depth range along the scour	WaterDepthMax-WaterDepthMin
IncisionWidthMin	minimum scour incision width derived from accepted points along the scour	Incision width is calculated as the distance between two datum (zero) crossing points

Table C-1(continued) Summary scour statistics

Scour Parameter	**Parameter Description**	**Comments**
IncisionWidthMax	maximum scour incision width derived from accepted points along the scour	meters
IncisionWidthAvg	average scour incision width derived from accepted points along the scour	meters
BaseWidthMin	minimum scour base width derived from accepted points along the scour	A point on the scour profile is considered to be part of the scour base if it is between the datum (zero) crossings and not more than 10% shallower than the deepest point
BaseWidthMax	maximum scour base width derived from accepted points along the scour	meters
BaseWidthAvg	average scour base width derived from accepted points along the scour	meters
RatioMin	minimum base width to incision width ratio derived from accepted points along the scour	The ratio is calculated as the BaseWidth / IncisionWidth. This is an indicator of the shape of the scour profile.
RatioMax	minimum base width to incision width ratio derived from accepted points along the scour	unitless

Table C-1(continued) Summary scour statistics

Scour Parameter	**Parameter Description**	**Comments**
RatioAvg	minimum base width to incision width ratio derived from accepted points along the scour	unitless
BTBWidthMin	minimum Berm To Berm width derived from accepted points along the scour	BTBWidth is calculated as the distance between the tops of berms on either side of the scour centerline
BTBWidthMax	maximum Berm To Berm width derived from accepted points along the scour	meters
BTBWidthAvg	average Berm To Berm width derived from accepted points along the scour	meters
BermLeftHeightMin	minimum height of berms on the ‘left’ side of the scour centerline, derived from accepted points along the scour	Berm height is calculated as the vertical distance from berm top to the coincident datum point
BermLeftHeightMax	maximum height of berms on the ‘left’ side of the scour centerline, derived from accepted points along the scour	meters
BermLeftHeightAvg	average height of berms on the ‘left’ side of the scour centerline, derived from accepted points along the scour	meters
BermRightHeightMin	minimum height of berms on the ‘right’ side of the scour centerline, derived from accepted points along the scour	meters

Table C-1(continued) Summary scour statistics (FJG, 2005a)

Scour Parameter	Parameter Description	Comments
BermRightHeightMax	maximum height of berms on the 'right' side of the scour centerline, derived from accepted points along the scour	meters
BermRightHeightAvg	average height of berms on the 'right' side of the scour centerline, derived from accepted points along the scour	meters
SidewallLeftAverageMaxSlope	average of all the maximum slopes found on the left sidewall of the scour, derived from accepted points along the scour	sidewall is taken as that section of a profile between the datum (zero) crossing and deepest point
SidewallLeftAvgSlopeAtZeroCrossing	average of all the slopes found at the datum (zero) crossing on the left sidewall of the scour, derived from accepted points along the scour	degrees
SidewallRightAverageMaxSlope	average of all the maximum slopes found on the right sidewall of the scour, derived from accepted points along the scour	degrees
SidewallRightAvgSlopeAtZeroCrossing	average of all the slopes found at the datum (zero) crossing on the right sidewall of the scour, derived from accepted points along the scour	degrees

Table C-1(continued) Summary scour statistics

Scour Parameter	Parameter Description	Comments
MinDepthDisturbAvg	Average of min. depth disturbance values derived from accepted points along the scour.	meters
MaxDepthDisturbAvg	Average of max. depth disturbance values derived from accepted points along the scour.	meters
AvgDepthDisturbAvg	Average of avg. depth disturbance values derived from accepted points along the scour.	meters
OrientationAvg	average of all orientations calculated at each sampled point along the scour	Grid Azimuth in degrees. Uses digitized vector data and is irrespective of quality flags
ScourLength	Length of scour derived from digitized vector data. Irrespective of quality flags.	meters
TotalProfiles	total number of profiles sampled along the scour	
PercentUsed	Percentage of profiles meeting quality flags specifications	

Appendix D

Summary of Data and Digital Files on DVD

Appendix D: Summary of Data and Digital Files on DVD

Directory: Arc Files

accepted_scours.dbf
accepted_scours.prj
accepted_scours.sbn
accepted_scours.sbx
accepted_scours.shp
accepted_scours.shp.xml
accepted_scours.shx
rejected_scours.dbf
rejected_scours.prj
rejected_scours.sbn
rejected_scours.sbx
rejected_scours.shp
rejected_scours.shp.xml
rejected_scours.shx
SOBI_Scour_Profile_Data.DBF
SOBI_Scour_Summary_Data.DBF

Directory: Fledermaus

2007_2009_SOBI_AllVessels_5m.sd
2007_2009_SOBI_AllVessels_5m_JECA.sd
2007_2009_SOBI_AllVessels_5m_SLOPE.sd
sample.jpg

Directory: Images

2009_combined_5m_Neg_Depth.tfw
2009_combined_5m_Neg_Depth.tif
2009_combined_5m_Neg_Depth.txt
2009_combined_5m_Neg_Depth-PaletteLegend.tif
Anticosti_SOBI_Color.tif
Anticosti_SOBI_Color.txt
Forteau_Point_2009_2m.tfw
Forteau_Point_2009_2m.tif
Forteau_Point_2009_2m.txt
marineeagle_Jeca_5m_Neg_Mean.tfw
marineeagle_Jeca_5m_Neg_Mean.tif

marineeagle_Jeca_5m_Neg_Mean.txt
Point_Amour_2009_2m.tfw
Point_Amour_2009_2m.tif
Point_Amour_2009_2m.txt
Read_Me.xls

Directory: Report
C-CORE R-10-039-781 V1 Nalcor SoBI Iceberg Cable Risk.doc
10056SGN-001-BTY-SOBI-01-0 Version1.pdf

Directory: SOBI_Scour_Metrics
SOBI_Scour_Profile_Data_07-12-10.xls
SOBI_Scour_Summary_Data_15-12-10.xls

Directory: xyz_Bathymetry
2009_2m_Nalcor_Forteau_Point_XYZ.xyz
2009_2m_Nalcor_Point_Amour_XYZ.xyz
Anticosti_SOBI_AllSoundings.xyz
Anticosti_2009_combined_5m.xyz
MarineEagle_2007_5m.xyz
Read_Me.xls

LAST PAGE OF DOCUMENT